

Applications and Industry®

UNIVERSITY OF HAWAII
LIBRARY

JUN 3 8 38 AM '70

May 1961



Transactions Papers

Industry Division

60-1018	Stochastic-Time Optimal-Control Systems.....Aoki . . .	41
60-649	A-C Contactors Supplied by Long Control Lines.....Alley . . .	46
60-1019	Synthesis Technique for Feedback Systems.....Weaver, Sage, Miller . . .	50
61-83	Linear Switching Condition for Feedback Control Systems.....Garrett . . .	53
60-642	Automatic Speed Regulation of D-C Motors.....Hansen, Wilkerson . . .	59
61-78	Control Sys. Standards....Gibson, Rekasius, McVey, Sridhar, Leedham . . .	65
61-109	Ignitron Firing Circuits Utilizing Controlled Rectifiers.....Graham . . .	78
	Optimum Nonlinear Bang-Bang Control Systems With Complex Roots	
60-1266	I—System Synthesis.....Chandaket, Leondes . . .	82
61-79	II—Analytical Studies.....Chandaket, Leondes, Deland . . .	95
60-645	Wide-Range D-C Center-Wind Drive.....Jones, Pare . . .	102
61-67	Grounding of D-C Structures and Enclosures.....Hoffmann . . .	106
	Conference Papers Open for Discussion.....	See 3rd Cover

© Copyright 1961 by American Institute of Electrical Engineers

NUMBER 54

Published Bimonthly by

AMERICAN INSTITUTE OF ELECTRICAL ENGINEERS

Instrumentation Division

61-17	Digital Telemetering Techniques.....	Brothman, Brothman, Reiser . . .	81
61-63	Analysis of Errors in Calibration of Electric Instruments.....	Hermach . . .	90

Power Division

61-134	A 20,000-Ampere Mechanical Switch.....	Newgard . . .	96
--------	--	---------------	----

Communication Division

61-47	Antenna Matching Unit for H-F Vehicular Whip.....	Gruber, Seward . . .	99
61-60	Telegraph Distortion and Distortion Measuring.....	Wüsteney . . .	104
61-61	Single-Ring Circular Antenna Array.....	Hickman, Neff, Tillman . . .	110
61-29	Proposed Electronic Method for High-Speed Teleprinters.....	Biswas . . .	115
61-69	Low-Cost Number Identifier for Small Telephone Systems...	Redington . . .	117
61-111	Completely Transistorized 600-Channel Multiplex System.....	Sparks . . .	121
61-117	Telephone Circuit and Equipment Impedances.....	Radue . . .	126

Science and Electronics Division

61-25	Elimination of Null in Modulating and Demodulating Devices.....	Jones . . .	135
60-1290	Method of Calculating Gain and Phase Margins.....	Schlereth . . .	139
61-90	Movement of Air in Electric Wind of Corona Discharge.....	Robinson . . .	143
61-1	Low-Level Linear Rundown Circuit...Endsley, Grannemann, Summers . . .		150
T-121	Magnetic-Controlled Rectifier Power Amplifier.....	Morgan . . .	152
61-91	Discharges Preceding Sparkover at Low Gradients.....	Penney, Craig . . .	156
61-89	Commutation and Destructive Oscillation in Diode Circuits.....	Somos . . .	162
61-35	Ampere-Turn Gain of Ordinary Saturable Reactors.....	Geyger . . .	173
61-98	Transistor Morse-to-Teleprinter Code Converter.....	Cunniff, Theall . . .	178
61-5	Synthesis of General Parameter Insertion Loss Filters.....	Temes . . .	181
61-24	Fatigue-Free Silicon Device Structure.....	Green . . .	186
	Late Discussion.....		192

(See inside back cover)

Note to Librarians. The six bimonthly issues of "Applications and Industry," March 1961–January 1962, will also be available in a single volume (no. 80) entitled "AIEE Transactions—Part II. Applications and Industry," which includes all technical papers on that subject presented during 1961. Bibliographic references to Applications and Industry and to Part II of the Transactions are therefore equivalent.

Applications and Industry. Published bimonthly by the American Institute of Electrical Engineers, from 20th and Northampton Streets, Easton, Pa. AIEE Headquarters: 33 West 39th Street, New York 18, N. Y. Address changes must be received at AIEE Headquarters by the first of the month to be effective with the succeeding issue. Copies undelivered because of incorrect address cannot be replaced without charge. Editorial and Advertising offices: 33 West 39th Street, New York 18, N. Y. Nonmember subscription \$8.00 per year (plus 75 cents extra for foreign postage payable in advance in New York exchange). Member subscriptions: one subscription at \$5.00 per year to any one of three divisional publications: Communication and Electronics, Applications and Industry, or Power Apparatus and Systems; additional annual subscriptions \$8.00 each. Single copies when available \$1.50 each. Second-class mail privileges authorized at Easton, Pa. This publication is authorized to be mailed at the special rates of postage prescribed by Section 132.122.

The American Institute of Electrical Engineers assumes no responsibility for the statements and opinions advanced by contributors to its publications.

Printed in United States of America

Number of copies of this issue 5,100

Stochastic-Time Optimal-Control Systems

MASANAO AOKI

NONMEMBER AIEE

CONTROL SYSTEMS which are so designed that the control system outputs become identical with the control system inputs in the minimum amount of time are known as "time optimal-control systems." In other words, a time optimal-control system is one which, when the final desired state, moves from the initial state to the final state in the minimum time. The final state may be the origin of the phase space in which the state of a control system is represented by a point. In general, however, the desired final state will be a function of time. Since essential complications enter into the problem when the desired state of a control system is a function of time, only the problem with the origin as the desired state will be considered in this paper.

Time optimal-control systems possess features which have attracted the attention of several investigators; Bushaw,¹ Llanman, Glicksburg, and Gross,² Gamidze,³ Pontryagin,⁴ and LaSalle,⁵ among others.

One feature concerns the utilization of the so-called "bang-bang," or maximum principle, type of control forces. For a linear deterministic control system, LaSalle showed, among other things, that under suitable assumptions if there is an optimal control force, then there is always a bang-bang type of control force that is optimal.

Another feature of interest is the fact that the criterion of control is implicit. That is, in a time optimal-control system, the criterion of performances is the time required to reach the desired final state from the initial state and this time is dependent upon control actions of the system in a complicated way. Therefore, an explicit expression of the criterion function is generally not available. This

point is important if an optimal sequence of control actions is sought by formulating control processes as multistage decision processes.

Dynamic programming provides a powerful investigation tool for multistage decision processes, since the functional equation techniques apply to nonlinear control systems and with suitable modification of criteria of performances to non-deterministic control systems as well,⁶ whereas most of the work on time optimal-control systems so far has been concerned with deterministic, linear, or quasi-linearized systems.

Functional equations are written in terms of criterion functions of control processes. If the criteria are implicit, the resulting functional equations are, in general, more difficult to solve analytically. When analytic solutions are not easily available, computational solutions may be necessary.

In this paper, optimal sequences of control forces are investigated for a linear time optimal system with random disturbances, using functional equation techniques of dynamic programming. Computational solutions of resulting functional equations are also discussed. In sections dealing with computational solutions, control forces are restricted to a finite number of values. This does not mean, however, that in stochastic-time optimal-control systems bang-bang-type control forces are optimal.

Stochastic-Time Optimal Processes

Roughly speaking, there are two ways by which random variables enter into control processes. One way is via random disturbances n contaminating the ideal input signal s to the system. That is, the actual input to the system is some function of s and n , $h(s, n)$. The most common situation is where $h(s, n) = s + n$. (If some function of error, such as a mean-square error, is to be minimized—which is the usual situation—under certain assumptions, an optimal predictor followed by a bang-bang controller is an optimal control configuration.^{7,8}) The other is the situation where some parameters entering into control systems exhibit randomness. That is, control systems are assumed to contain some noisy components.

In the absence of randomness, with the origin of the phase space as the desired final state, the existence of switching hyperplane in the phase space is well known for bang-bang systems. Because of random elements in the control systems, however, for a given initial point and a desired final point in the phase space, points where the control forces change sign and consequently the time required to reach the desired state will no longer be definite but will be random variables.

One of the natural extensions of criteria of performances to stochastic control systems is, therefore, the expected time required to reach the origin from the given initial point in the phase space. Control systems with this criterion of performance will try to minimize the expected time to reach the origin. An optimal policy here consists of a sequence of control forces which minimizes this expected time.

Another criterion of performance, pertinent to stochastic-time optimal problems, is the probability of reaching the origin (or ϵ -neighborhood thereof) in the next t seconds, given the present state of the system, i.e., the present position of the system in the phase space. Control systems with this type of performance criterion, therefore, would try to maximize this probability.⁹ An optimal policy, here, consists of a sequence of control forces which maximizes this probability.

In this paper, the criterion of performance is taken to be the expected time. Random variations in system parameters will be assumed which are independently and identically distributed for each time instant.

Functional Equation Formulation

Consider a general control system described by the differential equation:

$$\dot{s} = As + Bu + f \quad (1)$$

where

s = n -dimensional state vector of the system
 u = r -dimensional control force of the system
 f = n -dimensional disturbing force of the system

A = n -by- n matrix, some elements of which may exhibit random variation with time

B = n -by- r matrix, some elements of which may exhibit random variation with time

In the following, the time discrete system will be considered, either because the system is of the sampling control type or because time must be quantized in order for a computational solution to be obtained.

With elementary time step Δt , the

60-1018, recommended by the AIEE Feedback Control Systems Committee and approved by the AIEE Technical Operations Department for presentation at the AIEE Pacific General Meeting, San Diego, Calif., August 8-12, 1960, and presented for discussion only at the Winter General Meeting, New York, N. Y., January 29-February 3, 1961. Manuscript submitted March 18, 1960; made available for printing November 23, 1960.

MASANAO AOKI is with the University of California, Los Angeles, Calif.

The work reported in this paper was supported in part by the U. S. Office of Naval Research under contract no. N00014-59-1-1192 and reproduction in whole or in part is permitted for any purpose of the United States Government.

The author wishes to acknowledge his fruitful discussions with Dr. R. Bellman of the Rand Corporation, Santa Monica, Calif.

differential equation becomes the difference equation:

$$\mathbf{s}_{n+1} = C\mathbf{s}_n + D\mathbf{u}_n + \mathbf{v}_n \quad (2)$$

where

$$\begin{aligned} \mathbf{s}_n &= \mathbf{s}(n\Delta t) \\ \mathbf{u}_n &= \mathbf{u}(n\Delta t) \\ \mathbf{v}_n &= \Delta t \cdot \mathbf{f}(n\Delta t) \\ C &= \Delta t \cdot A + I \\ D &= \Delta t \cdot B \\ I &= n\text{-by-}n \text{ unit matrix} \end{aligned}$$

That is, if the present state of the system is \mathbf{s}_n , the next state is given by \mathbf{s}_{n+1} . Since C , D , and \mathbf{v}_n may contain components with random variations, \mathbf{s}_{n+1} will, in general, be a random variable.

Define

$g(\mathbf{s})$ = expected minimum time required to reach the state at the origin $\mathbf{0}$ starting from the initial state \mathbf{s} following an optimal policy

Then

$$g(\mathbf{0}) = 0$$

Noting the fact that if the present state is given by \mathbf{s} , then the next possible state of the control system, \mathbf{s}' , after Δt elapses is given by equation 2 with $\mathbf{s}_n = \mathbf{s}$, the application of the principle of optimality⁶ gives the functional equation for $g(\mathbf{s})$:

$$\begin{aligned} g(\mathbf{s}) &= \min_{\mathbf{u}} [\Delta t + E\{g(\mathbf{s}')\}] \\ &= \Delta t + \min_{\mathbf{u}} E\{g(\mathbf{s}')\} \end{aligned} \quad (3)$$

where the expected value operator E is taken over the possible next state \mathbf{s}' , which can be seen from equation 2 to be the function of the present state vector \mathbf{s} , control force \mathbf{u} , and random variables in the form of \mathbf{v} or C and D .

For example, if the control system is second order and is subjected to a step input, then \mathbf{s} has two components, the error e and the error derivative \dot{e} , and the next state \mathbf{s}' is given by

$$\begin{aligned} e' &= \phi_1(e, \dot{e}, \mathbf{u}, \alpha) \\ \dot{e}' &= \phi_2(e, \dot{e}, \mathbf{u}, \alpha) \end{aligned} \quad (4)$$

where ϕ_1 and ϕ_2 are linear in e and \dot{e} , \mathbf{u} is the control force, and α is used to represent the effects of random variations in the next state.

If the random disturbance in equation 2 is such that for any fixed \mathbf{s} and \mathbf{u} , there are two possible next states \mathbf{s}^+ and \mathbf{s}^- with probability p and $1-p$ respectively, then equation 3 becomes

$$g(\mathbf{s}) = \Delta t + \min_{\mathbf{u}} [pg(\mathbf{s}^+) + (1-p)g(\mathbf{s}^-)] \quad (3A)$$

where

$$\begin{aligned} \mathbf{s}^+ &= C^+\mathbf{s} + D^+\mathbf{u} + \mathbf{v}^+ \\ \mathbf{s}^- &= C^-\mathbf{s} + D^-\mathbf{u} + \mathbf{v}^- \end{aligned}$$

C , D , and \mathbf{v} are assumed to take two forms

with superscripts $+$ and $-$ with probability p and $1-p$ respectively. For bang-bang control systems, the minimization over \mathbf{u} reduces to that over $u^i = \pm 1$ where $\mathbf{u} = (u^1, u^2, \dots, u^r)$.

Before the solution of equation 3, approximate or otherwise, is discussed another formulation which allows straightforward solution (at least computationally) to problems will be considered.¹⁰

Since the desired state is $\mathbf{0}$, the distance from the origin of the point \mathbf{s} in the phase space representing the present state gives a measure of how close the system is to the final desired state. Define

$k_n(\mathbf{s})$ = expected value of the distance of the state from the origin starting from \mathbf{s} after an optimal sequence of n control actions

The usual application of the principle of optimality gives

$$k_1(\mathbf{s}) = \min_{\mathbf{u}} \{E[\mathbf{s}']\} \quad (5)$$

$$k_{n+1}(\mathbf{s}) = \min_{\mathbf{u}} E\{k_n(\mathbf{s}')\}, n=1, 2, \dots$$

where \mathbf{s}' and E are as in equation 3.

Since the interest here is not so much in the system deviation at any time instant, but rather in the first time the deviation becomes zero (or less than a predetermined quantity ϵ) for any given \mathbf{s} , N^* is sought such that

$$\begin{aligned} k_{N^*}(\mathbf{s}) &\leq \epsilon \\ k_n(\mathbf{s}) &> \epsilon \\ n &< N^* \\ \epsilon &\geq 0 \end{aligned}$$

where ϵ is the predetermined nonnegative quantity.

In the above, the distance from the origin may be replaced by some more general norm of deviation $T(\mathbf{s})$. Then

$$k_1(\mathbf{s}) = \min_{\mathbf{u}} E\{T(\mathbf{s}')\} \quad (5A)$$

replaces $k_1(\mathbf{s})$ in equation 5.

Computational Techniques

In this section, computational techniques will be discussed since it is often necessary to resort to computational solutions of functional equations of the type of equation 3 and of the recurrence equation of the type of equation 5.

EXPANDING GRID

The recurrence equation is solved computationally for a certain given domain of \mathbf{s} by first computing $k_1(\mathbf{s})$ of points in the domain and then using these computed $k_1(\mathbf{s})$ to compute $k_2(\mathbf{s})$, employing suitable interpolation if necessary.

At the same time optimal \mathbf{u} for each \mathbf{s}

in the domain is recorded. What desired here is to represent $k_1(\mathbf{s})$ for \mathbf{s} in the domain using as few points in the domain of \mathbf{s} as is compatible with the accuracy of computation. Let these points be called $\mathbf{z}_1, \mathbf{z}_2, \dots, \mathbf{z}_m$. Then, computing $k_2(\mathbf{z}_i)$, $1 \leq i \leq m$, for a given control force \mathbf{u} , it is necessary to know $E\{k_1(\mathbf{s}')\}$. Since \mathbf{z}'_i will not, in general, coincide with one of $\mathbf{z}_1, \dots, \mathbf{z}_m$, $k_1(\mathbf{z}'_j)$, $j=1, 2, \dots, m$, are used to represent approximately $E\{k_1(\mathbf{s}')\}$. This process is repeated for a set of all allowable values and the minimum is chosen as $k_2(\mathbf{z}_i)$ and the corresponding \mathbf{u} which gives the minimum is recorded as $\mathbf{u}_2(\mathbf{z}_i)$.

Thus, $k_2(\mathbf{z}_i)$, $i=1, 2, \dots, m$, are computed, and this process is continued to compute a sequence $\{k_n(\mathbf{z}_i)\}$, $i=1, 2, \dots, m$, $n=1, 2, \dots$. Each computation $k_n(\mathbf{s})$ is examined to ascertain whether $k_n(\mathbf{s}) \leq \epsilon$ is realized for the first time, so, that value of \mathbf{s} will be removed from further computation of $k_L(\mathbf{s})$, $L > n$, and the value of n will be associated with that \mathbf{s} . That is, on the average it takes $(n\Delta t)$ seconds to reach the origin from the point \mathbf{s} using an optimal policy. Since $\{\mathbf{u}_n(\mathbf{s})\}$ will be recorded at the same time, this sequence of optimal-control forces is used to construct the switching hyperplanes in the phase space.

In the foregoing discussion, it was tacitly assumed that the set $(\mathbf{z}_1, \mathbf{z}_2, \dots, \mathbf{z}_m)$ is sufficient to compute $k_n(\mathbf{s}')$ with the same order of accuracy for all n . There exist, however, cases where \mathbf{s}' falls outside the domain for which the set $(\mathbf{z}_1, \dots, \mathbf{z}_m)$ is chosen. Then, in order to maintain the accuracy of computation, it is necessary to expand the set of points at which $k_n(\mathbf{s})$ is computed. Thus, the set of \mathbf{s} over which $k_1(\mathbf{s})$ is computed must be expanded continually to be able to compute $k_n(\mathbf{s})$ for increasing n . The net effect is such that to compute $k_n(\mathbf{s})$ for the domain D , it is necessary to compute $k_1(\mathbf{s})$ for a much larger domain D .

APPROXIMATION IN POLICY SPACE⁶

Discussions in this section again will consider $g(\mathbf{s})$ of equation 3. It is often true in practice that there is some approximate policy, that is, some rule of choosing the control force, derived from some approximate analysis of the problem or perhaps from past experience although no good approximation for $g(\mathbf{s})$ is available.

Assume that an approximate policy $\mathbf{u}^0(\mathbf{s})$, i.e., an approximation $\mathbf{u}^{(0)}(\mathbf{s})$ to $\mathbf{u}(\mathbf{s})$ in equation 3. Obtain the initial approximation to $g(\mathbf{s})$ by solving

$$g^{(0)}(\mathbf{s}) = \Delta t + E\{g^{(0)}(\mathbf{s}')\} \mathbf{u}^{(0)} \quad (6)$$

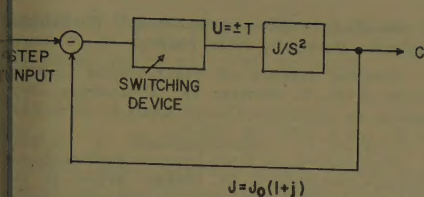


Fig. 1. Simple control system

compute the sequence

$$\{g^{(i)}(\mathbf{s})\}$$

$$g^{(i)}(\mathbf{s}) = \Delta t + \min_{\mathbf{u}} E\{g^{(i-1)}(\mathbf{s}')\} \quad (7)$$

where

$$g^{(0)} = 0, i = 1, 2, \dots$$

then, clearly,

$$g^{(i)}(\mathbf{s}) \leq g^{(i-1)}(\mathbf{s})$$

It can be shown that $g^{(i)}(\mathbf{s})$ is monotonically decreasing in i , and $g(\mathbf{s})$ is unique.⁶ This provides a steadily improving computational scheme to obtain $g(\mathbf{s})$. However, the difficulty of expanding grid discussed in the previous section still remains.

Since it is a much easier problem to obtain the switching hyperplanes to reach the origin in the minimal time from \mathbf{s} if there are no random parameters in the control system, these switching hyperplanes may be used to obtain $g^{(0)}(\mathbf{s})$. Another possibility might be to replace the random parameters by their expected values and instruct switching hyperplanes accordingly, and use the resulting minimal time $g^{(0)}(\mathbf{s})$.

The choice of initial approximation is important in so far as it affects the accuracy and speed of convergence of computations. To illustrate these points, the simple example will be discussed. Although it is possible in principle to carry a formal n -dimensional formulation, for the sake of ease of presentation, the example will be developed for the case $n=2$. (When computational solutions are desired, problems with n greater than 3 or 4 generally present substantial practical computational difficulties because of the limited capabilities of present-day digital computers, although there are several techniques to solve special cases of this type.)

Example

Fig. 1 shows the control system in question. For the sake of simplicity, the control force u is taken to be scalar, the noise term is dropped, and only the parametric disturbance term is retained. It is assumed that the inertial load J

exhibits the random disturbance given by

$$J = J_0(1 + j_n) \quad (8)$$

where J is assumed to be constant over Δt and change stepwise at $n\Delta t$. Furthermore j_n is assumed to be of the Bernoulli type,

$$j_n = \begin{cases} a & \text{with probability } p \\ -a & \text{with probability } 1-p \end{cases}$$

The state vector \mathbf{s} has two components, the error e and the error derivative \dot{e} . The distribution function of j_n is assumed to be independently and identically distributed for each n .

If $j_n \equiv 0$, $n=1, 2, \dots$ is assumed, then the switching curve is well known. The phase space is divided into two regions and in one region, $u = +T$ is used until it reaches the switching curve, then $u = -T$ is used. In the other region the reverse sequence takes place.

The switching curves are given by

$$e = \pm \frac{1}{2M} \dot{e}^2$$

where

$$M = T/J_0$$

If

$$j_n \neq 0$$

then

$$\begin{aligned} \frac{\dot{e}_n}{M} &= \frac{\dot{e}_{n-1}}{M} \mp \frac{\Delta t}{1+j_{n-1}} \\ \frac{e_n}{M} &= \frac{e_{n-1}}{M} \mp \frac{1}{2} \frac{(\Delta t)^2}{1+j_{n-1}} + \frac{\dot{e}_{n-1}}{M} \Delta t \end{aligned} \quad (9)$$

These equations correspond to ϕ_1 and ϕ_2 of equation 4. Equation 9 can be normalized to

$$\left. \begin{aligned} y_n &= y_{n-1} - \frac{\Delta t}{1+j_{n-1}} u \\ x_n &= x_{n-1} - \frac{(\Delta t)^2}{2(1+j_{n-1})} u + y_{n-1} \Delta t \end{aligned} \right\} \quad (9A)$$

with

$$u = \pm 1$$

where

$$x_n = \frac{e_n}{M}$$

and

$$y_n = \frac{\dot{e}_n}{M}$$

First, consider as $u^{(0)}(e, \dot{e})$ in equation 6, the control forces given by the switching curves of the deterministic case with $j_n = 0$ and as $g^{(0)}(e, \dot{e})$ take the time required by these curves. Then, because of the simple nature of this example,

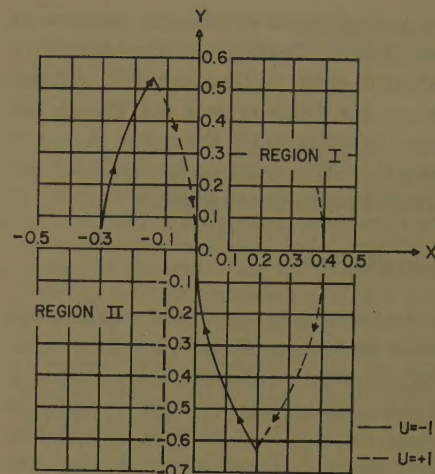


Fig. 2. Examples of switching of control forces for the deterministic control system

$$g^{(0)}(e, \dot{e}) = g^{(0)}(-e, -\dot{e}) = \frac{\dot{e}}{M} + \frac{2}{M} \sqrt{Me + \frac{\dot{e}^2}{2}} \quad (10)$$

or in its normalized form

$$g^{(0)}(x, y) = y + 2\sqrt{x + y^2/2} \quad (10A)$$

In Fig. 2 if (x, y) is in region I, use

$$g^{(0)}(x, y)$$

and if in region II, use

$$g^{(0)}(-x, -y)$$

Since this choice of $u^{(0)}(x, y)$ and $g^{(0)}(x, y)$, although convenient, does not satisfy equation 6 for all (x, y) , the relation $g^{(i)}(x, y) \leq g^{(i-1)}(x, y)$ does not necessarily follow for all (x, y) . However, the computational solution with varying mesh size Δx and Δy seems to indicate that in most cases $g^{(i)}(x, y) \leq g^{(i-1)}(x, y)$ results. Fig. 3 shows the switching boundary for this stochastic-time optimal system for $a=0.1$, $p=0.25$. The deterministic case with $a=0$ is also shown for comparison.

The dependence of the switching curve on p is another interesting and very im-

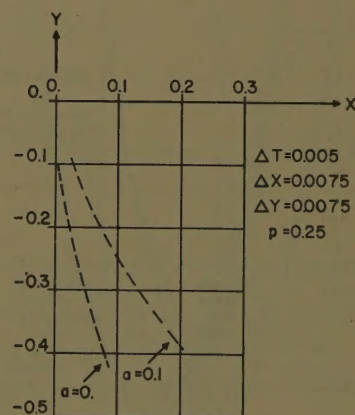


Fig. 3. Parts of switching curves for the deterministic and stochastic control system

portant point to investigate, because of its possible bearing on the design of adaptive-time optimal-control systems where the value of p is not known but must be estimated in the course of control actions. This subject is scheduled for discussion in a future paper.

Conclusions

In this paper, an initial attempt has been made to apply the functional equation formulation of dynamic programming to stochastic-time optimal systems in order to provide an analytic formulation and computational algorithm for the derivation of an optimal sequence of control forces. Some of the techniques are

illustrated by a simple second-order control system.

References

1. OPTIMAL DISCONTINUOUS FORCING TERMS (book), D. W. Bushaw. "Contribution to the Theory of Nonlinear Oscillations—IV," Princeton University Press, Princeton, N. J., 1958.
2. ON THE BANG-BANG CONTROL PROBLEM, R. Bellman, I. Glicksburg, O. Gross. *Quarterly of Applied Mathematics*, Providence, R. I., vol. 14, 1956, pp. 11–18.
3. THEORY OF TIME OPTIMAL PROCESSES FOR LINEAR SYSTEMS, R. V. Gamkrelidze. *Izvestiya Akademii Nauk, SSSR*, Moscow, USSR, vol. 22, 1958, pp. 449–74.
4. OPTIMAL CONTROL PROCESSES, L. S. Pontryagin. *Uspekhi Mate Nauk*, Moscow, USSR, vol. 14, 1959, pp. 3–20.
5. TIME OPTIMAL CONTROL SYSTEMS, J. P. LaSalle. *Proceedings, National Academy of Sciences*, Washington, D. C., vol. 45, 1959, pp. 573–77.

6. DYNAMIC PROGRAMMING (book), R. Bellman. Princeton University Press, 1957.
7. OPTIMAL DESIGN OF FINAL-VALUE CONTROL SYSTEMS, R. C. Booton, Jr. *Proceedings, Symposium on Nonlinear Circuit Analysis*, New York, N. Y., vol. 6, 1956, pp. 233–41.
8. TECHNIQUES OF TIME-DOMAIN SYNTHESIS FOR CONTROL SYSTEMS, C. W. Steeg. *Report no. 100*, Dynamic Analysis and Control Laboratory, Massachusetts Institute of Technology, Cambridge, Mass., 1957.
9. COMPUTATIONAL DETERMINATION OF THE NATURE OF SOLUTIONS OF NONLINEAR SYSTEMS WITH STOCHASTIC INPUTS, R. Bellman, P. Brock, M. Mizuki. *IEEE Special Publication no. T-1*, "Proceedings of the Computers in Control Systems Conference," May 1958, pp. 109–10.
10. ON AN APPLICATION OF DYNAMIC PROGRAMMING TO THE SYNTHESIS OF LOGICAL SYSTEMS, R. Bellman, J. Holland, R. Kalaba. *Journal of the Association for Computing Machinery*, New York, N. Y., vol. 6, 1959, pp. 486–93.
11. ON A ROUTING PROBLEM, R. Bellman. *Quarterly of Applied Mathematics*, vol. 16, 1958, pp. 87–90.

Discussion

P. K. C. Wang (International Business Machines Corporation, San Jose, Calif.): The author has presented an interesting formulation of the stochastic-time optimal-control problem. A check on the relative location of the stochastic optimal switching curve for the given example (Fig. 3) and that obtained by the following simple reasoning leads to unexpected disagreement. It is hoped that the author will explain this point.

Since j_n can assume only two distinct values, the over-all process trajectory is a composite of four types of trajectories (i.e., those corresponding to $u=+1, j_n=a$; $u=-1, j_n=-a$; $u=-1, j_n=a$; and $u=+1, j_n=-a$). Let the initial state of the process be $(x=0.2, y=0)$, then the subsequent trajectory for a fixed polarity of forcing u (say $u=+1$) and $j_n=\pm a$ must be inside a region bounded by the trajectories corresponding to $u=+1, j_n=a$, and $u=+1, j_n=-a$ (shaded region in Fig. 4). Similarly, the upper and lower bounds of the trajectory

variation can be constructed for an arbitrary, deterministic initial state with fixed polarity of forcing. Following the above reasoning leads to the conclusion that the stochastic optimal switching curve should lie in a region bounded by the deterministic switching curves corresponding to $j_n=a$ and $j_n=-a$. These curves also correspond to the limiting cases where $p=0$ and $p=1.0$. However, the author's switching curve lies outside the expected region. As a result, the decelerating trajectory will always follow the switching curve to the null state with rapid "chattering" of the forcing u . On the other hand, if a deterministic switching curve for $j_n=0.1$ is used, the decelerating trajectory will also follow the deterministic switching curve in the same manner but with less expected total response time. Therefore, it is suspected that the author's switching curve is in error.

As a minor remark, it is felt that the term "gain disturbance" would be more appropriate for the given example instead of "inertial load disturbance," since the dynamic effect of inertia variation is not taken into account.

To complement the paper, I would like to discuss the stochastic-time optimal-control problem briefly in general terms from a practical standpoint. It has been pointed out by the author that considering only the case where the desired process state is deterministic, there are roughly two ways by which random variables enter into control systems: external disturbance and internal-process parameter variations. The external disturbances can be classified as follows:

1. Disturbances entering at the input of the control system: In many practical situations, the differences in the intrinsic nature of signal and noise permit estimation of signal by appropriate filtering. If the residue noise due to imperfect filtering is small, then the time optimal controller designed for the deterministic part of the input is generally satisfactory.

2. Disturbances acting on the dynamic process: The effect of this type of disturbance may be reduced by introducing appropriate minor loops in the process itself. The controller is designed using the math-

ematical model of the modified process.

When the process parameters vary randomly with time, the time optimal-control problem becomes considerably more complex. However, in many practical situations, the parameters vary about some fixed mean values. For the linear process described by equation 1, the parameter matrices have the forms:

$$A = \bar{A} + \alpha(t)$$

with

$$|\alpha_{ij}| \leq \epsilon_{ij}$$

and

$$B = \bar{B} + \beta(t)$$

with

$$|\beta_{ij}| \leq \delta_{ij}$$

where \bar{A} and \bar{B} are the mean-value matrices, $\alpha(t)$ and $\beta(t)$ are random matrices whose elements have bounded variations.

If ϵ_{ij} and δ_{ij} are small, then the time optimal controller designed for a process characterized by \bar{A} and \bar{B} is applicable. The effect of $\alpha(t)$ and $\beta(t)$ on the over-all system response may be estimated by perturbation techniques. On the other hand, if the random components have significant effect on the process dynamics, then the process itself is basically nonstationary. An adaptive time-optimal controller would be required. Here, the practical problem of process identification must be solved.

The dynamic programming approach to the general optimum control problem involving stochastic processes was formulated by Bellman in 1958.¹ Recently, Krasovskii² presented an interesting treatment of the stochastic-time optimal-control problem by introducing a "generalized Liapunov function." However, there remains a large gap between the theoretical results and practical applications.

REFERENCES

1. DYNAMIC PROGRAMMING AND STOCHASTIC CONTROL PROCESSES, R. Bellman. *Information and Control*, New York, N. Y., vol. 1, no. 3, 1958, pp. 228–39.
2. ON OPTIMUM CONTROL IN THE PRESENCE OF

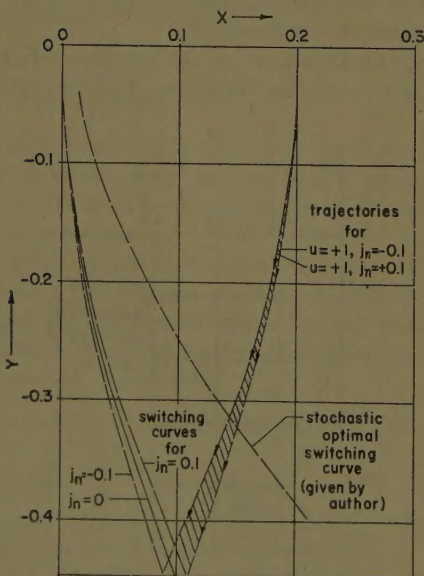


Fig. 4

Ralph J. Kochenburger (University of Connecticut, Storrs, Conn.): This paper describes, in very general terms, an application of dynamic programming techniques to the response-time optimization of bang-bang systems subjected to stochastic disturbances and variations of parameters. It is suspected, but difficult to prove, that such bang-bang systems do represent the optimum scheme of control under such circumstances. The problem being treated is an admittedly difficult one even when dealing with a deterministic system described by differential equations of higher order. It becomes discouragingly complicated when the stochastic variation of parameters must be taken into account as well. Considering this, the author has undertaken an exceedingly difficult task and has done an excellent job of formulating the general optimizing procedures that might be followed.

I have no reason to question the results as such, but would like to introduce the engineering viewpoint by raising the following questions: (1) Is this a contrived problem introduced for the purpose of providing an exercise in analysis, or is it likely to occur in actual practice? One reason for raising this question is the author's example of a randomly varying inertia. (2) What promise is there that the tremendous intellectual labor that has gone into the study of optimum switching criteria involving higher orders of phase space will bear fruit from an engineering standpoint. I am aware of, and have had successful experience with, such criteria applied to systems describable in the phase plane. However, my experience with these criteria applied to higher order systems has been successful when applied to analog simulations of systems, but not when applied to the actual "hardware." I wonder whether the analytic sophistication of the phase-space technique is justified in consideration of various assumptions and approximations that must be made in order to adapt most practical systems to this method of analysis.

One other point I would like to raise in regard to phase-space analysis in general is the fact that optimum switching criteria prescribe what are essentially nonlinear phase-lead corrective networks of the type that introduce new s-plane zeros but no new poles. Such networks are notorious for their accentuation of higher frequency noise and ripple; with bang-bang systems they can be especially detrimental by causing chatter of the relay elements or their electronic equivalents. On the other hand, the introduction of additional poles would increase the order of the phase space and further complicate the analysis.

The above comment relates to switching criteria in general and not to the specific subject treated in the paper. As far as that paper is concerned, I must agree with the author's statement that present-day computers are not adequate for performing the computations called for by his approach when the order of the differential equation involved exceeds 3 or 4. Unfortunately, for most practical problems, it does exceed that order. Even when computers become

adequate for such tasks, the question will arise as to how often the expense of such computations will be justified.

Here, I would like to offer a possible answer to my own question. It is obvious that the dynamic programming computations described in the paper are far too complicated to be performed on a real-time basis and so cannot be used directly in the self-optimization of control systems. They could, however, be performed in advance of actual system operation and used to prepare a program, probably approximate, from which the system could select the switching criterion most appropriate to the immediate situation. From this standpoint, techniques such as those described here might, if applied to a sufficiently large ensemble of systems and situations, result in an improvement of performance that would "pay off" from an economic standpoint.

Many papers in this field have confined themselves to the high plane of relatively abstract mathematics and have not favored the engineering reader with examples of actual results that might be obtained in practice. The author should be congratulated for not following this policy. The example he furnishes consists of a second-order system which is necessarily oversimplified in order to make its analysis practical for presentation in a paper of reasonable size. It does, however, provide some insight into the question of how stochastic parameter variations might affect optimum switching criteria in general. His Fig. 3 is especially enlightening in this respect but more detail, such as the effect of other a 's and p 's, would have been helpful. Also of interest would have been a typical appearance of the Δx , Δy computation mesh that resulted during this dynamic programming computation procedure. How fine did such a mesh have to be in order to represent a reasonable approximation of the actual system? Answers to such questions

would be of value to many engineers interested in applying the procedure proposed by Mr. Aoki.

Masanao Aoki: I would like to express my appreciation to the discussers of my paper.

First, concerning Dr. Wang's comment on the location of the optimal switching curve: perhaps what was not made clear in the paper is the fact that in stochastic-time optimal systems it is more meaningful to use not a single point, say the origin of the phase space, but some finite neighborhood, say the ϵ -neighborhood of the origin, as the set of desired states, D ; for example, in order to avoid the expected time becoming infinite. The same holds true for the probability criterion. Fig. 5 shows the case where D is taken to be the ϵ -neighborhood of the origin defined by

$$D = \{(x, y) : \max(|x|, |y|) \leq \epsilon\}$$

With D consisting of more than a single point, the optimal switching curve lying in the fourth quadrant for the deterministic case, $j_n = 0$, will move as shown in Fig. 5 in the positive x direction. For example, the initial point is taken to be at $(0.2, 0)$. Then the switching curve passing through the origin will require the extra time to travel along ABC in Fig. 5.

In the stochastic situation it is true that the point initially at $(0.2, 0)$ will be found somewhere in the shaded region of Fig. 5 before the switching occurs.

However, in the absence of a distribution function for the time to reach D , it is not at all clear intuitively how the expected times to reach D behave as a function of the initial point and the size and the shape of the ϵ -neighborhood. Of course, one cannot exclude the possibility that the effects of the finite boundaries which must be introduced in computational solution as dis-

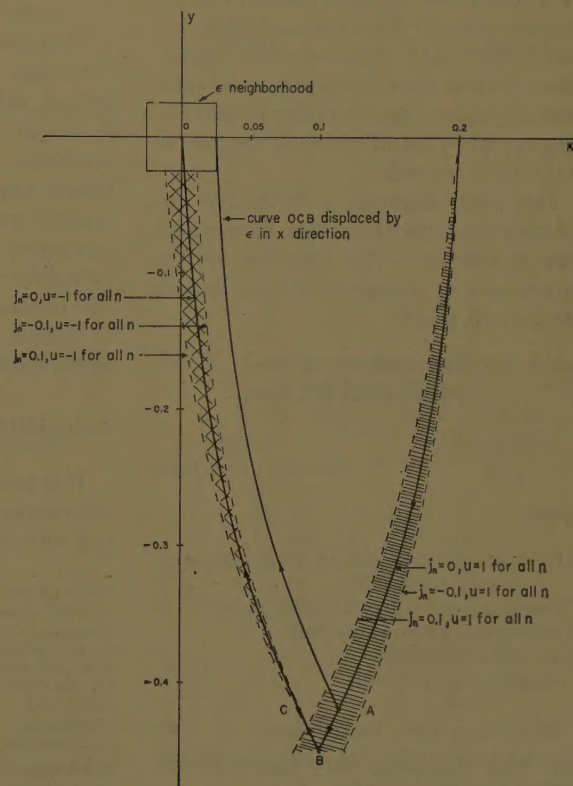


Fig. 5. Case for D taken as the ϵ -neighborhood of the origin

cussed in the section on the "expanding grid" are affecting the computed optimal switching curve. Similarly, the effect of the computational errors due to the mesh size and the degree of interpolating polynomial must also be considered. In this case, these effects were tested.

As in many problems involving random variables, one way of evaluating solutions would be to test these solutions by simulation. More specifically, Monte Carlo techniques may be used to perform the simulation numerically to compare the computed switching curve with the deterministic switching curve for $f_n \equiv 0$, say.

With regard to Professor Kochenburger's comments, when a control vector u enters into the dynamic equation of the system in a linear manner, then it can be shown that u will take on the boundary value even in stochastic situations with suitable assumptions.¹

Heuristically speaking, if the dynamic equation of a 2-dimensional system is given by

$$\dot{y} = f_1(x, y, \alpha) + a(\alpha)u$$

$$\dot{y} = f_2(x, y, \alpha) + b(\alpha)u$$

where α is a random parameter and u is a scalar control variable, then defining $g(x, y)$ as in the paper, $g(x, y)$ can be shown to satisfy the partial differential equation

$$0 = 1 + \frac{\partial g}{\partial x} E(f_1(x, y, \alpha)) + \frac{\partial g}{\partial y} E(f_2(x, y, \alpha)) + \min_{u \in \Omega} \left[\left(\frac{\partial g}{\partial x} E(a) + \frac{\partial g}{\partial y} E(b) \right) u \right]$$

Therefore, it is seen that

$$u = -A \cdot \text{sign} \left\{ \frac{\partial g}{\partial x} E(a) + \frac{\partial g}{\partial y} E(b) \right\}$$

if admissible control variables are such that

$$\Omega = \{u : -A \leq u \leq A\}$$

I manufactured the example in the paper to illustrate the procedure discussed where a system parameter shows random variations.

As already discussed elsewhere, one of the major uses of the functional equation

approach to a problem lies in the fact that the solution to the functional equation, when obtained, can serve as a standard against which various approximations and assumptions can be tested.² For example, one of the most promising approaches to problems of high dimensions may be said to lie in exploiting "good" suboptimal policies and in policy improvement. In this connection it is significant that dynamic programming, unlike ordinary numerical technique, may give structural information on optimal policy.

Finally, a great deal more needs to be done in the area of numerical analysis in the solution of the functional equations.

REFERENCES

1. SOME PROPERTIES OF STOCHASTIC TIME OPTIMAL CONTROL SYSTEMS, M. Aoki. Report no. 60-100, Department of Engineering, University of California, Los Angeles, Calif., Nov. 1960.
2. Discussion of DYNAMIC PROGRAMMING APPROACH TO A FINAL-VALUE CONTROL SYSTEM WITH A RANDOM VARIABLE HAVING AN UNKNOWN DISTRIBUTION FUNCTION, M. Aoki. Transactions Institute of Radio Engineers, New York, N. Y. vol. AC-5, no. 4, Sept. 1960, pp. 270-83.

A-C Contactors Supplied by Long Control Lines

R. P. ALLEY
MEMBER AIEE

WHEN a-c operated contactors are controlled by push buttons located at some distance from the contactor, the wire-to-wire and wire-to-ground capacitance of these control leads may be sufficient to prevent the contactor from dropping out when the off button at the remote station is depressed.

This paper discusses a method of calculating the capacitance wire to wire and wire to conduit. The equation for the capacitance of a single wire lying against the conduit wall is

$$C_1 = \frac{(17.52 \times 10^{-12}) K_1 K_2}{\cosh^{-1} \left(\frac{R_1^2 + R_2^2 - (R_1 - r_t)^2}{2 R_1 R_2} \right)} \text{ farads/ft (per foot)}$$

where

- K_1 = dielectric constant of wire insulation (usually about 3)
- K_2 = experimental factor (usually about 0.5)
- R_1 = internal radius of conduit
- R_2 = conductor radius
- r_t = total conductor radius

Similarly, the capacitance of two parallel wires lying so that the insulations of the two touch is

$$C_2 = \frac{(8.467 \times 10^{-12}) K_1 K_2}{\cosh^{-1} \left(\frac{(R_1 - r_t)}{2 R_2} \right)} \text{ farads/ft}$$

Because this is a linear conservative system, the two results can be combined to obtain answers for more complicated problems. International Business Machines Corporation 650 computer programs have been written to calculate line constants, maximum safe line length desirable with various contactors, and the necessary value of shunt resistance to detune a contactor coil to secure reliable drop-out.

Calculation of Line Capacitance

This paper is concerned primarily with the calculation of the capacitance of control wires in conduits, and as such will not

Paper 60-649, recommended by the AIEE Industrial Control Committee and approved by the AIEE Technical Operations Department for presentation at the AIEE Great Lakes District Meeting, Milwaukee, Wis., April 27-29, 1960, and re-presented for discussion only at the Winter General Meeting, New York, N. Y., January 29-February 3, 1961. Manuscript submitted February 23, 1960; made available for printing December 13, 1960.

R. P. ALLEY is with the General Electric Company, Bloomington, Ill.

directly cover the calculation of the characteristics of telephone-type open-wire control lines. Open-wire lines can be calculated from equation 2 or from the "Electrical Engineers' Handbook."¹

$$C_2 = \frac{3.677 \times 10^{-3}}{\log_{10} \frac{2D}{d}} \text{ microfarads/1,000 ft}$$

where

D = wire-to-wire distance
 d = conductor diameter

ASSUMPTIONS

Unfortunately, while a good determination of the capacitance of wires in a conduit is theoretically possible, a number of uncertainties arise to render such an exact calculation rather impractical. The best way to examine this physical problem is to list the assumptions made in the capacitance formula developments in this paper:

1. Linearity: The capacitance system is assumed to be linear so the problem may be solved in a piecemeal manner and the results superimposed. In general, this is the case.
2. Grounding: In all cases the conduit is assumed to be grounded. This should be universally true.
3. Position: The wires are assumed to lie on the inside wall of the conduit, and yet be lying next to each other. Although such an arrangement is clearly impossible if three wires are in the conduit, it was adopted to calculate the maximum possible capacitance for a given line. Also, this means that the wire-to-wire capacitance may be expected to vary more widely than that from wire to

Table I. Typical Measurements Summary

Description	Measured, Microfarads	Calculated, Microfarads	K2, Measured/ Calculated
51 feet 1-inch conduit, three no. 12 wires:			
Wire to wire	0.00067	0.00108	0.62
Wire to ground	0.00161	0.00307	0.52
582 feet 1-inch conduit, one no. 6 wire:			
Wire to ground	0.0400	0.0700	0.57
20 feet 1/2-inch conduit, three no. 14 wires:			
Wire to wire	0.000224	0.000561	0.40
Wire to ground	0.000557	0.001076	0.418
20 feet 1/2-inch conduit, no. 12 wire:			
Wire to wire	0.000142	0.000591	0.24
Wire to ground	0.000612	0.001156	0.53

conduit. A water-filled conduit would clearly change the apparent size of the conduit.

4. Insulation: Because the maximum electric field intensity always occurs in the wire insulation, the dielectric constant of this insulation was used as that for the insulation filling the conduit. This approximation is not too serious a factor in that this dielectric constant occurs only to the first power, and an experimental constant is used to adjust for this and other inaccuracies. Again, a water-filled conduit could give widely different results.

CAPACITANCE FORMULAS

With the foregoing limitations, two characteristic capacitances for wires in a conduit may be calculated. For a single wire lying against a conduit wall:

$$C_1 = \frac{17.52 \times 10^{-12} K_1 K_2}{\cosh^{-1} \left[\frac{R_1^2 + R_2^2 - (R_1 - r_i)^2}{2 R_1 R_2} \right]} \text{ farads/ft} \quad (1)$$

where

r_i = total conductor radius (with insulation)
 C_1 = capacitance wire to conduit

Similarly, the capacitance of two parallel wires lying so that the insulations touch is

$$C_2 = \frac{(8.467 \times 10^{-12}) K_1 K_2}{\cosh^{-1} \left(\frac{R_1 - r_i}{2 R_2} \right)} \text{ farads/ft} \quad (2)$$

By using the above equations, the capacitances of lines may be measured and calculated and the results compared. Actually, this is the method of obtaining the factor K_2 .

Considering Table I, a factor of 0.5 for K_2 appears reasonable in most cases. It may also be observed that the K_2 factor for the wire-to-wire capacitance varies over a wider range than that for the wire to ground as was explained in the assumptions.

Line Capacitance in Control Circuits

POSSIBLE CIRCUITS

If the start-stop push buttons are remotely located from the contactor, there are six possible wiring combinations for the components, especially if the location of the grounded line is arbitrarily assumed. These six cases are shown in Figs. 1-6, and if the equivalent circuits are studied, cases II and V are found to be identical. The capacitances defined somewhat arbitrarily earlier are seen to correspond to the needed capacitors in these circuits, C_1 being the wire-to-conduit and C_2 the wire-to-wire capacitance.

MAXIMUM CONDUIT LENGTH

One use for this capacitance calculation is to determine the maximum length of line which may be used for a given contactor. If the circuit reduces to a simple series capacitor as in Fig. 1 (cases I, II, IV, V), the critical hold-in capacitance reactance is given by

$$X_c = X_L \pm \sqrt{X_L^2 - (X_L^2 + R^2) \left[1 - \left(\frac{E}{E_z} \right)^2 \right]} \quad (3)$$

where

X_c = maximum magnitude capacitive reactance required

X_L = inductive reactance magnitude of contactor coil

R = resistance of contactor coil

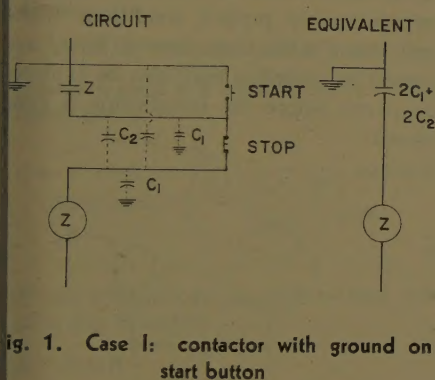


Fig. 1. Case I: contactor with ground on start button

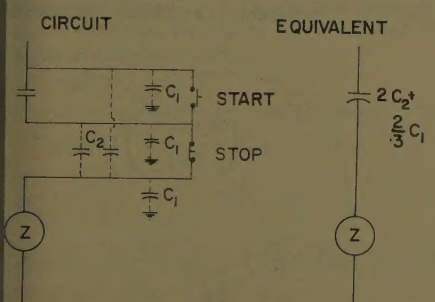


Fig. 2. Case II: contactor with start button on ungrounded supply

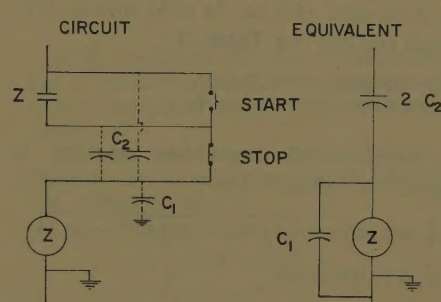


Fig. 3. Case III: contactor with coil grounded, start button to supply

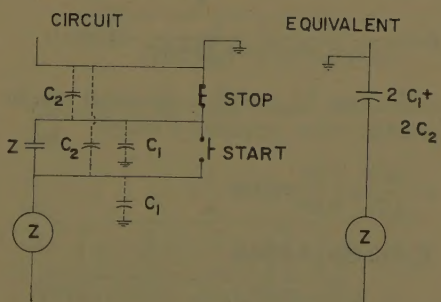


Fig. 4. Case IV: contactor with ground at stop button

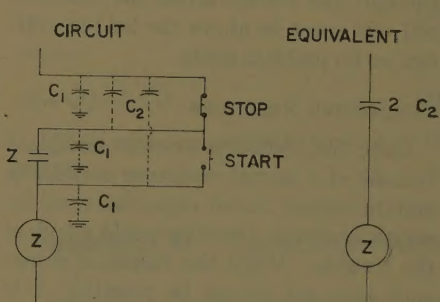


Fig. 5. Case V: contactor with stop button on ungrounded supply

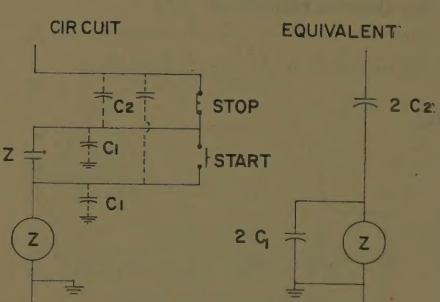


Fig. 6. Case VI: contactor with coil grounded, stop button to supply

Table II. Calculated Capacitances for Conduits of 1/2- to 1-Inch Nominal Diameter

Cable	Capacitance, Farads per Ft	
	C1	C2
No. 14 solid....	0.19×10^{-10}	0.9×10^{-10}
No. 12 solid....	0.22	0.10
No. 10 solid....	0.36	0.16

E =line voltage
 E_z =minimum alternating voltage to hold the contactor closed

If C_t is the total capacitance of the line per foot for the particular case, the maximum length (D) of the control conduit is given by

$$D = \frac{1}{w C_t X_c}$$

where
 $w = 2\pi f$
 f =line frequency

For the case where some of the line capacitance shunts the contactor coil, the calculation becomes slightly more cumbersome.

If a is the ratio shunting capacitance to series capacitance for cases III and IV (Figs. 3 and 4),

$$X_c = X_L(a+1) \pm$$

$$\sqrt{(R^2 + X_L^2) \left(\frac{E}{E_z} \right)^2 - R^2(a+1)^2} \quad (4)$$

Obviously, if the ratio of the series and shunt capacitances is correct (i.e., is large enough), the voltage across the contactor coil will never be above the hold-in voltage, so no problem exists.

CORRECTIVE RESISTORS

Since the contactor remains energized because of a partial resonance between it and the control circuit capacitance, an increase in circuit damping would alleviate the trouble. While the values of resistance may not always be practical, it is often worth the trouble to calculate their size. For the simple series case of Figs. 1, 2, 4, and 5, the quadratic equation for the desired resistor is

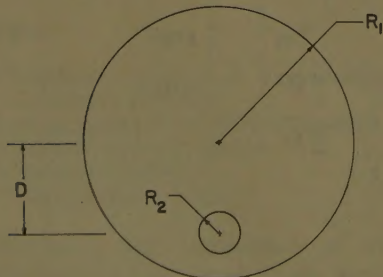


Fig. 7. Eccentric cylindrical conductors then

$$R_2 \left\{ Z^2 \left[1 - \left(\frac{E}{E_z} \right)^2 \right] - 2X_L X_c + X_c^2 \right\} + R_2 \{ 2R_1 X_c^2 \} + X_c^2 Z^2 = 0 \quad (5)$$

where

Z =total impedance magnitude of contactor coil

X_c =series impedance magnitude of the circuit

R_1 =resistance of the contactor coil

R_2 =desired shunting (or detuning) resistor

The power dissipated continuously by this resistor is also

$$P = E^2 / R_2 \text{ watts}$$

For the more complex cases with both series and shunt capacitances illustrated in Figs. 3 and 4, the quadratic equation in R_2 becomes more complex.

$$R_2 \left\{ Z^2 \left[(1+a)^2 - \left(\frac{E}{E_z} \right)^2 \right] + X_c^2 - 2X_L X_c(1+a) \right\} + R_2 \{ 2X_c^2 R_1 \} + X_c^2 Z^2 = 0 \quad (6)$$

where the meaning of all the terms remains the same as previously.

EXAMPLE

Consider a 440-volt size 2 contactor with the following characteristics:

$$\begin{aligned} Z &= 3,140 \text{ ohms} \\ X_L &= 3,070 \text{ ohms} \\ R &= 659 \text{ ohms} \end{aligned}$$

Drop-out voltage=30% of rated 60-cycle voltage

It is used with no. 14 solid wire in 1/2-inch conduit (for Table II):

$$\begin{aligned} C1 &= 0.19 \times 10^{-10} \text{ farads/ft} \\ C2 &= 0.09 \times 10^{-10} \text{ farads/ft} \end{aligned}$$

The critical capacitive reaction is given by equation 3 or

$$\begin{aligned} X_c &= 3,070 \pm \sqrt{(3,070)^2 - (3,140)^2(-10.11)} \\ X_c &= 17,994 \text{ ohms} \end{aligned}$$

For case I, Fig. 1, the effective series capacitance is $C1+2C2$ or 0.37×10^{-10} farads/ft.

$$D = \frac{1}{(377)(0.37)(10^{-10})(17,944)} = 3,980 \text{ ft}$$

For case VI, which is the usual one in practice, from equation 4 where

$$a = \frac{2C2}{2C1} = \frac{0.09}{0.19} = 0.474$$

$$\begin{aligned} X_c &= (3,070)(1.474) \pm \\ &\sqrt{(3,140)^2(11.11) - (659)^2(1.474)^2} \\ &= 14,946 \text{ ohms} \end{aligned}$$

$$D = \frac{1}{(377)(0.18)(14,946)(10^{-10})} = 9,900 \text{ ft}$$

If it is now desired to operate this contactor on 12,000 ft of conduit, a shunt resistor will be needed to allow this operation. For case I ($X_c \cong 6,000$ ohms), equation 5 gives

$$\begin{aligned} R_2^2 \{ (3,140)^2[-10.11] - 2(3,070)(6,000) + (A) \\ (6,000)^2 \} + R_2 \{ 2(654)(6,000)^2 + (B) \\ (6,000)^2(3,140)^2 = 0 \quad (C) \end{aligned}$$

Using the quadratic formula

$$R_2 = \frac{-B \pm \sqrt{B^2 - 4AC}}{2A} \cong 60 \text{ ohms}$$

This is not very practical in this case because of the high power dissipation.

For case VI, $x_c = 12,260$ ohms for this wiring. Using equation 6 and considering it to be

$$AR_2^2 + BR_2 + C = 0$$

each of the coefficients may be evaluated in turn:

$$A = (3,140)^2(1.474)^2(-11.11) + (12,260)^2 - 2(3,070)^2(12,260)(1.474) = 34 \times 10^{-12}$$

$$B = 2(12,260)^2(659) = 1,977 \times 10^9$$

$$C = (12,260)^2(3,140)^2 = 1,478 \times 10^{-12}$$

Thus $R_2 \cong 66$ ohms, which is again rather impractical. The conclusion would be that splitting this line into two sections would be the most feasible alternative. Thus calculations can be made which will approximately predict conditions which will occur with long control lines, and corrective remedies may also be explored on paper before the installation is completed.

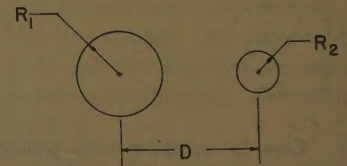


Fig. 8. Adjacent cylindrical conductors

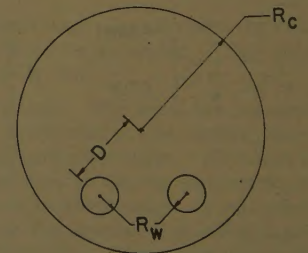


Fig. 9. Conduit cross section

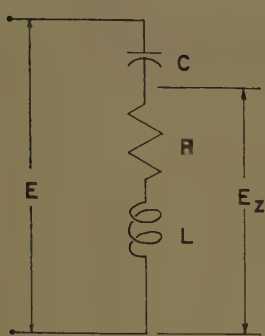


Fig. 10. Basic series circuit

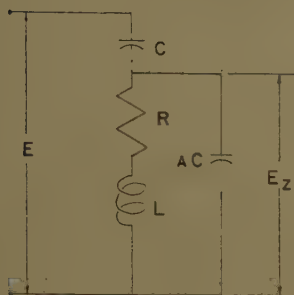


Fig. 11. Basic series and shunt circuit

Appendix I. Cable Capacitance Derivations

Assume that a cylindrical conductor lies eccentric in a conducting sheath, as shown in Fig. 7. The capacitance for this case is given by Smythe:²

$$C = \frac{2\pi\epsilon}{\cosh^{-1}\left(\frac{R_1^2 + R_2^2 - D^2}{2R_1R_2}\right)} \text{ farads/meter} \quad (7)$$

where

$$\epsilon = 8.85 \times 10^{-12} \text{ farads/meter (for air)}$$

However, since it is usual to convert this to farads per ft,

$$C = \frac{2\pi\epsilon}{3.281 \cosh^{-1}\left(\frac{R_1^2 + R_2^2 - D^2}{2R_1R_2}\right)} \text{ farads/ft} \quad (8)$$

If two cylinders are parallel to each other as in Fig. 8, and if

$$R_1 = R_2 = R$$

the capacitance may be derived from the same Smythe equation by reversing the signs in the denominator:

$$C = \frac{2\pi\epsilon}{\cosh^{-1}\left(\frac{D^2 - 2R^2}{2R^2}\right)} \text{ farads/meter} \quad (9)$$

or

$$C = \frac{2\pi\epsilon}{3.281 \cosh^{-1}\left(\frac{D^2}{2R^2} - 1\right)} \text{ farads/ft} \quad (10)$$

or this may be further reduced to

$$C = \frac{8.467 \times 10^{-12}}{\cosh^{-1}\left(\frac{D}{2R}\right)} \text{ farads/ft} \quad (11)$$

In an actual cable, both previous conditions are present, as shown in Fig. 9, but since the system may be assumed linear and conservative, superposition of the two capacitances should give a meaningful answer.

For wires pulled in conduits, the medium is not filled with a homogeneous dielectric constant, but rather the wires have insulating sheaths, with the majority of the conduit normally filled with air.

Appendix II. Calculations

Consider the basic circuit as shown in Fig. 10. The following voltage relationships hold:

$$\frac{E_z}{E} = \frac{R + jX_L}{R + j(X_L - X_C)} \quad (12)$$

Then

$$\left| \frac{E_z}{E} \right| = \frac{\sqrt{R^2 + X_L^2}}{\sqrt{R^2 + (X_L - X_C)^2}} \quad (13)$$

Considering E_z and E to be magnitudes only, the above may be rewritten:

$$R^2 + (X_L - X_C)^2 - \left(\frac{E}{E_z}\right)^2 (R^2 + X_L^2) = 0$$

or

$$X_C^2 - 2X_LX_C + (X_L^2 + R^2) \left[1 - \left(\frac{E}{E_z}\right)^2 \right] = 0$$

or solving for X_C

$$X_C = X_L \pm \sqrt{X_L^2 - \underbrace{(X_L^2 + R^2)}_{Z^2} \left[1 - \left(\frac{E}{E_z}\right)^2 \right]} \quad (14)$$

If E_z represents the critical hold-in voltage of the contactor, X_C then represents the critical capacitive reactance to achieve this condition.

For the case where the contactor is shunted by a capacitor as in Fig. 11, the voltage division is

$$\frac{E_z}{E} = \frac{-j\frac{1}{a}X_C(R + jX_L)}{R + j\left(X_L - \frac{1}{a}X_C\right)} \quad (15)$$

$$= \frac{-j\frac{1}{a}X_C(R + jX_L)}{-jX_C + \frac{R + j\left(X_L - \frac{1}{a}X_C\right)}{R + j\left(X_L - \frac{1}{a}X_C\right)}}$$

Clearing of fractions results in the following:

$$\frac{E_z}{E} = \frac{+\frac{1}{a}(R + jX_L)}{\left[R + j\left(X_L - \frac{1}{a}X_C\right) \right] + \frac{1}{a}(R + jX_L)}$$

Taking several steps, let E_z and E be simply numbers:

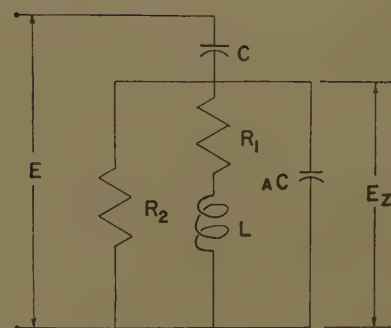


Fig. 12. Series and shunt circuit with resistor

$$\left(\frac{E_z}{E}\right)^2 = \frac{(R^2 + X_L^2)}{(1+a)(R) + j[X_L(1+a) - X_C]}$$

$$\left(\frac{E_z}{E}\right)^2 = \frac{R^2 + X_L^2}{(a+1)^2 R^2 + [X_L(a+1) - X_C]^2}$$

$$\left(\frac{E_z}{E}\right)^2 = \frac{R^2 + X_L^2}{2X_LX_C(a+1) + X_C^2}$$

$$X_C^2 - 2X_CX_L(a+1) + (R^2 + X_L^2)(a+1)^2 - (R^2 + X_L^2)\left(\frac{E}{E_z}\right)^2 = 0$$

$$X_C^2 - 2X_CX_L(a+1) + (R^2 + X_L^2) \times \left[(a+1)^2 - \left(\frac{E}{E_z}\right)^2 \right] = 0$$

So

$$X_C = X_L(a+1) \pm \sqrt{X_L^2(a+1)^2 - (R^2 + X_L^2) \times \left[(a+1)^2 - \left(\frac{E}{E_z}\right)^2 \right]}$$

$$X_C = X_L(a+1) \pm \sqrt{Z^2 \left(\frac{E^2}{E_z^2}\right) - R^2(a+1)^2} \quad (16)$$

where

$$Z = \sqrt{R^2 + X_L^2} \quad (17)$$

All six wiring cases may be covered by the above.

Appendix III. Corrective Action

A corrective action sometimes used is to shunt the contactor coil by a resistor as shown in Fig. 12.

$$Z_2 = \frac{jR_2 \frac{1}{a} X_C (R_1 + jX_L)}{R_2(R_1 + jX_L) - j\frac{1}{a} X_C (R_1 + R_2 + jX_L)} \quad (18)$$

$$\frac{E_z}{E} = \frac{Z_2}{Z_2 - jX_C}$$

$$\frac{E_z}{E} = \frac{R_2(X_L - jR_1)}{R_2X_L + aR_2X_L - R_1X_C - R_2X_C - j(R_1R_2 + aR_1R_2 + X_CX_L)}$$

Using magnitudes only, this reduces to

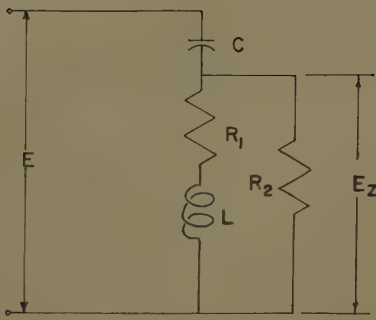


Fig. 13. Series circuit with resistor

$$\left(\frac{E_z}{E}\right)^2 = \frac{R_2^2 Z^2}{R_2^2 R_1^2 (1+a)^2 + X_L^2 (1+a)^2 + X_c^2 - 2X_L X_c (1+a) + R_2^2 R_1 X_c^2 + X_c^2 Z^2} \quad (19)$$

Solving for a quadratic in R_2 :

$$R_2 = Z^2 (1+a)^2 - \left(\frac{E}{E_z}\right)^2 + X_c^2 - 2X_L X_c (1+a) + R_2^2 X_c^2 R_L + X_c^2 Z^2 = 0 \quad (20)$$

This may be solved for R_2 .

For the simpler case as shown in Fig. 13,

$$Z_2 = \frac{(R_1 + jX_L)R_2}{R_1 + R_2 + jX_L} \quad (21)$$

$$\frac{E_z}{E} = \frac{(R_1 + jX_L)R_2}{(R_1 + jX_L)R_2 - jX_c(R_1 + R_2 + jX_L)}$$

$$\frac{E_z}{E} = \frac{(R_1 + jX_L)R_2}{(R_1 + jX_L)R_2 - jX_c(R_1 + R_2 + jX_L)}$$

Expanding

$$\frac{E_z}{E} = \frac{R_1 R_2 + jR_2 X_L}{R_1 R_2 + X_c X_L + j(R_2 X_L - R_1 X_c - R_2 X_c)}$$

$$\left|\frac{E_z}{E}\right|^2 = \frac{R_1^2 R_2^2 + R_2^2 X_L^2}{(R_1 R_2 + X_c X_L)^2 + [R_2 X_L - R_1 X_c - R_2 X_c]^2}$$

If magnitudes only are of concern,

$$\left(\frac{E_z}{E}\right)^2 = \frac{R_2^2 (Z^2)}{R_1^2 R_2^2 + 2R_1 R_2 X_c X_L + X_c^2 X_L^2 + R_2^2 X_L^2 - R_1 R_2 X_L X_c - R_2^2 X_L X_c - R_1 R_2 X_L X_c + R_1^2 X_c^2 + R_1 R_2 X_c^2 - R_2^2 X_L X_c + R_1 R_2 X_c^2 + R_2^2 X_c^2}$$

$$\left(\frac{E_z}{E}\right)^2 = \frac{R_2^2 Z^2}{R_2^2 [R_1^2 + X_L^2 - 2X_L X_c + X_c^2] + Z^2 R_2 [2R_1 X_c^2 + X_c^2 X_L^2 + R_1^2 X_c^2] + X_c^2 X_L^2 + R_1^2 X_c^2}$$

$$R_2^2 \left\{ Z^2 \left[1 - \left(\frac{E}{E_z}\right)^2 \right] - 2X_L X_c + X_c^2 \right\} + R_2 [2R_1 X_c^2 + X_c^2 X_L^2 + R_1^2 X_c^2] + X_c^2 Z^2 = 0$$

$$R_2^2 \left\{ Z^2 \left[1 - \left(\frac{E}{E_z}\right)^2 \right] - 2X_L X_c + X_c^2 \right\} + R_2 [2R_1 X_c^2 + X_c^2 Z^2] = 0 \quad (22)$$

Thus one can solve for the necessary R_2 .

References

1. ELECTRICAL ENGINEERS' HANDBOOK. ELECTRIC POWER (book), Harold Pender, William A. Del Mar, editors. John Wiley & Sons, Inc., New York, N. Y., 1950, sect. 14-37, eq. 4.
2. STATIC AND DYNAMIC ELECTRICITY (book), W. R. Smythe. McGraw-Hill Book Company, Inc., New York, N. Y., 1950, p. 77.

A Digital Time-Domain Synthesis Technique for Feedback Control Systems

LYNN E. WEAVER
MEMBER AIEE

ANDREW P. SAGE
ASSOCIATE MEMBER AIEE

ROBERT L. MILLER, JR.
ASSOCIATE MEMBER AIEE

IN THE DESIGN of feedback control systems, the ultimate goal is the synthesis of a system to perform according to prescribed specifications. This paper develops a method of synthesis for feedback control systems which is partially based upon previous work in network theory and sampled-data systems. Synthesis is realized in the complex plane by obtaining the open-loop-system transfer function from the desired closed-loop input and output time functions. Specifications are introduced in terms of the system response to a deterministic input such as a step or ramp function. A plot

of the desired closed-loop transient response is made which is then sampled at equal time intervals.

From the sampled output time function and system error function the open-loop system function required to meet the system time-domain specifications is obtained. The prescribed open-loop transfer function and the fixed part of the system yield the necessary compensation required to meet the specifications.

In this paper, the developed synthesis technique is applied to several problems. The resulting systems are simulated on an analog computer and a comparison is made with the prescribed specifications showing the effectiveness of the synthesis technique presented. A discussion follows which points out the limitations of this technique.

Considering the block diagram of a unity feedback system as shown in Fig. 1, the well-known transfer function is

$$\frac{C(s)}{R(s)} = \frac{G(s)}{1 + G(s)} \quad (1)$$

Solving for $G(s)$ results in

$$G(s) = \frac{C(s)}{R(s) - C(s)} \quad (2)$$

The system input, $r(t)$, and output, $c(t)$, are sampled at equal time intervals T , thus,

$$c^*(t) = \sum_{n=0}^{\infty} c(nT) \delta(t - nT) \quad (3)$$

$$r^*(t) = \sum_{n=0}^{\infty} r(nT) \delta(t - nT) \quad (4)$$

$$C^*(s) = \sum_{n=0}^{\infty} c(nT) e^{-snT} \quad (5)$$

$$R^*(s) = \sum_{n=0}^{\infty} r(nT) e^{-snT} \quad (6)$$

In terms of the sampled input and output, the open-loop transfer function is approximately given by

$$G(s) = \frac{\sum_{n=0}^{\infty} c(nT) e^{-snT}}{\sum_{n=0}^{\infty} [r(nT) - c(nT)] e^{-snT}} \quad (7)$$

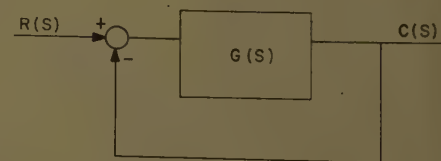


Fig. 1. Feedback control system

Paper 60-1019, recommended by the AIEE Feedback Control Systems Committee and approved by the AIEE Technical Operations Department for presentation at the AIEE Pacific General Meeting, San Diego, Calif., August 8-12, 1960, and represented for discussion only at the Winter General Meeting, New York, N. Y., January 29-February 3, 1961. Manuscript submitted May 31, 1960; made available for printing December 15, 1960.

LYNN E. WEAVER and ANDREW P. SAGE are with the University of Arizona, Tucson, Ariz.; ROBERT L. MILLER, JR., is a captain, U. S. Army Signal Corps.

Equation 7 is a ratio of two polynomials in the delay operator e^{-snT} . Division of these two polynomials results in another polynomial which is the discrete Laplace transform for the open-loop system function. The coefficients of the polynomial are the areas under the impulse response curve of the open-loop system between the sampling instants, if the sampling period T is sufficiently small.

The input function to be considered in this paper will be a unit step function. Other inputs, such as a ramp, can be handled in exactly the same fashion.

After division, the coefficient of the polynomial will be of the form

$$G(s) = g_0 + g_1 e^{-sT} + g_2 e^{-2sT} + \dots + g_n e^{-nsT} \quad (8)$$

The polynomial described by equation 8 may be of finite or infinite order. If there is to be zero steady-state error for the unit step input, the system must contain at least one open-loop integration. In this case, the final value of the impulse response of the open-loop system will not be zero but some finite or infinite value. If the open-loop system contains one integration, $G(s)$ may be represented as

$$G(s) = \frac{K_v}{s} \frac{\pi(1+T_1s)}{\prod_j (1+T_j s)} \quad (9)$$

where the coefficients T_1 and T_j may be complex. $G(s)$ must, of course, be realizable. By partial fractions equation 9 becomes

$$G(s) = \frac{K_v}{s} + \sum_j \frac{C_j}{1+T_j s} \quad (10)$$

The discrete Laplace transform of equation 10 is

$$\frac{G(s)}{T} \approx K_v \sum_{n=0}^{\infty} e^{-snT} + \sum_j \sum_{n=0}^{\infty} \frac{C_j}{T_j} e^{-\frac{nT}{T_j}} e^{-snT} \quad (11)$$

As n becomes large, $G(s)$ approaches

$$TK_v e^{-snT}$$

If there is more than one open-loop integration, the coefficients of the discrete impulse response approach infinity for large n . If the polynomial of equation 8 is of infinite order, it will be necessary to define a modified polynomial of finite order in order to apply the proposed synthesis technique. For convenience, it will be assumed here that there is a single open-loop integration. By defining

$$G(s) = \frac{K_v}{s} + G'(s) \quad (12)$$

it follows that

$$G'(s) = G(s) - \frac{K_v}{s} \quad (13)$$

$$G'(s) = G(s) - TK_v \sum_{n=0}^{\infty} e^{-snT} \quad (14)$$

since the discrete transform corresponding to s/K_v is

$$TK_v \sum_{n=0}^{\infty} e^{-nsT}$$

The constant TK_v is subtracted from each coefficient of the polynomial of equation 8 resulting in

$$G'(s) = \sum_{n=0}^{\alpha} A_n e^{-nsT} \quad (15)$$

Since $G'(s)$ as given by equation 15 is irrational, e^{-snT} is expanded in a Taylor's series about $s=0$ to give

$$G'(s) = \sum_{n=0}^{\alpha} A_n - s \sum_{n=0}^{\alpha} n T A_n + \frac{s^2}{2!} \sum_{n=0}^{\alpha} n^2 T^2 A_n + \dots \quad (16)$$

Equation 16 is a rational function in the complex variable s .

To put $G'(s)$ in transfer-function form the method of undetermined coefficients is used. It is convenient to define

$$d_m = \frac{(-1)^m}{m!} \sum_{n=0}^{\alpha} (nT)^m A_n \quad (17)$$

such that equation 16 becomes

$$G'(s) = \sum_{m=0}^{\infty} d_m s^m = d_0 + d_1 s + d_2 s^2 + \dots = \frac{a_0 + a_1 s + a_2 s^2 + \dots + a_n s^n}{b_0 + b_1 s + b_2 s^2 + \dots + b_m s^m} \quad (18)$$

Cross-multiplying and equating coefficients of s , in equation 18, results in the set of linear algebraic equations

$$\begin{aligned} d_0 b_0 &= a_0 \\ d_0 b_1 + d_1 b_0 &= a_1 \\ d_0 b_2 + d_1 b_1 + d_2 b_0 &= a_2 \\ &\vdots \\ d_0 b_n + d_1 b_{(n-1)} + \dots + d_n b_0 &= a_n \\ d_0 b_{(n+1)} + d_1 b_n + \dots + d_{(n+1)} b_0 &= 0 \end{aligned} \quad (19)$$

Here the assumption is made that $m > n$ when making an approximation of $G'(s)$. The denominator may be normalized by making b_0 equal to 1 without changing the nature of the approximation.

As an example, suppose an approximation is desired in the form of two poles and no zeros. Then

$$G'(s) = \frac{a_0}{1 + b_1 s + b_2 s^2} \quad (20)$$

which results in

$$\begin{aligned} d_0 &= a_0 \\ d_0 b_1 + d_1 &= 0 \\ d_0 b_2 + d_1 b_1 + d_2 &= 0 \end{aligned} \quad (21)$$

which may be solved for the three unknowns a_0 , b_1 , and b_2 . After $G'(s)$ has been realized as the ratio of two polynomials in s , $G(s)$ is obtained by addition of s/K_v to $G'(s)$.

In a large number of automatic control systems, it is necessary to place a restriction on the minimum pole zero excess in order that a physically realizable compensation network may be used. Thus, care must be exercised in selecting the form of the $G'(s)$ if a pole zero excess greater than one is to be obtained. For example, if it is desired that $G(s)$ be of the form

$$G(s) = \frac{K_v(1 + \alpha s)}{s(1 + b_1 s + b_2 s^2)} \quad (22)$$

then $G'(s)$ must be of the form

$$G'(s) = \frac{a_0 + a_1 s}{1 + b_1 s + b_2 s^2} \quad (23)$$

which gives the desired $G(s)$ only if,

$$K_v b_2 + a_1 = 0 \quad (24)$$

In some cases, the method of undetermined coefficients will either not satisfy equation 24 or will result in negative values for α , b_1 , or b_2 . In such cases, a modified $G''(s)$ may be defined by

$$G''(s) = G(s) - \frac{K_v \beta}{s(\beta + s)} \quad (25)$$

In terms of the discrete transform, equation 25 is equivalent to

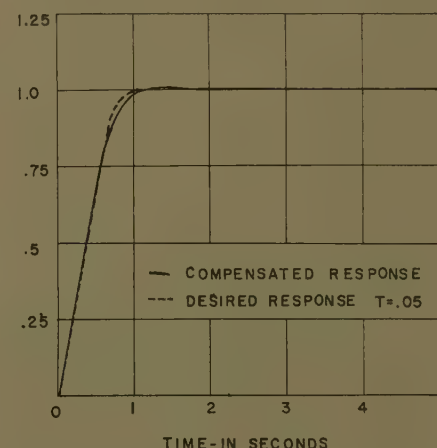


Fig. 2. Transient response for 0.05-second sampling period

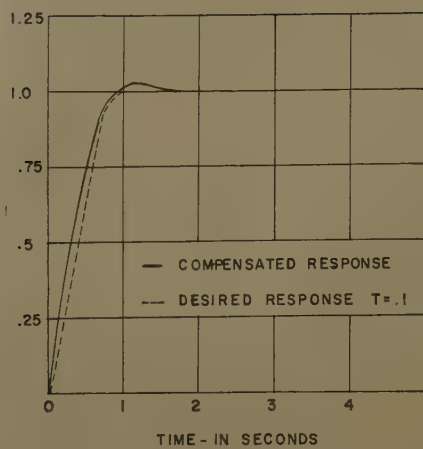


Fig. 3. Transient response for 0.1-second sampling period

$$G''(s) = G(s) - TK_v \sum_{n=0}^{\infty} (1 - e^{-\beta nT}) e^{-snT} \quad (26)$$

The term

$$TK_v (1 - e^{-\beta nT})$$

would then be subtracted from each term of equation 8. $G''(s)$ is then substituted $G'(s)$ in equations 15–21. After $G''(s)$ or has been realized as a ratio of two polynomials in s , $G(s)$ is obtained from equation 25.

Example

As an example of the synthesis technique, consider the desired step response curve shown in Fig. 2. Equations 26, 27, and 28 give the resulting $G'(s)$ for three different sampling rates.

$$G'(s) = -0.36 + 0.058s - 0.0055s^2 + 0.00049s^3 - 0.00009s^4 \quad (27)$$

$$T = 0.05 \text{ second, } K_v = 2.9663$$

$$G'(s) = -0.41 + 0.08s - 0.0085s^2 + 0.00067s^3 - 0.000076s^4 \quad (28)$$

$$T = 0.1 \text{ second, } K_v = 3.18725$$

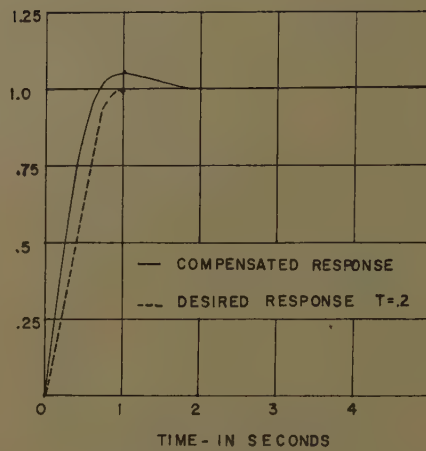


Fig. 4. Transient response for 0.2-second sampling period

$$G'(s) = -0.53 + 0.137s - 0.0185s^2 + 0.0016s^3 - 0.000069s^4 \quad (29)$$

$$T = 0.2 \text{ second, } K_v = 3.74528$$

The final form of $G'(s)$ or $G(s)$ may be designed to have any given pole zero excess. Using as an approximation $G'(s)$

$$G'(s) = \frac{K}{1 + bs} \quad (30)$$

the method of undetermined coefficients yields

$$a = d_0$$

$$b = -\frac{d_1}{d_0} \quad (31)$$

where the d 's are given by equations 26, 27, and 28 for three sampling intervals. The resulting open-loop transfer functions are

$$G(s) = \frac{2.963(1 + 0.0404s)}{s(1 + 0.161s)} = \frac{0.742(s + 24.8)}{s(s + 6.21)} \quad (32)$$

$$T = 0.05$$

$$G(s) = \frac{3.187(1 + 0.0675s)}{s(1 + 0.195s)} = \frac{1.09(s + 15)}{s(s + 5.13)} \quad (33)$$

$$T = 0.1$$

$$G(s) = \frac{3.74(1 + 0.123s)}{s(1 + 0.264s)} = \frac{1.74(s + 8.15)}{s(s + 3.79)} \quad (34)$$

$$T = 0.2$$

The step response of these three systems is shown in Figs. 2–4. The effect of changing the sampling interval is clearly shown.

If the constraint is imposed that $G(s)$ contain no zeros and two poles, then

$$G(s) = \frac{K_v}{s(1 + \alpha s)} = \frac{2.963}{s(1 + 0.121s)} \quad (35)$$

The transient response for the closed-loop system of equation 35 shows a 1% overshoot and a time to peak of 1.06 seconds, which is very close to the desired response.

Example II

As another example of the synthesis technique, consider the desired step response curve shown in Fig. 5. Sampling at 0.2-second intervals, the resulting $G'(s)$ and K_v are

$$G'(s) = -0.788 + 0.994s - 1.16s^2 + 1.40s^3 - 1.64s^4 + \dots \quad (36)$$

$$K_v = 0.875$$

Approximating $G'(s)$ by

$$\frac{a_0}{1 + b_1s}$$

the undetermined coefficients method yields

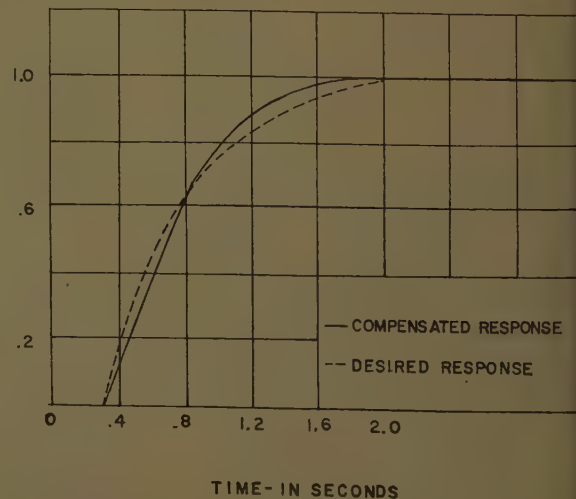
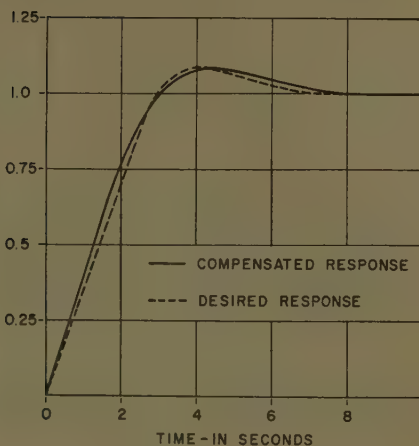
$$a_0 = d_0$$

$$0 = d_1 + d_0b_1 \quad (37)$$

and $G(s)$ is therefore obtained as shown in equation 38:

Fig. 5 (left). System response

Fig. 6 (right). Transient response for system with dead-time delay



$$s) = \frac{0.875(1+0.362s)}{s(1+1.26s)} \\ = \frac{0.252(s+2.76)}{s(s+0.794)} \quad (38)$$

comparison of the specified and actual closed-loop response is shown in Fig. 5.

Example III

Consider the desired step-response curve shown in Fig. 6. It is known that the open-loop function $G(s)$ must contain a time delay of 0.3 second. It is therefore convenient to define

$$G(s) = e^{-0.3s} G(s) = e^{-0.3s} \frac{C(s)}{R(s) - C(s)} \quad (39)$$

Sampling at 0.05-second intervals leads

$$K'(s) = -0.06210 + 0.0041s - 0.000003s^2 + \dots \quad (40)$$

$$K_e = 1.29$$

For an approximation in the form of two

poles and no zeros, the method of undetermined coefficients gives

$$K'(s) = \frac{-0.0621}{1 + 0.06602s + 0.00431s^2} \quad (41)$$

The open-loop transfer function is therefore

$$G(s) = \frac{1.29(1 + 0.0179s + 0.00431s^2)}{s(1 + 0.06602s + 0.00431s^2)} e^{-0.3s} \quad (42)$$

Fig. 6 compares the desired and actual response for this example.

Conclusions

The advantages and disadvantages of this technique may be enumerated as follows:

1. The approximation of the transfer function may be of any order or any pole zero excess.
2. It is possible to specify the location of one or more poles in the open-loop transfer function.

3. There is no assurance that the final open-loop transfer function will be minimum phase.

4. The method of synthesis is very amenable to machine calculation.

Much of the difficulty associated with the technique appears to be connected with the undetermined coefficient method of specifying $G'(s)$. This is a major shortcoming of the synthesis technique as presented here.

References

1. A GENERAL METHOD OF TIME DOMAIN NETWORK SYNTHESIS, F. Ba Hli. *Transactions, Professional Group on Circuit Theory, Institute of Radio Engineers*, New York, N. Y., vol. CT-1, Sept. 1954.
2. THEORY AND APPLICATIONS OF INFINITE SERIES (book), K. Knopp. Hafner Publishing Company, New York, N. Y., 1949, p. 348.
3. AUTOMATIC FEEDBACK CONTROL SYSTEM SYNTHESIS (book), J. G. Truxal. McGraw-Hill Book Company, Inc., New York, N. Y., 1955, chap. 5.
4. A STUDY OF DEAD TIME IN FEEDBACK CONTROL SYSTEMS, L. E. Weaver. *Report*, Argonne National Laboratory, Purdue Research Foundation, Lafayette, Ind., May 1, 1957.

A Linear Switching Condition for Third-Order Positive-Negative Feedback Control Systems

S. J. GARRETT
NONMEMBER AIEE

Synopsis: A third-order switching servomechanism is investigated that operates with positive feedback for the first part of the transient response period and is switched to negative feedback for the last part. The optimum switching condition is determined for third-order systems with both a step position input and a step velocity input. The analysis is extended to higher-order systems. Experimental results of an analog computer study are presented.

SEVERAL types of switching servomechanisms appear in the literature.¹⁻⁴ McDonald¹ and Hopkin² describe a switching servomechanism that applied full forward torque for the first part of the transient response period and full reverse torque for the latter part. When the system reached the rest position, no torque was applied. The switching instant was determined as a nonlinear function of the error signal and its first

derivative so that the system came to rest with no overshoot. The minimum number of switching instances necessary for minimum response time was determined. In 1954, Bogner and Kazda³ extended the idea to third- and higher-order systems.

The difficulty with this type of switching servo system is that any slight disturbances will cause full forward torque to be applied to the output. Hence, a dead zone near the rest position must be provided to keep the system from chattering excessively.

In 1958, Meiksin⁴ introduced a switching control system that operates as a positive feedback control system for part of the transient response period and as a negative feedback control system for the remaining part. The switching condition for minimum time response with no overshoot for a step input was determined for second- and third-order systems.

Again, the switching system had a faster time response for a position step input than did a corresponding linear negative feedback control system.

This p-n feedback system has the added advantage that small inputs or disturbances result in small torques that drive the error of the system to zero. Thus, the p-n feedback system does not produce severe chattering. The switching condition for second-order systems was given by a linear relationship between the error of the system and the first time derivative of the error. However, for a third-order system, the switching condition determined by Meiksin is difficult to obtain either by analysis or by a physically realizable system.

In this paper a third-order p-n feedback switching control system is investigated. The optimum switching condition is developed for a p-n feedback control system for both a step position input and a step velocity input. This switching con-

Paper 61-83, recommended by the AIEE Feedback Control Systems Committee and approved by the AIEE Technical Operations Department for presentation at the AIEE Winter General Meeting, New York, N. Y., January 29-February 3, 1961. Manuscript submitted March 18, 1960; made available for printing November 25, 1960.

S. J. GARRETT is with the Westinghouse Electric Corporation, East Pittsburgh, Pa.

This paper is a partial abstract of a thesis submitted by the author to the Graduate School of the University of Pittsburgh in partial fulfillment of the requirements for an M.S. degree in Electrical Engineering. The valuable suggestions and constructive criticisms made by Dr. Z. H. Meiksin are gratefully acknowledged.

dition is a linear function of the position error and the first and second time derivatives of the position error. In the analysis, the system is assumed to be piecewise linear. Phase-space analysis is used to determine the switching condition. Results of an analog computer study are presented in the following.

Analysis

The transient response period is divided into two intervals. During the first interval, which begins at $t=0$, the system is in the positive feedback mode. The second interval begins as the system is switched into the negative feedback mode. During each interval the system may be described by a linear differential equation.

The negative feedback mode is analyzed first. Phase-space analysis^{5,6} similar to that given by Meiksin⁴ is applied to determine the negative feedback trajectories.

Analysis of the positive feedback mode consists of determining which negative feedback phase-space trajectories are intersected by the positive feedback phase-space trajectories. The switching condition is derived in terms of these negative feedback trajectories. It is then shown that if the p-n feedback control system switches at the instant prescribed by the switching condition, minimum response time with no overshoot is obtained.

Negative Feedback

The general expression for the error of a type 1 third-order negative feedback control system with a step position input is

$$\ddot{\theta}_e + a\dot{\theta}_e + b\theta_e + c\theta_e = 0 \quad (1)$$

Equation 1 may be rewritten as

$$\begin{aligned} \ddot{\theta}_e &= \dot{\theta}_{e1} \\ \ddot{\theta}_e &= \dot{\theta}_{e2} \\ -c\theta_{e1} - b\dot{\theta}_{e2} - a\theta_{e3} &= \dot{\theta}_{e3} \end{aligned} \quad (2)$$

where $\theta_{e1} = \theta_e$

It is convenient to consider the set of equations as a linear transformation of a vector

$$\|A\|\theta_e = \dot{\theta}_e \quad (3)$$

The set of equations 3 is transformed to its normal co-ordinates by the following transformation:

$$\begin{aligned} \theta_e &= \|M\|\mathbf{X}_e \\ \dot{\theta}_e &= \|M\|\dot{\mathbf{X}}_e \end{aligned} \quad (4)$$

where $\|M\|$ is the modal matrix and \mathbf{X}_e is the column matrix of the normal co-

ordinates. The modal matrix $\|M\|$ is composed of rows which are proportional to the direction cosines of the normal co-ordinates. When the modal matrix is applied as in equation 4, the three dependent original equations 2 are separated into three independent equations such as those shown in equation 8.

Equation 3 in terms of the normal co-ordinates may be written as

$$\|A\| \|M\| \mathbf{X}_e = \|M\| \dot{\mathbf{X}}_e \quad (5)$$

Premultiplying by the inverse modal matrix gives

$$\|A\| \mathbf{X}_e = \dot{\mathbf{X}}_e \quad (6)$$

where

$$\|A\| = \|M\|^{-1} \|A\| \|M\| = \begin{bmatrix} \lambda_1 & 0 & 0 \\ 0 & \lambda_2 & 0 \\ 0 & 0 & \lambda_3 \end{bmatrix} \quad (7)$$

and λ_1 , λ_2 , and λ_3 are the roots or eigenvalues of the characteristic equation of the system. It is assumed that λ_1 , λ_2 , and λ_3 are distinct negative real roots. The solution to equation 6 may be written as

$$\begin{aligned} X_{e1} &= X_{e10} e^{\lambda_1 t} \\ X_{e2} &= X_{e20} e^{\lambda_2 t} \\ X_{e3} &= X_{e30} e^{\lambda_3 t} \end{aligned} \quad (8)$$

where X_{e10} , X_{e20} , and X_{e30} are the initial values of X_{e1} , X_{e2} , and X_{e3} respectively.

Plotting the projections of the trajectories on the X_{e2} - X_{e1} and X_{e3} - X_{e1} planes may be accomplished by the method of isoclines.⁷ The projection of the trajectory for a typical third-order system is shown in Fig. 1.

The first equation of the set of equations 4 is expanded to yield

$$\begin{aligned} \theta_{e1} &= M_{11}X_{e10}e^{\lambda_1 t} + M_{12}X_{e20}e^{\lambda_2 t} + M_{13}X_{e30}e^{\lambda_3 t} \\ \theta_{e2} &= M_{21}X_{e10}e^{\lambda_1 t} + M_{22}X_{e20}e^{\lambda_2 t} + M_{23}X_{e30}e^{\lambda_3 t} \\ \theta_{e3} &= M_{31}X_{e10}e^{\lambda_1 t} + M_{32}X_{e20}e^{\lambda_2 t} + M_{33}X_{e30}e^{\lambda_3 t} \end{aligned} \quad (9)$$

From equation 9 it follows that the transient response of the position error, θ_{e1} , is the sum of the projections of the normal components of the trajectory on to the θ_{e1} axis. Since the eigenvalues were assumed distinct, it may be assumed that $|\lambda_1| < |\lambda_2| < |\lambda_3|$. Thus, the eigenvector corresponding to λ_1 will be associated with the term $X_{e10}e^{\lambda_1 t}$. Hence, this eigenvector will be designated the slow eigenvector. Similarly, the eigenvectors associated with λ_2 and λ_3 are designated the intermediate and fast eigenvectors respectively.

Next, the equations for the eigenvectors are obtained in the θ -space, i.e., in terms of the co-ordinates θ_{e1} , θ_{e2} , and θ_{e3} . The eigenvectors constitute the axes of the

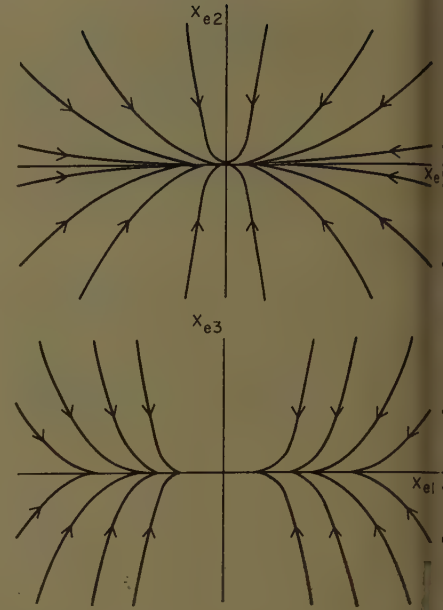


Fig. 1. Projections on X_{e2} - X_{e1} and X_{e3} - X_{e1} planes of negative feedback control system phase-space trajectories

normal co-ordinate system. In normal co-ordinates the equation for the slow eigenvector is

$$\begin{aligned} X_{e2} &= 0 \\ X_{e3} &= 0 \end{aligned} \quad (10)$$

Equation 10 may be transformed into the θ -space giving

$$\begin{aligned} \theta_{e2} &= \lambda_1 \theta_{e1} \\ \theta_{e3} &= \lambda_1^2 \theta_{e1} \end{aligned} \quad (11)$$

which are the desired equations for the slow eigenvector.

In a similar manner the equations for the intermediate and fast eigenvector in that order are found:

$$\begin{aligned} \theta_{e2} &= \lambda_2 \theta_{e1} \\ \theta_{e3} &= \lambda_2^2 \theta_{e1} \end{aligned} \quad (12)$$

$$\begin{aligned} \theta_{e2} &= \lambda_3 \theta_{e1} \\ \theta_{e3} &= \lambda_3^2 \theta_{e1} \end{aligned} \quad (13)$$

Positive Feedback

The general expression for a type 1, third-order positive feedback control system in terms of actuating signal is

$$\ddot{\theta}_s + a\dot{\theta}_s + b\dot{\theta}_s - c\theta_s = 0 \quad (14)$$

The equation relating the actuating signal of the positive feedback mode to the actuating error of the negative feedback mode for a position step input is derived as follows: the actuating signal may be expressed in terms of the position input and output as

$$\theta_s = \theta_i + \theta_o \quad (15)$$

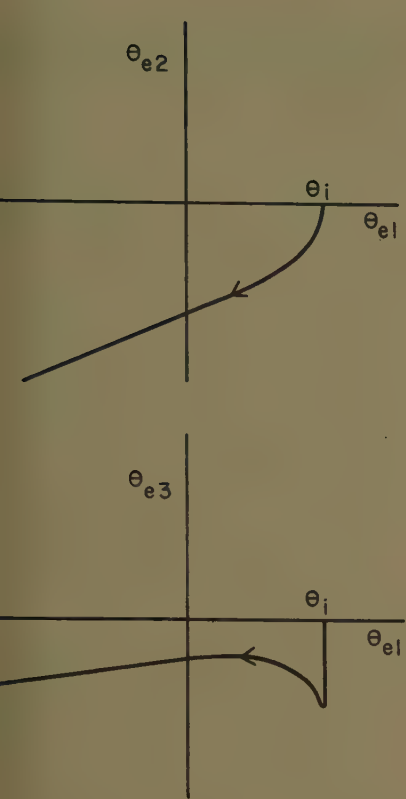


Fig. 2. Projection on θ_{e2} - θ_{e1} and θ_{e3} - θ_{e1} planes of positive feedback control system phase-space trajectories

where θ_i is the position input and θ_o the position output. Similarly, the actuating force may be written as

$$F = \theta_i - \theta_o \quad (16)$$

Eliminating θ_o between equations 15 and 16 gives the desired result

$$F = 2\theta_i - \theta_s \quad (17)$$

Differentiating equation 17 twice results

$$F = -\ddot{\theta}_s \quad (18)$$

$$F = -\ddot{\theta}_s \quad (19)$$

One method of showing the general projection of the positive feedback trajectories may be explained as follows: The Laplace transform of equation 14 for a step position input, θ_i , is

$$\frac{\theta_i(s^2 + as + e)}{(s^3 + as^2 + es - c)} \quad (20)$$

Using Routh's criterion the characteristic equation

$$s^3 + as^2 + es - c = 0 \quad (21)$$

has one positive root and two negative roots. The positive root, designated by δ_1 , must be real and the negative roots, $-\delta_2$ and $-\delta_3$, may be real or complex. Repeating equation 20 yields

$$\frac{\theta_i(s^2 + as + e)}{(s - \delta_1)(s + \delta_2)(s + \delta_3)} \quad (22)$$

The solution of equation 14 for a step position input is

$$\theta_s = \theta_i \left[\frac{\delta_1^2 + a\delta_1 + e}{(\delta_2 + \delta_1)(\delta_3 + \delta_1)} e^{+\delta_1 t} + \frac{\delta_2^2 - a\delta_2 + e}{(-\delta_1 - \delta_2)(\delta_3 - \delta_2)} e^{-\delta_2 t} + \frac{\delta_3^2 - a\delta_3 + e}{(-\delta_1 - \delta_3)(\delta_2 - \delta_3)} e^{-\delta_3 t} \right] \quad (23)$$

Differentiating equation 23 twice leads to

$$\dot{\theta}_s = \theta_i \left[\frac{\delta_1(\delta_1^2 + a\delta_1 + e)}{(\delta_2 + \delta_1)(\delta_3 + \delta_1)} e^{+\delta_1 t} - \frac{\delta_2(\delta_2^2 - a\delta_2 + e)}{(-\delta_1 - \delta_2)(\delta_3 - \delta_2)} e^{-\delta_2 t} - \frac{\delta_3(\delta_3^2 - a\delta_3 + e)}{(-\delta_1 - \delta_3)(\delta_2 - \delta_3)} e^{-\delta_3 t} \right] \quad (24)$$

$$\ddot{\theta}_s = \dot{\theta}_i \left[\frac{\delta_1^2(\delta_1 + a\delta_1 + e)}{(\delta_2 + \delta_1)(\delta_3 + \delta_1)} e^{+\delta_1 t} + \frac{\delta_2^2(\delta_2^2 - a\delta_2 + e)}{(-\delta_1 - \delta_2)(\delta_3 - \delta_2)} e^{-\delta_2 t} + \frac{\delta_3^2(\delta_3^2 - a\delta_3 + e)}{(-\delta_1 - \delta_3)(\delta_2 - \delta_3)} e^{-\delta_3 t} \right] \quad (25)$$

Since only the root δ_1 is positive, the transient response of θ_s , $\dot{\theta}_s$, and $\ddot{\theta}_s$ will depend eventually on the term $e^{+\delta_1 t}$ and θ_e will begin positive and decrease through zero. $\dot{\theta}_e$ and $\ddot{\theta}_e$ will both be negative. In any event, the projection of the trajectories of the positive feedback mode may be plotted on the θ_{e2} - θ_{e1} and θ_{e3} - θ_{e1} planes from the solution of equations 23, 24, and 25 for different values of t . A plot of typical projections of the positive feedback trajectory is shown in Fig. 2.

Switching Condition

The response of the system will begin in the positive feedback mode. At a certain point on the positive feedback trajectory the system is switched into the negative feedback mode; the particular point is determined by the switching condition. An optimum switching condition is defined to exist (1) if the switching condition may be simply obtained from the variables of the system, or (2) if the switching results in minimum time response with no overshoot.

The optimum switching condition based upon the above criteria for a position step input is positive feedback for

$$\theta_{e1} > 0, \quad X_{e1} > 0, \text{ or} \quad \theta_{e1} < 0, \quad X_{e1} < 0 \quad (26)$$

and negative feedback for

$$\theta_{e1} \geq 0, \quad X_{e1} \leq 0, \text{ or} \quad \theta_{e1} \leq 0, \quad X_{e1} \geq 0 \quad (27)$$

When this switching condition is used

the system responds in positive feedback until the projection of the trajectory on the normal co-ordinate $X_{e1} = 0$, in which case the system is switched to the negative feedback mode. Thus, the slow eigenvector is eliminated in the p-n feedback switching system.

In the θ_{e1} , θ_{e2} , and θ_{e3} co-ordinates the switching plane, $X_{e1} = 0$, becomes

$$\begin{aligned} \theta_{e1} &= M_{12}X_{e2} + M_{13}X_{e3} \\ \theta_{e2} &= M_{22}X_{e2} + M_{23}X_{e3} \\ \theta_{e3} &= M_{32}X_{e2} + M_{33}X_{e3} \end{aligned} \quad (28)$$

where M_{ij} is the element in the i th row and the j th column of $||M||$. Equation 28 is a simultaneous equation involving five variables and three equations. Two equations and two variables may be eliminated to obtain

$$\begin{aligned} \theta_{e1} &+ \left[\frac{M_{12}M_{33} - M_{13}M_{32}}{M_{23}M_{32} - M_{22}M_{33}} \right] \theta_{e2} + \\ &\left[\frac{M_{22}(M_{13}M_{32} - M_{12}M_{33}) - M_{12}}{M_{32}(M_{23}M_{32} - M_{22}M_{33}) - M_{32}} \right] \theta_{e3} = 0 \end{aligned} \quad (29)$$

Equation 29 may be reduced to

$$\theta_{e1} \frac{\lambda_2 + \lambda_3}{\lambda_2 \lambda_3} \theta_{e2} + \frac{1}{\lambda_2 \lambda_3} \theta_{e3} = 0 \quad (30)$$

From equation 30 it may be seen that the switching plane passes through zero and the intermediate and fast eigenvectors. It must be noted that the positive feedback trajectory will intersect the switching plane for any step position input.

Another method of deriving the equation for the switching plane is to pre-multiply the first equation of the set in equation 4 by the inverse modal matrix,

$$||M||^{-1} \theta_e = X_e \quad (31)$$

Equation 31 may be expanded to give

$$\begin{aligned} N_{11}\theta_{e1} + N_{12}\theta_{e2} + N_{13}\theta_{e3} &= X_{e1} \\ N_{21}\theta_{e1} + N_{22}\theta_{e2} + N_{23}\theta_{e3} &= X_{e2} \\ N_{31}\theta_{e1} + N_{32}\theta_{e2} + N_{33}\theta_{e3} &= X_{e3} \end{aligned} \quad (32)$$

where N_{ij} is the element in the i th row and j th column of the inverse modal matrix $||M||^{-1}$. The switching plane becomes

$$X_{e1} = N_{11}\theta_{e1} + N_{12}\theta_{e2} + N_{13}\theta_{e3} = 0 \quad (33)$$

In a similar manner, equation 32 may be used to obtain the switching plane that will eliminate any eigenvector.

The switching condition for a position step input may now be summarized as follows: the system is in positive feedback when

$$\begin{aligned} \theta_{e1} > 0 \text{ and } \theta_{e1} + K_1\theta_{e2} + K_2\theta_{e3} > 0, \text{ or} \\ \theta_{e1} < 0 \text{ and } \theta_{e1} + K_1\theta_{e2} + K_2\theta_{e3} < 0 \end{aligned} \quad (34)$$

and in negative feedback when

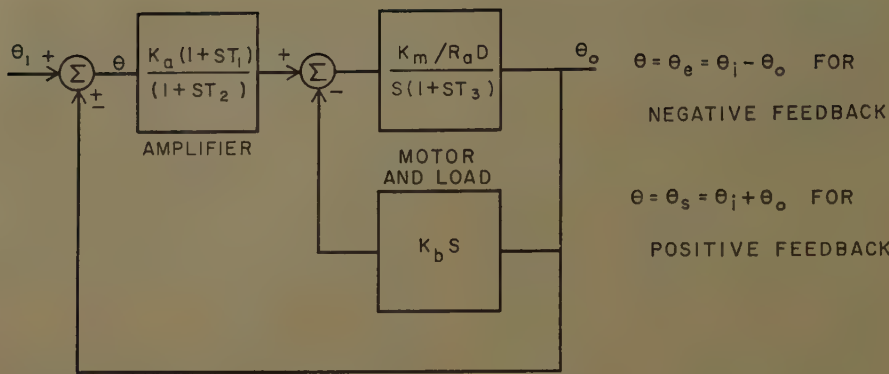


Fig. 3. Typical type 1, third-order feedback control system

$$\begin{aligned} \theta_{e1} \geq 0 \text{ and } \theta_{e1} + K_1\theta_{e2} + K_2\theta_{e3} &\leq 0, \text{ or} \\ \theta_{e1} \leq 0 \text{ and } \theta_{e1} + K_1\theta_{e2} + K_2\theta_{e3} &\geq 0 \end{aligned} \quad (35)$$

where

$$K_1 = -\frac{\lambda_2 + \lambda_3}{\lambda_2 \lambda_3} \quad (36)$$

and

$$K_2 = \frac{1}{\lambda_2 \lambda_3} \quad (37)$$

It is now necessary to show that switching condition as given by equations 34 and 35 results in minimum time response of the system to a position step input. The time response of a system is inversely proportional to the area between the projection of the trajectory on the $\theta_{e2}-\theta_{e1}$ plane and the θ_{e1} axis.⁷

From Fig. 2 it may be seen that the area under the positive feedback trajectory is increasing as θ_{e1} decreases.

Therefore, for minimum time response the system must remain in the positive feedback mode as long as possible. That the system must reach the rest position with no overshoot is the requirement that limits the time the system may stay in the positive feedback mode. It is shown that this requirement is equivalent to requiring the system to switch before a change in algebraic sign occurs in the projection of the systems trajectory on the X_{e1} axis. This is shown as follows: Equation 4 may be expanded to give

$$\begin{aligned} \theta_{e1} &= M_{11}X_{e1} + M_{12}X_{e2} + M_{13}X_{e3} \\ \theta_{e2} &= M_{21}X_{e1} + M_{22}X_{e2} + M_{23}X_{e3} \\ \theta_{e3} &= M_{31}X_{e1} + M_{32}X_{e2} + M_{33}X_{e3} \end{aligned} \quad (38)$$

If equation 8 is substituted in the first equation of set 38, the result is

$$\theta_{e1} = M_{11}X_{e10}e^{\lambda_1 t} + M_{12}X_{e20}e^{\lambda_2 t} + M_{13}X_{e30}e^{\lambda_3 t} \quad (39)$$

Since the terms $M_{12}X_{e20}e^{\lambda_2 t}$ and $M_{13}X_{e30}e^{\lambda_3 t}$ decay toward zero faster than $M_{11}X_{e10}e^{\lambda_1 t}$, (because $|\lambda_1| < |\lambda_2| < |\lambda_3|$ as stated above) θ_{e1} must have the same sign as $M_{11}X_{e1}$ as time approaches infinity. Further-

more, since the negative feedback system does not have overshoot for a position step input, and since $X_{e1} = X_{e10}e^{\lambda_1 t}$ does not change sign in the negative feedback mode, θ_{e1} must have the same sign as $M_{11}X_{e1}$ when the system is switched from positive to negative feedback. If $M_{11}X_{e1}$ and θ_{e1} have the same sign at the switching instant and if in the negative feedback mode θ_{e1} and $M_{11}X_{e1}$ have the same sign as time approaches infinity, the requirement that the system come to rest with no overshoot requires the system to be switched before X_{e1} changes sign.

The system remains in the positive feedback mode for the longest possible time and yet comes to rest with no overshoot if the system is switched whenever the positive feedback trajectory intersects the plane $X_{e1} = 0$. Thus, the switching condition, given by equations 34 and 35, results in minimum time response for a

system that employs one switching instance in the transient response period

Ramp Input

The preceding discussion was for a step position input. In this case the differential error equation is equal to zero there is at least one integrator (type 1 system) in the forward loop. On the other hand, for a step velocity input the error equation is equal to zero for a system that has at least two integrators (type 2 system) in the forward loop. If a type 1 system is subjected to a step velocity input, a constant error will result. Meiksin⁴ concluded that for a type 2 second-order positive-negative feedback switching control system the time response for a step velocity input was greatly improved.

By an analysis similar to that given for a type 1 p-n feedback control system, it can be shown that for a type 2 p-n feedback switching control system the switching condition 34 and 35 results in minimum time response for both a step velocity input and a step position input. It would seem plausible that the same switching condition would result in minimum time response with no overshoot for any combination of step position and step velocity inputs.

Furthermore, it appears that a step acceleration input could be handled with the same switching condition for a type 3 p-n feedback switching control system. However, a type 3 third-order negative

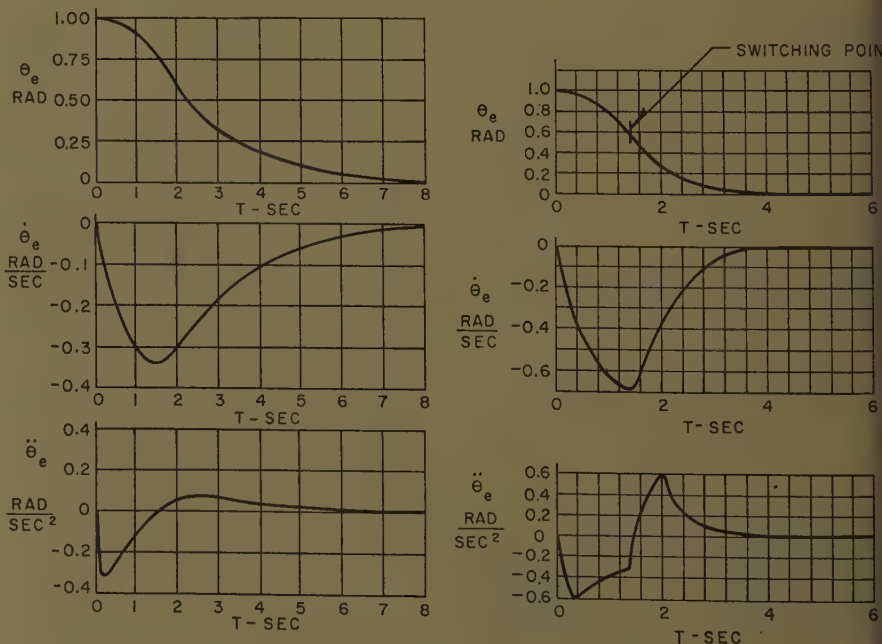


Fig. 4. Transient response of control systems as recorded on analog computer

A—Linear third-order negative feedback
B—P-n feedback switching

feedback control system is not stable. A higher-order type 3 control system may be stable, and hence could probably be used in a p-n feedback switching system that would have a final value of zero error or a step acceleration input.

Extension to Higher-Order Systems

It is interesting to note that as the value of an eigenvalue tends to infinity, the third-order system tends to a second-order system and the switching plane for the third-order system tends to the switching line derived by Meiksin for a second-order control system, i.e.,

$$\lim_{\lambda_3 \rightarrow \infty} \left[\theta_{e1} - \frac{\lambda_2 + \lambda_3}{\lambda_2 \lambda_3} \theta_{e2} + \frac{1}{\lambda_2 \lambda_3} \theta_{e3} \right] = \theta_{e1} - \frac{1}{\lambda_2} \theta_{e2} \quad (40)$$

The switching condition is such that the slow eigenvector is eliminated in both the second- and third-order system. In other words, the p-n control system is contrived to eliminate the slowest mode of the transient response. This idea may be extended to a system of any order. For an n th-order system the modal matrix may be found by a process similar to the method presented for the third-order system. The transformation to the normal co-ordinates will be made using the modal matrix.

$$\begin{aligned} \theta_e &= \|M\| X_e \\ \dot{\theta}_e &= \|M\| \dot{X}_e \end{aligned} \quad (41)$$

The inverse transformation will be made using the inverse modal matrix

$$\|M\|^{-1} \theta_e = X_e \quad (42)$$

which may be expanded to give

$$\begin{aligned} N_{11}\theta_{e1} + N_{12}\theta_{e2} + \dots + N_{1n}\theta_{en} &= X_{e1} \\ N_{21}\theta_{e1} + N_{22}\theta_{e2} + \dots + N_{2n}\theta_{en} &= X_{e2} \\ \vdots \\ N_{n1}\theta_{e1} + N_{n2}\theta_{e2} + \dots + N_{nn}\theta_{en} &= X_{en} \end{aligned} \quad (43)$$

If X_{e1} is the slow eigenvector, the switching condition will then be positive feedback for

$$\begin{aligned} \theta_{e1} > 0 \text{ and } X_{e1} > 0, \text{ or} \\ \theta_{e1} < 0 \text{ and } X_{e1} < 0 \end{aligned} \quad (44)$$

and negative feedback for

$$\begin{aligned} \theta_{e1} \geq 0 \text{ and } X_{e1} \leq 0, \text{ or} \\ \theta_{e1} \leq 0 \text{ and } X_{e1} \geq 0 \end{aligned} \quad (45)$$

The system will switch from positive to negative feedback when

$$N_{11}\theta_{e1} + N_{12}\theta_{e2} + \dots + N_{1n}\theta_{en} = 0 \quad (46)$$

If the system is to be switched only once during the transient response period, the optimum switching condition is

given by equations 44 and 45. For, if the system were switched in the transient response period any later than it would be if switched according to equations 44 and 45, it would overshoot. On the other hand, if the system were switched earlier in the transient response period, it would respond more slowly because it would be in negative feedback longer.

Numerical Example

Consider a system shown in Fig. 3 and described by the following differential equation in the negative feedback mode.

$$\ddot{\theta}_e + 6.0\dot{\theta}_e + 9.4\theta_e + 4.0\theta_e = 0 \quad (47)$$

The characteristic equation of this system is given by

$$\lambda^3 + 6.0\lambda^2 + 9.4\lambda + 4.0 = 0 \quad (48)$$

The roots of this equation are

$$\begin{aligned} \lambda_1 &= -0.7070 \\ \lambda_2 &= -1.4863 \\ \lambda_3 &= -3.8067 \end{aligned} \quad (49)$$

Then, by equations 36 and 37

$$\begin{aligned} K_1 &= 0.9354 \\ K_2 &= 0.1767 \end{aligned} \quad (50)$$

The switching condition is given by equations 34 and 35 and may be written as positive feedback when

$$\begin{aligned} \theta_{e1} > 0 \text{ and } \theta_{e1} + 0.9354\theta_{e2} + 0.1767\theta_{e3} > 0, \text{ or} \\ \theta_{e1} < 0 \text{ and } \theta_{e1} + 0.9354\theta_{e2} + 0.1767\theta_{e3} < 0 \end{aligned} \quad (51)$$

and negative feedback when

$$\begin{aligned} \theta_{e1} \geq 0 \text{ and } \theta_{e1} + 0.9354\theta_{e2} + 0.1767\theta_{e3} \leq 0, \text{ or} \\ \theta_{e1} \leq 0 \text{ and } \theta_{e1} + 0.9354\theta_{e2} + 0.1767\theta_{e3} \geq 0 \end{aligned} \quad (52)$$

Thus, for a step position input the system will respond in positive feedback initially and will switch into negative feedback when the switching condition given by equations 51 and 52 is reached. This was demonstrated on an analog computer as described in the following paragraph.

Analog Computer Study

An analog computer study was conducted for a system represented by the block diagram in Fig. 3. The differential equation describing the system in the negative feedback mode is

$$\ddot{\theta}_e + 6.0\dot{\theta}_e + 9.4\dot{\theta}_e + 4.0\theta_e = 0 \quad (53)$$

The initial conditions were $\theta_{e1} = 1$, $\theta_{e2} = \theta_{e3} = 0$. The equation for the switching plane is

$$\theta_{e1} + 0.9354\theta_{e2} + 0.1767\theta_{e3} = 0 \quad (54)$$

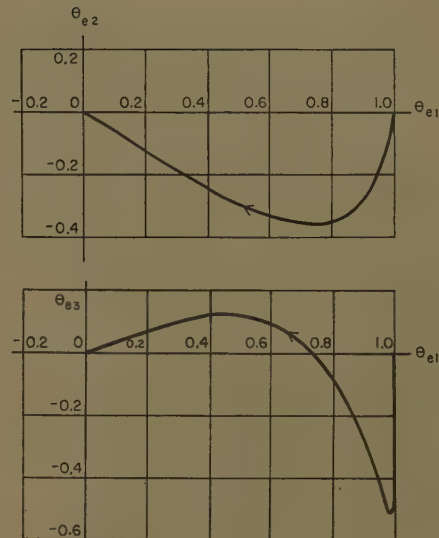


Fig. 5. Projections of trajectories of linear negative feedback control system as recorded on analog computer X-Y plotter

LINEAR NEGATIVE FEEDBACK CONTROL SYSTEM

The transient response for the linear negative feedback control system is shown in Fig. 4(A). The time response (measured from $t = 0$ the time the system reaches 95% of its final value) is 6.33 seconds.

An X-Y plotter was used to plot the projection of the trajectories of the response of the system on the $\theta_{e2}-\theta_{e1}$ and $\theta_{e3}-\theta_{e1}$ planes. These trajectories are shown in Fig. 5.

P-N FEEDBACK SWITCHING CONTROL SYSTEM

The transient response for the p-n feedback control system is shown in Fig. 4(B); the time response as measured from this is 3.33 seconds.

The projections of the trajectories on the $\theta_{e2}-\theta_{e1}$ and $\theta_{e3}-\theta_{e1}$ planes were plotted for several values of step position input; see Fig. 6(A). To contrast the linear system with the switching system, the projections of the trajectories of both systems are shown on the same planes in Fig. 6(B).

The switching condition was varied by changing the value of the constants in the equation for the switching plane:

$$\theta_{e1} + P\theta_{e2} + R\theta_{e3} = 0 \quad (55)$$

When P and R were equal to the values given in equation 54, the system switched at the proper time to eliminate the slow eigenvector. The output of the system reached the final value with no overshoot.

When either P or R , or both P and R , were increased, the system switched earlier in the transient response period. Also, the system switched from negative to positive feedback and back again

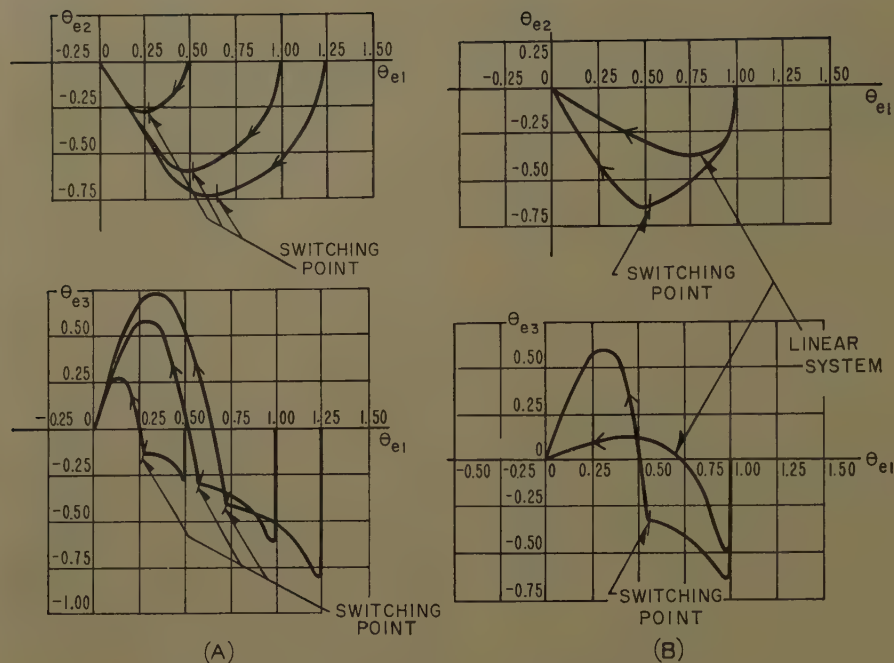


Fig. 6. Projection of trajectories on θ_{e2} - θ_{e1} and θ_{e3} - θ_{e1} planes

A—P-n control system
B—Linear and switching systems

several times during the negative feedback part of the transient response period. The output of the system reached the final value with no overshoot.

When either P or R , or both P and R , were decreased, the system switched later in the transient response period. The output reached the final value with overshoot. However, the value of P and R is not critical. A decrease of 20% in P and R resulted in less than 5% overshoot.

Interpretation of Results

The results of the analog computer study confirm the validity of the analytical treatment. The time response was decreased 47% by using the p-n feedback switching control system instead of the linear negative feedback control system with the same power-handling capacity.

The amount of damping in the system was not changed during the transient response. The time response of the system may be further reduced if the amount of damping during the positive feedback mode is held to the minimum inherent in the system and if additional damping is introduced into the system when the system is switched into the negative feedback mode. This can be accomplished easily by switching in a proper feedback network.

The switching condition will be determined from the characteristic equation of the highly damped linear negative feedback system using equations 34 through

37. It may be expected that a similar decrease in time response will be obtained by operating other linear negative feedback systems as p-n feedback switching systems.

The results obtained by varying the constants in the switching plane equation are explained by considering the position of the switching plane with respect to the positive feedback trajectories. When the constants P and R of equation 55 are made higher than the calculated value for optimum switching, the switching plane is tilted so that the positive feedback trajectories will intersect it before the projection of the trajectories on the normal co-ordinate X_{e1} is zero. The equation for the transient response will therefore contain a term that corresponds to the slow eigenvector. The trajectory of the system in negative feedback will not remain in the switching plane but will travel toward the slow eigenvector. When this occurs, the system is switched back into the positive feedback mode.

In the positive feedback mode the trajectory of the system is driven toward the switching plane once again. The system is switched in and out of positive feedback several times. This switching is undesirable and may be eliminated by decreasing the constants P and R in the switching plane equation.

When the constants P and R are decreased, the switching plane is tilted so that the positive feedback trajectory will intersect it after the projection of the

trajectory on the normal co-ordinate X_{e1} has changed in algebraic sign. The trajectory will leave the switching plane and travel toward the slow eigenvector, but in a direction that carries it deeper into the negative feedback region. It has been shown that if the system is switched after the projection of the trajectory on the normal co-ordinate X_{e1} has changed sign, the output of the system will overshoot its final value.

In a practical system it would be good design to decrease the constants P and R below the theoretical value for optimum switching, to insure that the system switched only once during the transient response period. The overshoot of the output of the system is barely noticeable if the constants P and R are made 10% to 20% below the theoretically optimum values.

The switching condition is not critical i.e., if the switching instant is missed slightly the system will reach the steady state without hunting or noticeable overshoot.

Conclusions

For a linear third-order type 1 negative feedback control system that has three distinct real roots to its characteristic equation, the following new conclusions may be drawn for a step position input:

1. The time response can be decreased by operating the first part of the transient response period in positive feedback, and switching according to the derived switching condition into negative feedback.
2. The transient response of the system may be considered as being composed of three independent modes. The modes decay exponentially with an increasing time. Any mode can be eliminated by switching into negative feedback when the initial value of the mode is zero.
3. If the system is switched from positive to negative feedback when the initial value of the slowest mode is zero, the system responds with the fastest time response and no overshoot. This switching condition is the optimum switching condition.

If a type 2 p-n feedback control system is used instead of a type 1 system, the following new conclusions are drawn:

4. The analysis and operation of the type 2 system is the same as the type 1 system for a step position input.
5. The optimum switching condition results in the fastest time response with no overshoot for a step velocity input.

If a higher-order p-n feedback control system is used instead of a third-order system, the following new conclusions are drawn:

6. The transient response can be separated into three distinct parts: a positive feedback period, a negative feedback period, and a final steady state period.

ated into independent modes by an analysis that is similar to the method used for the third-order system.

The slowest mode of the transient response can be eliminated by switching into negative feedback when the initial value of the slowest mode is zero.

Eliminating the slowest mode in an n th-order system results in the fastest time response with no overshoot for a system that only switches once during the transient period.

Nomenclature

b, c, e = constant coefficients of third-order differential equations
 A = linear transformation matrix
 K_1, K_2 = constant coefficients of equation defining switching condition
 M = modal matrix of negative feedback control system
 m_{ij} = element of i th row and j th column of modal matrix
 m_{ij}^{-1} = element of i th row and j th column of inverse modal matrix
 t = time

X_{e1}, X_{e2}, X_{e3} = normal co-ordinates of third-order negative feedback error phase-space
 $\delta_1, \delta_2, \delta_3$ = eigenvalues of positive feedback system
 θ_e = error signal of negative feedback control system
 $\theta_e = \begin{bmatrix} \theta_{e1} \\ \theta_{e2} \\ \theta_{e3} \end{bmatrix}$ = vector from origin of co-ordinates to point in "error" phase-space
 θ_i = input signal of system
 θ_o = output signal of system
 θ_s = actuating signal of positive feedback control system
 $\lambda_1, \lambda_2, \lambda_3$ = eigenvalues of negative feedback system
 $\|A\|$ = diagonal matrix of negative feedback eigenvalues
 $\| \|$ = matrix
 D = damping coefficient
 J = moment of inertia
 K_a = amplifier gain
 K_b = voltage-velocity constant of d-c motor
 K_m = torque-current constant of d-c motor
 K_p = pilot motor constant
 R_a = armature resistance of d-c motor
 s = Laplacian operator
 t_1, t_2 = amplifier time constants
 t_3 = motor and load time constant

References

1. NONLINEAR TECHNIQUES FOR IMPROVING SERVO PERFORMANCE, D. McDonald. *Proceedings, National Electronics Conference, Chicago, Ill.*, vol. 6, 1950, pp. 400-21.
2. A PHASE-PLANE APPROACH TO THE COMPENSATION OF SATURATING SERVOMECHANISMS, Arthur M. Hopkin. *AIEE Transactions*, vol. 70, pt. I, pp. 631-39.
3. AN INVESTIGATION OF THE SWITCHING CRITERIA FOR HIGHER ORDER CONTACTOR SERVOMECHANISMS, Irving Bogner, Louis F. Kazda. *Ibid.*, pt. II (*Applications and Industry*), vol. 73, July 1954, pp. 118-27.
4. POSITIVE-FEEDBACK PHASE-SPACE TRAJECTORIES AND APPLICATION TO SERVO SYSTEMS, Z. H. Meiksin. *Ibid.*, 1958 (Jan. 1959 section), pp. 673-79.
5. THE MATHEMATICS OF CIRCUIT ANALYSIS (book), E. A. Guillemin. John Wiley & Sons, Inc., New York, N. Y., 1949.
6. ANALYSIS AND DESIGN PRINCIPLES OF SECOND AND HIGHER ORDER SATURATING SERVOMECHANISMS, R. E. Kalman. *AIEE Transactions*, pt. II (*Applications and Industry*), vol. 74, Nov. 1955, pp. 294-310.
7. AUTOMATIC FEEDBACK CONTROL SYSTEM SYNTHESIS (book), J. G. Truxal. McGraw-Hill Book Company, Inc., New York, N. Y., 1955.

Automatic Speed Regulation of D-C Motors Using Combined Armature Voltage and Motor Field Control

ANSGAR HANSEN
MEMBER AIEE

ALAN W. WILKERSON
NONMEMBER AIEE

THE MOST commonly available adjustable speed drives of today use the d-c motor. The speed can be controlled by armature voltage variation, field current variation, or a combination of both. Where the load torque is essentially constant throughout the speed range, armature voltage control is used. The second method, motor field adjustment, is most economical where the load power is substantially constant over a speed range not wider than 4 to 6. When an extremely wide speed range is desired with reduced torque at the higher speeds, the combination of both armature and field control gives good results. At low speeds, the motor field is usually maintained at a constant level and the motor speed is varied by changing the armature voltage. When rated armature voltage is reached, the speed can be further increased by weakening the field. The armature voltage, in any case, may be supplied from a Ward-Leonard generator, magnetic amplifiers, tubes, or semiconductors.

On early drives, the combination of armature and field control was accomplished by operating rheostats or potentiometers in the field circuits of a Ward-Leonard system. The rheostats were either two independent units, or they were tandem mounted so that a single knob would provide operation over the entire range. Such systems are still commonly used. However, it is frequently necessary to obtain better speed regulation with varying load than can be obtained with the rheostat systems, and the users of the drives often will not tolerate the physical size of the rheostats capable of handling the field power. Accuracy of the drive and miniaturization of speed setters can best be met by closed-loop feedback systems, which in recent years have become very popular.

This paper deals with closed-loop feedback circuits for combined armature and field control. Because these circuits automatically change from armature voltage control to field control at a pre-

determined point, they are commonly called crossover circuits. Two types will be discussed: one has been developed for conditions requiring very close regulation, low drift, and a linear relationship between input signal and output speed. This type utilizes a tachometer generator connected to the motor.

The other type was developed for drives where accuracy and linearity can be sacrificed to reduce cost. This system does not require a tachometer generator. It is believed that each type of system represents a new approach to the problem of wide range automatic speed control of d-c motors.

Crossover Control Using a Tachometer Generator

With combined armature voltage and motor field control, it is usually desirable that the motor field be fully excited at all speeds below base speed, and that the armature voltage remain at the rated level for all speeds above base speed. If this is accomplished, optimum motor performance will be obtained. One of the most difficult problems in an automatic

Paper 60-642, recommended by the AIEE Industrial Control Committee and approved by the AIEE Technical Operations Department for presentation at the AIEE Great Lakes District Meeting, Milwaukee, Wis., April 27-29, 1960, and re-presented for discussion only at the Winter General Meeting, New York, N. Y., January 29-February 3, 1961. Manuscript submitted February 23, 1960; made available for printing December 14, 1960.

ANSGAR HANSEN and ALAN W. WILKERSON are with The Louis Allis Company, Milwaukee, Wis.

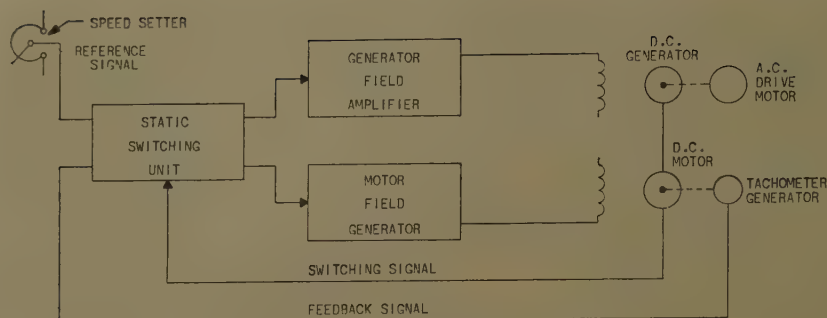


Fig. 1. Block diagram of tachometer crossover system

control with this type of operation is to effect the crossover from armature control to field control smoothly, without any discontinuities, yet also precisely, so that the two ranges do not excessively overlap. Another problem is to avoid a major change in system gain at the point of crossover. Such abrupt changes in gain are frequently accompanied by over-all system instability and oscillations, or hunting. It is desirable that the system should not require complex or numerous adjustments for proper operation.

The circuit discussed here meets all these requirements, and needs only one simple adjustment to determine the crossover point, regardless of the range of motor field control. The use of a tachom-

eter generator for feedback results in a linear relationship between speed and reference signal, and also makes extremely accurate speed regulation possible.

The general scheme of the circuit for crossover control using a tachometer generator for feedback is shown in the block diagram of Fig. 1. Although a Ward-Leonard generator is used as the source of armature power, any of the increasingly popular static d-c supplies would serve equally well.

At the input to the static switching unit, a comparison is made between a reference signal corresponding to desired speed and a tachometer feedback signal proportional to actual drive motor speed. The entire system works to keep these two

signals as nearly equal as possible, and any difference between them acts through the generator and motor field amplifiers to change the motor speed in a manner that reduces the unbalance. This difference between reference and feedback signals is known as the error signal and the accuracy of the system is dependent upon keeping the error as small as possible.

The generator and motor field amplifiers can, of course, be vacuum-tube, thyatron, magnetic, or semiconductor amplifiers. In fact, all of these types have been used successfully. In the system to be described, transistor amplifiers provide high-gain and low-input power requirements. They are followed by magnetic amplifiers for the relatively high power required to excite the fields.

The static switching unit channels any changes in error signal to the proper field amplifier, depending on whether the drive is below or above base speed. Actual switching from generator field amplifier to motor field amplifier is directed by a signal from the motor armature voltage. Switching occurs when this signal reaches a predetermined level, corresponding to base speed.

Below base speed, any increase in error signal is applied through the static switching unit to the generator field amplifier to

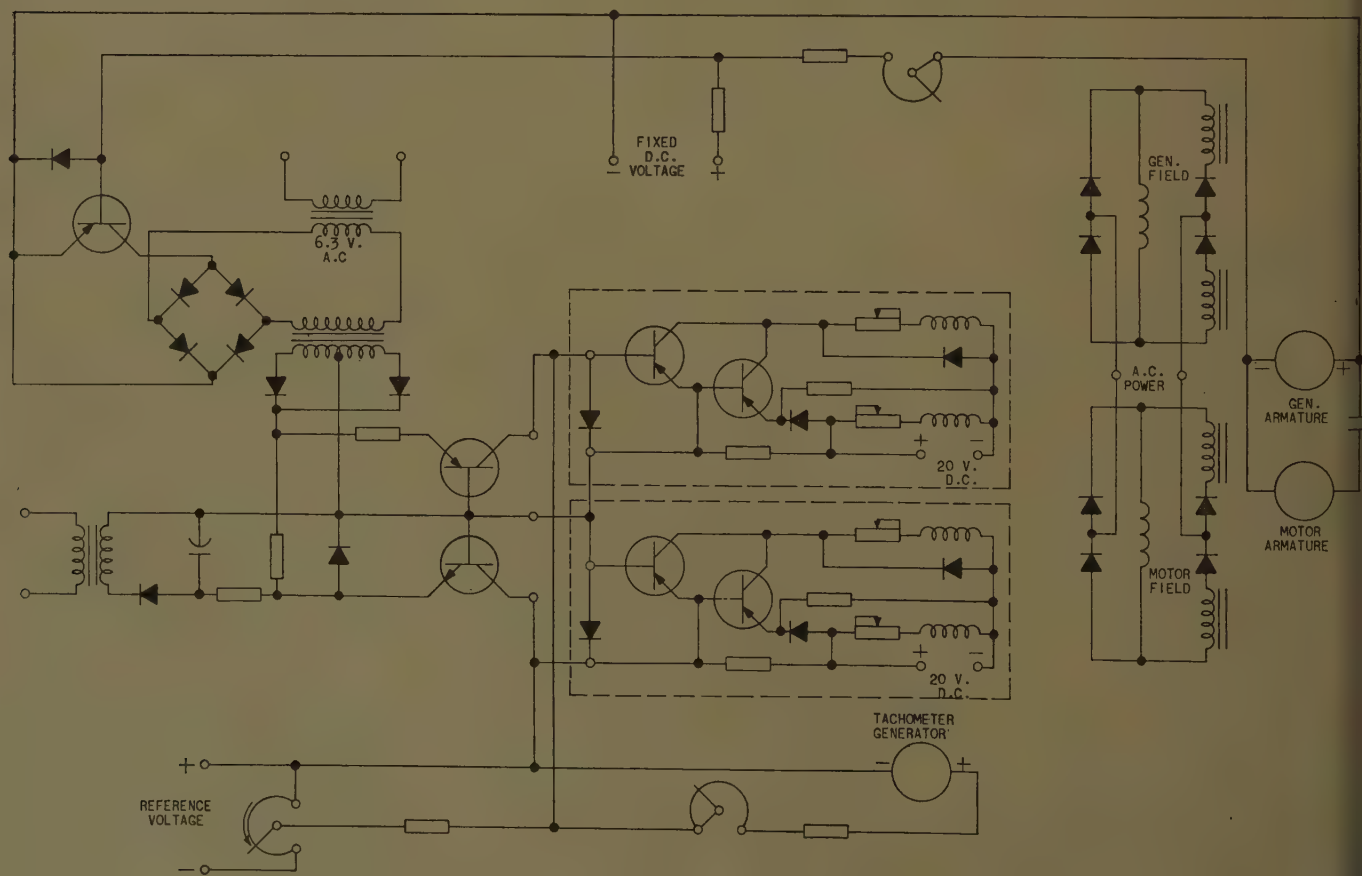


Fig. 2. Complete schematic of transistorized tachometer crossover system

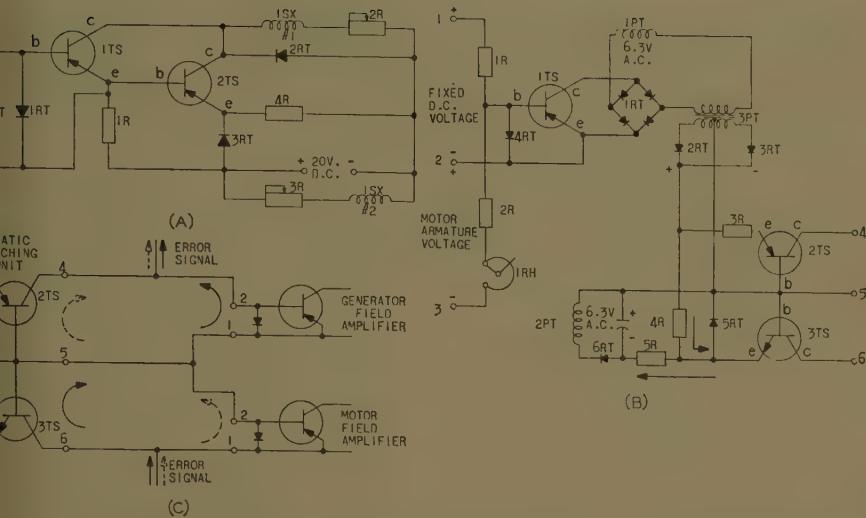


Fig. 3. A—Transistor preamplifier. B—Static switching circuit. C—Detailed interconnection diagram of circuit and preamplifier

se the motor armature voltage and rease motor speed. Motor field length does not change. When base ed is reached, further increases in or signal are switched to the motor field plifier, which weakens the motor field, in increasing motor speed.

Accuracy of speed regulation depends on the stability of the reference signal d also upon the relative magnitudes of reference and error signals. For mple, if the maximum reference signal 100 times as large as the error signal necessary to operate at maximum speed, n the steady-state difference between ual and desired speed will never be ater than 1.0% of top speed, since a % error is sufficient to cause full opera- n of both field amplifiers. With a hometer generator for feedback, out- t speed will be directly proportional to erence signal, and nonlinearities in the er components of the system will not use significant variations in this linear ationship.

The entire control circuit is shown in . 2. To aid in understanding the sys- a, operation of the field amplifiers and ion of the static switching unit will be cribed separately.

Fig. 3(A) is a transistorized preamplifier t drives the magnetic power amplifiers plying each of the two fields. The ee elements of the transistors are elled *e*, *b*, and *c* for emitter, base, and ector respectively. Current entering ut terminal 2 and leaving through ninal 1 passes through the emitter- e junction of transistor 1TS and causes uch larger current between the emitter collector of 1TS. Except for a very ll amount through 1R, this emitter rent of 1TS must flow through the tter-base junction of 2TS, where it

causes a still larger current in the emitter-to-collector path of 2TS. The collector current of 2TS, 5,000 to 10,000 times larger than the original signal, becomes the input current to control winding 1 of 1SX, the magnetic amplifier. Resistor 2R is adjusted to limit the output of 2TS to a safe value. Rectifier 2RT acts as a discharge path for the inductive current of the control winding when transistor 2TS is suddenly turned off by an incoming signal.

The forward voltage drop across rectifier 3RT provides a small reverse bias for transistor 2TS, necessary for operation above 50 degrees centigrade. Resistor 3R adjusts a fixed current through winding 2 of 1SX, to bias the magnetic amplifier for the desired output when 2TS is not conducting. In the case of the generator field magnetic amplifier, this bias is used to obtain minimum output in the absence of a control current from the transistor preamplifier. Transistor output current then acts to increase the magnetic-amplifier output. With the motor field magnetic amplifier, the fixed bias provides rated field excitation, and the transistor output causes the magnetic amplifier to weaken the field.

Of considerable importance to the use of this transistor amplifier is its input impedance. When terminal 2 is positive with respect to terminal 1, a path of very low resistance exists through the emitter-base junction of 1TS. When terminal 1 is positive with respect to terminal 2, a similar low-resistance path exists through diode 1RT. The input terminals therefore represent a very low impedance to current flow in either direction. Because of this low impedance, signals must be applied as currents, rather than voltages, since a voltage of more than a few tenths of a volt would cause destructive currents.

Fig. 3(B) shows the static switching circuit, containing three transistor switches. Transistor 1TS senses armature voltage, and switches 2TS and 3TS when the rated base speed level is reached. A fixed d-c voltage applied to terminals 1 and 2 causes a current through 1R and 4RT, tending to keep transistor 1TS in the nonconducting state. A second current through 2R and 1RH, proportional to motor armature voltage, tends to switch transistor 1TS to the conducting state. When this second current exceeds the first one, transistor 1TS turns ON and applies the 6.3 volts from 1PT to the primary of 3PT through bridge rectifier 1RT. Rectifiers 2RT and 3RT convert the a-c output voltage of 3PT to d-c, for switching 2TS and 3TS. The crossover point at which 1TS switches is adjusted by rheostat 1RH.

Transistors 2TS and 3TS are the static switches that direct the error signal to the two field amplifiers. Below base speed when there is no voltage on transformer 3PT, transistor 2TS has no signal applied to its base and emitter. The base-to-collector path through this transistor therefore represents an essentially open circuit, available as an output function at terminals 4 and 5. Transistor 3TS also receives no signal from transformer 3PT below base speed, but a direct current from the rectified output of transformer 2PT flows through resistor 5R and the

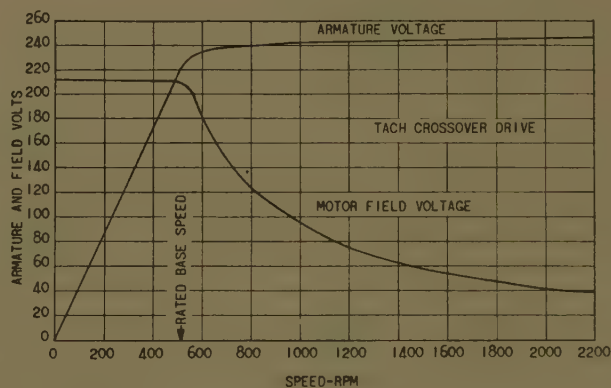


Fig. 4. Curves of armature and field voltage versus motor speed

base-emitter junction of 3TS, to make the collector-to-base path through 3PT essentially a short circuit. This short circuit appears at terminals 5 and 6. Note that 3TS is an n-p-n transistor, in contrast to the p-n-p types used elsewhere in the system.

When the armature voltage becomes large enough at base speed to switch 1TS ON, the voltage from 3PT sends a current through 3R and the emitter base junction of 2TS, changing the resistance at terminals 4 and 5 from an open circuit to a short circuit. In addition, a current through 4R exceeds the turn-on current through 5R, and transistor 3TS switches to the open-circuit state at terminals 5 and 6. To summarize, below base speed, terminals 4 and 5 are open-circuited and terminals 5 and 6 are short-circuited; above base speed, the reverse is true.

Fig. 3(C) shows in detail how the static switching unit is interconnected with the two transistor field amplifiers. The error signal is shown as a solid arrow below base speed and as a dashed arrow above base speed. Below base speed, the error signal current does not pass through the input of the motor field amplifier, since an easier path exists through terminals 6 and 5 of the static switching unit. The motor field excitation therefore will not change. Error signal current will flow, however, through the generator field amplifier, since terminals 5 and 4 of the static switching unit are open-circuited. Thus the error signal causes changes in the motor armature voltage. Above base speed, the opposite action takes place, and error signal current goes through the motor field amplifier and by-passes the generator field amplifier. To be absolutely correct, however, not all of the

error signal above base speed goes through terminals 5 and 4 of the static switching unit, since a certain amount is required through the generator field amplifier input to maintain rated armature voltage. Similarly, some of the error current will necessarily pass through terminals 6 and 5 above base speed. The static switching unit redirects only the amount of error signal which exceeds the value required to bring the motor to base speed.

The curves in Fig. 4 show actual measurements taken on a drive using this control circuit, demonstrating the variations in armature and field voltages with speed. There is very little overlap between the armature and field ranges of control. Although these curves represent motor field control over a 4-to-1 speed range, equally satisfactory performance is obtained without adjustment over any other range for which the motor may be designed.

Referring to Fig. 3(A), the method of comparing the reference and feedback signals may appear to be somewhat unconventional. However, since the low input impedance of the two transistor amplifiers requires a current for the input signal rather than a voltage, it is more convenient to add the reference and feedback currents in parallel, as opposed to the usual series connection used in adding voltages. With this summing method, it is not necessary that the reference and feedback voltages be equal, since equal currents may be derived from unequal voltages merely by proper sizing of series resistance. Tachometer generator selection is therefore correspondingly less critical than in a voltage comparison feedback system.

Current limit circuitry for protecting

the armature circuit of the motor and generator from damage by excessive currents is easily applied to this crossover system. Such a control introduces an additional signal, capable of overcoming the error current, whenever armature current is too large. This signal must be able to assume either polarity to protect for both forward and regenerative currents.

If desired, acceleration control may be inserted between the reference voltage from the speed setter and the input to the system. The reference current then rises and falls according to the internal characteristics of the acceleration circuit.

This system also readily adapts itself for use in applications where speed is not regulated, such as tension or position regulators, since the reference and feedback signals may be made proportional to any desired quantity, and a tachometer signal is not required to accomplish the crossover.

With the advent of the silicon-controlled rectifier, it has become possible to provide large amounts of field power economically with the use of semiconductors entirely. Such an amplifier is shown in Fig. 5. The dual transformation serves two purposes: it isolates the amplifier input and output, and it allows the use of low-voltage controlled rectifiers to supply high-voltage fields. Since the input characteristics are identical with the transistor amplifier described earlier, this controlled rectifier amplifier can be directly substituted in the crossover circuit or in another system where the first amplifier is used.

Crossover Circuits Without Tachometer Feedback

Many applications for wide-speed-range adjustable speed drives do not require the accurate speed regulation and the extreme linearity obtainable with the tachometer feedback schemes discussed in the previous section. For such applications it is desirable to eliminate the tachometer generator, which is a fairly delicate component, thereby also eliminating possible long tachometer leads, and cutting the cost. Such tachometer-free control schemes have been developed, meeting the requirements stated in the previous section, to obtain a smooth transition between the armature voltage control range and the field-weakening range with little overlap and negligible change in system gain.

In the previous section the control components, amplifiers, and switching circuits were of prime interest; in the

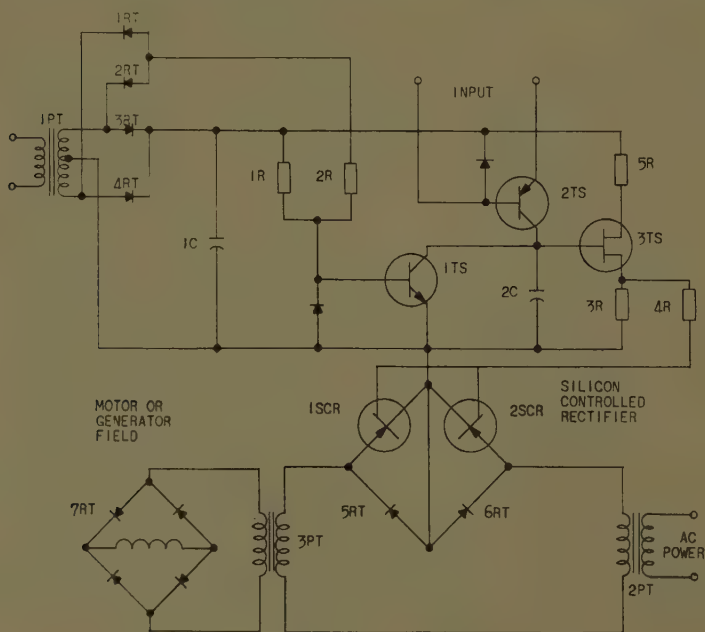
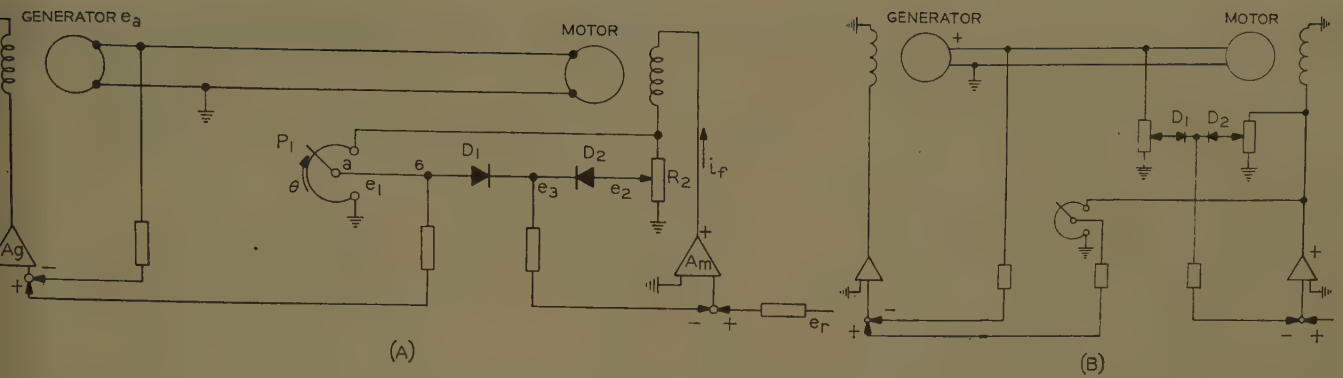


Fig. 5. Complete semiconductor field amplifier



6. A—Schematic 1-line diagram for crossover without tachometer feedback. B—Modified circuit where low-gain motor field amplifier can be used

on, in which the new circuits are dis-
ed, amplifiers are shown only as blocks
hasizing the basic idea. The ampli-
actually used are of the same type
scussed previously.

Fig. 6(A) one of the schemes is
own, for simplicity, as a 1-line diagram;
current-resistance drop compensation
current limit devices (which would
nally be incorporated) are not shown.
he speed is set by means of the
ntiometer P_1 parallel-connected to a
ntiometer P_2 which is series-connected
parallel-connected) to the motor field
ling. P_2 is used to adjust for desired
-weakening range. The outputs of
nd P_2 are connected through back-to-
connected diodes D_1 and D_2 . The
ut e_1 of P_1 is used for reference voltage
ne generator field amplifier A_g , which
upplied with a negative feedback
al from the armature voltage e_a . The
age e_3 appearing at the diode center
is used for the feedback signal to the
or field amplifier A_m , which is pro-
d with a substantially constant refer-
signal e_r .

he crossover point is the point at
h P_1 is set so that $e_1 = e_2$. Below this
t, when $e_1 < e_2$, the diode D_1 blocks and
conducts, rendering the feedback volt-
 e_r equal to $-e_2$ and proportional to the
or field current. The field current
be proportional to the reference volt-
 e_r , and for proper adjustment the field
ent will be equal to the rated field
ent. The voltage e_1 will vary linear-
with the displacement of the speed
r P_1 . Because e_1 is the reference sig-
to the generator field amplifier and
use the motor field current is con-
st, the motor speed will be a linear
tion of the speed setter displacement
 θ as indicated in Fig. 7.

should be noted that a change in
reference voltage e_r will affect the
l to a minor degree only. If the
r is nonsaturated it will not affect
speed at all, because both armature

voltage and field voltage will change with
changing e_r .

If the speed setter is turned up so that
 $e_1 > e_2$ the diode D_1 will be conducting and
 D_2 will be nonconducting. Thus, the
feedback voltage e_3 is now equal to the
output voltage e_1 of the potentiometer P_1
and, because of the feedback, the motor
field current i_f is proportional to e_r and
not i_f .

$$e_1 = K_1 e_r \quad (1)$$

Also, because the armature voltage e_a
is proportional to e_1 ,

$$e_a = K_a e_1 \quad (2)$$

Hence, if e_r is constant, the armature volt-
age will be constant. The motor field
current i_f will be inversely proportional
to the displacement angle θ of the speed
setter P_1 , which can easily be shown.
From the figure

$$i_f R \theta_2 \theta / \theta_{\max} = e_1 \quad (3)$$

As already shown, e_1 is constant, and
 i_f and θ are therefore inversely propor-
tional. Further, if the motor is non-
saturated, then, as will be seen, the motor
speed ω is proportional to θ .

$$\omega = K_w e_a / i_f \quad (4)$$

Equations 1 through 4 render

$$\omega = K \theta \quad (5)$$

where

$$K = K_a K_w R_2 / \theta_{\max} \quad (6)$$

It has been shown that in the armature
voltage adjustment range ω is propor-
tional to θ . Equation 5 shows that if the
motor is nonsaturated, the inherent linear
relation between ω and θ holds also in the
field-weakening range; see Fig. 7. Al-
though the linear relation is distorted by
saturation, the distortion is usually tol-
erable and considerably less than that
found in many other crossover schemes
without tachometer feedback.

As seen, if the motor field is non-

saturated, the change in the reference
voltage e_r will not affect the speed; equa-
tion 5 shows that, also in the field-weak-
ening range, ω will be independent of e_r when
the motor is not saturated. It is known
that the control is fairly insensitive to
changes in the reference voltage e_r even
with some saturation in the motor; con-
sequently the line voltage will usually be
sufficiently constant as a reference source.

By taking the feedback to the motor
field amplifier from the armature voltage
instead of from the output of the speed
setter potentiometer, a motor field ampli-
fier with lower power gain can be used.
Such a modification is shown in Fig. 6(B).
The performance of this scheme is the
same as that in Fig. 6(A), except that a
small dependency is introduced between
armature voltage and field voltage. This
dependency can under certain conditions
affect the stability.

A modification further decreasing the
necessary power gain of the motor field
amplifier is shown in Fig. 8(A). In the
armature voltage range, this control oper-
ates as in previously discussed schemes
except that the motor field circuit is an
open-loop circuit, with amplifier A_m
biased to saturation with a low bias;
see Fig. 8(B). There is no feedback be-
cause in this range $e_f' > e_a'$ and the diode
 D is nonconducting. The potentiom-

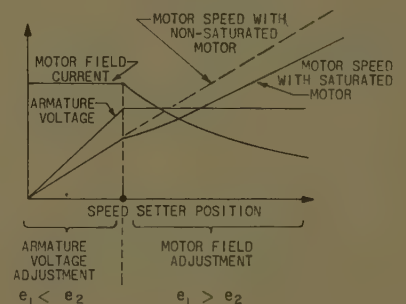


Fig. 7. Curves for motor field current, armature voltage, and motor speed versus speed setter position

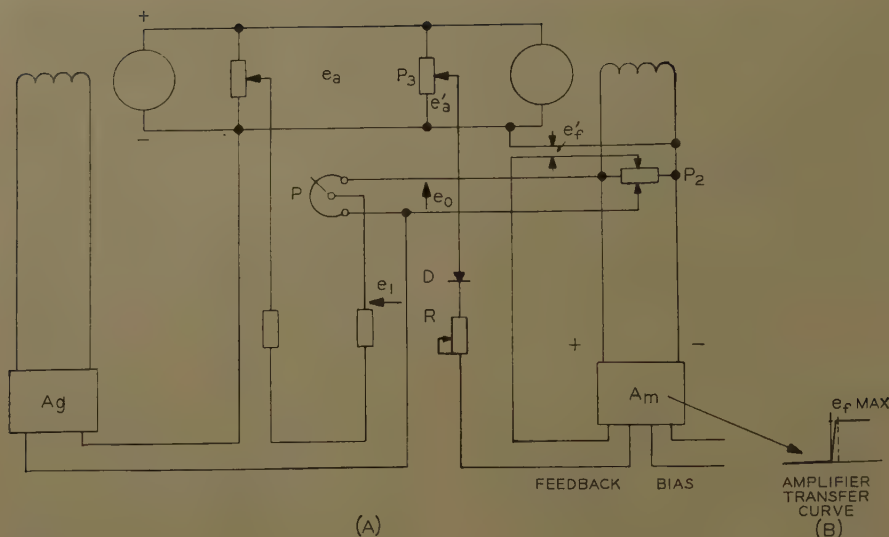


Fig. 8. Schematic diagram for simplified crossover without tachometer feedback

eters P_2 and P_3 and the resistor R are set so that when e_a with increasing displacement angle θ of the speed setter P approaches the rated value $e_{a\max}$ a feedback current will flow to A_m , decreasing the motor field voltage.

The control operates as the schemes shown in Figs. 6(A) and (B) except that the crossover is somewhat less sharp and the dependence between armature circuit and motor field circuit is greater; however, it can be shown that stability is not a problem if R is set so that e_a increases slightly with decreasing field current. The scheme is a little more susceptible to drift than the other schemes but it has been proved for a large number of applications. One of its great advantages lies in the small number of components required by the control, as a result of which it is noncomplex and extremely reliable.

Figs. 6 and 8 comprise a family of three tachometer-free crossover schemes of varying complexity for varying requirements. They are all compatible with standard current-resistance drop compensation schemes and current limit circuits. If special precaution is taken in the connection, they are also compatible with standard timed acceleration-deceleration schemes of the electronic and transistor types. Because it is very often desirable to use timed acceleration-deceleration, special consideration is given in this discussion to the problem.

As a general rule, most acceleration-deceleration circuits for adjustable speed d-c drives are, like the one shown in Fig. 9(A), interposed between the speed setter and the first-stage amplifier feeding both armature voltage control and motor field control. When the input signal to the acceleration circuit changes, the output

also changes, but at a slower rate, determined by the internal characteristics of the acceleration circuit.

If the acceleration control shown in Fig. 9(A) is applied between the speed setter and the amplifier A_g in the scheme of Fig. 8, the control works very well in the armature voltage range of speed control, but above base speed acceleration control is lost, and the motor field weakens immediately in response to a rapid increase in speed setter position.

To understand this action, it is necessary to remember that above base speed the armature voltage from the generator is essentially constant. When the speed setter is suddenly advanced above base speed, the input the acceleration circuit increases, and the output will begin to increase slowly. However, only a slight increase in the output of the acceleration circuit is needed to increase the armature voltage so much that the feedback signal through diode D is large enough to turn the motor field amplifier off. The field will weaken almost immediately, just enough to make e_1 equal e_1' . Thus, if the scheme of Fig. 9(A) combined with Fig. 8 is used above base speed, the new speed will be obtained immediately without any control of the acceleration in spite of the presence of an acceleration control unit. It can therefore be seen that a standard acceleration circuit cannot be used in the usual way on this type of crossover circuit.

Fig. 9(B) shows how a timed acceleration-deceleration control must be connected to the basic scheme of Fig. 8(A).

The voltage signal e_b is a bias voltage equal to the value of e_0 at full field. Thus, below base speed, the potential of the points A and B are equal and the control

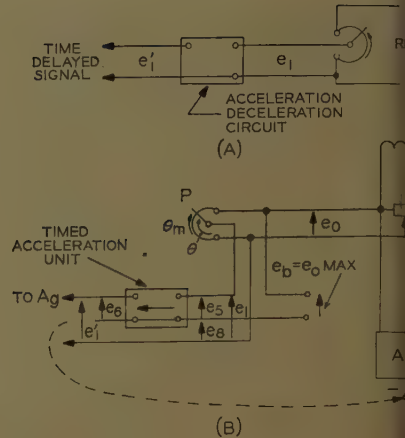


Fig. 9. Acceleration-deceleration control. A—Normal connection. B—Connected crossover without tachometer feedback

operates in this range exactly as applied to a drive without field weakening. In the field-weakening range the operation can best be illustrated by calculating the response to a step change $\Delta\theta$ in the speed setter displacement angle θ . Assuming that the control is a log-acceleration control unit with time constant T ; assuming that the time lag in amplifiers and in feedbacks is negligible compared with T (a reasonable assumption), and let the gain from signal e_1' back to the signal be k ; then

$$e_0 = k(e_f - e_1')$$

$$e_0 = e_b + e_8$$

$$e_1 = e_0\theta/\theta_{\max}$$

$$e_1' = e_6 + e_8$$

$$e_1 = e_6 + e_8$$

$$e_0 = e_6 + Tde_6/dt$$

Considering incremental changes of the equations yield

$$\Delta e_0 = e_0\Delta\theta/\theta_{\max} (1 - e^{-t/T'})$$

A step change in θ is represented by and

$$T' = T\theta_{\max}/\theta$$

The corresponding incremental change in speed $\Delta\omega$ will be

$$\Delta\omega = \Delta\omega_f(1 - e^{-t/T'})$$

where $\Delta\omega_f$ is the final change in speed. Equation 9 shows that in response to a step change in speed setter position speed will change smoothly until the new speed is reached but that the rate of change will be different from the rate of change in the armature adjustment range. The different rate of change in the armature voltage range and in the field-weakening range has usually proved acceptable.

A Set of Standard Specifications for Linear Automatic Control Systems

J. E. GIBSON
MEMBER AIEE

Z. V. REKASIUS
ASSOCIATE MEMBER AIEE

E. S. McVEY
ASSOCIATE MEMBER AIEE

R. SRIDHAR
NONMEMBER AIEE

C. D. LEEDHAM
NONMEMBER AIEE

A WIDESPREAD FEELING exists throughout the automatic control field that the art has matured to the point where standardization of performance specifications should be considered. In fact, during a 2-year study in which contact was made with approximately 100 control system vendors, only once were the authors told that the problem was unimportant. This paper reports on the first portion of the study: linear systems. The specifications discussed fall naturally into three groups: frequency domain, time domain, and generalized performance indices. Recommendation of a nonconflicting set of specifications is made in these groups. In addition, a discussion of statistical specifications and recommendations on data presentation are given.

Two points should be made at the outset. First, while a fairly complete discussion of recommended specifications is attempted, space limitations prohibit inclusion of those rejected. Second, specifications meant for industry-wide acceptance must not invade the province of design; that is, they must not dictate design techniques and procedures, but rest solely on input-output measurements. Only those specifications necessary to performance of a particular system are to be called out.

Finally, the authors admit some precipitation in beginning this task; attempting to mediate, as it were, between innumerable armed and warlike camps of implacable servo designers. They discovered, however, an excellent spirit of

co-operation and a feeling that the time is ripe for such an attempt.

Nomenclature

Definition of symbols used throughout the paper is introduced here for reference.

BW=bandwidth
C=output from control system
D-R factor=deviation reduction factor
E=error signal
 ϵ_{ss} =steady-state error
FVE=final value of error
G=open-loop transfer function; see Fig. 1
IAE=integral of absolute error
IRAR=impulse response area ratio
ISE=integral squared error
ITAE=integral time absolute error
ITSE=integral time squared error
ISTSE=integral squared time squared error
ISTAE=integral squared time absolute error
K=direct-current loop gain
 K_bH =feedback transfer function
 K_fG =forward transfer function
 $K_{(n)}$ =error constants
L=compliance
LD=logarithmic decrement
 M_p =peak overshoot of absolute output-input ratio
PO=per cent overshoot
Q=load disturbance
R=input to control system
 T_1 =time for output to first reach final value after step input
 T_D =delay time
 T_p =time at which peak overshoot occurs after step input
 T_R =rise time
 T_S =settling time
 T_t =sum of delay time, and one half the rise time
Z=output impedance
 α =damping factor
 ζ =damping ratio
 ω =real frequency
 ω_p =peak frequency (frequency at which M_p occurs)

Operational Definition of a Quasi-Linear System

The assumption that a system is linear is made frequently in analyzing actual control systems, implying that the system can be described by either one or a set of linear differential equations with constant coefficients. Strictly speaking, sys-

tems with time-varying coefficients can be linear. Since, however, their analysis and behavior is in many respects similar to the nonlinear systems, they will not be considered as linear in this paper.

The mathematical criterion to prove that a system is linear is the principle of superposition.¹¹ The experimental application of this criterion cannot, however, be used to prove linearity since any system will become nonlinear for sufficiently small or sufficiently large inputs. The use of a linear mathematical model in the analysis of a practical control system simplifies appreciably the procedure of analysis. For the same reason (simplicity), such models are used in this paper to arrive at a set of specifications for actual control systems. If a practical system deviates slightly from its linearized model, its response will closely resemble the response of an ideal, or linear, system and may fall within the specifications of such a system. If the nonlinearities are pronounced, the response may deviate considerably from that of a linearized model and, consequently, specifications for linear systems may no longer be applicable.

The purpose of control system specifications is to assure satisfactory response over a range of inputs which the system is expected to follow. Hence, from the point of view of specifications, a system will be considered linear if its response lies within the tolerances placed upon the linear specifications recommended for its idealized (linearized) mathematical model.

The convenience of mathematical analysis cannot justify the requirement that an actual control system be linear. As long as the response of an actual control system does not differ appreciably from the specified response of the linear system, however, no basis exists for discriminating such a system against an idealized one.

In all practical cases, the system inputs will be bounded in magnitude. As long as the response satisfies the specifications for linear systems, pronounced nonlinearities of the servo system are immaterial. If, however, the expected inputs exceed the range of input magni-

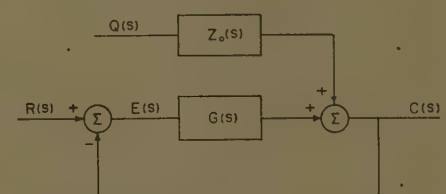


Fig. 1. Block diagram of system with load disturbance

per 61-78, recommended by the AIEE Feedback Control Systems Committee and approved by the AIEE Technical Operations Department for presentation at the AIEE Winter General Meeting, New York, N. Y., January 29-February 3, 1961. Manuscript submitted November 1, 1960; made available for printing December 1, 1960.

J. E. GIBSON, Z. V. REKASIUS, E. S. McVEY, R. SRIDHAR, and C. D. LEEDHAM are all with Purdue University, Lafayette, Ind.

The research upon which this paper is based was supported by the Air Research and Development Command, Air Force Materiel Development Center, Holloman Air Force Base, N. Mex., J. Engelbach, project engineer; Contract AF 500-1933.

$$\frac{C(j\omega)}{R(j\omega)}$$

$$\frac{C(o)}{R(o)}$$

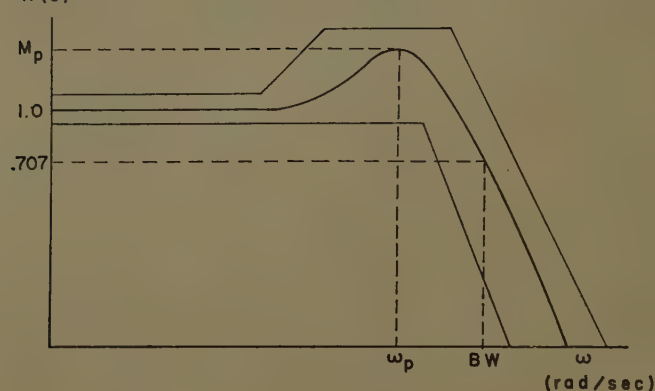


Fig. 2. Frequency response enclosure diagram

tudes over which the linear system specifications are to be applicable, additional specifications—based on a nonlinear mathematical model of the system—will be necessary to assure satisfactory performance.

Since the recommended specifications for linear systems are based upon step and sinusoidal inputs, the range of magnitudes of these inputs, within which the specifications are to be met, must be specified.

The criteria outlined are intended for use only in deciding the applicability of linear system specifications to actual control systems; not for equivalent linearization in the analysis of nonlinear systems.

Frequency Domain Specifications

Four specifications, which deal with frequency response characteristics of a system, are recommended:

1. M -peak (M_p).
2. Peak frequency (ω_p).
3. Bandwidth (BW).
4. Peak output impedance (Z_p).

Several other frequency domain specifications were considered but are not recommended. These are: gain margin, phase margin, crossover frequency, compliance, carrier frequency, gain-bandwidth product, error constant-bandwidth ratio, average value of time delay, and deviation ratio.

Only those specifications that have direct interpretation in terms of closed-loop system performance were chosen; others offered no unique value to make their inclusion desirable. The number recommended was kept to a minimum to avoid possible overspecifying of the system. Also, some performance characteristics, such as speed of response and accuracy, can be better dealt with in the time domain.

It is recommended that closed-loop frequency response data be presented in the manner indicated by Fig. 2. The tolerances on the recommended frequency domain specifications are used to establish the main outline of the "box" which encloses the frequency response. A specific form for the enclosure or box cannot be specified because the shape of the response varies from one system to another and the required characteristics depend upon a specific application. It should be noted that Fig. 2 is a log-log plot and that the response magnitude is normalized.

General agreement appears to have been reached on the definition of the M -peak specification. M -peak is defined as the maximum value of the closed-loop transfer function. The recommended definition, however, is the normalized M -peak,

$$M_p = \max \left| \frac{C(s)}{R(s)} \right| \quad (1)$$

$$s = j\omega$$

where

ω = frequency in rad/sec (radians per second)
 $C(s)$ = Laplace transform of output
 $R(s)$ = Laplace transform of input

M -peak is a relative stability specification. The input of a control system may contain periodic components near the frequency at which the M -peak occurs. Hence, it is necessary to restrict the amplification to a tolerable magnitude so that the system will not destroy itself. With time domain, as with gain and phase margin specifications, it is difficult to guarantee that the response to sinusoidal inputs will stay within tolerable bounds. The M -peak specification has a unique property of placing restrictions on the worst possible steady-state response to

periodic inputs. Hence, it is the most reliable measure of the degree of system stability.

The normalization of M -peak is accomplished by dividing the maximum magnitude of the closed-loop transfer function by the magnitude at sufficiently low frequencies where the transfer function is essentially flat. The normalized M -peak is a dimensionless number. Without normalization, the value of M -peak in unity feedback systems would depend upon the dimensions of input and output variables. Hence, the M -peak must be normalized in order to have a meaningful comparison of stability of different systems.

Peak frequency ω_p is defined as the frequency in rad/sec at which M -peak occurs. The term resonant frequency is often used to designate ω_p . Resonance, however, is also defined as the frequency at which the output of a network is in phase with the input, which is not the same as the definition given for M -peak. Hence, confusion may be avoided if the term "resonant frequency" is not used to specify ω_p .

Peak frequency may have little, if any, importance in most systems and need not always be specified. It is recommended only for cascaded systems which, with the same ω_p , will amplify an input of frequency ω_p by a factor equal to the product of all the individual system M_p 's. In such cases, ω_p together with a bandwidth (BW) specification may be used to insure satisfactory sinusoidal response characteristics. In general, however, an M -peak specification need not be accompanied by ω_p .

There is no general agreement in the automatic control field regarding bandwidth. The bandwidth concept is borrowed from the field of communications electronics, where it is defined as the frequency range between two half-power frequencies near resonance. K pfm ller, therefore, uses the term border frequency (*Grenzfrequenz*) to designate what is called bandwidth in control systems.² However, the use of bandwidth for what should more correctly be called border frequency has become a tradition in control system literature, and an attempt to correct the terminology seems to be a hopeless task. The following definition is recommended in this paper: Bandwidth is the range of frequencies in rad/sec between zero and the frequency of which the normalized closed-loop transfer function has the magnitude of 0.707, or 3 decibels down. The latter is referred to as the half-power frequency.

In view of recommended time domain specifications including the system's speed

response and peak frequency, the need for a BW specification is not obvious. However, it should be recalled that a given system may follow satisfactorily the step changes in input although its response to periodic or nearly periodic inputs may still be unsatisfactory, as shown in Table I. Therefore, while the tendency of the designer or vendor may be to keep the system bandwidth to a minimum—the anti-high-fidelity philosophy of control system synthesis—in order to minimize the cost, the user may require sufficient speed of response for other than step inputs; e.g., ramp, etc. This may require specification of a range of frequencies of inputs (minimum BW), which the system should be able to follow. On the other hand, if noise is expected to contain a predominant frequency component, a BW specification, together with peak frequency specification, can guarantee sharp cutoff or rejection of noise.

Any simple example of a second-order system can show that the relationship between BW and either rise time, delay time, or settling time involves circuit parameters of the system. For several possible BW definitions, examples have been worked out, using ITAE optimum zero-velocity and zero-position systems to show that the correlation between the domain specifications and BW is unsatisfactory, as seen in Table I. For example, increase in BW is accompanied by shorter rise time in the zero-position error systems and a decrease in zero-velocity error systems.

The correlation can be obtained only in the case of the ideal rectangular filter, which is not realizable physically.² Hence, time domain specifications do not, in general, assure satisfactory BW.

The concept of compliance ("stiffness" sometimes used to designate the reciprocal of compliance) represents an attempt to secure satisfactory performance of systems with time-varying parameters. Variation of load, or load disturbance, can always be represented as a change in system parameters. Unfortunately, expressing time variation of

system parameters in terms of load disturbance is difficult.

Compliance, a time domain specification, is defined as³

$$L \triangleq \frac{\frac{C(t)}{C_{\max}'}}{\left| \frac{Q}{Q_{\text{rated}}} \right|} \quad (2)$$

An analogous specification in the frequency domain is the compliance frequency function, defined as

$$L(j\omega) \triangleq \frac{\frac{C(j\omega)}{C_{\max}'}}{\left| \frac{Q(j\omega)}{Q_{\text{rated}}} \right|} \quad (3)$$

where

$C(j\omega)$ = sinusoidal output resulting from load disturbance

C_{\max}' = maximum value of time derivative of output; e.g., rated speed of motor

$Q(j\omega)$ = sinusoidal load disturbance

Q_{rated} = rated load of system

Output impedance is defined as

$$Z(j\omega) = \frac{C(j\omega)}{Q(j\omega)} = \frac{Z_0(j\omega)}{1 + G(j\omega)} \quad (4)$$

where

$G(j\omega)$ = the open-loop transfer function; see Fig. 1

and

$$Z_0(j\omega) = \left. \frac{C(j\omega)}{Q(j\omega)} \right|_{E(j\omega)=0} \quad (5)$$

is the open-loop output impedance, without the corrective action of the feedback loop.³

Comparison of equations 3 and 4 shows that compliance frequency function is nothing more than the normalized output impedance; hence, a separate specification for each is unnecessary.

The compliance transfer function has an advantage over output impedance in that it enables qualitative comparison of two systems, operating under different rated loads and output speeds. Output impedance, however, is more appropriate when comparing systems which are per-

forming the same function. The numerical value of compliance transfer function depends upon the rated values of load and response which cannot be precisely defined. Output impedance is free from this ambiguity. Hence, the loading effects on servosystems should be specified in terms of output impedance rather than compliance.

In instrument servomechanisms, the loading effect is negligible and consequently no output impedance specifications are necessary. Where a control system drives an appreciable load, a change in the load may seriously affect system stability. In such cases, the system should be designed to meet all the specifications, other than output impedance under specified rated load. If the load is expected to vary appreciably, additional specifications must be used to guarantee that the system will still follow the input in a satisfactory manner. Speed of response to a load disturbance is of secondary importance; ideally, no response is desired. Accuracy and stability considerations, however, may be required to minimize the effect of load disturbance. Restriction on loading effects in the time domain would not be sufficient, for the worst effects on output may occur because of periodic variations in load.

Hence, the frequency domain specification of maximum magnitude of the output impedance (Z -peak) is recommended for systems that are expected to operate under appreciable variations in load. Z -peak is defined as the maximum value of the magnitude of the output impedance function $Z(j\omega)$ as given by equation 4. No other loading specifications are recommended.

Time Domain Specifications

RECOMMENDATIONS

The time domain specifications listed below are those found most frequently in the literature. All can be interpreted directly in terms of time response, and are meaningful for systems with deterministic inputs. This list includes: delay time T_D , rise time T_R , time for output to first reach final value T_1 , time at which peak overshoot occurs T_p , damping ratio ζ , damping factor α , logarithmic decrement $\cdot LD$, settling time T_s , percentage overshoot PO , final value of error FVE , conventional error series, compliance or output impedance, and deviation reduction factor.

The word conventional, as used in association with error series, implies that the series is a power series, written in

Table I. Correlation Between Bandwidth and Time Domain Specifications for Optimum ITAE Systems

System		BW, Rad/Sec	$\frac{\pi}{T_R}$	$\frac{\pi}{T_D}$	$\frac{\pi}{T_t}$	T_R , Sec	T_D , Sec
Type	Order						
Position	2nd	1.01	1.43	2.12	1.23	2.20	1.48
	3rd	1.03	1.73	1.42	1.10	1.81	2.20
Velocity	4th	0.90	2.04	1.10	1.00	1.54	2.86
	2nd	2.05	3.93	10.08	3.88	0.80	0.81
	3rd	1.89	3.61	4.19	2.64	0.87	0.75
	4th	1.77	3.14	2.96	1.93	1.00	1.06

terms of positive powers of a complex variable and expanded about the point where the variable is zero; or in any equivalent form.⁴ It is possible to derive a similar power series for the error, expanded about the point where the variable is infinite. Such a series is termed nonconventional.

Five specifications, chosen from the foregoing list, are recommended for general use:

1. Delay time (T_D).
2. Rise time (T_R).
3. Settling time (T_S).
4. Percentage overshoot (PO).
5. Final value of error (FVE).

These quantities should be specified, together with their maximum or minimum values or their tolerance, as is dictated by the requirements of a particular system.

Using some or all recommended specifications, a region can be defined in the output magnitude-time space within which the system average response must fall. The particular interpretation to be placed on the word "average" and the reason for its inclusion is explained in the next section, where T_D , T_R , T_1 and T_p are discussed.

Using all five specifications, a region of the form shown in Fig. 3 will be defined for a step input. This choice of boundaries is not the only one possible,⁵ but boundaries should be related to some or all of the recommended specifications and with the requirements of a particular system in mind. Constraint of the required time response in this fashion is recommended after consultation with the control industry and the realization that such methods are used and are effective.

Interrelationships exist between the recommended time domain specifications and other recommended specifications;

e.g., frequency domain specifications. The severe restrictions that must be placed on these interrelationships in practical systems, however, preclude their recommendation for general use.

TIME—DELAY, RISE, FINAL VALUE, AND PEAK OVERSHOOT

The quantities T_D , T_R , T_1 , and T_p are related to the initial transient response of a control system when excited by a step at the input. The first two named appear to have been borrowed for control system applications from the theory developed earlier for filters in communication networks. Close similarity between the function of a control system transfer function and a communication filter justifies the plagiarism. Furthermore, precise relationships exist between T_D and T_R and characteristics of the filter for the case of an ideal filter and an ideal change in input.^{2,6,7} The fact that an ideal communication filter cannot be built and that ideal control systems do not exist does not necessarily dictate a change in the basic definition.^{3,8-10} A definition makes a strong foundation if it is supported by a precise mathematical derivation for the ideal case, and if it is readily interpretable for the usual deviation from the ideal in actual systems. Such is the case for T_D and T_R , defined mathematically in references 2, 6, and 7 and approximated for actual systems in references 3, 8, 9, and 10.

T_D = time elapsed, after application of step input, until the *average* output reaches half its final value

T_R = projection, on the time axis, of that part of the tangent to the *average* response curve, at $t = T_D$, that lies between zero and the final value

The time scale chosen should be such that the tangent, in the definition for T_R , is at an angle close to 45 degrees to

the positive time axis, thus minimizing measurement errors.

These definitions, excluding the word *average*, are not always satisfactory, however, because response to a high-order system may well be far from smooth. With this type of response, the literal interpretation of either of the definitions could give an uncertain or a misleading result.

The ambiguity can be removed and the definitions made meaningful if they are applied to an *average* response, obtained by drawing the best smooth curve through the actual response. The recommended definitions are, therefore, those previously written, including the word *average*.

It is impossible to relate specifications T_1 and T_p to any other characteristics of the filter, even in the ideal case, and they add no significant information as to characteristics of the initial transient response. Therefore, they are not recommended as general specifications.

The precise relationships between T_D and T_R and the characteristics of an ideal filter or transfer function do not exist for most physical systems. The correlation is poor, even with second-order systems; consequently, time-frequency domain relations are not recommended.

DAMPING RATIO, DAMPING FACTOR, LOGARITHMIC DECREMENT, SETTLE TIME, AND PER CENT OVERSHOOT

These specifications are concerned with the oscillatory nature of a system response about its final value.

When a system is disturbed, it is necessary to know how fast the resulting transient will decay, or, alternatively, how much time will elapse before the transient falls below any given value. For a second-order system, damping ratio,³ damping factor or damping constant,¹ and logarithmic decrement¹⁰ are defined and can be used to indicate the duration of the transient. For high

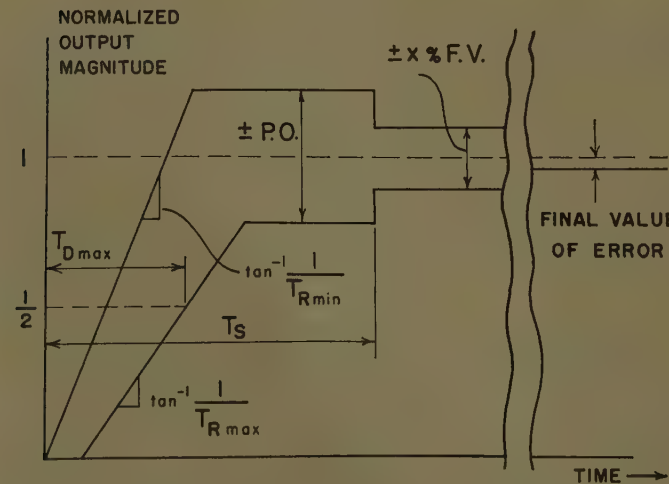


Fig. 3. Diagrammatic representation of recommended specifications

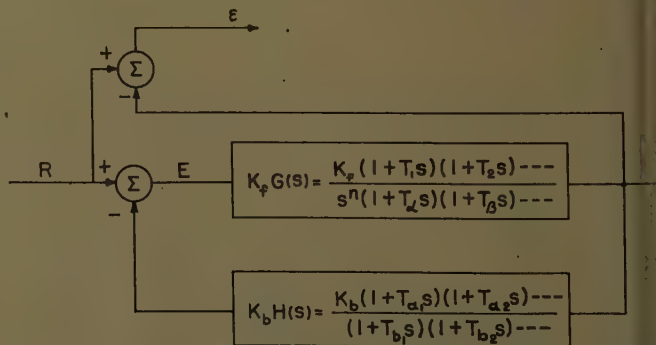


Fig. 4. A system reduced to forward and feedback transfer functions

der systems, these quantities lose their significance. It is possible, however, to define an equivalent damping ratio for systems of higher order than the second. To do this, some other criteria, usually a performance index such as $IRAR$,¹⁹ is calculated for the higher-order system, and the damping ratio of the second-order system that would give the same value of the performance index is assigned as the equivalent damping ratio. However, correlation between high-order systems of the same equivalent damping ratio is poor.¹³

These facts prevent the use of quantities ξ , α , and LD as general system specifications. Nevertheless, the rate of transient decay must be specified and a time chosen after which the transient effect can be considered small. To do this, a range of magnitude about the final value is chosen, the extent of which must depend on the requirements for each particular system. Settling time is defined as:¹⁴⁻¹⁶

T_s = the time elapsed after application of a step input until the response of a system falls to, and remains within, $\pm x\%$ of its final value. Where x is to be specified for each particular system under consideration, $x=5$ is a typical value

Systems are designed, frequently, to meet the specifications of time delay and rise time, which have already been discussed, and for certain classes of systems, these times will be short. It is conceivable that, with a short rise time, the system overshoot will become large and reduce the system effectiveness. It is evident, without further justification, that response of this nature must be controlled.

Any specification for the control of overshoot must necessarily include information as to the magnitudes of the response final value and of the comparative overshoot. Therefore, a natural choice is the fraction that results from a comparison of the overshoot with the final value. The quantity can be expressed, conveniently, as a percentage overshoot.

$$O = \frac{\text{maximum value of response} - \text{final value}}{\text{final value}} \quad (6)$$

FINAL VALUE OF ERROR AND CONVENTIONAL ERROR SERIES

The specifications of this paragraph are concerned with the system's ability to follow input commands with accuracy. A system may possess a fast response, good dynamic behavior, etc., but it may not be completely satisfactory unless it is statically accurate; at least, limits of

static accuracy are necessary. The static accuracy can be measured in terms of FVE which is defined as

$$\epsilon_{ss} = \lim_{t \rightarrow \infty} \{e(t)\} = \lim_{s \rightarrow 0} \{se(s)\} = \lim_{s \rightarrow 0} \times \left\{ sR(s) \left[\frac{1 + K_f K_b G(s) H(s) - K_f G(s)}{1 + K_f K_b G(s) H(s)} \right] \right\} \quad (7)$$

where

$$\begin{aligned} R(s) &= \text{input} \\ K_f G(s) &= \text{forward transfer function} \\ K_b H(s) &= \text{feedback transfer function} \end{aligned}$$

The gain constants, associated with the over-all transfer functions, are separated out as they play a special part in the calculation of error. It is important to note that the error associated with a control system is defined

$$\text{error } \epsilon = C_d - C \quad (8)$$

where C is the system output variable and C_d the desired value of the output variable. With linear systems, the desired value C_d is related, linearly, to the input variable R ; i.e., $C_d = f(R)$ where f is a linear function, or $C_d = kR$ where k is a constant.

If the system is one of unity feedback, the constant k is unity and dimensionless. The error as defined in equation 8 and the system actuating error are now identical quantities and are given by the relation $E = \epsilon = R - C$. For certain nonunity feedback systems, the constant k is also unity and dimensionless. The system error, but not the actuating error, is then also given by $\epsilon = R - C$.

Equation 7, defining steady-state error, is derived from these latter relations,³ thus allowing for all systems that have been

reduced to a forward and a feedback path and for which k is unity and dimensionless.

If the system can be reduced to one of unity feedback, some simplification results. The system errors for deterministic inputs $R(s) = A/s^n$, termed type- n inputs, and for all systems classed according to the number of free integrations in the transfer function are easily calculable in a well-known fashion which need not be detailed here. The errors and error constants, K_0, K_1, \dots, K_n , are tabulated in many references; see reference 10, p. 145.

Alternatively, if the system is of the form shown in Fig. 4; i.e., reduced to a forward path and a feedback path, the determination of error follows a similar pattern but with some added algebraic complexity. The steady-state error of these nonunity feedback systems can be evaluated, directly, by taking the limit in equation 7. It is also possible to generate, mathematically, an equivalent unity feedback transfer function from the known forward and feedback transfer functions and then apply the definitions for the error constants.

The unity feedback system that will be generated from systems of the form displayed in Fig. 4 will either have one free integration, or it will be without free integrations in the transfer function. The only finite error constant is therefore, K_0 unless $K_b = 1$; then, K_0 approaches infinity and K_1 is the only finite error constant. Thus, systems of this form with time constants in the feedback path cannot be expected to follow inputs greater than type 2 with finite error.

Feedback transfer functions with

Table II. Steady-State Errors for Nonunity Feedback System $K_b = 1$

Type of Input	Type of Forward Transfer Function			
	0	1	2	3
0	0	0	0	0
1	$A \frac{1}{1 + K_f}$	0	0	0
2	∞	$A \left[\frac{1}{K_f} + \sum_{n=1}^N T_{a_n} - \sum_{n=1}^N T_{b_n} \right]$	$A \left[\sum_{n=1}^N T_{a_n} - \sum_{n=1}^N T_{b_n} \right]$	
3	∞	∞	∞	

Table III. Steady-State Error for Nonunity Feedback System $K_b \neq 1$

Type of Input	Type of Forward Transfer Function		
	0	1	2
0	0	0	0
1	$A \frac{[1 + K_f K_b - K_f]}{1 + K_f K_b}$	$A \left[1 - \frac{1}{K_b} \right]$	$A \left[1 - \frac{1}{K_b} \right]$
2	∞	∞	∞
3	∞	∞	∞

factors of type s^n , where s is a positive or negative integer, are not considered because they are of little use in control applications.

The errors that result from systems of the type in Fig. 4 have been generalized for different types of inputs, and are displayed in Tables II and III.

Therefore, in expressing the degree of accuracy of any system for deterministic inputs, the rule is to:

Specify directly a region about the input quantity, referred to the output terminals, within which the steady-state value of the response must remain.

Or, for systems where $C_d = R$; i.e., k equals unity and is dimensionless, to:

Specify the error constants and associated tolerances which contain, in a concise form, the information necessary to determine accuracy.

The conventional error series and, in particular, the error coefficients, describe the value of a system's error when a "long time" has elapsed following application of the input. The accuracy with which the error is described, compared with the number of terms of the series considered, depends on two factors: first, on the behavior of the derivatives of the input (here, the faster the magnitude of these derivatives decreases, the fewer terms will be required), and second, on the magnitude of the loop gain K (here, in general, the greater the value of K , the smaller the successive coefficients and the fewer the terms that will be required).³

Three procedures are available for determining coefficients,³ each of which requires knowledge of the system's forward and feedback transfer functions in algebraic form. Each requires algebraic manipulation, which for anything but the simplest system, does not fall far short of that necessary to determine the error exactly by taking the inverse Laplace transform.

One method for defining and determining the error coefficients is to take time moments of area of the system error impulse response.¹⁴ These moments of area, i.e., coefficients of the error series, can be interpreted in terms of the rise time and delay time of the whole system to a step response.¹⁷ This interpretation is, however, restricted to systems where the error impulse response decreases monotonically towards zero, or, in the terminology of second-order systems, where the damping is greater than critical damping. The interpretation, furthermore, is restricted to systems with error impulse response symmetrical about a time equal to the delay time. These restrictions appear to eliminate use of these rela-

tions in practical systems. As an example, there is a 19% error, compared with the true delay time, when a step is applied to a second-order system that is critically damped and the delay time is calculated from the conventional error coefficients.

The preceding remarks indicate that the conventional error series and its coefficients have limited value for either specification of the error itself or for estimation of rise time, delay time, etc., and are not recommended for use in specifying systems.

OUTPUT IMPEDANCE AND DEVIATION REDUCTION FACTOR

Compliance or output impedances undoubtedly can be considered as functions of time, but, in the authors' opinion, they are more appropriately considered as functions of frequency and have been discussed in that section of this paper.

Deviation reduction factor, suggested by Rutherford,¹⁸ is defined

$$D-R \text{ factor} = \frac{\text{potential deviation}}{\text{actual deviation}} \quad (9)$$

where potential deviation is the error that results, as time approaches infinity, between the controlled and the required variable, because of a step disturbance with the system open loop. The actual deviation is the maximum value of this same error, but with the system operating closed loop.

The quantity is a measure of system effectiveness in smoothing disturbances, but suffers from the disadvantage of becoming infinite should the system under consideration be open-loop unstable, no matter whether the system is closed-loop stable or not.

There are no advantages to this specification, and it does not add to the information given by other recommended specifications; e.g., output impedance. Consequently, it is not recommended for use.

Performance Indices

A performance index or figure of merit has been defined by Anderson, et al.,¹⁹ as: "Some mathematical function of the measured response, the function being chosen to give emphasis to the system specifications of interest." A performance index is a single number in which a designer attempts to place his engineering judgment. The performance index may be chosen so that only one or a few system properties affect its value. Or, it may be chosen so that a designer attempts to place his whole engineering judgment in a

single number; i.e., the performance index is a function of all properties of a system's response. This type of performance will be defined here as a general performance index. In this paper, performance indices will be considered only for this general case. If a performance index is rejected as a general performance index, this does not mean that it is unacceptable for specific cases.

Control engineers have been interested in performance indices for more than a decade. This interest has received a new impetus from recent research on adaptive control systems. The purpose of using performance indices in adaptive systems is the same as for previous work, namely, for any given set of conditions, to determine the optimum values of system parameters which are at the command of the designer or adaptive system. The performance index replaces the usual design specifications for system response.

It is impossible to define a general practical performance index which would be considered perfect by all control engineers. This is because performance indices are adjudged good or bad, depending upon the response characteristics of systems when they are optimized by the performance index; and, control engineers are not in complete agreement as to what constitutes the best general system. Because no control system is perfect (i.e., the response is not identical to the input for all inputs), one performance index will emphasize some properties of the response more than others. It is this matter of trading one part of the response off against another part that causes control engineers to disagree. There are a few general rules which can be followed in the selection of a general performance index, but they too depend upon individual judgment so that the results are debatable. These rules are an elaboration upon comments by Graham and Lathrop:²⁰

1. A general performance index should lead to systems of higher orders, as well as second order, which judgment indicates are good systems when their over-all response is considered. This property is called reliability.
2. A performance index should be selective. That is, the optimum value of system parameters should be clearly discernible from some characteristic such as a minimum, zero, or maximum value of a plot of the performance index value versus system parameters.
3. The ease with which a performance index can be applied is a consideration.

A number of performance indices have been considered with the hope that one or more of them could be recommended.

for general use. The results of the study are shown in Table IV.

In conclusion, none of the performance indices considered can be recommended for general use at this time. *TAE*, *ITSE*, *ISTAE*, and *ISTSE* are the best of those considered, and may be used only after careful study with the system or family of systems of concern. In any attempt to apply these four performance indices to general work, they should serve only as an aid in engineering judgment—not as an absolute guide. Further study is in progress, and the results will be published in a few months.

Specifications of a Control System on a Statistical Basis

The ever-increasing prominence of control system design based on statistical theory raises the question whether the performance of a system may be specified statistically. Before this question is answered, it may be worthwhile to discuss briefly the statistical design methods presently available.

This discussion will be restricted to linear, time-invariant lumped parameter systems. The present methods of statistical analysis of control systems have stemmed from the work of Wiener³³ in connection with optimum physically realizable filters. Wiener defined optimum in the basis of a minimum mean square error (mse) when the input is a stationary random process obeying the ergodic hypothesis. Here, error is defined as the difference between a desired output and the actual output. The desired output is some function of the input. The minimum mse is now widely adopted to define an optimum control system for statistical design. However, various other criteria have been proposed by different authors. For instance, Zaborzky and Diesel³⁴ suggest a generalized error criterion which is applicable for both deterministic and random inputs. They show that most of the other known performance criteria are special cases of their general criterion.

There is no loss of generality in considering subsequent arguments on the basis of a system designed for a minimum mse, since the latter is widely accepted in control literature. Most of the arguments are, however, valid for other types of criteria.

One of the serious limitations of the mse criterion for optimization is that it is doubtful at the present moment whether it does yield the best system. This statement by Johnson³⁵ is self-explanatory.

Table IV. Classification for Performance Indexes

Performance Index	Mathematical Formulation	System Input	References	Comments	Recommendation
<i>IRAR</i> (impulse response area ratio)	$IRAR = -\frac{A}{A} + \frac{A}{A}$ $A \rightarrow$ positive area under impulse response curve $A \rightarrow$ negative area under impulse response curve	impulse	19	Good for second-order systems. Poor correlation between <i>IRAR</i> and system response characteristics for higher-order systems.	
Logarithmic decrement	$LD = \frac{(1 - \xi^2)^{1/2}}{2\pi\xi}$ system	impulse or step	12	Logarithmic decrement for a second-order system is $LD = 2 \log IRAR$. It has the same deficiencies as <i>IRAR</i> and, in addition, is sensitive to irregularities in the response waveform.	
Control area	$\int_0^\infty e(t) dt$	step	21, 22	Control area $= 2\xi$ for a second-order system. Extremal values do not indicate that system is optimum. Criterion gives difference of positive and negative area under error curve.	
Weighted control area	$\int_0^\infty e(t) dt$	step	22	Extremal values do not indicate optimum system. If zero value is taken as optimum, systems result that are underdamped.not recommended
<i>IAE</i> (integral of absolute value of error)	$\int_0^\infty e(t) dt$	step	23	<i>IAE</i> is adequate for a second-order system but has inadequate selectivity for higher-order systems.	
<i>ISE</i> (integral of squared error)	$\int_0^\infty e^2(t) dt$	step	24	<i>ISE</i> has poor selectivity. Optimum systems tend to be underdamped. Used mainly because of mathematical convenience. With appropriate modification, criterion can be used with stochastic inputs.	
Solution time		step	25, 26	Adequate for second-order systems. Higher-order optimum systems are underdamped.	
Fett's criteria		step	20, 26	Inadequate selectivity. Has no meaning for overdamped system.	
Beta	signal feedback to input divided by output signal	sinusoidal	27, 28, 29	Used with electronic feedback amplifiers but not with electromechanical systems.	
<i>ITAE</i> (integral of time multiplied by absolute value of error)	$\int_0^\infty t e(t) dt$	step	20, 30, 31	Selects good type-1 systems (systems with 1 integration in open-loop transfer function). Type-2 systems have excessive overshoot. Graham and Lathrop studied unity numerator systems through the eighth order.	
<i>ITSE</i> (integral of time multiplied by squared error)	$\int_0^\infty te^2(t) dt$	step	20	This criterion has not been studied extensively. However, all results available indicate that it is one of the more valuable performance indices.	...qualified recommendation, see text
<i>ISTSE</i> (integral of squared time multiplied by squared error)	$\int_0^\infty t^2e^2(t) dt$	step	20, 32	This criterion selects good type-1 systems. Information is not available on optimum type-2 systems.	
<i>ISTAE</i> (integral of squared time multiplied by absolute value of error)	$\int_0^\infty t^2 e(t) dt$	step	20	The limited information available indicates this criterion may be of general value.	

ture: "It should be clearly understood that the greatest advantage of the mean square error criterion is that it leads to a mathematical problem that is tractable. A different error criterion often might be preferable except for the attendant mathematical difficulties."

It is true, however, that the mean square value of a random process is one of the easier parameters to evaluate experimentally. It is sometimes argued that the mean square together with the mean value of a random process yields information about the process when it is Gaussian. The central limit theorem is often invoked to assume Gaussian processes. In this connection, Sherman³⁶ has an interesting development. He shows that all the error criteria (the only restriction being that the function of error be a single-valued even function, which is monotonically nondecreasing for positive errors) yields the same type of linear predictor as the Wiener filter for Gaussian inputs.

Truxal¹⁴ points out the case of a second-order system described by a closed-loop transfer function of the form

$$\frac{C}{R}(s) = \frac{5K_v}{s^2 + 5s + 5K_v} \quad (10)$$

whose input consists of a signal component with a particular spectral density and white noise. Optimizing K_v on the basis of minimum mse, for the case when the desired output is equal to the signal component of the input, yields a value of K_v which makes the system have a damping ratio of 0.215. Obviously, the transient response characteristics of a second-order system with such a low damping ratio would, in general, be unacceptable.

This solution may not necessarily imply that the mse criterion is useless. However, the very fact that one feels the necessity of checking the optimized (in the mse sense) system, by means of the step response characteristics, implies either a lack of faith with the former criterion or overfamiliarity with the latter. Granting that a step input is a drastic and relatively uncommon input to most systems, designing on the basis of a good step response may actually amount to overdesigning, with attendant disadvantages such as additional complexity, weight, cost, etc.

This may be one strong argument in favor of indices of performance on the basis of statistical inputs, which may describe the actual inputs to the system better than any of the synthetic ones such as sine waves and step functions. Moreover, in the final reckoning, one system is said to be better than another if it operates better on the actual input, if some

criterion for comparing systems can be accepted. It really is not at all important how good or bad the step function response looks. Two serious drawbacks should be pointed out, however: (1) the amount of confidence with which the actual inputs may be described statistically, and (2) the degree of confidence in the statistical performance index. Extensive research is warranted before any such index may be recommended.

One other present disadvantage is that the statistical method of analysis appears to be highly restrictive as far as the inputs are concerned. The inputs are assumed to be stationary and ergodic, in general, but since the conditions of ergodicity are nebulous, it may be rather difficult to deduce from actual data whether the assumption is true or not.

Often the observation is made that the design of systems, using statistical procedures, is unrealistic since the final result requires the poles and zeros of the original system to be completely canceled out and poles and zeros placed at new and more suitable locations by the equalizer. Hence, the method is not very satisfactory for designing equalizers.

To recommend statistical performance specifications at this time seems rather premature, considering the fact that the statistical design of control systems has not matured sufficiently to warrant any great degree of confidence in systems optimized on that basis. Until the theory is developed further, performance specifications of a control system should necessarily depend on well-known system characteristics obtained from sinusoidal or step responses. These have been discussed elsewhere in this paper.

Graphical Presentation of System Design Data

Performance specifications are used to:

1. Judge the performance quality of a system.
2. Compare systems quantitatively and qualitatively.
3. Set minimum standards on an accept-reject basis.

Performance specifications contain all of the information needed to evaluate a system on an operating basis as they describe the system's input and output. However, additional factors less tangible than the values of the performance specifications must be considered when evaluating proposals and selecting designs which offer simplicity and sensitivity of parameter variation; e.g., Nyquist or conditional stability. The considerations

require interpretation and manipulation of system design data. Thus arises the problem of the kind of design data to present and the method of presentation.

System data should be given in a form familiar to those who must use them since experience and judgment are required in any evaluation. To be able to determine the specified performance specifications directly from the graphical presentation, would be desirable, also, but this is of secondary importance. The requirement for a presentation scheme can best be met by commonly known design procedures.

Methods which have been considered are: Bode diagram, Nyquist diagram, root locus, Nichols charts, Routh-Hurwitz criteria, Leonhard-Michaelov method, differential equation solutions, and the Guillemin-Truxal method.

Standardizing on particular schemes for system data presentation does not imply that a designer should necessarily use these schemes. He should always be free to use methods he considers best for a particular problem. However, after the design is complete, standard diagrams should be prepared so that various competitive systems can be compared, using the same kind of data. This obviously makes an evaluator's job easier since he need not be familiar with all of the possible methods of presenting design information; also, the danger of errors by the evaluator are minimized in converting from one scheme to another.

All of the methods considered for system data presentation except the Bode, root locus, Nyquist diagrams, and Nichols charts are either inappropriate or are not used to any great extent by the industry. A critical appraisal of the information available from Bode, Nyquist, Nichols, and root-locus plots shows that it is possible by manipulation, calculation, etc., to obtain the same amount of information from any of them. The same information is inherent in each diagram (this is also true for other methods) because the system transfer function can be obtained from the diagram and the system information is contained in the transfer function.

Thus, it appears to be a difficult, if not impossible, task to differentiate between the methods, other than on the basis of convenience. What one considers convenient depends upon training and experience although most engineers would agree that there are salient features of each method which make it most convenient in determining certain aspects of system performance. For example, the root locus is considered to be of much value in gaining

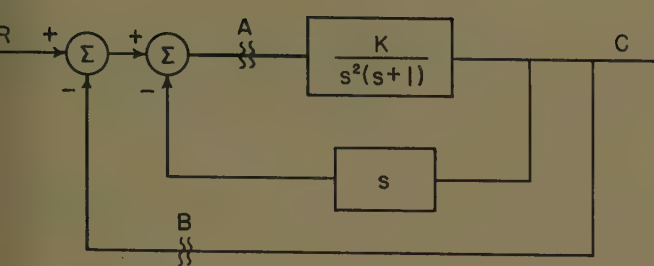


Fig. 5. Multiple loop system

sight into the transient behavior of a system; the Nyquist diagram is convenient for the determination of M_p for unity feedback systems, closed-loop frequency response, bandwidth, and conditional stability; the Bode diagram is the most convenient diagram on which to obtain the system transfer function from frequency response data, values of error coefficients, and for making a preliminary judgment as to the method of equalization, etc.

Of the four most appropriate methods selected, the root-locus and Nyquist diagrams are recommended for use in the presentation of system data. It is believed that specifying four diagrams could defeat the purpose of minimizing the number of methods to be used. However, it is desirable to have more than one presentation. Nyquist and root-locus are better than Bode diagrams as they may possibly be extended to nonlinear systems; e.g., describing function analysis, polar plots and because a separate phase diagram must be plotted for a Bode presentation in the case of nonminimum phase systems. Probably more engineers use Nichols charts for design than Nyquist diagrams. However, for data presentation and for its basic nature, the Nyquist is preferred.

Both equalized and unequalized Nyquist system diagrams may be plotted to make the results of equalization apparent or to present alternate schemes. The plot of $G(j\omega)H(j\omega)$ is required for nonunity single-loop feedback systems. The presentation procedure shall not be specified for multiple-loop systems. The design engineer must decide how the Nyquist diagram or diagrams should be presented. The reason a unique procedure is not specified for multiple-loop systems is apparent after considering an example. If the feedback path is broken at point B in the system of Fig. 5, the transfer function that would be plotted is

$$G(s) = \frac{K}{s(s^2 + s + K)} \quad (11)$$

If the loop is broken at point A, the transfer function that would be plotted is

$$G(s) = \frac{K}{s^2} \quad (12)$$

The Nyquist diagrams thus obtained are quite different. Another Nyquist diagram that may be of interest for this system is the minor loop by itself. One way to obtain a unique Nyquist diagram is to convert a multiple-loop system to an equivalent single-loop unity feedback system. However, this method has not received sufficient attention in the literature to justify its recommendation as the only way to treat multiple-loop systems.

To keep the amount of data herein to a minimum, only the equalized system root locus will be presented.

It is recommended that the closed-loop transfer function be included as a part of system data because the transfer function defines the system concisely, uniquely, and it may be needed for analysis and synthesis of larger systems of which the system in question may be a part.

The number of terms that should be included in the transfer function is a matter of engineering judgment since no practical system is ever given an exact description. As a rule of thumb, it is satisfactory to neglect those time constants which correspond to frequencies ten times greater than the bandwidth of the system. Whether or not it is always necessary to include all time constants to such a high frequency must remain a matter of engineering judgment. Inclusion of the open-loop transfer function is not necessary since it is available from other information presented, although it would sometimes be desirable to have it written on the diagrams.

A detailed explanation of the root-locus and Nyquist diagrams will not be given here since there is an abundance of literature available concerning them; indeed, this is one of the most important reasons for choosing them.

Conclusions

An operational definition of a linear control system is given. The frequency domain specifications recommended are: M -peak, peak frequency, bandwidth, and peak output impedance. Time domain specifications recommended are: time delay, rise time, settling time, per cent overshoot, and final value of error. In both cases, a template is defined that in-

corporates these specifications and permits a go-no-go determination on the basis of a frequency response test and a step response test. The generalized indexes of performance given tentative approval are: $ITAE$, $ITSE$, $ISTSE$, and $ISTAE$, but more work must be done in this area before a firm recommendation can be made.

Only specifications necessary for a particular application should be called out. Since overspecification invariably results in a more expensive and possibly less reliable system, this point deserves special emphasis.

Use of statistical design specifications is not recommended. Of course, all available statistical input and performance data should be supplied the vendor. Finally, although it is impossible to differentiate on an engineering basis, within the constraints of this work, between various data presentation schemes, the root locus and the Nyquist plot are recommended because they are familiar to engineers and have anticipated usefulness in specification of nonlinear systems.

References

1. TRANSIENTS OF LINEAR SYSTEMS, VOL. I (book), F. M. Gardner, G. L. Barnes. John Wiley & Sons, Inc., New York, N. Y., 1942, pp. 5, 171.
2. ÜBER BEZIEHUNGEN ZWISCHEN FREQUENZCHARAKTERISTIKEN UND AUSGLEICHVORGÄNGEN IN LINEAREN SYSTEMEN, K. Küpfmüller. *Elektrische Nachrichten-Technik*, Berlin, Germany, vol. 5, pt. 1, 1928, pp. 18, 23.
3. INTRODUCTION TO THE DESIGN OF SERVOMECHANISMS (book), J. L. Bower, P. M. Schultheiss. John Wiley & Sons, Inc., 1958, pp. 69, 226-33, 237, 248-57, 261-62.
4. ANALYTIC FUNCTION THEORY, VOL. I (book), E. Hille. Ginn and Company, Boston, Mass., 1959, chap. 5.
5. LECTURES ON THE THEORY OF AUTOMATIC CONTROL (in Russian), M. A. Aizerman. State Publishing House of Physical and Mathematical Literature, Moscow, USSR, 1958, pp. 302-19.
6. COMMUNICATION NETWORKS, VOL. II (book), E. A. Guillemin. John Wiley & Sons, Inc., 1935, p. 477.
7. ÜBER EINSCHWINGVORGÄNGEN IN WELLENFILTREN, K. Küpfmüller. *Elektrische Nachrichten-Technik*, vol. 1, 1924, pp. 141-52.
8. PRINCIPLES OF SERVOMECHANISMS (book), G. S. Brown, D. P. Campbell. John Wiley & Sons, Inc., 1948, p. 351.
9. FUNDAMENTAL THEORY OF SERVOMECHANISMS (book), L. A. Macoll. D. Van Nostrand Company, Inc., Princeton, N. J., 1945, pp. 35-37.
10. THEORY OF SERVOMECHANISMS (book), H. M. James, N. V. Nichols. McGraw-Hill Book Company, Inc., New York, N. Y., 1947, pp. 108, 142.
11. NONLINEAR CONTROL SYSTEMS (book), R. L. Cosgriff. John Wiley & Sons, Inc., 1958, p. 5.
12. TRANSIENT ELECTRIC CURRENTS (book), H. H. Skilling. McGraw-Hill Book Company, Inc., 1952.
13. SPECIFICATION AND DATA PRESENTATION IN LINEAR CONTROL SYSTEMS, J. E. Gibson, C. D. Leedham, E. S. McVey, Z. V. Rekasius. *Technical Report no. 1*, Air Force Missile Development Center, Holloman Air Force Base, N. Mex.; Purdue University, Lafayette, Ind., July 1959.
14. AUTOMATIC FEEDBACK CONTROL SYSTEM

SYNTHESIS (book), F. G. Truxal. McGraw-Hill Book Company, Inc., 1955, pp. 80, 86.

15. CONTROL ENGINEERING MANUAL (book), B. K. Ledgerwood, editor. McGraw-Hill Book Company, Inc., 1957, p. 29.

16. AUTOMATION, COMPUTATION AND CONTROL (book), E. M. Grabbe, editor. John Wiley & Sons, Inc., 1957, pp. 14-19.

17. ELECTRONICS: EXPERIMENTAL TECHNIQUES (book), W. C. Elmore, M. Sands. McGraw-Hill Book Company, Inc., 1949, p. 137.

18. THE PRACTICAL APPLICATION OF FREQUENCY RESPONSE ANALYSIS OF AUTOMATIC PROCESS CONTROL, C. I. Rutherford. *Proceedings, American Society of Mechanical Engineers*, New York, N. Y., vol. 162, 1950, pp. 334-54.

19. A SELF-ADJUSTING SYSTEM FOR OPTIMUM DYNAMIC PERFORMANCE, G. W. Anderson, J. A. Aseltine, A. R. Mancini, C. W. Sarture. *Convention Record, Institute of Radio Engineers*, New York, N. Y., pt. 4, 1958, pp. 182-90.

20. THE SYNTHESIS OF "OPTIMUM" TRANSIENT RESPONSE: CRITERIA AND STANDARD FORMS, Dunstan Graham, R. C. Lathrop. *AIEE Transactions*, pt. II (*Applications and Industry*), vol. 72, Nov. 1953, pp. 273-88.

21. THE DYNAMICS OF AUTOMATIC CONTROLS (book), R. C. Oldenbourg, H. Sartorius. American Society of Mechanical Engineers, 1948.

22. SOME DESIGN CRITERIA FOR AUTOMATIC CONTROLS, Paul T. Nims. *AIEE Transactions*, vol. 70, pt. I, 1951, pp. 606-11.

23. ANALOGUE METHODS FOR OPTIMUM SERVOMECHANISM DESIGN, F. C. Fickeisen, T. M. Stout. *Ibid.*, pt. II (*Applications and Industry*), vol. 71, Nov. 1952, pp. 244-50.

24. THE ANALYSIS AND SYNTHESIS OF LINEAR SERVOMECHANISMS (book), A. C. Hall. Technology Press, Cambridge, Mass., 1947.

25. COMMUNICATION NETWORKS, VOL. I (book), E. A. Guillemin. John Wiley & Sons, Inc., 1931.

26. INVESTIGATION OF SEVERAL CRITERIA FOR THE SYNTHESIS OF OPTIMUM TRANSIENT RESPONSE OF SERVOMECHANISM SYSTEMS OF HIGHER ORDERS, J. W. Frogatt. USAF Institute of Technology, Wright-Patterson Air Force Base, Dayton, Ohio, 1954.

27. STABILIZED FEEDBACK AMPLIFIERS, H. S. Black. *AIEE Transactions (Electrical Engineering)*, vol. 53, Jan. 1934, pp. 114-20.

28. REGENERATION THEORY, H. Nyquist. *Bell System Technical Journal*, New York, N. Y., vol. 11, 1932, pp. 126-47.

29. ENGINEERING ELECTRONICS (book), G. E. Happell, W. M. Hesselberth. McGraw-Hill Book Company, Inc., 1953.

30. THE TRANSIENT PERFORMANCE OF SERVOMECHANISMS WITH DERIVATIVE AND INTEGRAL

CONTROL, Richard C. Lathrop, Dunstan Graham. *AIEE Transactions*, pt. II (*Applications and Industry*), vol. 73, Mar. 1954, pp. 10-17.

31. THE INFLUENCE OF TIME SCALE AND GAIN ON CRITERIA FOR SERVOMECHANISM PERFORMANCE, Dunstan Graham, Richard C. Lathrop. *Ibid.*, July, pp. 153-58.

32. AN INTEGRAL CRITERION FOR OPTIMIZING DUPLICATOR SYSTEMS ON THE BASIS OF TRANSIENT RESPONSES, J. H. Crow. *Ph.D. Thesis*, Washington University, St. Louis, Mo., June 1957.

33. EXTRAPOLATION, INTERPOLATION AND SMOOTHING OF STATIONARY TIME SERIES (book), M. Wiener. Technology Press, Cambridge, Mass., 1949.

34. PROBABILISTIC ERROR AS A MEASURE OF CONTROL-SYSTEM PERFORMANCE, J. Zaborzki, J. W. Diesel. *AIEE Transactions*, pt. II (*Applications and Industry*), vol. 78, July 1959, pp. 163-6.

35. CONTROL SYSTEMS ENGINEERING (book), William W. Seifert, Carl W. Steeg, Jr., editors. McGraw-Hill Book Company, Inc., 1960, p. 611.

36. NON-MEAN SQUARE ERROR CRITERIA, Sherman. *Transactions, Professional Group on Information Theory, Institute of Radio Engineers*, vol. 4, no. 3, Sept. 1958, pp. 125-26.

37. SERVOMECHANISM AND REGULATING SYSTEM DESIGN, VOL. II (book), H. Chestnut, R. V. Mayer. John Wiley & Sons, Inc., 1955.

Discussion

N. W. Trembath (Space Technology Laboratories, Los Angeles, Calif.) The authors have completed a difficult task, and this report of their work represents a thorough and accurate treatment of performance specifications for linear automatic control systems. Their recommendations and conclusions should provide a basis for standardizing specifications for large segments of the automatic control and servomechanisms industry. In addition, the results presented in this paper will be even more useful when combined with a similar paper on specifications for nonlinear automatic control systems which, it is hoped, the authors will soon present.

There is only one major problem which occurs to this writer with the conclusions presented in this paper. All recommended specifications deal with control system input-output characteristics. This is as it should be when a complete closed-loop system is to be specified; however, a problem occurs when a control system must be specified and its designer has no voice in selecting major elements of the closed-loop system. Such is frequently the case in the aircraft-missile industry, for example.

If input-output specifications are to be employed when major variances can exist in fixed elements of the system, then a complete specification would require specifications corresponding to each of the parameter variations or to statistical combinations of such variances. When large numbers of parameters are involved, it is more workable to employ the results of experience gained with similar systems and specify over-all gain and phase margins. These specifications are not of the input-output type and are not recommended by the subject paper.

It can be argued that such margins can be readily obtained from the graphical presentations of system design data, which are recommended in the paper under discussion. Such presentations can be used to evaluate

system margins or sensitivity to parameter variations. Nevertheless, there sometimes exists the need to specify such margins or equivalent indices of tolerance to parameter variations as constraints on the basic design.

V. C. Rideout (University of Wisconsin, Madison, Wis.) and W. C. Schultz (Cornell Aeronautical Laboratory, Cornell University, Buffalo, N. Y.): The authors are to be congratulated on their extensive treatment of control system performance specification. Particularly important are the summaries in their Table IV and the series of frequency-domain figures of merit, a class of figures of merit which has not been widely discussed.

In our series of papers,¹⁻³ aspects of the performance measure problem were discussed from a time-domain point of view. We treated upon a type of performance index (for the transient input case), which is not mentioned in this paper. This performance index is defined by the equation

$$E = \int_0^{\infty} W(t)F(e)dt \quad (13)$$

where $F(e)$ is an amplitude-weighting function of the error e and $W(t)$ is a time-weighting function. Special cases of this form are discussed in the Gibson paper in the section on performance indices (*ITAE*, *ISE*, *IAE*, et al.), but some of the broader aspects of interpretation are not indicated. We feel that such interpretation lends support to views expressed by the authors of this paper in a number of ways: first, we have come to the same general conclusion that there is no one best way of specifying an "optimum" servo response; second, we agree not only that performance measures and their applications should not invade the province of the designer, but should serve as an aid to the designer rather than an obstacle; third, the concept illustrated by Fig. 3 of their paper bears a strong resemblance to a type of formulation that can be derived from equation 13, as will be

illustrated. The illustrations are based on an assumed viewpoint that also bears on the matter of mathematical convenience mentioned by these authors. Mathematical convenience does not justify requiring that a system be linear; no more should mathematical difficulties prevent the use of certain performance measures, especially, we feel, when computing devices are available

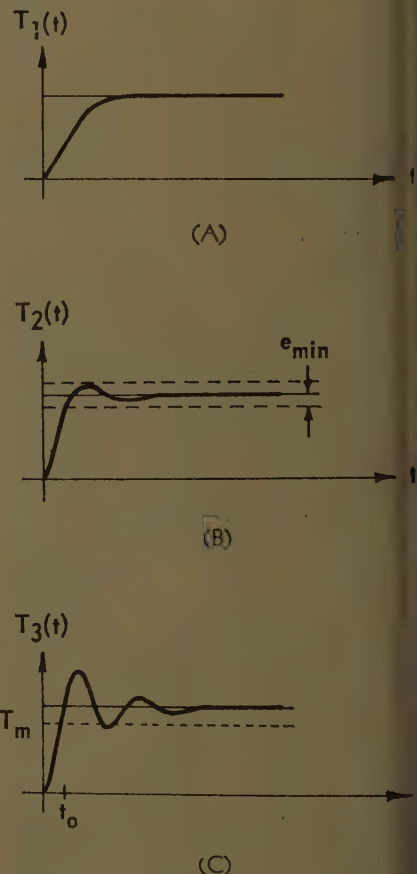
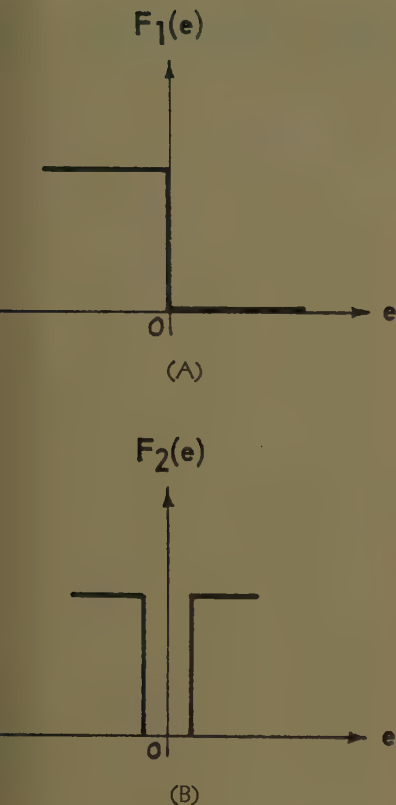


Fig. 6. Three catastrophe cases in system response illustrated by (A), (B), and (C)



7. *F*-functions used in system-performance evaluation

Considering the three temperature control system specifications⁴ shown in Fig. 6, these might be referred to as *calastrophe* cases. A calamity occurs in system 6(A) if overshoot occurs; in system 6(B), once certain minimum value of error is reached, *calastrophe* results if the error again exceeds this limit; and in system 6(C), *calastrophe* results if the undershoot is greater than a prescribed amount; e.g., the process ceases prematurely. Granted that these are extreme cases; yet it is in such extremes that the designer cannot rely on mathematical convenience and employ the *ISE* or *TAE* with any success. Many other extreme cases could be cited for which the well-known indices would not produce satisfactory results.

It is in such situations where we feel that a different interpretation, namely a metric interpretation, offers some help to the designer. For example, in the three cases of Fig. 6, time-weighting is relatively important, since the same calamity occurs whenever the specifications are not met. Thus, equation 13 can be written in the simpler form

$$\int_0^{\infty} F(e) dt \quad (14)$$

for cases 6(A) and 6(B). *F*-functions, which could be used in evaluating system performance, might then be selected as shown in Fig. 7. The system of Fig. 6(C) is somewhat different, since a time-weighting function, $W_1(t)$ can be used to formulate a meaningful measure. For example, $W_1(t)$ can be defined as being equal to zero until t_0 , the time at which the output function first crosses the value T_m , and it is equal to one thereafter. For simplicity, equation 13 could be rewritten as

$$E = \int_{T_m}^{\infty} F(e) dt \quad (15)$$

An *F*-function that could then be used for this case might be one of those shown in Fig. 8. These examples serve to illustrate how a performance measure can be formulated to handle very special cases.

Although the template concept of Fig. 3 provides a formulation that may achieve similar results, a geometrical interpretation of equation 13 permits a formulation that can readily be mechanized on an electronic computer. The repetitive analog computer is particularly well-suited for doing this, although slow-time analog computers or digital computers can also be used for evaluation of these performance indices. Fig. 9 illustrates how such performance measures are mechanized.

Several degrees of sophistication are implied in Fig. 9. For example, the model may be defined as unity, so that model error is simply input minus output; or, the model may be defined as a pure delay of τ units, so that model error is delayed input minus output (delay-error); or, the model might be defined as some desired transfer function, so that the model error is some sort of comparison error. If the system parameters are subject to change, then the model might be selected as a satisfactory (optimum) set of parameter values of the system transfer function. Then the performance index is a measure of the deviation from the desired output, and may be used to form a basis for adaptation in the sense of Aseltine.⁵ We are currently engaged in research activities oriented along these lines.

In reference to Fig. 9, mention was made of the delay-error $e(t, \tau)$. This delay-error has been used in connection with deterministic inputs and also, to a greater extent, for certain types of statistical inputs. In the latter case, the error measure of equation 14 is modified to become

$$E(\tau) = \lim_{T \rightarrow \infty} \frac{1}{2T} \int_{-T}^T F[e(t, \tau)] dt \quad (16)$$

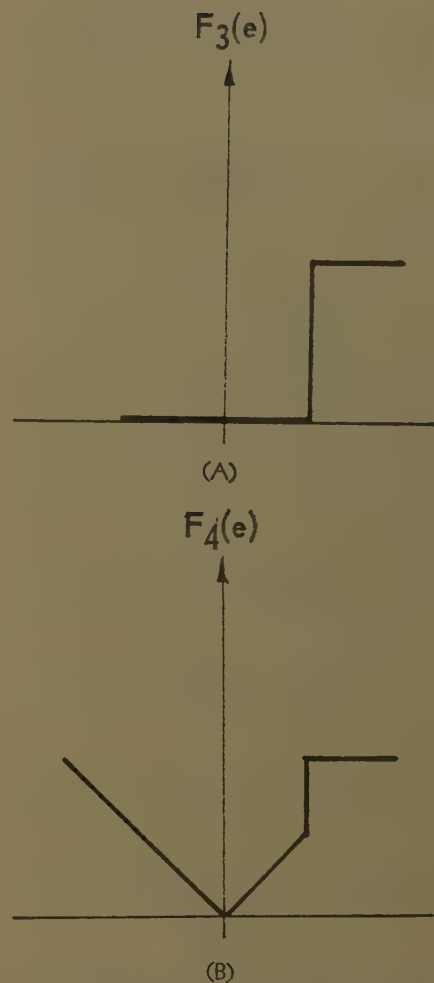
The well-known special case of this form is

$$E(\tau) = \lim_{T \rightarrow \infty} \frac{1}{2T} \int_{-T}^T e^2(t, \tau) dt \quad (17)$$

which can be expanded under certain conditions (linear system, stationary, and ergodic input) into the form

$$E(\tau) = \phi_{rr}(0) + \phi_{cc}(0) - 2\phi_{rc}(\tau) \quad (18)$$

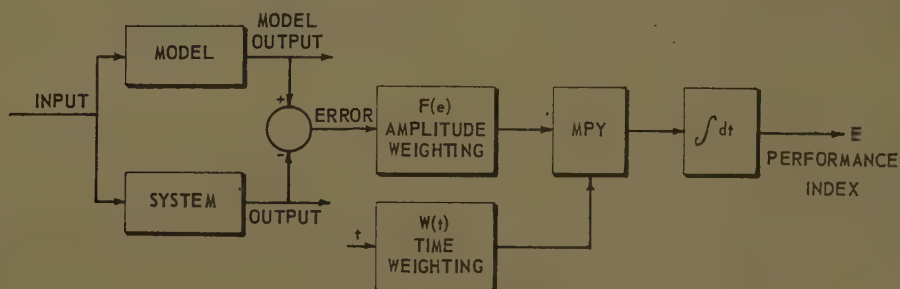
where ϕ_{rr} and ϕ_{cc} are auto-correlation functions and ϕ_{rc} is the cross-correlation of input and output. Studies of equation 18, used as



8. *F*-functions which could be used for case of equation 15

a performance measure, have been made.⁶ We have also reported on studies of the interrelationships between the measure of equation 17 and the corresponding case for deterministic input.³ Also discussed are a number of papers that describe interesting applications of statistical methods to performance measures. In this connection, we would like to point out that several other writers^{7,8} previously had discussed the findings of Sherman (see reference 37 of the paper) that any symmetrical function of error yields the same optimum filter for Gaussian inputs, provided the function is nondecreasing.

We agree that further development of the theory of statistical performance measures is needed. However, we wonder if a statement can or should be made that statistical



9. Mechanized evaluation of performance indices

design specifications should not be employed. Might we not say, rather, that no standard method or methods can be recommended at this present state of the art?

REFERENCES

1. THE SELECTION AND USE OF SERVO PERFORMANCE CRITERIA, W. C. Schultz, V. C. Rideout. *AIEE Transactions*, pt. II (*Applications and Industry*), vol. 76, 1957 (Jan. 1958 section), pp. 383-88.
2. A GENERAL CRITERION FOR SERVO PERFORMANCE, W. C. Schultz, V. C. Rideout. *Proceedings, National Electronics Conference*, Chicago, Ill., vol. 13, 1957, pp. 549-60.
3. PERFORMANCE MEASURES: PAST, PRESENT, AND FUTURE, W. C. Schultz, V. C. Rideout. *Transactions, Professional Group on Automatic Control, Institute of Radio Engineers*, New York, N. Y., vol. AC-6, no. 1, Feb. 1961, pp. 22-35.
4. HOW TO ESTABLISH THE CONTROL PROBLEM FOR AN ON-LINE COMPUTER, E. W. James, A. S. Boksenbom. *Control Engineering*, New York, N. Y., vol. 4, Sept. 1957, pp. 148-59.
5. Discussion by J. Aseltine of Technical Report No. 59-49, "Proceedings of the Self-Adaptive Flight Control System Symposium," Wright Air Development Center, ASTIA no. AD-209389, Armed Services Technical Information Agency, Dayton, Ohio, Mar. 1959.
6. CORRELATION STUDIES OF LINEAR AND NON-LINEAR SYSTEMS, M. G. Spooner, V. C. Rideout. *Proceedings, National Electronics Conference*, vol. 12, 1956, pp. 321-35.
7. A NON-MEAN-SQUARE-ERROR CRITERION FOR THE SYNTHESIS OF OPTIMUM FINITE-MEMORY SAMPLED DATA FILTERS, A. R. Bergen. *National Convention Record*, Institute of Radio Engineers, pt. 2, 1957, pp. 26-32.
8. ON A PROPERTY OF WIENER FILTERS, T. R. Benedict, M. M. Sondhi. *Proceedings, Institute of Radio Engineers*, vol. 45, July 1957, pp. 1021-22.

E. J. Groth (Motorola, Inc., Scottsdale, Ariz.): The writer is gratified to have been asked to comment on this paper. It is understood that the purpose of the study is to establish, principally for procurement efforts, a minimum list of specifications. To become a standard, it is necessary that such minimum specifications apply in a large number of cases, with serious deviations required only occasionally. To test the value of a proposed set of specifications, some sample cases should be tried. The writer has explored this to some extent, and has reached the conclusion that only the simplest of controls can be specified without extensive additional specifications.

For example, it appears that the study ignores the situation where a given control may be only a portion of a much larger control system. For instance, an autopilot, which is certainly a control system, may well be a portion of a bombing- or fire-control system. Could an autopilot be procured against the list of minimum specifications? Certainly not. Would the minimum list, augmented as required, be of any real value? Here again the answer is no. Such a control system requires shaping of its characteristics so that the response of the total system meets some set of requirements again not specifiable by the minimum list. Any control system which is to operate on a load member which has resonances, or whose supports have resonances in the bandwidth of interest, must be specified in entirely different terms than those developed for the minimum list. This category includes a great portion of the high-performance control systems being procured by the military at the present time.

The foregoing statements imply that control systems must frequently perform a filtering function. This is the actual case, and procurement involves a total system specification rather than simplified control system specifications.

Another point of importance is that the approach taken in the study tends to look at servo specifications under certain well-defined and common types of inputs such as, for example, step functions. It is considered that an important specification is the per cent overshoot of a system when subjected to a step input. It is really much more important to specify the output performance in terms of the expected input, or more generally the spectra of expected inputs. It may well turn out that a given control system will never be subjected to a step input. This example leads to the generalization that the newer design techniques and specification techniques for control systems, which spell out the performance of a system in a statistical fashion with the inputs and outputs considered as spectra, have been slighted. The writer believes that the design of control systems using these newer techniques is more realistic than the normal noise-free design techniques that have been used in the past and around which nearly all of the specifications are developed.

It is stated that a performance index will emphasize some properties of the response more than another index. This is true for the simple approaches to design. However, there are cases in which performance indices provide quite useful and necessary information. Such an example occurs with distortionless systems. A distortionless system is defined as one having outputs equal to the inputs for all inputs (restricted to some bandwidth including all frequencies of interest). Distortionless systems are not considered in the paper and indeed, it is implied that such do not exist. Recently, the efforts of the writer have been associated with placing two different distortionless control systems in the field. Optimization of these systems against noise spectra present at the inputs and against certain system biases was carried out. The specifications for these highly successful systems had to be statistical, and the quantities comprising the minimum list of specifications had no useful meaning.

It is agreed that standardization is required in the procurement of control systems. However, the writer believes that such should extend only to standardizing the meaning of terms and this should, of course, be a developing thing as new techniques of design and implementation develop. The standardization should not extend to delineating a minimum list of specifications because of its lack of applicability for other than the simplest control systems. The writer believes the examples cited above support this view.

J. E. Gibson, Z. V. Rekasius, E. S. McVey, R. Sridhar, and C. D. Leedham: The authors wish to thank the discussers for their complimentary remarks and their technical criticism. It is extremely important to have several viewpoints when trying to establish a standard set of specifications.

Mr. Trembath's remarks regarding the

difficulty of specifying large, complex systems are certainly appreciated; in fact, that difficulty was exactly the motivation which spurred this study. His point that a designer often does not have complete freedom within the performance specifications applies without exception to systems that authors have encountered. There will always be limited space, weight, price, reliability, and other specifications, in addition to performance specifications. It is also true that certain elements within the loop frequently are specified in advance. It may come as a disappointment to missile designers, but the authors feel that, in this regard at least, aerospace and military problems are simpler than industrial ones. In industrial applications, a "clean" set of specifications is extremely rare. Generally, a greater proportion of the system is specified in advance than is common in design, starting from the ground up, as in a new aerospace system.

It must be emphasized that the specifications given are definitely designed for those systems that are a part of a larger, over-all system, and apply as directly as they do for isolated systems. Indeed, the interaction of the over-all system upon the automatic control subsystem is the source from which the input-output specifications on the subsystem are derived—and why, incidentally, untrustworthy specifications, such as gain and phase margin, cannot be used. The sum total effect on a system of statistical variations within a supposedly identical lot of components is certainly of serious concern. In fact, this is exactly why non-zero tolerances must be placed upon the response specifications. The authors feel that the go-no-go templates are quite reasonable—in fact, conventional—solutions to this problem.

The authors, of course, concur with Mr. Trembath in the viewpoint that experience and insight will yield better systems; and it is the authors' intent to place in the hands of the buyer and the vendor a consistent set of specifications that will help to minimize confusion and disappointment. Good work and an intent to meet the spirit of specifications are, of course, always necessary; but this appears somewhat beyond the present discussion.

The discussion by Mr. Rideout and Mr. Schultz adds materially to the presentation on performance indices, and we are in agreement with the views they express. It might be pointed out, for example, that Aseltine et al.¹ achieved excellent results in a particular system with *IRAR*, which is, in general, unreliable. It appears difficult and perhaps not even desirable to force all systems into a single mold by the use of a single general index. This may be read as a trivial statement, but the authors did not allow themselves to make it until the end of their study. Rideout and Schultz are well known for their work in the area, and it is interesting that our conclusions concurred with theirs.

In regard to statistical design specifications, it was the authors' intent in the last paragraph of the statistical specification sections and the last paragraph of the conclusions to convey the information expressed by Rideout and Schultz; i.e., no method can be recommended for statistical specifications at the present state of the art; but most certainly engineering research should

ected at improving this situation; A her extensive research effort is presently der way at Purdue on statistical design of stems, and it is hoped that results may on be reported.

Mr. Groth's closely reasoned remarks de- ve answers as closely reasoned; hence, reply paragraph by paragraph. The tement of principle in his opening lines excellent; but he realizes, as do the thors, that one or two pathological exam- ers could be chosen to prove almost any- ing. His autopilot example in the second ragraph does not fall into this category, r does the general problem of a control stem which is a part of a larger system.

We feel that this point has been dis- ssed in commenting on Mr. Trembath's marks. However, to be specific, we do that these specifications "as aug- mented" would be of real value in procuring autopilot. Our reasoning is: *Some* ecifications must be set on the autopilot be placed out for bid. Naturally, these ecifications should be set by a team of erts in the area. A number of vendors ll respond to the invitation to bid. There ll follow the usual dialogue between ven- r and buyer. Since it is to everyone's con- rn that the conversations and reports be clear and explicit as possible, it appears vious that the terms be defined. The thors flatter themselves that they in- ded on their preliminary lists every term common use in control system terminology every western language. These were re- ced and weeded to those here presented. ne authors maintain that with their ilosophy of a common language there ould be no argument. Naturally, how- er, there will be argument with specifics. Certain specifications may be found to e useless or misleading and will be re- ced; others will doubtless be added. aturally, if a buyer wished to specify other ms, other terms could be used, but "... y control system which is to operate on load member which has resonances, or ose supports have resonances in the band- dth of interest . . ." or "... a con- ol system which requires shaping of characteristics so that the response e the total system meets some set of uirements. . ." could be specified rms of the specifications here given. fact, exactly this problem was under cussion when the frequency response velope, the M -peak, the bandwidth, d the impedance specifications were ined.

Mr. Groth's third and shortest paragraph tes a position entirely in accordance with e authors' view, but they emphasize that ese specifications most definitely can be ed if the buyer or vendor cares to take e filter point of view for a system which a portion of a larger system. For instance, certain applications, it might be advis-

able to call out a specification on closed-loop phase shift versus frequency in the form of a go-no-go template, along with specifica- tions from the standard set. The buyer is at liberty to do this, but it must be re- membered that overspecifying the system will add to its cost.

Mr. Groth's opening sentence in the fourth paragraph is exactly correct. Fur- thermore, the authors are well aware of the desirability of closely tailoring a system to actual inputs and this is the point of that section in the paper dealing with statistical specifications. Rather close association with the actual state of the art in statistical design, however, has left the authors with the opinion that statistical specification is rather academic at present, and that it will remain so until a more realistic approach becomes mathematically tractable. Atten- tion is directed to the text following equa- tion 10. Mr. Groth is reminded that the authors specifically avoid the area of design, and point out that this must remain the province of the vendor. They further state in the conclusion that all available statisti- cal input information should be given to the vendor, and that it may be used in the design as the vendor sees fit.

No doubt Mr. Groth feels at a disadvan- tage, as do the authors, because security restrictions prevent the citation of examples that might prove a point. The missile in- dustry's aversion to step functions is well- known, and to be required to meet difficult specifications, in the face of other severe constraints, is unpleasant. Mr. Groth might be reminded, however, of the rather dramatic films shown on television of the successful *Polaris no. 2* firing. It was our distinct impression that the missile erupted from the water at about a 35-degree angle from the vertical, and an abrupt change in command heading of 35 degrees is usually considered a step function.

In the fifth paragraph, the authors agree with Mr. Groth's first three sentences. It was hoped, in fact, that the class of sys- tems for which IP 's (indices of perform- ance) proved useful would be broad enough to warrant the term "general," although this has not proved to be the case. Per- haps the best approach is that of Rideout and Schultz in which a class of IP 's is tailored to meet specific situations. At Purdue, we have had some success with a new class of indices, based on extensions of the second method of Liapunov. These results are soon to be published by Rekasius.

With regard to the remainder of the fifth paragraph, the authors are somewhat con- fused. If we understand the discussor correctly, he is defining a class of systems in which the difference between the output and a nonzero input is *actually* zero over a finite bandwidth; not merely *desired* to be zero. We are not aware that in the paper

we implied or stated anything concerning such systems. However, we will be happy to do so. The authors believe that such systems do not physically exist and can never physically exist. In fact, we believe it can be shown that such a physical device is theoretically impossible. These state- ments apply whether zero-error is defined on a steady-state sinusoidal basis or on an rms-error basis. Doubtless Mr. Groth does not mean what he seems to be saying since he goes on to speak of optimizing such sys- tems, which seems to imply (or, so we infer) that the error is not zero at all.

An interesting case of a distortionless sys- tem (distortionless, in the mean-squared sense) is considered by Peterson² who treats of an optimum linear time-varying sys- tem. In the closing comments, Peterson claims for optimum time-varying systems that "I have never found a case where it (mean-square error) does not vanish if the message has a nonstationary ensemble cor- relation for which it is possible to write an analytic closed-form expression for a repre- sentative member of the ensemble."

The fallacy in Peterson's argument is evi- dent if one considers equation 25 in the refer- ence. The expression for the optimum sys- tem relies on the fact that the *rhs* of equa- tion 25 is always positive. This is true only if the inputs are independent, and this certainly is not true for the example chosen in the paper as evidenced by Fig. 1, where both the inputs $i(t)$ and $r(t)$ have com- ponents dependent on the acceleration $\ddot{x}(t)$. However, if one does consider statistically independent inputs, equations 33 through 38 are not valid. Hence, the expression for the mean-square error, equation 6, from which the conclusion of no distortion is drawn, is invalid.

On the final paragraph, the authors agree with the discussor's opening statement. They also agree that terms and definitions should certainly be subject to continual re- view and modification. However, we must point out that this is not a *minimum* list but rather a *standard* list. A buyer is free to use more specifications, or fewer, as his application demands. It is the authors' opinion that this is a *preferred* list in the sense of the RETMA tube list, and will fit a great majority of linear systems. If we can agree to use these terms and definitions, progress will have been made. In addition, for many systems, the necessary and suffi- cient specifications for the performance as- pects of the system may be chosen from this list, thus again yielding progress.

REFERENCES

1. See reference 19 of the paper.
2. OPTIMIZATION OF MULTIOUTPUT LINEAR TIME-VARYING SYSTEMS SUBJECT TO MULTIPLE OR REDUNDANT NONSTATIONARY INPUTS, E. L. Peterson. *AIEE Transactions*, pt. II (*Applications and Industry*), vol. 79, 1960 (Jan. 1961 section), pp. 471-75.

Design of Ignitron Firing Circuits Utilizing Controlled Rectifiers

D. C. GRAHAM
ASSOCIATE MEMBER AIEE

IGNITRON TUBES have been applied as the basic rectifying device in electronic power converters for many years. The fields of application have been both broad and varied. New applications and new requirements on old-type applications stipulate more stringent performance characteristics and an even greater reliability than ever before required.

Voltage control of an ignitron power converter is achieved by controlling the time in the cycle where conduction is initiated. The passing of a current pulse through the ignitor at the proper time initiates the conduction. The circuit which generates these current pulses, and controls their phase position, is called the firing circuit. Therefore, the operating characteristics of the electronic converter, as a whole, are dependent on the firing circuit characteristics.

Nonlinear reactor firing circuits obtain phase delay by means of phase-shift reactors.¹ The phase-shift reactors, which operate on the principle of the magnetic amplifier, have a high volt-ampere operating level which results in a speed of response of approximately 15 to 20 cycles for conventional-type firing circuits. This response time has become marginal, even with forcing, by the trend to individual power supplies for the multiple stands of continuous hot mills, coupled with increased rolling speeds. The application of rectifiers as power supplies for reversing mills, electronic exciters, and magnet power supplies for particle accelerators, requires a phase-control range greater than conveniently available with reactor-type firing circuits. This increased range of phase shift is necessary to operate over the entire range of rectification and inversion.²

Most reactor firing circuits have rather nonlinear phase-shift characteristics which introduce a variable gain in the closed-loop regulating circuits employed on such applications.

Paper 61-109, recommended by the AIEE Industrial Power Rectifiers Committee and approved by the AIEE Technical Operations Department for presentation at the AIEE Winter General Meeting, New York, N. Y., January 29-February 3, 1961. Manuscript submitted November 3, 1960; made available for printing December 14, 1960.

D. C. GRAHAM is with the Westinghouse Electric Corporation, East Pittsburgh, Pa.

The reactor firing circuit, while possessing a high degree of reliability and certain economic advantages, cannot meet the more stringent requirements of modern-day applications.

The older capacitor-thyratron circuit¹ overcame most of these disadvantages but, because the power-handling capabilities of commercially available thyratrons were not compatible with the power requirements of the firing circuit, poor thyatron life resulted. This type of circuit did not meet with industry acceptance, since reliability and long trouble-free life of components are required on these important applications.

The foregoing considerations dictated the need for a firing circuit having:

1. A fast speed of response.
2. An extended phase control range.
3. A high degree of reliability.
4. A controllable phase-shift characteristic that is linear, and therefore does not introduce a variable gain in the regulating loop.

This paper describes a firing circuit which meets these more stringent present-day requirements. The circuit analysis and the necessary theoretical considerations to permit the design of a firing circuit for any given set of pulse requirements are included.

Circuit Operation

CONTROLLED RECTIFIER CHARACTERISTICS

In order to understand the operation of the circuit to be presented, it will first be necessary to become familiar with the basic characteristics of the controlled rectifier. The controlled rectifier is a 3-terminal device which is the semiconductor counterpart of the thyatron. The reverse characteristic is similar to that of a thyatron or a silicon diode, since it essentially blocks current when negative anode to cathode voltage is applied, providing the critical breakover voltage is not exceeded and providing no signal is applied to the gate terminal.

The device may be switched to the conducting state either by exceeding the forward breakover voltage (V_{BO}) or by

applying an appropriate gate signal. The device will regain its forward blocking characteristic only after the forward current falls below a certain minimum value and the gate signal has been removed.

Fig. 1 shows a schematic diagram of the controlled rectifier. The controlled rectifier is made conductive or "gated" by a positive current from the gate to cathode connections. Fig. 2 illustrates the typical device characteristics.

EXPLANATION OF CIRCUIT OPERATION

With the preceding basic knowledge of the controlled rectifier characteristics, we may now proceed with the explanation of the firing circuit proper, as seen in Fig. 3.

Fig. 4 illustrates the voltages of the various circuit components during one complete cycle. During the positive half-cycle of the supply voltage (e_s), the silicon controlled rectifier (SCR) is in the blocking state. The firing capacitor (C_f) is charged through the charging rectifier (D_c) and the current-limiting resistor (R_c), as long as the supply voltage (e_s) is more positive than the firing capacitor voltage (e_{cf}). The firing capacitor retains its charge as the applied voltage decreases and becomes negative since the charging rectifier (D_c), the shunt rectifier (D_s), and the controlled rectifier (SCR) prevent the draining off this charge by their blocking action. The gate signal is applied only during the negative half-cycle of the charging voltage (e_s), thus eliminating power-follow current from the supply and maintaining the circuit stability. If the controlled rectifier (SCR) is released during the positive half-cycle of the supply voltage (e_s), it will lose control.

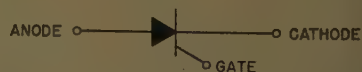


Fig. 1. Controlled rectifier schematic

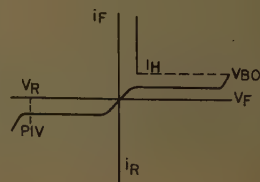


Fig. 2. Controlled rectifier characteristics

i_F = forward current
 i_R = reverse current
 V_F = forward voltage
 V_R = reverse voltage
 PIV = peak inverse voltage
 V_{BO} = forward breakover voltage
 I_H = minimum holding current

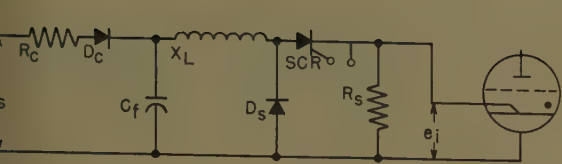


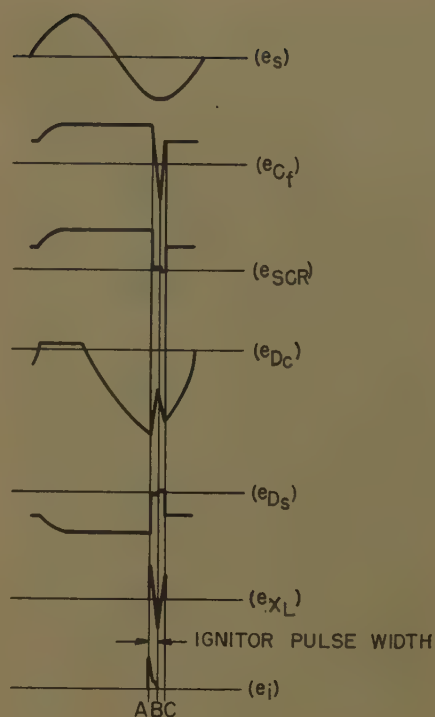
Fig. 3. Firing circuit schematic

e_g = ignitor voltage
 e_s = supply voltage
 e_{Cf} = charging resistor
 e_{CR} = charging rectifier
 e_i = firing capacitor

X_L = series inductor
 R_s = shunting resistor
 D_s = shunting rectifier
 SCR = silicon controlled rectifier

Fig. 4 (right). Component voltage characteristics

e_s = transformer output voltage
 e_{Cf} = capacitor voltage
 e_{CR} = controlled rectifier voltage
 e_{D_s} = charging rectifier voltage
 e_{D_s} = shunt rectifier voltage
 e_{X_L} = inductor voltage
 e_i = ignitor voltage



In Fig. 4 the gate pulse is applied at point A. When the gate signal is applied, the controlled rectifier becomes conductive and allows the firing capacitor to discharge through the inductor (X_L) and the ignitor, as shown between points A and B. The result is an R - L - C oscillatory discharge. The frequency and the magnitude of the discharge is predetermined by the values of the firing capacitor (C_f), the series inductor (X_L), and the ignitor resistance.

The purpose of the shunt resistor (R_s) in parallel with the ignitor is to maintain the discharge oscillatory, regardless of the ignitor resistance. Since the discharge is oscillatory, the capacitor is charged negatively at the end of this forward discharge period, shown as point B. The capacitor then discharges back through the shunt rectifier (D_s) and the inductor (X_L), and reverses its polarity, as shown between points B and C.

By the time the current through the controlled rectifier falls to zero, the gate signal has been removed and the controlled rectifier regains its blocking characteristic. The width of the gate pulse is important since the controlled rectifier must have sufficient time to return to its forward blocking characteristic after the ignitor pulse and prior to the application of forward voltage. Since the controlled rectifier regains its blocking characteristic, the capacitor maintains its partial positive charge for the remainder of the negative half-cycle. The capacitor is then fully recharged during the next positive half-cycle. By allowing the circuit to oscillate and partially recharge the capacitor, this stored energy can be reused and it reduces the power requirements from the source. The power consumed by the circuit increases at either high delay or no delay, as the capacitor is charged to a value negative at the end of its forward discharge period than the supply voltage and a current pulse flows from the source. The power increase is not excessive, and therefore is not detrimental.

The firing circuit has no time delay

since the controlled rectifier will phase shift as fast as the gate pulse is shifted. This is true since, as the gate signal is phase shifted, the turn-on time of the controlled rectifier will remain a constant. The only time delay involved is in the regulating equipment supplying the gate pulse. The power level required for "gating" the controlled rectifier is small, and therefore regulating equipment may be utilized that has a fast speed of response.

Pulse-position modulators, for supplying the gate signals to the controlled rectifiers, comprise a complete subject in themselves and will not be covered in this paper. There are a variety of circuits available for this purpose and the response times vary from less than a cycle to several cycles. The pulse characteristics of a suitable gate circuit for use with the firing circuit may be readily determined. The pulse should have a sharp wave front, a pulse width of 10 to 15 degrees duration, and a magnitude of approximately 3 volts and 60 milliamperes, depending on the particular controlled rectifier utilized. The particular pulse-position modulator chosen will depend on the characteristics required of the rectifier installation.

Since the firing circuit operation is completely linear, the output pulse characteristics may be determined analytically.

Circuit Design

PULSE CHARACTERISTICS

The first step of the circuit design is to determine the pulse characteristics desired. Ignitor characteristics vary within predetermined manufacturing tolerances. The range of acceptable ignitors is determined from experience and exhaustive ignitor tests by the individual manufacturers. Characteristics of ignitor firing may be illustrated as in Fig. 5. All acceptable ignitors must fall within the range represented by the cross-hatched area.

In addition to the volt-amperes neces-

sary for reliable ignitor firing as shown on the curve, a margin must be allowed for ignitor aging and variations in the supply voltage of the excitation circuit. Limits established by applicable standards stipulate satisfactory operation from 85% to 110% of rated voltage.³ The margin necessary is based on experience.

The broken sloping line of Fig. 5 represents the characteristics of a firing circuit capable of meeting the given requirements. The intercept on the ordinate is the peak voltage developed by the circuit with infinite resistance (open ignitor). The intercept on the abscissa is the peak amperes developed with zero resistance (short-circuited ignitor). Different points

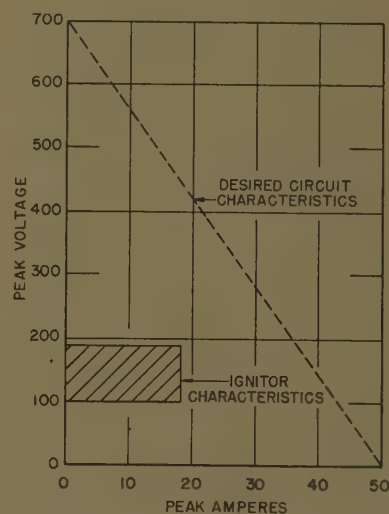


Fig. 5. Volt-ampere characteristics of desired circuit

on the curve may be calculated by substituting various values of resistance in place of the ignitor. The controlled-rectifier excitation circuit operation is linear, and thus the volt-ampere characteristic will fall on a straight line connecting the two intercepts.

The values of the peak amperes and peak volts of the example circuit taken from the curve are 50 amperes and 700 volts respectively.

In addition to the peak amperes and peak voltage, the desired pulse width must be decided. The pulse width must be sufficient to allow the establishment of the cathode spots and the transfer of the arc to the auxiliary anode, grid, or the main anode of the ignitron. The pulse width affects the power required. A shorter pulse will require less power. Thus, the minimum reliable pulse width should be used. A pulse width of 12 degrees has been determined as satisfactory, based on experience.

The circuit analysis may proceed once the pulse characteristics have been decided.

CIRCUIT ANALYSIS

The circuit may be analyzed by considering the charging period and the discharge period separately. The energy required for the discharge will determine the charging characteristics required, and therefore the discharge part of the circuit will be discussed first.

The discharge circuit, as shown in Fig. 3, consists of the capacitor, controlled rectifier, inductor, and the parallel combination of the ignitor and shunt resistor. The circuit operation is dependent on an oscillatory discharge. The basic equation for an R - L - C oscillatory discharge may be written as⁴

$$i = \frac{2CEe^{-\alpha t} \sin \beta t}{\sqrt{4LC - R^2C^2}} \quad (1)$$

where

E = initial voltage of the capacitor
 L = inductance
 C = capacitance
 R = resistance
 t = time

$$\beta = \sqrt{\frac{1}{LC} - \frac{R^2}{4L^2}}$$

and

$$\alpha = \frac{R}{2L} \quad (2)$$

The condition that must be met for the discharge to remain oscillatory is

$$R < R_c$$

where

$$R_c = 2\sqrt{\frac{L}{C}} \quad (3)$$

The equation for the peak current of an oscillatory discharge may be derived from equation 1 by setting the first derivative equal to zero and solving for t . The value of t obtained, which is the time at which the peak current occurs, may then be substituted in equation 1. The new equation will be the peak current of the discharge.

Let

$$K = \frac{2CE}{\sqrt{4LC - R^2C^2}}$$

Equation 1 may then be written

$$i = Ke^{-\alpha t} \sin \beta t \quad (4)$$

and

$$\frac{di}{dt} = K[(\beta e^{-\alpha t} \cos \beta t) + (-\alpha \sin \beta t e^{-\alpha t})]$$

setting

$$\frac{di}{dt} = 0$$

and solving for t

$$t = \frac{\tan^{-1} \beta / \alpha}{\beta} \quad (5)$$

Substituting this value of t in equation 4,

$$I_{\max} = Ke^{-\alpha \left(\frac{\tan^{-1} \beta / \alpha}{\beta} \right)} \sin \left(\tan^{-1} \frac{\beta}{\alpha} \right) \quad (6)$$

For any given pulse width it may be seen that regardless of the value of L and C ,

$$\begin{aligned} \alpha &= \text{constant} \\ \beta &= \text{constant} \\ \sqrt{4LC - R^2C^2} &= \text{constant} \end{aligned}$$

Thus, equation 6 may be simplified as follows:

The frequency of oscillation of the 12-degree pulse is

$$f = \frac{360}{24} \times 60 = 900 \text{ cps (cycles per second) =}$$

$$\frac{1}{2\pi\sqrt{LC}} \quad (7)$$

thus

$$LC = 3.11 \times 10^{-8}$$

Assume

$$L = 1 \times 10^{-4}$$

then

$$C = 3.11 \times 10^{-4}$$

and solve for the values of α , β , and $\sqrt{4LC - R^2C^2}$. R_c in equation 3 is the value of resistance at which the discharge becomes nonoscillatory. There-

fore, a value of resistance less than R_c must be used that has sufficient margin to allow for inherent circuit resistance. A value of $0.8 R_c$ will assure an oscillatory discharge.

Assume

$$R = 0.8 R_c$$

then

$$R = 1.6 \sqrt{\frac{L}{C}} = 0.91$$

Solving for the constants α , β , and $\sqrt{4LC - R^2C^2}$ with $R = 0.8 R_c$

$$\alpha = \frac{R}{2L} = 4550$$

$$\beta = \sqrt{\frac{1}{LC} - \frac{R^2}{4L^2}} = 3390$$

$$\sqrt{4LC - R^2C^2} = 2.1 \times 10^{-4}$$

It may be seen from equation 6 that when $R = 0$, $\alpha = 0$, and $I_{\max} = K$.

Substituting these constants in equation 6, first for the condition of $R = 0$, R_c and then for $R = 0$, results in two simplified equations for the two peak currents.

$$I_{\max} = 0.566 CE \times 10^4 \text{ where } R = 0$$

$$I_{\max} = 0.24 CE \times 10^4 \text{ where } R = 0.8 R_c$$

The peak voltage of the circuit with an open ignitor is

$$E_{pk} = I_{\max} \times 0.8 R_c \quad (1)$$

Substituting the desired values of 700 volts and 50 amperes in equations 8 and 10 respectively, gives

$$50 = 0.566 CE \times 10^4$$

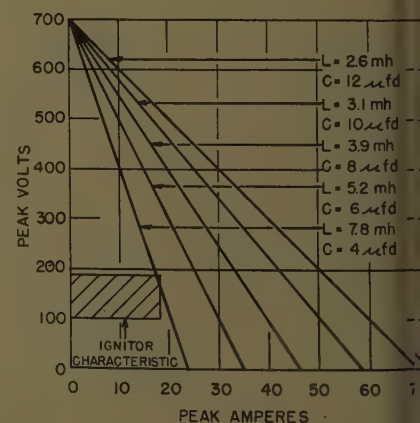
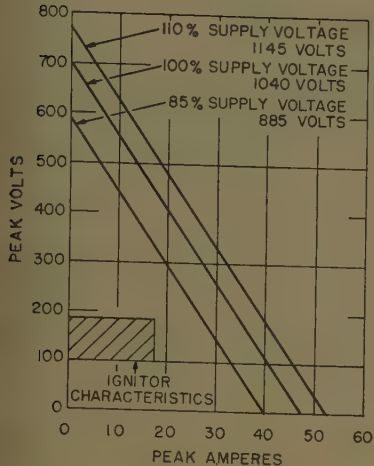


Fig. 6. Peak volt-ampere characteristic curves for various parameter combinations with a constant capacitor voltage and constant pulse width of 12 degrees

All curves for a constant peak capacitor voltage of 1,040 volts



7. Peak volt-ampere characteristic curves for the example circuit, 8 μ f and 4 mh

$$\frac{700}{\sqrt{2} \sqrt{\frac{L}{C}}} = 0.24CE \times 10^4$$

ving these two equations simultaneously

424.36

from equation 7

$$C = 3.11 \times 10^{-8}$$

se two equations, solved simultaneously, give the following values of L and C for the desired pulse:

3.7 mh (millihenry)

8.5 μ f (microfarad)

e value of the peak capacitor voltage V now be determined from equation 8, g the value of $C = 8.5 \mu$ f.

$$= \frac{50 \times 10^{-4}}{0.566C} = 1,040 \text{ volts}$$

nce equations 9 and 10 have been ved, the characteristics of the circuit easily be determined and plotted on peak volt-ampere curve for various combinations of L and C , provided the e pulse width is maintained. This edure enables the values of L , C , and peak capacitor voltage to be selected the most desirable combination. refore, the most suitable circuit onents may easily be chosen. Fig. a series of curves illustrating how the -ampere characteristics vary with erent combinations of L and C with a tant peak capacitor voltage of 1,040 s and a constant pulse width of 12 es. The higher the value of C , the er the peak amperes, and vice versa. peak voltage will remain the same as

long as the peak capacitor voltage remains unchanged. As seen from the curve, the circuit characteristic that most closely meets the requirements of the desired circuit is the 8- μ f-capacitor and 3.9-mh-inductor combination. The peak capacitor voltage of 1,040 volts will be satisfactory since the 700-volt ordinate intercept meets the desired value. The characteristics of the proposed circuit are shown separately in Fig. 7. The upper line represents the characteristic for the condition of 110% rated voltage, and the lower line is the characteristic for the condition of 85% rated voltage. The curve illustrates that the example circuit has sufficient margin for the 85% rated voltage condition and also ignitor aging.

DISCHARGE COMPONENTS

The current rating of the controlled rectifier will be determined at 110% rated voltage and the condition of a short-circuited ignitor as

$$I_{avg} = \int_0^{\pi/16} \frac{idt}{2\pi} = 1.12 \text{ amperes} \quad (11)$$

where I_{max} at 110% of rated voltage, as taken from Fig. 7, is 51.7 amperes at short circuit, and

$$I_{rms} = \sqrt{\int_0^{\pi/16} \frac{i^2 dt}{2\pi}} = 6.45 \text{ amperes} \quad (12)$$

The parallel resistor rating is determined from the current under the condition of an open ignitor and 110% supply potential. For the condition of an open ignitor:

$$I_{rms} = \sqrt{\int_0^{\pi/16} \frac{i^2 dv}{2\pi}} = 2.58 \text{ amperes} \quad (13)$$

where I_{max} at 110% of rated voltage, as derived from equation 9, is

$$I_{max} = 0.24CE \times 10^4 = 23.4 \text{ amperes}$$

The value of the parallel resistors is

$$R = 1.6 \sqrt{\frac{L}{C}} = 32 \text{ ohms}$$

The controlled rectifier utilized in this circuit is actually three devices connected in series. The various manufacturers of the controlled rectifier publish derating curves for various conduction periods and peak currents which must be adhered to in applying the devices. Each of the devices utilized in the circuit is rated 400 volts and 16 amperes average, and meets the derating requirements. The series connected devices support the 110% peak capacitor voltage of 1,145 volts in the forward direction. The device, applied in this circuit, is not subjected

to any reverse voltage other than the forward voltage drop of the shunt rectifier. The filter action of the circuit prevents forward voltage surges on the controlled rectifiers in excess of rated values. Potential dividing circuits are utilized around each device connected in series to assure equal voltage distribution. The number of controlled rectifiers in series may be reduced as higher voltage rated units become available commercially.

The inductor may be either an air or iron core type that is essentially linear in operation. The inductor carries the discharge current and also the oscillating current which flows through the shunt rectifier. The inductor is rated for the a-c pulse with the 110% supply voltage condition and shorted ignitor as

$$I_{rms} = \sqrt{\int_0^{2\pi/16} \frac{i^2 dt}{2\pi}} = 9.45 \text{ amperes} \quad (14)$$

The capacitor must be suitable for 1,145 volts.

CHARGING COMPONENTS

The charging voltage is approximately

$$E_{rms} = \frac{E_{cpk}}{\sqrt{2} \sin \left(\tan^{-1} \frac{X_c}{R} \right)} \quad (15)$$

and,

$$I_{rms} = \frac{E_{rms}}{\sqrt{2} \sqrt{X_c^2 + R^2}} \quad (16)$$

$I_{rms} = 0.62$ ampere, neglecting the reduction due to the shunt rectifier

The current rating is determined by neglecting the shunt rectifier power saving to allow sufficient margin for the condition of an open ignitor since under this condition the power which oscillates is small.

The resistor and the charging rectifier may be chosen accordingly. The charging rectifier must be capable of blocking the peak capacitor voltage in addition to the peak voltage of the charging source. This is true, since the capacitor may be fully charged at the time when the charging source voltage is at a negative crest. This is approximately 2,800 volts in the circuit described.

This design procedure is desirable in two respects. First, it enables the characteristics of a particular circuit to be predetermined analytically, and thus obtain the most desirable combination of parameters. Second, the ratings of the various components may be determined prior to any laboratory investigation.

Various circuits analyzed by this method were tried experimentally. The data obtained experimentally compared

favorably with the calculated characteristics.

Conclusions

The circuit operation and analysis procedure covers a firing circuit utilizing controlled rectifiers that meets the most stringent present-day firing circuit characteristics. Hence, the operating characteristics of the electronic converter as a whole, which are dependent on the firing

circuit characteristics, are capable of meeting the most stringent application requirements.

The controlled rectifier firing circuit presented, meets the required volt-ampere characteristics for reliable ignitor firing; is capable of 170-degree phase delay, which is adequate for all applications; has no time delay; is rugged and has unlimited life; and unlike the reactor firing circuits, is insensitive to frequency variations.

Optimum Nonlinear Bang-Bang Control Systems With Complex Roots

I—System Synthesis

PRAPAT CHANDAKET
ASSOCIATE MEMBER AIEE

C. T. LEONDES
ASSOCIATE MEMBER AIEE

ALMOST ALL OF THE WORK published on the synthesis of optimum nonlinear bang-bang or relay control systems has dealt with the case where the controlled system is characterized by real roots. For such systems there have been numerous papers devoted to the derivation of the optimum controller. Outside of Bushaw's work^{1,2} there has not been much in the literature on the explicit definition of the optimum nonlinear controller in the phase plane, or phase space, in the case where the controlled system is characterized by complex roots. Even in the case of Bushaw's work, the solution for the controller is presented only for regulator-type systems and his solution is not applicable to servomechanism-type systems. These points are discussed in more detail in the first part of this paper. There have been other very fine contributions to the literature on this problem.³⁻⁵ However, in these contributions the question of the complete optimum nonlinear controller as defined in the phase plane or space is still left unsolved.

It is the purpose of this paper to present the required phase-space solution for the optimum nonlinear controller for second-order systems, and thus to fill an important gap in the literature in the control-systems field. The derivation of the required optimum nonlinear controller is a fairly involved process as this paper demonstrates. The resultant con-

troller is a fairly complicated device (as is evident from Fig. 13 of the paper) and it presents some practical problems in its mechanization. As a result some compromise optimum nonlinear controllers are presented (see Figs. 16 and 17).

Because of the length of this paper, some results of analytical studies of the dynamic response capabilities of these systems are presented in Part II of this paper, "Analytical Studies," in which a variety of input forcing functions are applied to systems with optimum and compromised optimum nonlinear controllers.

Bushaw's Results

The optimum switching criterion for second-order systems was first derived by Bushaw in 1952.^{1,2} His system equation is represented by

$$\ddot{x} + g(x, \dot{x}) = \phi(x, \dot{x}) \quad (1)$$

where ϕ takes only the values $+1$ or -1 , and x, \dot{x}, \ddot{x} are the variable and its time derivatives which are to be reduced simultaneously to zero. His optimum criterion is to reduce x and \dot{x} to zero simultaneously, in minimal time. The results he developed are applicable to a second-order control system whose characteristic roots are complex. However, his result is applicable only to the special class of regulator control systems wherein the desired input may not change. This

References

1. EXCITATION CIRCUITS FOR IGNITRON RECTIFIERS, H. C. Myers, J. H. Cox. *AIEE Transactions (Electrical Engineering)*, vol. 60, Oct. 1941, pp. 943-48.
2. CONSIDERATIONS IN APPLYING RECTIFIERS TO A POWER SUPPLY FOR HOT STRIP MILLS, G. Zins, E. J. Cham. *AIEE Transactions, pt. 1 (Applications and Industry)*, vol. 73, May 1956, pp. 65-70.
3. POOL-CATHODE MERCURY-ARC POWER CONVERTERS. *ASA C34.1*, American Standards Association, New York, N. Y., 1958.
4. ALTERNATING-CURRENT CIRCUITS (book), M. Kerchner, G. F. Corcoran. John Wiley & Sons, Inc., New York, N. Y., 1960.

is due to the restriction that ϕ may only $+1$ or -1 . To make this statement clearer, consider a second-order predictor control system (complex roots) in Fig. 1, where F represents the maximum control effort. From this, one obtains the system equation

$$\ddot{e}(t) + 2\xi W_n \dot{e}(t) + W_n^2 e(t) = \delta K F$$

where

$$\delta = \pm 1$$

Using a step input

$$r(t) = a_0$$

one obtains the error equation

$$\ddot{e}(t) + 2\xi W_n \dot{e}(t) + W_n^2 e(t) = W_n^2 a_0 - \delta K F$$

with

$$\tau = W_n t$$

$$E(\tau) = \frac{W_n^2}{K F} e(\tau)$$

$$A_0 = \frac{a_0 W_n^2}{K F}$$

the normalized error equation becomes:

$$\ddot{e}(\tau) - 2\xi(\tau) + e(\tau) = A_0 - \delta$$

It should be noted that, where the input is allowed to change, the right half of equation 8 cannot be made $+1$ or -1 as was required in Bushaw's case.

It can be stated in general that the results, when applied to complex systems, are applicable only to the class of regulating control devices, where

Paper 60-1266, recommended by the AIEE Feedback Control Systems Committee and approved by the AIEE Technical Operations Department for presentation at the AIEE Fall General Meeting, Chicago, Ill., October 9-14, 1960. Manuscript submitted June 8, 1960; made available for printing September 13, 1960.

P. CHANDAKET is with the Royal Thai Navy Bangkok, Thailand, and C. T. LEONDES is with the University of California, Los Angeles, Calif.

This research was supported, in part, by the United States Air Force under Contract no. 49(638)-438, monitored by the Air Force Office of Scientific Research of the Air Research Development Command.

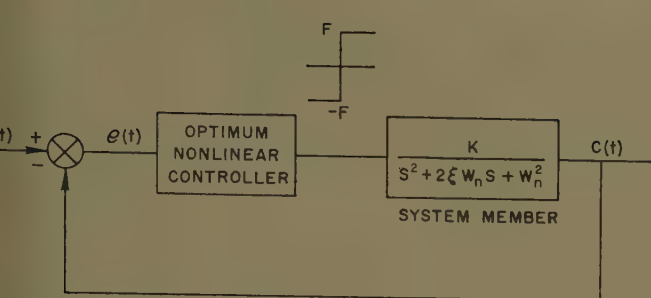


Fig. 1. Second-order optimum predictor control system (complex roots)

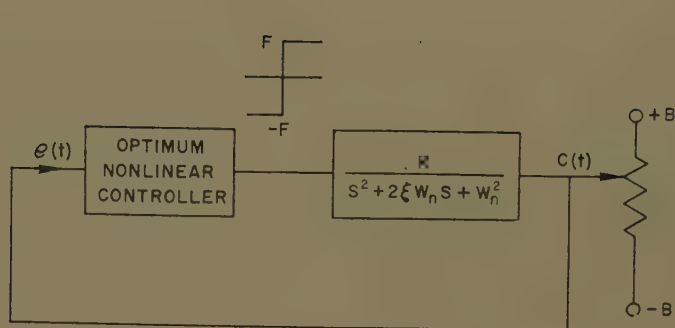


Fig. 2. Basic control system modified for Bushaw's result

output member has to be maintained at certain fixed level. In other words, the output member has its equilibrium state at a zero reference potential. This includes a class of control systems subjected to load disturbances. However, with a system arrangement which is slightly different than the usual control system, his results can be applied. The basic arrangement is suggested in Fig. 2. It should be emphasized that the equilibrium state is at $c = \dot{c} = 0$. With this arrangement, a desired input can be applied by moving the potentiometer (+B, -B) up or down. This is the same as introducing a new nonequilibrium state to the system. The optimum nonlinear controller is then designed to bring the system back to the equilibrium state where $c = \dot{c} = 0$ or $r(t) = c(t)$ in minimal time. With this mode of operation, the design of the nonlinear controller based on equation 2 for its optimum correcting process, since in this case $c = e(t)$ when c and $\dot{c} \neq 0$ and $c(t) = r(t)$ when $c = \dot{c} = 0$. With this arrangement, the obtained response will be optimal in this sense.

Comparing this to an ordinary control system (Fig. 1), the optimum nonlinear controller must be designed such that it brings $e(t)$ and $\dot{e}(t)$ in equation 4 to zero simultaneously, in minimal time. It is also that a_0 appears in the right half of equation 4, and this implies that the output information is needed as a pre-empting control factor in the required nonlinear controller. It may be seen that both systems will yield optimum response in their own senses.

Statement of the Problem

In this paper, the optimum switching criteria will be derived for a second-order optimum predictor control system of complex roots in the left-half plane ($\xi < 1$). These results will then represent a significant extension to Bushaw's work which is restricted to the special case of regulating control problems.

Since the system equation is different from that of Bushaw's in that

1. the direction of the force is opposite
2. the stable point is no longer at +1 and -1

all Bushaw's results must be modified. In order to facilitate the development of the results, the work in this paper will be developed on a self-contained basis, and a rigorous proof will be skipped, if basic reasoning can be applied. The approach to the problem will be slightly different from that of Bushaw's. In this work the optimum switching criteria will be directly derived from the use of inductive techniques which will then lead to a better understanding of the problem.

Since the obtained results will be quite complicated and very difficult to mechanize, a compromise switching criterion which will lead to a near-optimum response will be suggested. An analog study for this problem will also be discussed in Part II of this paper.⁶

Properties of Phase Trajectories

The system shown in Fig. 1 will be used for deriving the optimum switching criterion. Now, the optimum switching criterion is to reduce ϵ and $\dot{\epsilon}$ in equation 8 to zero simultaneously, in minimal time. Let

$$u(\tau) = \epsilon(\tau) \quad (9)$$

$$u(\tau) = \dot{\epsilon}(\tau) \quad (10)$$

then

$$\frac{du(\tau)}{d\tau} = u(\tau) \quad (11)$$

$$\frac{dv(\tau)}{d\tau} = -u(\tau) - 2\xi v(\tau) + M \quad (12)$$

where

$$M = A_0 - \delta \quad (13)$$

From equations 11 and 12, one obtains the slope of any phase trajectory in the $u-v$ plane as

$$\frac{dv(\tau)}{du(\tau)} = \frac{-u(\tau) - 2\xi v(\tau) + M}{V(\tau)} \quad (14)$$

where its stable point (focus) is at $u = M$ and $v = 0$. Since δ can take on values of either +1 or -1, then for convenience

$$M_n = A_0 + 1 \text{ (N-curve)}$$

$$M_p = A_0 - 1 \text{ (P-curve)} \quad (15)$$

Now, it can be stated that, in the $u-v$ plane, the stable point for the N-trajectory is $(M_n, 0)$ and for the P-trajectory $(M_p, 0)$ where N and P denote the negative (force) curve and positive (force) curve respectively.

LIMITATION ON a_0

Applying the Final Value Theorem to equation 2, one obtains the system steady-state position as

$$C_{ss} = \frac{\delta K F}{W_n^2}$$

as a result of this, if F is the maximum allowable control effort, the maximum limit of a_0 , the step input is, recalling that $|\delta| = 1$

$$|a_0| < \frac{KF}{W_n^2} \quad (16)$$

or by equation 7, one also obtains

$$|A_0| < 1 \quad (17)$$

In other words, if a_0 is greater than KF/W_n^2 there will be a nonzero steady error, which may be assumed to be undesirable.

USE OF CO-ORDINATE TRANSFORMATION

For convenience, the same transformation as used by Bushaw will also be used here, namely,

$$x = u + \xi v \quad (18)$$

$$y = \gamma v \quad (19)$$

where

$$\gamma = \sqrt{1 - \xi^2} \quad (20)$$

It should be noted that, with this linear transformation, the axis of abscissa is

left pointwise invariant, and the time length is the same. In fact, it simply represents a change to oblique co-ordinates. With these properties, the significant information, such as the corner condition (this term will be defined shortly) is unchanged. Therefore, all results can be derived in the x - y plane and are then applicable to the u - v plane by using the transformation equations 18 and 19.

Substitution of equations 18 and 19 into equations 11 and 12, yields

$$\frac{dx}{d\tau} = -\xi x + \gamma y + M\xi \quad (21)$$

$$\frac{dy}{d\tau} = -\gamma x - \xi y + \gamma M \quad (22)$$

Solving equations 21 and 22

$$x(\tau) = M + e^{-\xi\tau} [Ae^{j\gamma\tau} + Be^{-j\gamma\tau}] \quad (23)$$

$$y(\tau) = je^{-\xi\tau} [Ae^{j\gamma\tau} - Be^{-j\gamma\tau}] \quad (24)$$

where

$$A = \frac{1}{2} [x(0) - jy(0) - M]$$

and

$$B = \bar{A} \quad (25)$$

Slopes of trajectories in the rectangular x - y co-ordinates can be obtained from equations 21 and 22 as

$$\frac{dy}{dx} = \frac{\gamma}{\xi} - \frac{\gamma/\xi}{-\xi x + \gamma y + M\xi} \quad (26)$$

It can be seen from equation 26 that all x - y trajectories cross the x -axis at the angle $\theta = \tan^{-1} \gamma/\xi$, whereas in the rectangular u - v plane, all trajectories cross the u -axis with an infinite slope (see equation 14). However, when $v = u = 0$, $x = u$, and all trajectories in the upper (or lower) half of the x - y plane will also be represented by the corre-

sponding trajectories in the upper (or lower) half of the u - v plane. It should be stated that all derivations to follow will be performed in the x - y plane, if not stated otherwise and all figures will be drawn in the u - v plane. It is seen that there are two families of trajectories in the x - y plane, i.e., positive (force) and negative (force) trajectories. Both of them will spiral around their corresponding stable points on the x -axis at M_p or M_n . This fact can be shown from equations 23 and 24 as follows.

From equation 23

$$x(\tau) - M = e^{-\xi\tau} [(x(0) - M) \cos \gamma\tau + y(0) \sin \gamma\tau] \quad (27)$$

From equation 24

$$y(\tau) = -e^{-\xi\tau} [(x(0) - M) \sin \gamma\tau - y(0) \cos \gamma\tau] \quad (28)$$

Squaring and combining equations 27 and 28 yields

$$[x(\tau) - M]^2 + y^2(\tau) = e^{-2\xi\tau} [(x(0) - M)^2 + y(0)^2] \quad (29)$$

which indicates that any x - y phase trajectory will converge spirally around its stable point $(M, 0)$ and approaches this point when $\tau \rightarrow \infty$.

The travelling time from $[x(0), y(0)]$ to $[x(\tau), y(\tau)]$ can be obtained from equation 29 as

$$= \frac{1}{2\xi} \ln \frac{[x(0) - M]^2 + [y(0)]^2}{[x(\tau) - M]^2 + [y(\tau)]^2} \quad (30)$$

Another property that will be used in the derivation of the optimum switching criterion is the travelling time required for the successive intersection of any trajectory with the x -axis. This can be found from equation 24 by using the fact that $y = 0$ and $A = \bar{B}$, hence the imaginary part of $Ae^{j\gamma\tau} = 0$, and this yields

$$\tan \gamma\tau = \frac{y(0)}{x(0) - M}$$

Since $\tan \gamma\tau$ is multiple-valued $m\pi/\gamma$, one can state in general that the travelling time for any successive intersection of a trajectory with the x -axis is π/γ . The properties of trajectories in general, that have been derived in this section will be referred to from time to time, and for convenience are summarized.

Property I. All trajectories converge spirally around their focus at $(M, 0)$.

Property II. Slopes of x - y phase trajectories are given by

$$\frac{dy}{dx} = \frac{\gamma}{\xi} - \frac{\gamma/\xi}{-\xi x + \gamma y + M\xi}$$

Property III. The travelling time required for any successive intersection of a trajectory with the x -axis is π/γ .

Derivation of Other Necessary Properties

It has been shown that the phase trajectories in the x - y plane tend to spiral around the corresponding stable point $(M, 0)$ an infinite number of times. Among these, there are two zero trajectories (δ^+ and δ^-) that lead to the origin. However, due to Property I, if these two zero trajectories (δ^+ and δ^-) are traced backward (negative-time direction) they will diverge in a spiral about the corresponding focus, therefore, one would need to use some optimum cutoff criterion to discontinue these zero trajectories at certain points in order to find the optimum switching boundary. For convenience all properties necessary in the derivation of the optimum switching criterion will now be developed.

Property IV. Any optimum path must be canonical^{1,2}. A path will be called canonical if it contains no PN corners above the x -axis and no NP corners below. Note that, this is the opposite of Bushaw's canonical path.

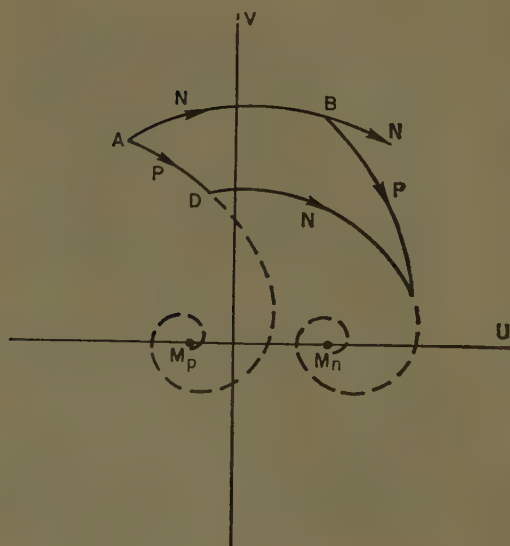


Fig. 3 (left). Example of canonical path in the upper u - v plane

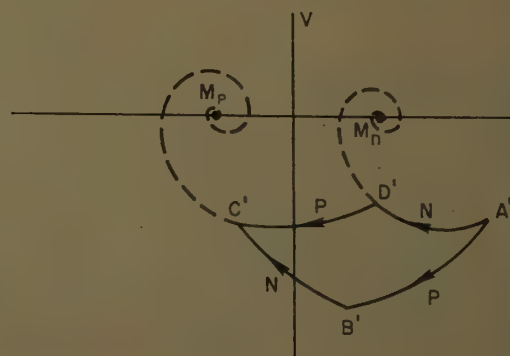


Fig. 4 (right). Example of canonical path in the lower u - v plane

Proof: Since the travelling time is only obtained in the u - v plane due to the fact that $v = du/d\tau$, the proof will be performed in this plane. Referring to equation 14 one obtains, for $v > 0$:

$$\left. \frac{dv}{du} \right|_{(P\delta^+)} < \left. \frac{dv}{du} \right|_{(P\delta^-)} \quad (32)$$

This property is illustrated at points A and B in Fig. 3. It can be seen that all points A , B , C , and D satisfy equation 14.

Therefore, this condition does exist in the u - v phase plane (also in the x - y plane). According to the definition, the path containing AB and BC is canonical, since it has an NP corner at B . The other path is composed of AD and DC and has a PN corner at D , therefore it is not canonical. These two paths have the same starting point and the same end point. Using the time relation

$$\int_{u(0)}^{u(\tau)} \frac{du}{v} \quad (33)$$

it can be seen that $\tau_{AB} + \tau_{BC} < \tau_{AD} + \tau_{DC}$. If this condition occurs, one can always find a canonical path which will take less time than the one with the wrong corner that is not canonical.

For $v < 0$, one obtains from equation

$$\left. \frac{dv}{du} \right|_{(P\delta^+)} < \left. \frac{dv}{du} \right|_{(P\delta^-)} \quad (34)$$

the condition shown in Fig. 4 may be seen. In this case, the canonical path contains $A'B'$ and $B'C'$ with a PN corner at B' . By using equation 33, one can see that $\tau_{A'B'} + \tau_{B'C'} < \tau_{A'D'} + \tau_{D'C'}$, which leads to the same conclusion that the time required for the canonical path is always less than that required for the path with the wrong corner. The canonical path will be used throughout the following derivation. It is easily seen that for a given path which is not canonical, one can always replace it with a canonical path which will take less time. Therefore the optimum path must be canonical,

whereas the opposite statement is not necessarily true.

Property V. The time required from all initial points on or within the boundary enclosed by either the zero trajectory (Γ_n or Γ_p) and the u axis in the u - v plane (or x -axis in the x - y plane) to reach the origin is less than π/γ (or equal at its limit). This is shown in Fig. 5.

Define: The zero trajectories Γ_p or Γ_n as the part of the phase trajectory that passes through the origin, and these can be obtained by tracing the trajectory (δ^+ or δ^-) backward from the origin for π/γ unit time. Referring to Fig. 5, it may be seen that these curves are unique and are represented by Γ_p for δ^+ -force and Γ_n for δ^- -negative force.

If the initial point falls in the P -loop, the required path is obtained by applying an N -force until it reaches Γ_p . The forcing function is then switched to a P -force and the trajectory follows Γ_p to the origin. One can obtain a similar result if the initial point falls in the N -loop by applying a P -force until it hits Γ_n then following Γ_n to the origin by using the N -force.

Proof: See Fig. 5. Assume the initial point at p , and let

$$\tau_{pr} = \lambda(\delta^- \text{-force})$$

$$\tau_{rt} = \sigma(\delta^+ \text{-force})$$

then we must prove that $\lambda + \sigma < \pi/\gamma$. For convenience, prove this by using negative time starting from the origin.

From equations 23 and 24

$$x_r = (A_0 - 1) + e^{\xi\sigma} (Ae^{-j\gamma\sigma} + Be^{j\gamma\sigma}) \quad (35)$$

$$y_r = je(\xi\sigma Ae^{-j\gamma\sigma} - Be^{j\gamma\sigma}) \quad (36)$$

where

$$A = \frac{1}{2}(1 - A_0) = B$$

$$x_p = (A_0 + 1) + e^{\xi\lambda} [A_1 e^{-j\gamma\lambda} + B_1 e^{j\gamma\lambda}] \quad (37)$$

$$x_p = je^{\xi\lambda} (A_1 e^{-j\gamma\lambda} - B_1 e^{j\gamma\lambda}) = 0 \quad (38)$$

where

$$A_1 = \frac{1}{2}[x_r - jy_r - (A_0 + 1)]$$

Solving the previous four equations using the fact that $y_p = 0$ implies

$$I_m[A_1 e^{-j\gamma\lambda}] = 0$$

yields

$$\frac{\sin \gamma\lambda}{\sin \gamma(\sigma + \lambda)} = \frac{e^{\xi\sigma}(1 - A_0)}{2} \quad (39)$$

By inspection of equation 39, the right side of the equation is positive [$|A_0| < 1$ by equation 17], $\sin \lambda > 0$ by Property III, hence, $\sin \gamma(\sigma + \lambda)$ must be positive and this implies $(\sigma + \lambda) < \pi/\gamma$ since either σ or λ cannot be greater than π/γ by Property III, and this completes the proof. A similar proof can be applied to the N -loop and will lead to the same conclusion.

Property VI. See Fig. 6.

A. If an N -trajectory crosses the axis at $x > M_n$, a shorter path can be found by shunting that path with a P -curve.

B. If a P -trajectory crosses the x -axis at $x < M_p$, a shorter path can be found by shunting that path with a N -curve.

The proof will be given in the u - v plane, because it is more easily seen and may be done with easier techniques. However, the results are applicable to the x - y plane due to the linear transformation in equations 18 and 19. For convenience, the slope characteristics in equations 32 and 34 are rewritten

for $v > 0$:

$$\left. \frac{dv}{du} \right|_N > \left. \frac{dv}{du} \right|_P \quad (40)$$

for $v < 0$:

$$\left. \frac{dv}{du} \right|_P > \left. \frac{dv}{du} \right|_N \quad (41)$$

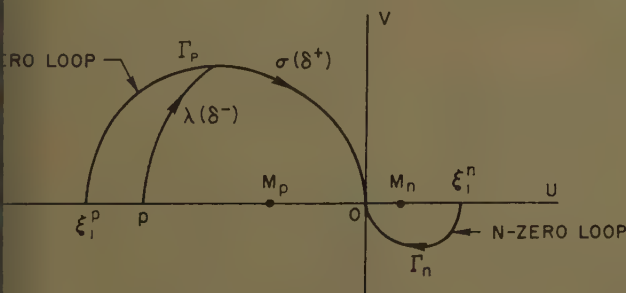


Fig. 5. Illustration for property V

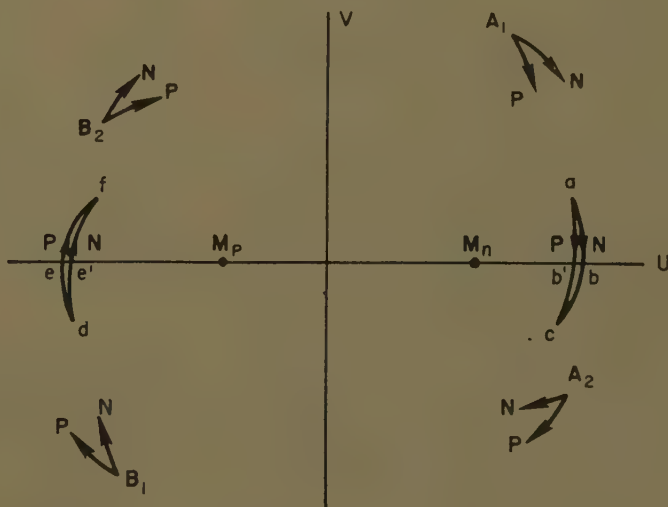


Fig. 6 (right). Short-path property VI in the u - v plane

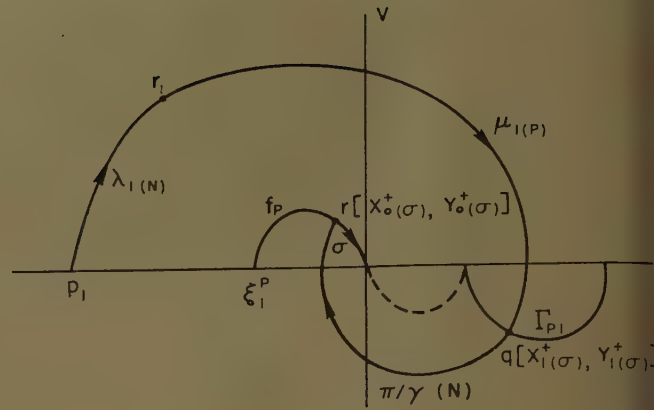
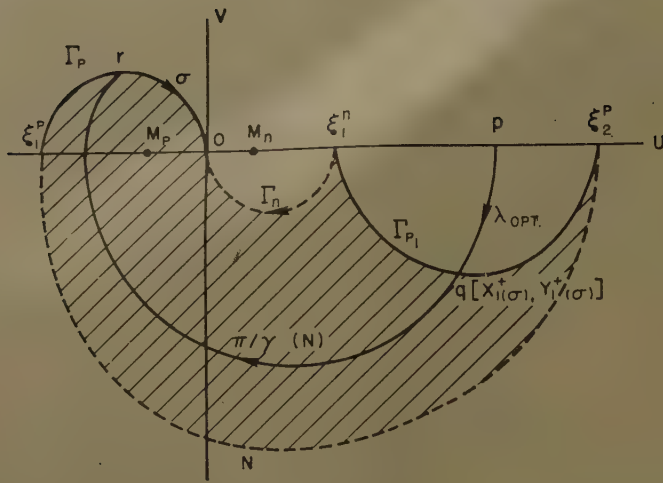


Fig. 10 (left). First positive optimum switching boundary

Fig. 11 (above). Derivation of the second positive switching corner

zero trajectory obtained will diverge in a spiral about its corresponding stable point an infinite number of times. Therefore, some criterion must be applied to discontinue the entire zero trajectory at a certain point, such that it will represent the optimum path to the origin see Fig. 8. By Property VI, if Γ_n or Γ_p are extended (backward) beyond ξ_1^n and ξ_1^p , then one can shunt them in the vicinity of the u -axis by the opposite (force) trajectories which will take less time. Therefore, the paths beyond ξ_1^n and ξ_1^p will not yield optimal path any more. With this fact, only the Γ_n and Γ_p portion of the zero trajectories will be used as part of the optimum switching boundary.

From now on, the complete optimum switching boundary will be derived on an inductive basis. Since the phase trajectory is unique, no other P -trajectories can intersect Γ_p . The only possibility is that they can join at either ξ_1^p or ξ_1^n , but this has been rejected by Property VI. Hence, only P -trajectories can reach Γ_n . Now, find the rest of the optimum switching boundary outside of the P - and N -zero loops. Let Γ_p and Γ_n be called the zero switching boundaries.

DERIVATION OF THE ZERO SWITCHING CORNERS $[x_{0(\sigma)}^\pm, y_{0(\sigma)}^\pm]$

Trace the curves backward from the origin by σ unit time. Applying equations 23 and 24 obtains the optimum switching corners $[x_{0(\sigma)}^\pm, y_{0(\sigma)}^\pm]$ as a function of time. See Fig. 8 for notations x_0^\pm and y_0^\pm where (x_0^+, y_0^+) belongs to Γ_p and (x_0^-, y_0^-) to Γ_n .

$$x_0^+(\sigma) = (A_0 \mp 1) + e^{\xi\sigma} [Ae^{-j\gamma\sigma} + Be^{j\gamma\sigma}]$$

$$y_0^+(\sigma) = je^{\xi\sigma} (Ae^{-j\gamma\sigma} - Be^{j\gamma\sigma})$$

where

$$A = -\frac{1}{2}(A_0 \mp 1) = \bar{B}$$

Solving the previous equations yields

$$\begin{aligned} x_0^\pm(\sigma) &= (A_0 \mp 1)\beta \\ y_0^\pm(\sigma) &= (A_0 \mp 1)\eta \end{aligned} \quad (51)$$

where

$$\begin{aligned} \eta &= -e^{\xi\sigma} \sin \gamma\sigma \\ \beta &= 1 - e^{\xi\sigma} \cos \gamma\sigma \end{aligned} \quad (52)$$

By taking $\sigma = \pi/\gamma$, one obtains

$$\xi_{1(n)}^p = [A_0(-1)](1 + e^{\xi\pi/\gamma}) \quad (53)$$

DERIVATION OF FIRST SWITCHING CORNER $[x_{1(\sigma)}^\pm, y_{1(\sigma)}^\pm]$

Define the first positive (or negative) switching corner as the next optimum switching point (backward) from Γ_p (or Γ_n), see Fig. 9.

Then derive the first positive switching corner, which the optimum path from a distant point must pass in order to reach the origin by the Γ_p -portion. Since the optimum path must reach the origin by Γ_p assume that this path will reach Γ_p at point r at σ unit time from the origin. Using a negative time direction, from this point one must trace backward along an N -trajectory. Certainly the first switching point must be outside of the P -zero loop (by Property VII-B), and it cannot pass the positive x -axis by Property VI. Therefore, let q represent the first positive switching point, and let p be the initial point. Assume

$$\tau_{pq} = \lambda \quad (P\text{-curve})$$

$$\tau_{qr} = \mu \quad (N\text{-curve})$$

$$\tau_{ro} = \sigma \quad (P\text{-curve})$$

The problem now, is to determine where q should be. By means of equation 51,

$$x_r(\sigma) = (A_0 - 1)\beta$$

$$y_r(\sigma) = (A_0 - 1)\eta \quad (54)$$

where

$$\beta = 1 - e^{\xi\sigma} \cos \gamma\sigma$$

$$\eta = -e^{\xi\sigma} \sin \gamma\sigma$$

$$x_q(\sigma) = (A_0 + 1) + e^{\xi\mu} (A_1 e^{-j\gamma\mu} + B_1 e^{j\gamma\mu})$$

$$y_q(\sigma) = je^{\xi\mu} (A_1 e^{-j\gamma\mu} - B_1 e^{j\gamma\mu})$$

where

$$A_1 = \frac{1}{2} [x_r(\sigma) - jy_r(\sigma) - (A_0 + 1)] = \bar{B}_1$$

$$x_p(\sigma) = (A_0 - 1) + e^{\xi\lambda} (A_2 e^{-j\gamma\lambda} + B_2 e^{j\gamma\lambda})$$

$$y_p(\sigma) = ie^{\xi\lambda} [A_2 e^{-j\gamma\lambda} - B_2 e^{j\gamma\lambda}] = 0$$

where

$$A_2 = \frac{1}{2} [x_q(\sigma) - jy_q(\sigma) - (A_0 - 1)] = \bar{B}_2$$

using

$$\alpha = \xi - j\gamma$$

one obtains by solving equations 54, and 56

$$1 + x_p = A_0 + 2e^{\alpha\lambda} - 2e^{\alpha(\mu+\lambda)} + (1 - A_0)e^{\alpha(\mu+\sigma+\lambda)}$$

Since the point p (given initial condition is fixed, then one can differentiate both sides of equation 57 with respect to λ to obtain

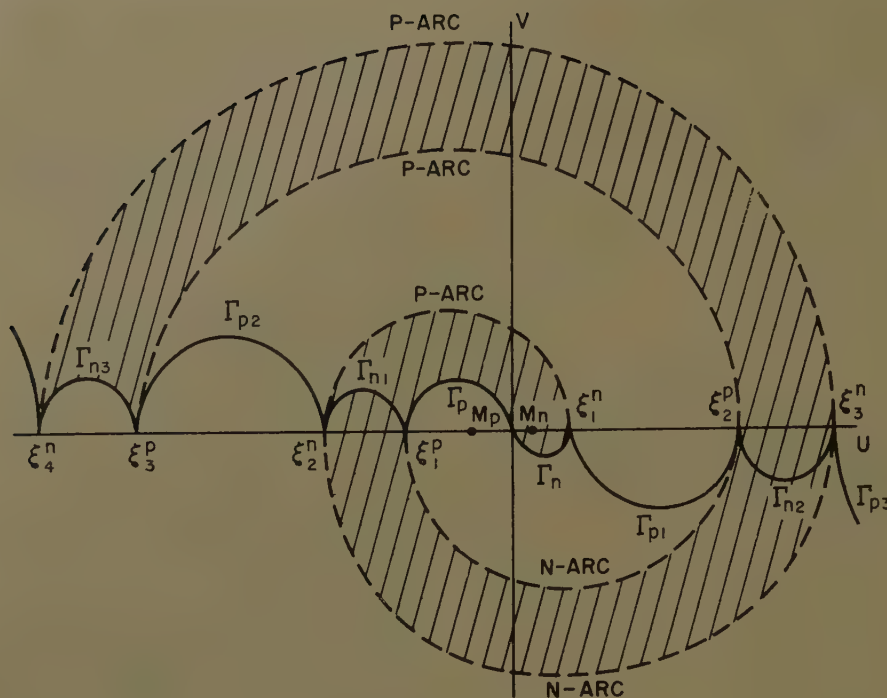
$$\frac{d}{d\lambda}(\sigma + \mu + \lambda) = \frac{2}{(1 - A_0)e^{\xi(\mu+\sigma)}} \frac{\sin \gamma\mu}{\sin \gamma\sigma}$$

The first optimum switching corner obtained by taking $d/d\lambda(\sigma + \mu + \lambda)$ yields

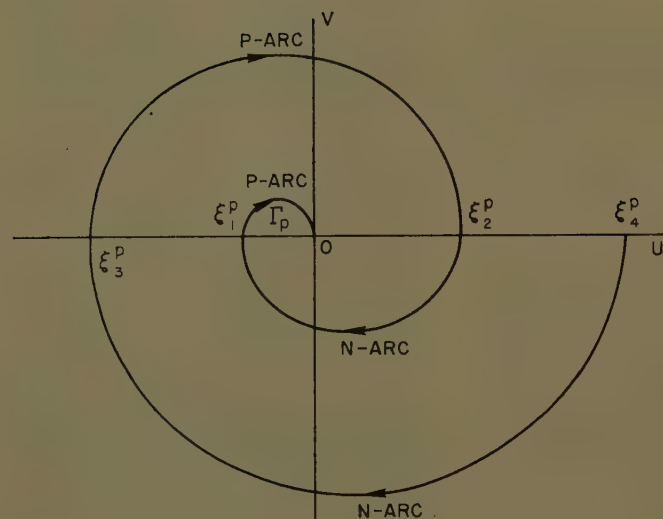
$$\mu = 0, \frac{\pi}{\gamma}, \frac{2\pi}{\gamma}, \dots, \frac{n\pi}{\gamma}$$

Judging from these values, $\mu = 0$ cannot exist, since the P -arc cannot intersect due to the uniqueness principle, and cannot join Γ_p at ξ_1^p due to Property VI. Also, it cannot be $2\pi/\gamma, 3\pi/\gamma, \dots$, since it will violate Property VI. The only choice left is $\mu = \pi/\gamma$. A further check

89



(A)



(B)

Fig. 13. (A) Complete optimum switching boundary and (B) tracing the phase-plane trajectory

equations 70 through 74 in conjunction with Property VI.) Constructing the switching locus this way, one will obtain the positive switching boundary extending from the origin to $\pm \infty$ on the u -axis with a gap in between (this gap will be filled by a negative switching boundary), and the area for all optimum trajectories that will reach the origin Γ_p will be limited by the spiral area as in Fig. 12. To obtain the complete optimum switching boundary, the negative switching loci must be derived and these will give the optimum switching corners for all optimum paths that will reach the origin by Γ_n . This can be obtained in the same manner as for the positive switching boundary. In fact, one also obtains the same result that, starting from Γ_n in nega-

tive time, π/γ units of time are required for Γ_{n1} , and Γ_{n2} will be π/γ units of time from Γ_{n1} and so on. By adding the positive and negative switching boundaries together, a complete optimum switching boundary is now composed of Γ_{nh} and Γ_{ph} where $h=1, 2, 3, \dots, \infty$, and it will extend from $-\infty$ to $+\infty$ along the u -axis. All optimum paths leading to the origin by Γ_n must be switched at all Γ_{nh} to be passed. A similar statement holds also for the optimum path that will reach the origin along the Γ_p trajectory. It will be shown later that all Γ_{ph} and Γ_{nh} are magnified versions of Γ_p and Γ_n obtained by multiplying the ordinates by ρ_h where $\rho = e^{\xi\pi/\gamma}$ and properly rotating and displacing them. The minimal time required for any given initial point

on the u -axis is easily estimated by the following relation:

For a given point P where $\xi_h \leq X_p \leq \xi_{h+1}$, the minimal time required falls within the limits

$$\frac{h\pi}{\gamma} \leq \tau_{\min} \leq (h+1)\frac{\pi}{\gamma} \quad (6)$$

The superscript p or n on ξ_h does not alter this relation. By inspecting the behavior of the optimum path in Fig. 13(A), one can give the optimum switching condition as follows.

If the present initial point is above the optimum switching boundary, a positive force is needed, whereas a negative force is needed when the present point is below the boundary. So far, the complete optimum switching boundary has not been derived in mathematical form. This will be presented next.

DERIVATION OF ξ_h^p AND ξ_h^n

Both ξ_h^p and ξ_h^n will represent the connecting points of the positive and negative switching boundaries; see Fig. 13. For example, determine the location of ξ_h^p . This is easily obtained by tracing the trajectory in the negative time direction by a series of forces as shown in Fig. 13(B). The time required from one to the next is π/γ by Property III. Since γ is always zero from equation 23

$$\xi_1^p = A_0 - [1 - (1 - A_0)e^{\xi\pi/\gamma}]$$

$$\xi_2^p = A_0 + [1 + 2e^{\xi\pi/\gamma} + (1 - A_0)e^{2\xi\pi/\gamma}]$$

$$\xi_3^p = A_0 - [1 + 2e^{\xi\pi/\gamma} + 2e^{2\xi\pi/\gamma} + (1 - A_0)e^{3\xi\pi/\gamma}]$$

$$\xi_4^p = A_0 + [1 + 2e^{\xi\pi/\gamma} + 2e^{2\xi\pi/\gamma} + 2e^{3\xi\pi/\gamma} + (1 - A_0)e^{4\xi\pi/\gamma}]$$

By the inductive method, one can write the obtained results in general form as

$$\xi_h^p = A_0 + (-1)^h \left[1 + 2 \sum_{k=1}^{h-1} \rho^k + (1 - A_0)\rho^h \right]$$

where

$$\rho = e^{\xi\pi/\gamma}$$

By the same technique,

$$\xi_h^n = A_0 + (-1)^{h+1} \times \left[1 + 2 \sum_{k=1}^{h-1} \rho^k + (1 + A_0)\rho^h \right]$$

DERIVATION OF THE OPTIMUM SWITCHING BOUNDARIES (Γ_{ph} AND Γ_{nh})

It is suggested from Fig. 13(A) that the equation for the general optimum switching corners (x_h^+, y_h^+) and (x_h^-, y_h^-) can be easily determined as functions of time (σ) from the origin along the zero loop Γ_p and Γ_n , by the inductive technique. I

ple, determine the relation for the
switching corners (x_h^+ ; y_h^+),
these corners represent the switch-
points for the optimum paths that will
ch the origin along the Γ_p loop trajec-
y.

The previous notation, the use of which
continue, is repeated here for con-
venience.

$\rho \xi \pi / \gamma$

$-e^{\xi \sigma} \sin -\gamma \sigma$

$1 - e^{\xi \sigma} \cos \gamma \sigma$

ere $0 \leq \sigma \leq \pi / \gamma$

Using equations 23 and 24, and tracing
trajectory backward with a positive
e ($\tau = -\sigma$), one finds

$$\begin{aligned} x(\sigma) &= (A_0 - 1)\beta \\ y(\sigma) &= (A_0 - 1)\eta \end{aligned} \quad (70)$$

ch $[x_0^+(\sigma), y_0^+(\sigma)]$ as the initial point,
Fig. 13, trace the trajectory in the
ative time direction by π / γ unit time
h a negative force, then obtain

$$\begin{aligned} x(\sigma) &= \xi_1^n - (A_0 - 1)\rho\beta \\ y(\sigma) &= -(A_0 - 1)\rho\eta \end{aligned} \quad (71)$$

ere

$$= (A_0 + 1)(1 + \rho)$$

again, use $[x_1^+(\sigma), y_1^+(\sigma)]$ as an initial
at and find the next switching point
g a positive force with $\tau = -\pi / \gamma$ and
ain

$$\begin{aligned} x(\sigma) &= \xi_2^n + (A_0 - 1)\rho^2\beta \\ y(\sigma) &= (A_0 - 1)\rho^2\eta \end{aligned} \quad (72)$$

repeating the process, one obtains

$$\begin{aligned} x(\sigma) &= \xi_3^n - (A_0 - 1)\rho^3\beta \\ y(\sigma) &= -(A_0 - 1)\rho^3\eta \end{aligned} \quad (73)$$

$$\begin{aligned} x(\sigma) &= \xi_4^n + (A_0 - 1)\rho^4\beta \\ y(\sigma) &= +(A_0 - 1)\rho^4\eta \end{aligned} \quad (74)$$

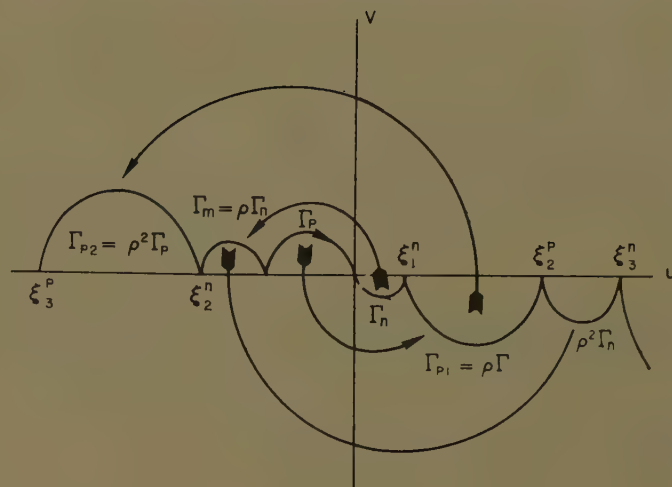
re ξ_1^n, ξ_2^n, \dots are the same as ob-
ed from equation 69. By inspecting
results developed in equations 70
ugh 74, one can write the positive
imum switching corner in general form

$$\begin{aligned} x(\sigma) &= \xi_h^n + (-1)^h(A_0 - 1)\beta\rho^h \\ y(\sigma) &= (-1)^h(A_0 - 1)\eta\rho^h \end{aligned} \quad (75)$$

where ξ_h^n can be obtained from equa-
69. With the same procedure, by
ting from Γ_n , one may obtain the
ative optimum switching corner, in
eral form, as

$$\begin{aligned} x(\sigma) &= \xi_h^p + (-1)^h(A_0 + 1)\beta\rho^h \\ y(\sigma) &= (-1)^h(A_0 + 1)\eta\rho^h \end{aligned} \quad (76)$$

Fig. 14. The tech-
nique for construct-
ing the optimum
switching boundary



By using the inverse transformation of
equations 18 and 19, one may obtain the
optimum switching corner in the $u-v$
plane as

$$\begin{aligned} u_h^+(\sigma) &= \xi_h^n + (-1)^h(A_0 - 1)\left(\beta - \frac{\xi\eta}{\gamma}\right)\rho^h \\ v_h^-(\sigma) &= (-1)^h(A_0 - 1)\frac{\eta}{\gamma}\rho^h \end{aligned} \quad (77)$$

and

$$\begin{aligned} u_h^-(\sigma) &= \xi_h^p + (-1)^h(A_0 + 1)\left(\beta - \frac{\xi\eta}{\gamma}\right)\rho^h \\ v_h^-(\sigma) &= (-1)^h(A_0 + 1)\frac{\eta}{\gamma}\rho^h \end{aligned} \quad (78)$$

Letting σ vary from 0 to π / γ , one may
obtain the complete optimum switching
boundary in the $x-y$ plane from equations
75 and 76 and in the $u-v$ plane from equa-
tions 77 and 78.

From the equations of the optimum
switching corners, 75 and 76, one finds that

$$\begin{aligned} [x_h^+{}_{(0)}, y_h^+{}_{(0)}] &= (\xi_h^n, 0) \\ [x_h^+{}_{(\pi/\gamma)}, y_h^+{}_{(\pi/\gamma)}] &= (\xi_{h+1}^p, 0) \end{aligned} \quad (79)$$

and

$$\begin{aligned} [x_h^-{}_{(0)}, y_h^-{}_{(0)}] &= (\xi_h^p, 0) \\ [x_h^-{}_{(\pi/\gamma)}, y_h^-{}_{(\pi/\gamma)}] &= (\xi_{h+1}^n, 0) \end{aligned} \quad (80)$$

Note that these relations can be applied
directly to the $u-v$ plane since $y=0$.

From equations 79 and 80 it is seen that

$$\Gamma_{ph} \text{ extends from } \xi_h^n \text{ to } \xi_{h+1}^p$$

and

$$\Gamma_{nh} \text{ extends from } \xi_h^p \text{ to } \xi_{h+1}^n$$

These results show that all initial points
on the v -axis (or x -axis) which fall between
 $|\xi_h^n|$ and $|\xi_{h+1}^p|$ will reach the origin along
 Γ_p and those which fall between $|\xi_h^p|$ and
 $|\xi_{h+1}^n|$ will reach the origin along Γ_n .

From equations 75 and 76 or 77 and 78
it is seen that all positive (or negative)

switching loci are related to the original
zero loop Γ_p (or Γ_n) by the factor ρ^h . In
order to understand the construction
techniques of the switching boundary one
may rewrite this in a simple form as

$$\begin{aligned} (\text{curve } \Gamma_{ph}) &= \xi_h^n + (-1)^{h+1}\rho^h (\text{curve } \Gamma_p) \\ (\text{curve } \Gamma_{nh}) &= \xi_h^p + (-1)^{h+1}\rho^h (\text{curve } \Gamma_n) \end{aligned} \quad (81)$$

Note that ξ_h^n and ξ_h^p are the limit ($\sigma =$
 π / γ) of $\Gamma_{h,n-1}$ and $\Gamma_{p,h-1}$. When h is an
even number $\xi_h^n < 0, \xi_h^p > 0$, and for h an
odd number, $\xi_h^n > 0, \xi_h^p < 0$. A study of
equation 81 and Fig. 13(A) will help to
clarify the construction technique. The
method of construction of the optimum
switching boundary is shown in Fig. 14.
First, one must construct Γ_p and Γ_n .
Next, Γ_{p1} is obtained by "magnifying"
 Γ_p by ρ , then revolving it by 180 degrees,
and displacing it along the u -axis until it
joins Γ_n . Γ_{n1} is obtained in the same
manner by magnifying Γ_n by ρ , then re-
volving it by 180 degrees, and then dis-
placing it until it joins Γ_p . Next one can
construct Γ_{p2} and Γ_{n2} and so on, in the
same manner. A four-loop optimum
switching boundary of a real system with
 $\xi = 0.2$ is shown in Fig. 3 of Part II.⁶

SPECIAL CASE ($\xi = 0$)

In a second-order system with an
undamped oscillatory element, one will
find $\xi = 0$. In this case $\gamma = 1$ and $\rho = 1$,
and the behavior in the $x-y$ plane is
identical to the behavior in the $u-v$ plane.
Therefore, it reduces equations 77 and
78 to

$$\begin{aligned} u_h^+(\sigma) &= \xi_h^n + (-1)^h(A_0 - 1)\beta \\ v_h^+(\sigma) &= (-1)^h(A_0 - 1)\eta \end{aligned} \quad (82)$$

$$\begin{aligned} u_h^-(\sigma) &= \xi_h^p + (-1)^h(A_0 + 1)\beta \\ v_h^-(\sigma) &= (-1)^h(A_0 + 1)\eta \end{aligned} \quad (83)$$

where ξ_h^p and ξ_h^n from equations 68 and
69 become

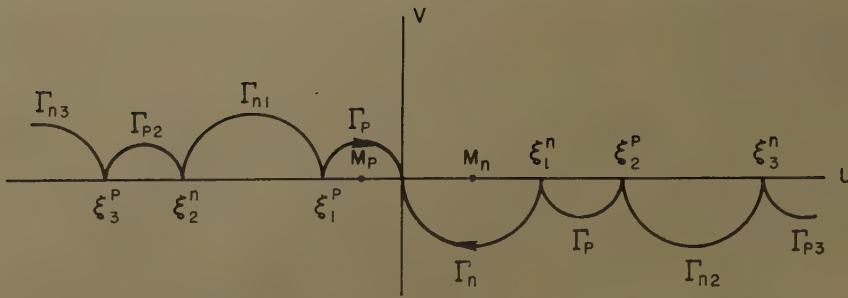


Fig. 15. Optimum switching boundary for an undamped oscillatory second-order system

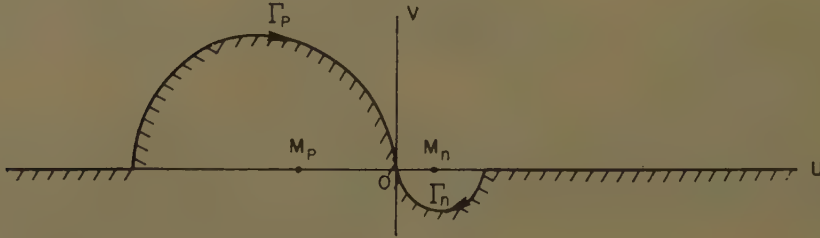


Fig. 16. Compromise switching boundary for a second-order complex system

$$\begin{aligned}\xi_h^p &= (-1)^h (2h + A_0 [(-1)^h - 1]) \\ \xi_h^n &= (-1)^{h+1} (2h + A_0 [(-1)^{h+1} + 1])\end{aligned}\quad (84)$$

where

$$\begin{aligned}\beta &= (1 - \cos \sigma) \\ \eta &= -\sin \sigma\end{aligned}\quad (85)$$

It can be seen that the zero switching corner can be obtained from 82 and 83 for Γ_p :

$$\begin{aligned}u_0^+ &= (A_0 - 1)(1 - \cos \alpha) \\ v_0^+ &= -(A_0 - 1) \sin \sigma\end{aligned}\quad (86)$$

for Γ_n :

$$\begin{aligned}u_0^- &= (A_0 + 1)(1 - \cos \sigma) \\ v_0^- &= -(A_0 + 1) \sin \sigma\end{aligned}\quad (87)$$

It is seen from equations 86 and 87 that the zero switching locus of Γ_p and Γ_n become perfect half circles centered at M_p and M_n which is $(A_0 - 1)$ and $(A_0 + 1)$ when σ varies from 0 to π . From equations 82 and 83, one can reduce the description to a simple form

$$\begin{aligned}(\text{curve } \Gamma_{ph}) &= \xi_h^p + (-1)^{h+1} (\text{curve } \Gamma_p) \\ (\text{curve } \Gamma_{nh}) &= \xi_h^n + (-1)^{h+1} (\text{curve } \Gamma_n)\end{aligned}\quad (88)$$

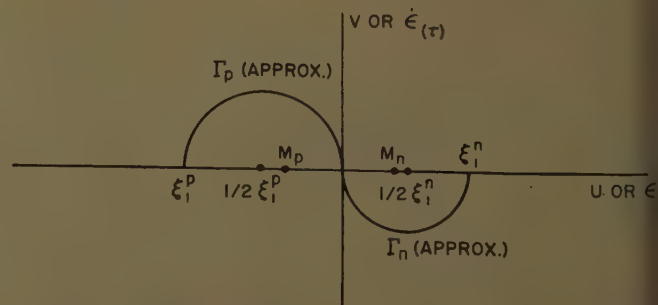
The optimum switching boundary is shown in Fig. 15.

Compromise Switching Boundary

The optimum switching boundary derived in the last section is rather complicated and the problem of mechanization is practically impossible, since for a system of low damping (small ξ), it might be necessary to use several boundary

loops to cover the large operating range of the error when the system is subjected to big load disturbances. For systems of large damping (large ξ), the error trajectories converge very rapidly to the origin (see Fig. 1 in Part II⁶), therefore the zero loops Γ_p and Γ_n can take care of larger error. However, in practical control problems, the systems usually have very small damping so that their predominant roots are close to the j -axis of the s -plane. These cases may be found in missile or airplane dynamic functions. For large load disturbances such as wind gusts, a nonlinear correcting process might be needed to correct a large error in the shortest time possible. Due to the difficulty in mechanizing the optimum switching boundary, a compromise switching boundary will be introduced in this section. The analog computer is used as the primary tool to study these effects. All the results are shown in Part II⁶. From these results (see Figs. 3 and 4 of Part II⁶), it is found that by taking the switching boundary outside of the Γ_p and Γ_n zero loops as a straight-line boundary along the error axis,

Fig. 17. Compromise switching boundary (approximate) of a second-order complex system



the time response is just slightly longer than the optimum time response. This study is performed for the case of $\xi = 0$. It was found that the error converges nearly as fast as in the optimum system. A typical compromise switching boundary is shown in Fig. 16. Γ_p and Γ_n are kept as part of the switching boundary to ensure that the system error and its derivative reach the origin simultaneously. However, as pointed out previously, perfect performance cannot be found in a physical system. If the system is switched slightly beyond the proposed switching point, steady-state oscillation will take place around the origin. However, since the system under discussion is of the quasi-stationary class,⁷ the modified dual mode concept must be used to maintain the system in the equilibrium state without any steady-state oscillation. In practice, one must use the equilibrium index ϵ and the criterion to switch the system from nonlinear mode to equilibrium mode is $|e| + |\dot{e}| < \epsilon$.⁷ With this concept, the steady-state oscillation can be eliminated at the cost of some steady-state error and ϵ should be set according to the degree of switching imperfection.

Further study shows that when ξ is decreased, Γ_p and Γ_n approach a perfect half circle. This effect is shown in Fig. 1 of Part II⁶. For small damping ratios, ($\xi \leq 0.2$), one can approximate the zero-loop boundary Γ_p and Γ_n by a half circle centered at $1/2 \xi_1^p$ and $1/2 \xi_1^n$ respectively with fairly good results. From equations 68 and 69 one obtains

$$\begin{aligned}\xi_1^p &= (A_0 - 1)(1 + \rho) \\ \xi_1^n &= (A_0 + 1)(1 + \rho)\end{aligned}\quad (89)$$

The compromise switching boundary approximate, is shown in Fig. 17. It should be emphasized that the approximate compromise switching boundary should be used only for systems with low damping ($\xi \leq 0.2$). With the use of the modified dual mode concept and ϵ set sufficiently large, the effect of steady state oscillation can be eliminated and reduced to a minimum.

By using equation 89 and the operation

one can obtain the compromise switching boundary, approximate in the normalized phase plane ($\epsilon - \dot{\epsilon}$) as follows:

$$= -\sqrt{\left(\frac{R^2}{2}\right) - \left(\epsilon - \frac{\epsilon}{|\epsilon|} \frac{R}{2}\right)^2} \text{ for } |\epsilon| < R \quad (90)$$

$$= 0 \text{ for } |\epsilon| > R \quad (91)$$

$$= \left(1 + \frac{\epsilon}{|\epsilon|} A_0\right) (1 + e^{\xi\pi/\gamma}) \quad (92)$$

The direction of the system forcing function is given by

$$\frac{\epsilon - \dot{\epsilon}_0}{|\epsilon - \dot{\epsilon}_0|} \quad (93)$$

It should be noted that $\dot{\epsilon}_0$ represents the normalized switching boundary error derivative. Using the modified dual mode concept the nonlinear force should be switched to the equilibrium force when the sum of the absolute values of ϵ and $|\dot{\epsilon}|$ is less than ϵ (equilibrium index). The normalized equilibrium force is A_0 .

Conclusions

In this paper, the optimum switching criterion for second-order predictor control systems with complex characteristic

roots was derived. Even though the derivation is rather lengthy, the final result of the optimum switching boundary is reduced to a pattern where it can be determined easily by using an electronic analog computer. Due to the practical difficulty of mechanizing the nonlinear controller which is required in this off-on type servosystem, a compromise switching boundary which was examined in an analog computer study⁶ is suggested. The compromise switching boundary is composed of only the zero-loop boundary (Γ_p and Γ_n) of the optimum system and the rest of this boundary extends along the error axis.

For ξ very small (≤ 0.2), an additional boundary approximation is suggested. The general switching criterion in this case was derived in the last section. It should be noted that the input information is used as a control factor in the error correcting process since the system is in the quasi-stationary class. Also, the modified dual mode concept must be used to switch the system from the nonlinear mode to the equilibrium mode when the error and error derivative are in the neighborhood of the origin. The switching point for the change from the nonlinear mode, in practice, is determined by the setting of the equilibrium index ϵ .

The analog study of a second-order system of this type is presented in Part II,⁶ wherein the approximate switching boundary is used in a system with the damping ratio 0.2. The system time responses to step, ramp, and sinusoidal input are recorded. The results obtained are quite satisfactory.

References

1. DIFFERENTIAL EQUATIONS WITH A DISCONTINUOUS FORCING TERM, D. W. Bushaw. *Report no. 469*, "Experimental Towing Tank," Stevens Institute of Technology, Hoboken, N. J., Jan. 1953.
2. DIFFERENTIAL EQUATIONS WITH A DISCONTINUOUS FORCING TERM, D. W. Bushaw. *Contributions to Nonlinear Oscillations*, Princeton University Press, Princeton, N. J., vol. IV, 1959.
3. AN OPTIMUM SWITCHING CRITERIA FOR A THIRD ORDER CONTACTOR ACCELERATION CONTROL SYSTEM, A. L. Passera, R. G. Willoh. *NACA Technical Note No. 3743*, National Advisory Committee for Aeronautics, Washington, D. C., Aug. 1956.
4. TIME OPTIMAL CONTROL OF LINEAR SYSTEMS, C. R. Stone, editor. *Report*, Aeronautical Division, Minneapolis-Honeywell Regulator Company, Minneapolis, Minn., 1959.
5. THE BANG-BANG SERVO PROBLEM TREATED BY VARIATIONAL TECHNIQUES, C. A. Desoer. *Information and Control*, New York, N. Y., vol. 2, no. 4, Dec. 1959, pp. 333-48.
6. OPTIMUM NONLINEAR BANG-BANG CONTROL SYSTEMS WITH COMPLEX ROOTS II.—ANALYTICAL STUDIES, P. Chandaket, C. T. Leondes. E. C. Deland, *AIEE Transactions*, see pp. 95-102, of this issue.
7. THE SYNTHESIS OF QUASI-STATIONARY OPTIMUM NONLINEAR CONTROL SYSTEMS, PARTS I AND II, P. Chandaket, C. T. Leondes. *Ibid.* (Paper nos. 61-705 and 61-706, to be published).

Discussion

Ch Yin (International Business Machine Corporation, Yorktown Heights, N. Y.): The authors treat the "second-order optimum predictor control system" in a fashion very similar to that of the "second-order optimum regulator problem" treated by Bushaw in 1952 (see reference 1 of the paper). The authors point out that the differences between their paper and Bushaw's are

The direction of the force is opposite. The stable points are no longer at 1 and -1.

They also point out that Bushaw's result is not applicable to the problem investigated in this paper. The culmination of their analysis is the derivation of the switching curve Γ shown in Fig. 13 of the text and the presentation of a compromise switching boundary.

After examining both papers, however, I fail to find any significant difference between them. The difference in the direction of the force is just a matter of nomenclature. While Bushaw denoted trajectories with focus at $(+1, 0)$ as P -arcs and trajectories with focus at $(-1, 0)$ as N -arcs, the authors choose to denote trajectories with focus at $(M_n, 0)$ as N -arcs and trajectories with focus at $(M_p, 0)$ as P -arcs, where M_n and M_p are given by equation 15 in the text. For $|A_0| < 1$, $M_n > 0$, and $M_p < 0$.

Upon examining equation 8, one realizes that the authors are actually considering the optimum regulator problem with an asymmetrical relay. In other words, instead of considering a relay with characteristics shown in Fig. 18, they consider one with characteristics shown in either Fig. 19(A) or Fig. 19(B) depending on the sign of A_0 . As pointed out by previous in-

vestigators,¹⁻⁶ the asymmetry of the relay poses no special difficulty to the solution of the problem. It is also evident from the fact that $A_0 \neq 0$ plays no part in the derivation of the optimum switching condition that two subsequent switching points on the switching curve must be π/γ time units apart. Thus Bushaw's result does not lose any generality by assuming symmetrical relay characteristics. While the method he used is rigorous, it is also tedious and his treatment does not lend itself to easy extension to higher order systems. Using any of the results given in references 1 through 5, one easily arrives at the optimal switching condition. From there on, the derivation of the switching curve in the phase plane is simple. I have re-derived Bushaw's results in reference 6. With trivial modifications the derivation is equally valid for the case considered in this paper. In particular, theorem 10 of

Fig. 18 (left). Relay characteristics

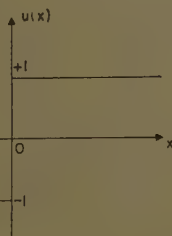
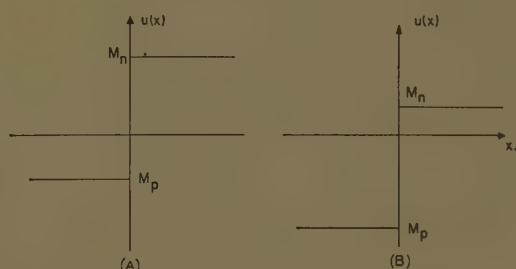


Fig. 19 (right). Relay characteristics depending on the sign of A_0

A— $A_0 > 0$
B— $A_0 < 0$



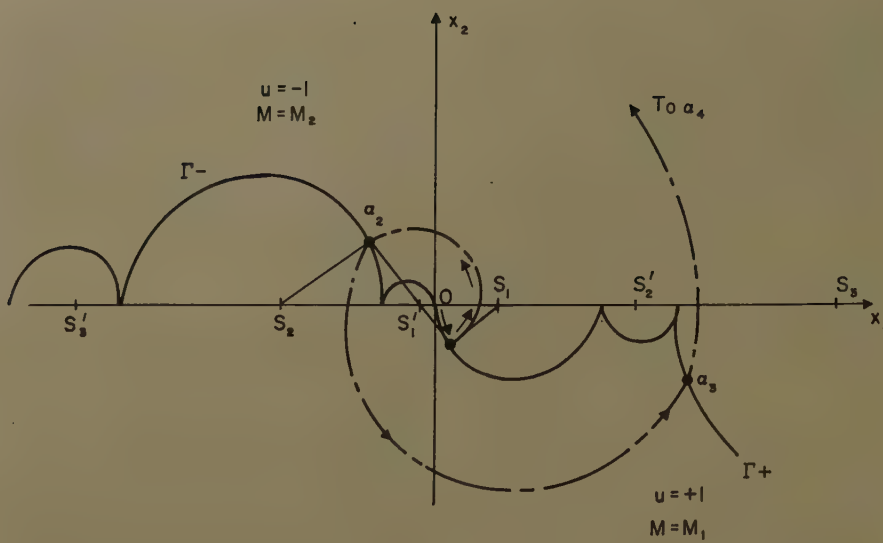


Fig. 20. $0 < \xi < 1$

reference 3 is directly applicable without any modification to the present problem. One may restate this theorem of Bass in the following manner

Consider the control system given by

$$\dot{x} = Ax + b[u(t) + w], \quad x(0) = x_0 \quad (94)$$

where $|u(t)| \leq 1$; b is a constant vector; w is a constant $|w| < 1$. Then the optimum control which will reduce $x(0)$ to 0 in minimum time is given by

$$u(t) = \text{sgn}[b, y(t)] \quad (95)$$

where $y(t)$ is the solution of the adjoint equation of equation 94.

$$\dot{y} = -A'y \quad (96)$$

A' is the transpose of A .

For the case at hand we have:

$$\frac{d}{dt} \begin{bmatrix} x_1 \\ x_2 \end{bmatrix} = \begin{bmatrix} -\xi & \gamma \\ -\gamma & -\xi \end{bmatrix} \begin{bmatrix} x_1 \\ x_2 \end{bmatrix} + \begin{bmatrix} \xi \\ \gamma \end{bmatrix} (u(t) + A_0) \quad (94A)$$

where

$$\gamma = \sqrt{1 - \xi^2}$$

During each switching interval $u = +1$ or -1 , the solution is given by

$$\begin{aligned} x_1 &= u + A_0 + r_0 e^{-\xi t} \cos(\gamma t - \theta_0) \\ x_2 &= -r_0 e^{-\xi t} \sin(\gamma t - \theta_0) \end{aligned} \quad (97)$$

Evidently, these are logarithmic spirals with foci at $(\pm 1 + A_0, 0)$ of $x_1 x_2$ plane.

The adjoint equation is

$$\frac{d}{dt} \begin{bmatrix} y_1 \\ y_2 \end{bmatrix} = \begin{bmatrix} \xi & \gamma \\ -\gamma & \xi \end{bmatrix} \begin{bmatrix} y_1 \\ y_2 \end{bmatrix} \quad (96A)$$

with solution

$$\begin{aligned} y_1 &= c e^{\xi t} \cos(\gamma t - \delta^*) \\ y_2 &= -c e^{\xi t} \sin(\gamma t - \delta^*) \end{aligned} \quad (98)$$

and the optimal control is

$$\begin{aligned} u(t) &= \text{sgn}[c \xi e^{\xi t} \cos(\gamma t - \delta^*) - c \gamma e^{\xi t} \sin(\gamma t - \delta^*)] \\ &= \text{sgn}[c e^{\xi t} \cos(\gamma t - \delta^* - \sigma)] \\ &= -\text{sgn}[\cos(\gamma t - \delta)] \end{aligned} \quad (95A)$$

where

$$c \geq 0, \quad \sigma = \cos^{-1}(-\xi)$$

and

$$\delta = \delta^* + \sigma$$

Upon introducing

$$M = u(t) + A_0$$

one has

$$M = M_1 = 1 + A_0 \text{ if } \cos(\gamma t - \delta) > 0$$

and

$$M = M_2 = -1 + A_0 \text{ if } \cos(\gamma t - \delta) < 0 \quad (99)$$

Fig. 21 (left). Construction of the $n+1$ th switching arc given the n th switching arc

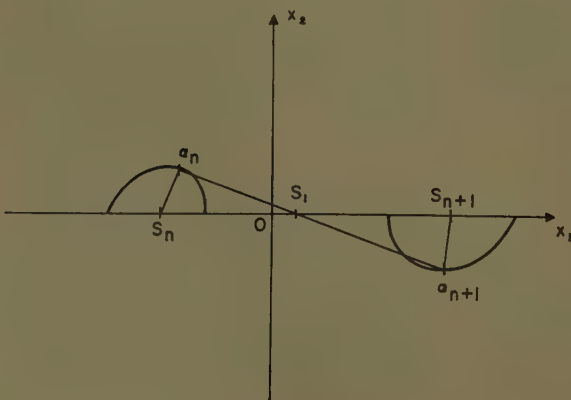


Fig. 22 (right). $-1 < \xi < 0$

This is the optimum switching condition. In terms of reverse time $\tau = -t$, equation 99 is written as

$$M(\tau) = M_1 \text{ if } \cos(\gamma\tau + \delta') > 0$$

$$M(\tau) = M_2 \text{ if } \cos(\gamma\tau + \delta') < 0 \quad (99)$$

Given δ' , trajectories starting from the origin are constructed. On each of the trajectories the switching points are determined. The locus of switching points for $0 \leq \delta' \leq 2\pi$ is the switching curve. The method of construction of the switching curve is the same as the text. One notes that in Fig. 20, the following relations hold

$$S_{2i-1} = \left[M_1 + (M_1 + M_2) \sum_{k=1}^{2(i-1)} e^{\frac{k\xi\pi}{\gamma}} \right]$$

$$S_{2i} = - \left[M_2 + (M_1 + M_2) \sum_{k=1}^{2i-1} e^{\frac{k\xi\pi}{\gamma}} \right] \quad (10)$$

and

$$S_{2i-1}' = \left[M_2 + (M_1 + M_2) \sum_{k=1}^{2(i-1)} e^{\frac{k\xi\pi}{\gamma}} \right]$$

$$S_{2i}' = \left[M_1 + (M_1 + M_2) \sum_{k=1}^{2i-1} e^{\frac{k\xi\pi}{\gamma}} \right]$$

where $i = 1, 2, 3, \dots$ along the x_1 -axis.

It will be shown that Fig. 20 corresponds to equation 99(A) by induction.

After choosing a particular value of δ' in $M(\tau)$, so that at $\tau = 0+$, $M = +M_1$ and constructing a trajectory in reverse time from the origin, we obtain the following sequence of switching points: $\alpha_1, \alpha_2, \dots, \alpha_n, \alpha_{n+1}, \dots$. For any δ' we want to show that the α 's are on Γ .

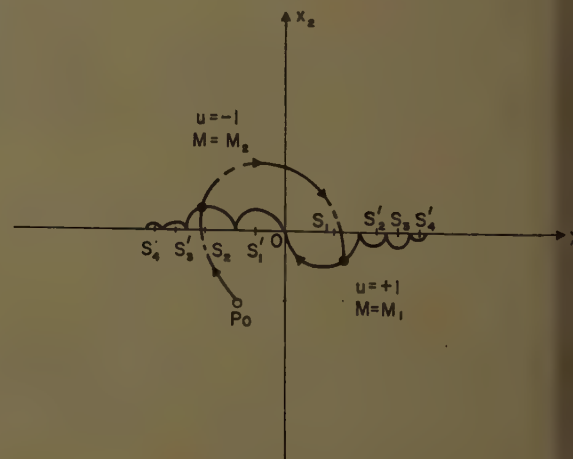
From construction α_1 must lie on the first arc of Γ^+ with focus at S_1 . The next switching point α_2 is obtained by constructing a spiral arc through α_1 with focus at S_1' , subtending an angle of π radians in the direction of increasing τ . In Fig. 21 one finds

$$\overline{S_1' \alpha_2} = \overline{S_1' \alpha_1} e^{\frac{\xi\pi}{\gamma}}$$

$$\overline{S_1' S_2} = (M_1 + M_2) e^{\frac{\xi\pi}{\gamma}} = \overline{S_1' S_1} e^{\frac{\xi\pi}{\gamma}}$$

and

$$\text{angle } \alpha_2 S_1' S_2 = \text{angle } \alpha_1 S_1' S_1$$



Therefore triangle $\alpha_2 S_1' S_2 \sim$ triangle $\alpha_1 S_1' S_2$

$$\frac{\xi\pi}{2\gamma} = \frac{\xi\pi}{S_1\alpha_1 e^\gamma} \quad (101)$$

Varying the position of α_1 on the first arc Γ_+ with focus at S_1 shows that α_2 lies on the spiral arc with focus at S_2 and the initial magnitude of the spiral arc is $M_1 e^\gamma$ while the final magnitude of the spiral arc is $M_1 e^{\frac{\xi\pi}{2\gamma}}$. Thus α_2 lies to the left of the origin on the second arc of Γ_- which is part of Γ .

Assume the switching point α_n lies on the n th spiral arc of Γ_- with focus at S_n where n is even. The initial and final magnitudes of this spiral arc are $M_1 e^{\frac{(n-1)\xi\pi}{n\xi\pi}}$ and $M_1 e^{\frac{n\xi\pi}{n\xi\pi}}$ respectively.

Then the subsequent switching interval corresponds to $\tau = +M_1$, and α_{n+1} is obtained by starting spiral arc from α_n with focus at S_2 subtending an angle of π radians as shown in Fig. 21. From equation 100,

$$\begin{aligned} S_{n+1} &= |S_{n+1}| - |S_1| \\ &= (M_1 + M_2) \sum_{k=1}^{n-1} e^{\frac{k\xi\pi}{\gamma}} \\ S_n &= |S_n| + |S_1| \\ &= M_1 + M_2 + (M_1 + M_2) \sum_{k=1}^{n-1} e^{\frac{k\xi\pi}{\gamma}} \\ &= e^{\frac{-\xi\pi}{\gamma}} (M_1 + M_2) \sum_{k=1}^n e^{\frac{k\xi\pi}{\gamma}} \end{aligned}$$

so

$$\frac{\xi\pi}{S_1 S_n e^\gamma} = \frac{\xi\pi}{S_1 S_{n+1}}$$

By construction,

$$\frac{\xi\pi}{S_1 \alpha_n e^\gamma} = \frac{\xi\pi}{S_1 \alpha_{n+1}}$$

$$\text{angle } \alpha_n S_1 S_n = \text{angle } \alpha_{n+1} S_1 S_{n+1}$$

$$\text{Therefore triangle } \alpha_n S_1 S_n \sim \text{triangle } \alpha_{n+1} S_1 S_{n+1}$$

and

$$S_{n+1} \alpha_{n+1} = S_n \alpha_n e^{\frac{\xi\pi}{\gamma}} \quad (102)$$

By assumption α_n lies on the n th arc Γ_- with focus at S_n . Varying the position of α_n through its allowed range shows that α_{n+1} lies on a spiral arc with focus at S_{n+1} , the initial and the final magnitudes of the spiral arcs are

$$M_1 e^{\frac{n\xi\pi}{\gamma}}$$

and

$$M_1 e^{\frac{(n+1)\xi\pi}{\gamma}}$$

respectively. Thus it has been shown that α_{n+1} lies on Γ_+ .

In exactly the same manner one can show that if α_n lies on Γ_+ where n is odd, then α_{n+1} lies on Γ_- , and starting with $M = -M_2$ at $\tau = 0+$ one obtains those arcs on Γ corresponding to foci at S_n' . This is what was to have been proved.

In this proof notice that nowhere has the fact been used that $1 > \xi > 0$, thus, setting $\xi = 0$ and $-1 < \xi < 0$ one gets the

switching curves for the undamped and negatively damped system as well. The switching curve for $\xi = 0$ is the same as that of Fig. 15 and the switching curve for $-1 < \xi < 0$ is shown in Fig. 22.

The idea of compromise switching boundary is interesting. There was some work done along this line by Knudsen,⁷ which might supplement the present paper.

REFERENCES

1. ON THE "BANG-BANG" CONTROL PROBLEMS, R. Bellman, I. Glicksberg, O. Gross. *Quarterly of Applied Mathematics*, Providence, R. I., vol. 14, 1956, pp. 11-18.
2. THE BANG-BANG PRINCIPLE, J. P. La Salle. *Report 59-5*, Research Institute for Advanced Studies, Baltimore, Md., Nov. 1959.
3. EQUIVALENT LINEARIZATION, NONLINEAR CIRCUIT SYNTHESIS AND THE STABILIZATION AND OPTIMIZATION OF CONTROL SYSTEMS, R. W. Bass. *Proceedings, Symposium on Nonlinear Circuit Analysis, "MRI Symposia Series"* Polytechnic Institute of Brooklyn, Brooklyn, N. Y., vol. 4, 1956, pp. 163-98.
4. THE BANG-BANG SERVO PROBLEM TREATED BY VARIATIONAL TECHNIQUES, C. A. Desoer. *Information and Control*, New York, N. Y., vol. 2, no. 4, Dec. 1959, pp. 333-48.
5. OPTIMAL CONTROL PROCESSES, L. S. Pontryagin. *Uspekhi Matematika Nauk*, Moscow, USSR, vol. 14, no. 185, Jan.-Feb. 1959, pp. 3-20.
6. ON THE OPTIMUM RESPONSE OF THIRD ORDER CONTACTOR CONTROL SYSTEMS, I. Flugge-Lotz, M. Yin. *Technical Report no. 125*, Division of Engineering Mechanics, Stanford University, Stanford, Calif., Apr. 1960.
7. MAXIMUM EFFORT CONTROL FOR OSCILLATORY ELEMENT, H. K. Knudsen. *Wescon Convention Record*, Institute of Radio Engineers, New York, N. Y., pt. 4, 1959, pp. 116-24.

(See Joint Discussion on p. 101)

Optimum Nonlinear Bang-Bang Control Systems With Complex Roots

II—Analytical Studies

PRAPAT CHANDAKET
ASSOCIATE MEMBER AIEE

C. T. LEONDES
ASSOCIATE MEMBER AIEE

E. C. DELAND
NONMEMBER AIEE

Part I of this paper¹ methods for the synthesis of the optimum nonlinear bang-bang control system with complex roots was presented. In this, the scope and utility of this synthesis are verified by analytical studies of the dynamic response capabilities of these systems.

Both the optimum and compromise optimum systems were studied. Various types of inputs were applied to these systems including steps, ramps, and sinusoidal inputs. As expected, the compromise optimum systems were slightly slower in response than the optimum systems. The compromise optimum system

is nevertheless nearly as fast as the optimum system, and this results in the important conclusion that the compromise optimum nonlinear control system can be used effectively particularly since in many cases system error may be expected to be maintained at a small value.

Study of Optimum and Near-Optimum System Responses

In this paper a second-order nonlinear predictor control system will be studied in both the optimum and near-optimum cases. From this study we shall draw cer-

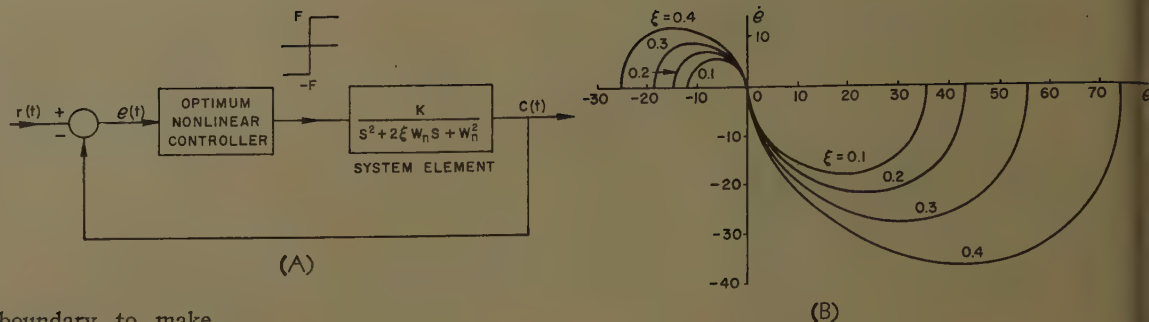
tain conclusions which will permit us to determine a most effective compromise boundary for particular problems. The TRAC analog computer (The Rand Corporation, Santa Monica, Calif.) was used for the entire study. The system time responses for both systems were studied by using a 4-loop switching boundary (Fig. 3) to confirm the results that for a system with small damping ratio, $\xi = 0.2$ in this study, the time response of the system using the compromise boundary is very close to the optimum time response. Finally, the function generator was designed to simulate the com-

Paper 61-79, recommended by the AIEE Feedback Control Systems Committee and approved by the AIEE Technical Operations Department for presentation at the AIEE Winter General Meeting, New York, N. Y., January 29-February 3, 1961. Manuscript submitted June 6, 1960; made available for printing December 7, 1960.

P. CHANDAKET is in the Royal Thai Navy, Bangkok, Thailand; C. T. LEONDES is with the University of California, Los Angeles, Calif.; and E. C. DELAND is with the Rand Corporation, Santa Monica, Calif.

This research was supported in part by the United States Air Force under Contract no. AF 49(638)-438 monitored by the Air Force Office of Scientific Research of the Air Research and Development Command.

Fig. 1. (A) System under study. (B). Optimum zero switching boundary for $a_0=5.0$, $F=10$



promise switching boundary to make possible a study of the system time response for various classes of input, such as the step, ramp, and sinusoid.

The system studied is shown in Fig. 1(A). For convenience, let K and w_n be unity. Then one obtains the following equations:

$$\ddot{e}(t) + 2\xi\dot{e}(t) + e(t) = \delta F \quad (1)$$

$$\ddot{e}(t) + 2\xi\dot{e}(t) + e(t) = a_0 - \delta F \quad (2)$$

for

$$r(t) = a_0 \quad (3)$$

where $a_0 = \text{constant}$. For all analog studies to follow the analog time is based on

$$\tau = 5t \quad (4)$$

where $t = \text{problem time}$.

EFFECT OF ξ ON Γ_p and Γ_n LOOP

Γ_p and Γ_n can be obtained by solving equation 2 in the negative time direction starting at the origin of the $e-\dot{e}$ plane. With $\tau = 5t$, equation 2 becomes

$$25\ddot{e}(\tau) + 10\xi\dot{e}(\tau) + e(\tau) = a_0 - \delta F \quad (5)$$

In the negative time direction, equation 5 becomes

$$25\ddot{e}(\tau) - 10\xi\dot{e}(\tau) + e(\tau) = a_0 - \delta F \quad (6)$$

By setting the analog system according to equation 6 one obtains Γ_p and Γ_n on the $e-\dot{e}$ plane as in Fig. 1(B). In this study, a_0 is set at 5, F at 10 and the zero

loops are obtained for $\xi = 0.1, 0.2, 0.3$, and 0.4 . It should be noted that to obtain Γ_p and Γ_n in the $e-\dot{e}$ plane, one must plot $-5e(\tau)$ versus $e(\tau)$ since the negative time direction is used. It can be seen that for $\xi = 0.1$ and 0.2 the shapes of Γ_p and Γ_n can be approximated with a fair result by a half circle centered at the mid-point of the zero-loop limit.

Next, the effect of a_0 upon Γ_p and Γ_n is recorded for a 2-loop optimum switching boundary. For this case ξ is set at 0.2 and F at 10 . The obtained optimum switching boundaries are shown in Fig. 2.

OPTIMUM AND NEAR-OPTIMUM SYSTEM TIME RESPONSES

To study the system time responses for the optimum and near-optimum systems, a 4-loop optimum switching boundary is recorded on the $e-\dot{e}$ plane. For this study ξ is set at 0.2 , F at 10 , and a_0 at 5 . The initial error is assumed at 260 . The 4-loop optimum switching boundary is plotted on the $e-\dot{e}$ plane as shown in Fig. 3. It should be recalled (as discussed in Part I¹) that the compromise switching boundary continues from the end of the zero loops Γ_n and Γ_p (Γ_n and Γ_p are included as part of the compromise switching boundary) along the error axis. The switching criteria are the same for both optimum and near-optimum cases,

namely, while the present point is above the boundary, a positive force is applied and when it is below the boundary a negative force is used. On this basis, the system time responses for both cases can be studied by manual switching. The phase plane behavior and the error time response are plotted at the same time. This can be easily done by watching the $e-\dot{e}$ plotter and pressing the "hold" button when the trajectory reaches the boundary, then switching to the opposite force. This process is repeated until the trajectory reaches the origin. The $e-\dot{e}$ phase-plane behaviors and the error time response for both cases are plotted in Figs 3 and 4.

On the phase-plane plot,* it is difficult to detect differences between the compromise phase-plane trajectory and the optimum phase trajectory. On the error time response plots (Fig. 4), the switching points for both cases are marked as 1 and 2. The results show that the time required for the optimum system is 11.25 seconds, whereas it takes 11.4 seconds for the near-optimum system. From these results, it can be concluded that by using the compromise switching boundary the time required is just slightly longer than that required in the optimum system, and the compromise switching boundary can be used effectively.

Design of Nonlinear Controller

It was stated in Part I¹ that for a system of low damping, the nonlinear controller using an approximate switching boundary can be used effectively. It is the purpose of this paper, and one to follow, to study the time responses of the system design based on this principle. To design a nonlinear controller, a function generator is generally needed to simulate the switching boundary. Based on equations 90, 91, and 92 of Part I¹ one can find the (approximated) switching boundary error derivative as a function of the real variable. Using $K = w_n = 1$, one obtains

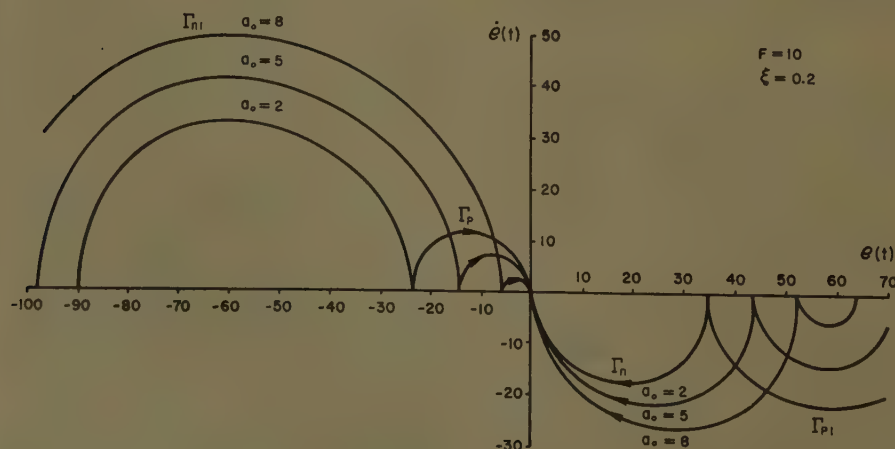


Fig. 2. Two-loop optimum switching boundary for $a_0=2, 5$, and 8

* The phase-plane plot in Fig. 3 is reduced half the size of the computer's plot.

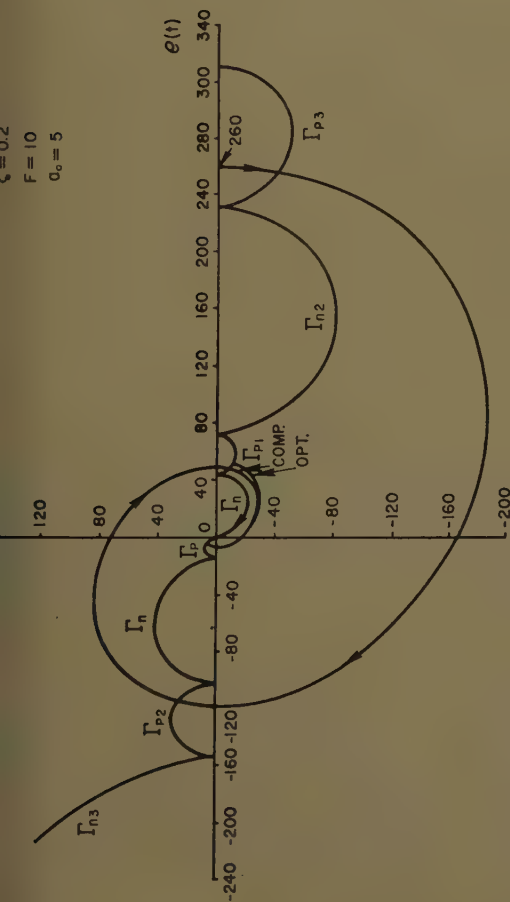


Fig. 3. Optimum and near-optimum $e-\dot{e}$ phase-plane behavior in a second-order complex system (equation 1)

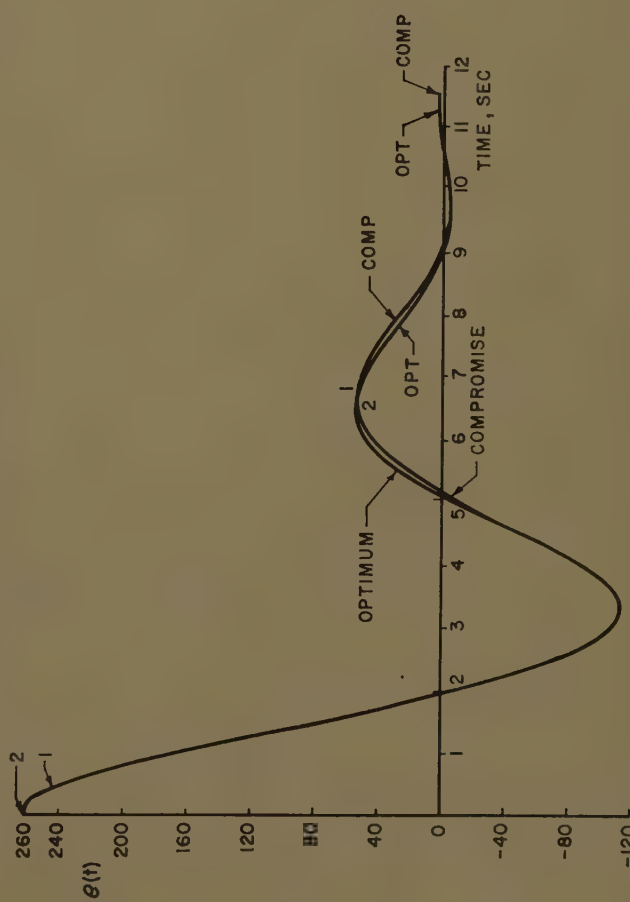


Fig. 4. Error time responses of the optimum and near-optimum second-order complex system (equation 1)

$\xi=0.2$
 $F=10$
 $a_0=5$

1 = optimum switching point
 2 = compromise switching point

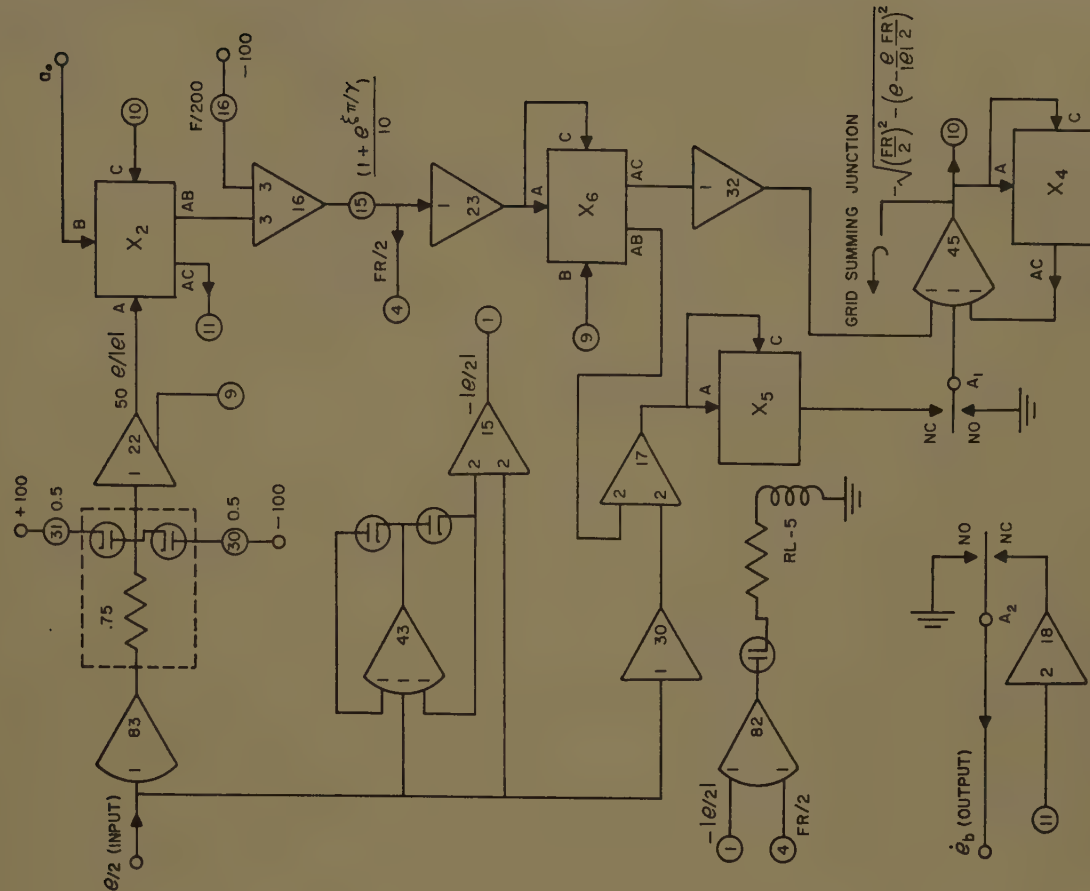


Fig. 5. Analog simulation of an approximated switching boundary (equations 7 and 8)

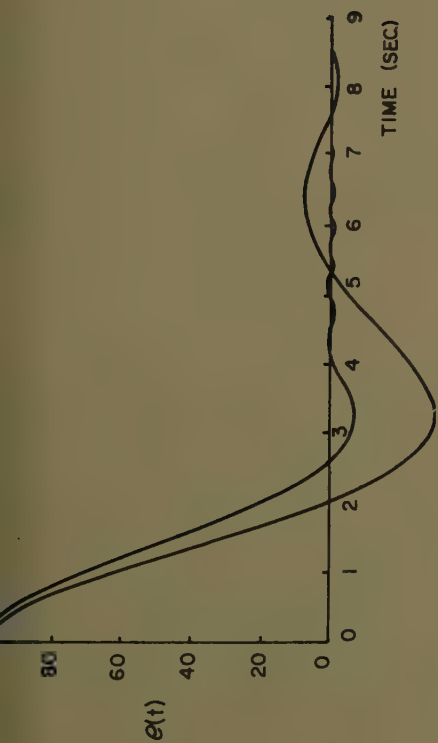


Fig. 8. Error time responses corresponding to the phase-plane plot in Fig. 7

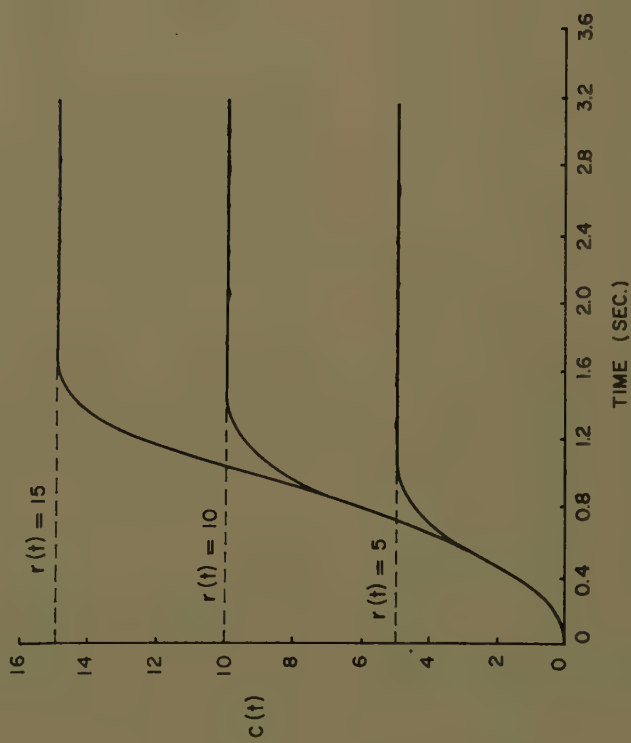


Fig. 9. System time responses to position inputs with $F=25$

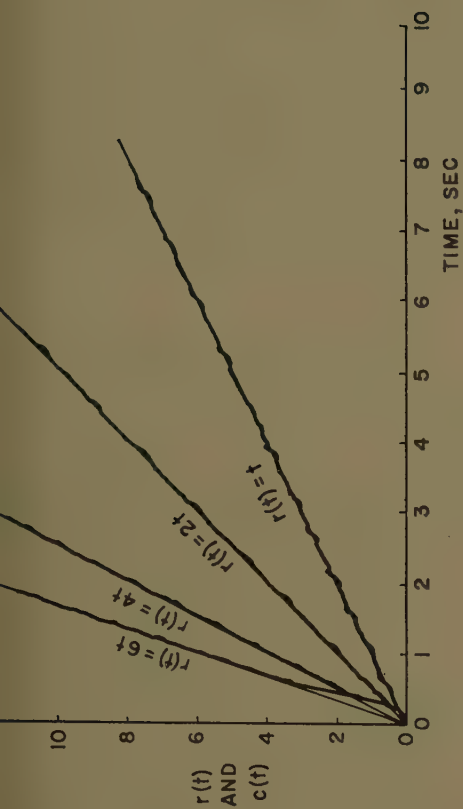


Fig. 10. System responses to velocity inputs

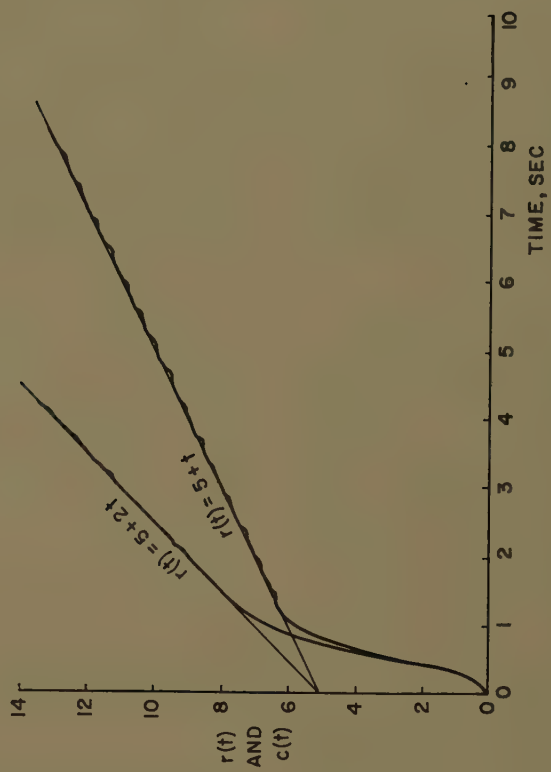


Fig. 11. System responses to a combination of position and velocity inputs

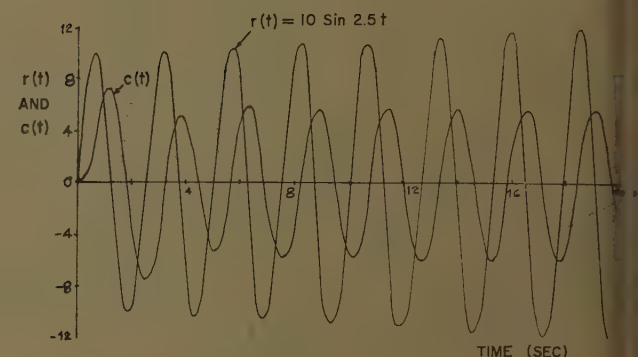
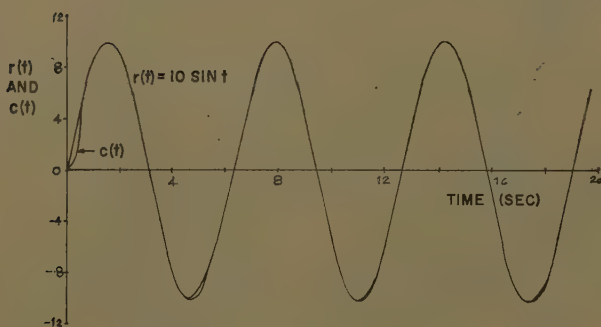
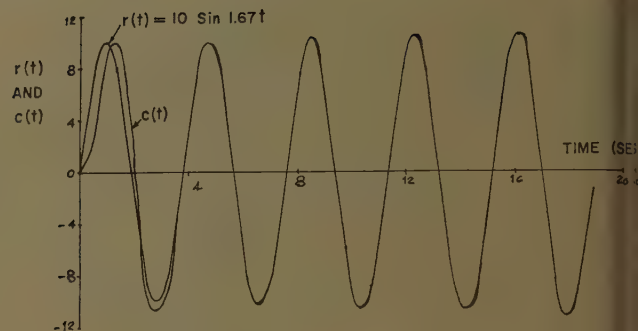
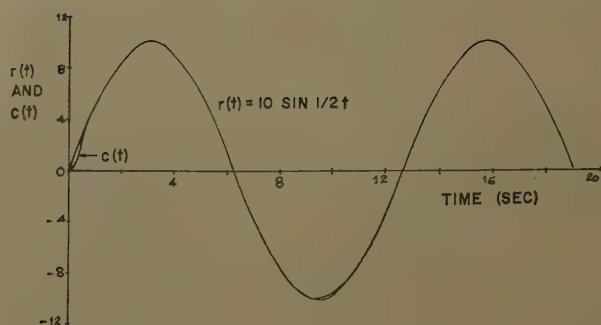


Fig. 12. System responses to sinusoidal inputs

stability in the circuit such that the high-gain amplifier output becomes positive at its saturation level, which in turn overloads amplifier 18 and multipliers no. 2 and 4. This effect can be prevented by connecting a diode of high back-resistance across the output and the summing grid junction of amplifier 45 as shown. The over-all system is then constructed as shown in Fig. 6 using analog time equal to five times the real time.

Results of Analog Studies

In this section various classes of inputs will be studied for the analog setup in Fig. 6. The damping ratio is selected at $\xi = 0.2$ which is the limit of the suggested value for using approximated switching boundary with satisfactory results.

First, the $e-\dot{e}$ phase behavior and the error response time were studied by using a step input of 5 with the maximum control effort (F) of 10 and 25. The error initial condition is assumed at 100. The $e-\dot{e}$ phase trajectories and the error time responses are shown in Figs. 7 and 8. It can be seen from both plots that oscillations in the origin exist due to slight deviations from perfect switching. The modified dual mode control² was not used for this study nor for the others to follow. It is believed that the use of this concept will greatly reduce the oscillatory effect.

The next study used $F=25$, $\xi=0.2$ and the system was assumed in the equilibrium

condition at $t \leq 0$. The results of the system responses for various types of inputs will be presented.

POSITION INPUTS

The system time responses to position inputs of 5, 10, and 15 are recorded as shown in Fig. 9. Oscillating effects result for system operation in the vicinity of the origin. However, these effects are very small and can hardly be seen on the plot. Excluding these effects (due to the imperfect switching) the system approaches the desired input in the same manner as in the optimum case.

VELOCITY INPUTS

It should be noted that the nonlinear controller is designed to give ideal performance for quasi-stationary² class inputs only, which in this case are limited to step-type inputs. However, in the nonlinear controller, the instantaneous location of the input (corresponding to a_0) is used as a control factor for the error correcting process. The input position is then limited to KF/w_n^2 at all times.

The systems responses to $r(t)=t$, $2t$, $4t$, and $6t$ are shown in Fig. 10. The responses to the combination of position and velocity inputs

$$r(t) = 5 + t$$

and

$$r(t) = 5 + 2t$$

are plotted in Fig. 11. The steady-state oscillations exist in all cases. These are normal (even with the perfect optimum nonlinear controller) since the desired inputs are moving and the system can give the ideal response only to position inputs. Therefore, with the velocity inputs, the error correcting process is needed all the time, and this results in the oscillating effects in the vicinity of the origin of the $e-\dot{e}$ plane.

SINUSOIDAL INPUTS

The sinusoidal inputs to be studied are

1. $r(t) = 10 \sin 0.5t$
2. $r(t) = 10 \sin t$
3. $r(t) = 10 \sin 1.67t$
4. $r(t) = 10 \sin 2.5t$

The system time responses to these inputs are plotted in Fig. 12. Note that the instantaneous position is limited to 25 (see equation 16 of Part I¹). For all cases studied, the maximum input were selected as 10. The system natural frequency is 1 radian/second. The system responses to cases 1, 2, and 3 are quite satisfactory. For case 4 where the input frequency is 2.5 radians/second the system cannot follow the desired input and the amplitude of the system is greatly reduced. This effect is caused by

1. Higher derivatives of the input are not used in the designed nonlinear controller
2. The demand of these higher derivative

input are much greater than the level system capacity.

conclusions

From the results of the analog studies the error response of a system using the compromise switching boundary is slightly slower than that of the optimum system. This experiment was performed by assigning the initial error in the fourth loop (γ_4) and the error in the compromise

case did converge nearly as fast as that in the optimum case. This results in the conclusion that the compromise switching boundary, which consists of only Γ_p and Γ_n loop, and the rest of the error axis can be used effectively. Further study shows that for a system with very small damping ratio ($\xi=0.2$), which is found frequently in practical control systems, the switching boundary can be approximated by replacing the Γ_p and Γ_n zero-loop boundaries by perfect half circles. With the

switching boundary designed as described, the system time responses to step, ramp, and sinusoidal inputs are quite satisfactory.

References

1. OPTIMUM NONLINEAR BANG-BANG CONTROL SYSTEMS WITH COMPLEX ROOTS—I. SYSTEM SYNTHESIS, Prapat Chandaket, C. T. Leondes. *AIEE Transactions*, see pp. 82-95 of this issue.
2. THE SYNTHESIS OF QUASI-STATIONARY OPTIMUM NONLINEAR CONTROL SYSTEMS, PARTS I AND II, P. Chandaket, C. T. Leondes. *Ibid.* (Paper nos. 61-705 and 61-706, to be published.)

Joint Discussion of Paper Nos. 60-1266 and 61-79

H. K. Knudsen (University of California, Berkeley, Calif.): I am surprised that the authors do not refer to the paper "Maximum Effort Control for an Oscillatory Element."¹ I am concerned with the derivation and construction of a bang-bang control system for complex roots with no damping. Comparing this with the authors' paper, Part I, the following is noted.

The authors used identically the same approximation that I conceived, and which has proved to be valid both mathematically and practically. This approximation is to make the switching boundary a straight line outside of the near origin region as shown in Fig. 17 of Part I of the authors' paper. Because of this, and the fact that the authors used a semicircular approximation to the true switching boundary in the near origin region $|e| < FR$, the equations describing the switching boundary, equation 16 in my paper and equations 7 and 9 in Part II of the authors' paper are very similar. In fact, for the case of no damping ($\xi=0$), equations 7 and 9 of Part II of the authors' paper and equation 16 of my paper are identical in the region where $|e| < FR$, making the necessary changes in notation between the papers. These changes are $F=1$, and $a_0=\tau$. Equation 9 of Part II of the authors' paper is in error. It should read:

$$R = \left(1 + \frac{e}{|e|} a_0\right) (1 + e^{\pm\pi/\gamma})$$

The analog simulation of the switching boundary is performed in both my paper and Part II of the authors' paper by the solution of the equation for the approximate switching boundary. However, the analog computer program in Fig. 6 of my paper is superior to that of Fig. 5 in Part II of the authors' paper because:

My program used only two multipliers and no relay, whereas, in the authors' paper (Part II), six multipliers and one relay were employed. Both programs used the same number of amplifiers.

A limiter was used in place of a relay to generate the straight-line portion of the switching boundary. This resulted in more positive, higher speed action.

This comparison is possible because the computer program in Fig. 6 of my paper can be modified to give the approximate

switching boundary given by equations 7, 8, and 9 of Part II of the authors' paper without the use of additional components. The necessary modifications which must be made on Fig. 6 of my paper are:

1. Increase the gain of the amplifier which has a gain of 2 to $1 + e^{\pm\pi/\gamma}$ so that

$$Z = (1 + e^{\pm\pi/\gamma}) |e|$$

2. Increase the magnitude of \bar{r} in the adder, which forms $\bar{r} + \bar{c}$, so that the output of the adder is $e^{\pm\pi/\gamma} \bar{r} + \bar{c}$.

3. Change the limits on the output limiter (c to \bar{c}) from $2 - \bar{r}$ and $-2 - \bar{r}$ to $(1 + \delta) - \delta \bar{r}$ and $-(1 + \delta) - \delta \bar{r}$ respectively, where

$$\delta = e^{\pm\pi/\gamma}$$

I have experimented with an approximate switching boundary different from the semicircles centered at $\xi_1^P/2$ and $\xi_1^N/2$ as given in Part I of the authors' paper. My approximation is to replace the optimum switching boundary in the region near the origin by two semiellipses centered at the foci (or centers) of the trajectories which occur for positive and negative applied force, respectively. These ellipses were adjusted so that they were "inside" the optimum switching boundary. "Inside" means that a trajectory traveling toward the optimum switching boundary will intersect the ellipse before the optimum boundary. It was desirable to have the approximate switching boundary inside the optimum switching boundary because in this case trajectories approaching the origin were confined inside the approximate switching boundary and thus trajectories could be made to arrive precisely at the origin. The modification of the analog computer in Fig. 6 of my paper, necessary to produce this elliptical switching boundary, was simply to change the gain of the amplifier which has a gain of $(1/2)\omega_n^2$ to a gain of k .

While the elliptical approximation gave a very good fit in the vicinity of the origin ($|e| < 0.25 FR$ for $\xi=0.2$) it failed badly outside of this region. It is suggested, therefore, that a combination of the semicircular approximation suggested in Part I of the authors' paper and my elliptical approximation be used. This approximate switching boundary would have the advantage that it would slightly increase the rise time of the system to a step input.

I have eliminated oscillations at the origin for the case where the applied force to the oscillatory element was limited by a saturating amplifier (as opposed to a relay) by adding error derivative to the output

of the computer in Fig. 6 of my paper. The amount of error derivative to be added to the computer output depends on the gain in the linear region of the saturable amplifier which drives the oscillatory element.²

In conclusion, it is felt that the work done in Part II of the paper could have been done more efficiently if the authors had referred to "Maximum Effort Control for an Oscillatory Element."¹

REFERENCES

1. MAXIMUM EFFORT CONTROL FOR AN OSCILLATORY ELEMENT, H. K. Knudsen. *Wescon Convention Record*, Institute of Radio Engineers, New York, N. Y., pt. 4, Aug. 1959, pp. 116-24.
2. MAXIMUM EFFORT CONTROL FOR AN OSCILLATORY ELEMENT, H. K. Knudsen. *M.S. Thesis*, University of California, Berkeley, Calif., Jan. 1960.

Closing Remarks

Prapat Chandaket and C. T. Leondes: The significant area of time-optimal control system synthesis has seen considerable activity in the past and, if anything, this activity seems to be on the upgrade. However, in spite of this activity some of the more important practical but nevertheless exceedingly interesting theoretical problems are, at the present time at least, being passed by. This is not surprising in view of the apparent difficult problems involved, for example, such questions as the synthesis of time-optimal controllers for random and nonrandom inputs to systems with bang-bang actuators of nonideal characteristics both for 2-port and multiport systems. As an applied example there is the question of synthesizing such controllers with the constraint of most efficient use of energy for a satellite attitude control system wherein the yaw and roll modes are tightly coupled, thus resulting in a 4-port system.

The results discussed in the papers are those obtained as part of a long-range program in this area and are in a certain sense not of primary interest. They are, nevertheless, of considerable practical interest since they show the manner in which a control system of this type would be operated, and Part I of our paper constitutes the first explicit presentation of these results. It is interesting to observe from Mr. Yin's comments that he did not carry out his derivation in terms of the more general and useful result for the control problem as presented in Part I.

A point which is not clear to Mr. Yin is that in this paper we are dealing with a

quasi-stationary control system,¹ and as such there are very real problems of system mechanization which perhaps can best be answered with the explicit results before us.

Mr. Knudsen expresses surprise that we did not refer to his paper. There were many papers that could have been listed as references, but anyone with real interest in the field is generally aware of the literature in the field. If Mr. Knudsen feels offended in any way he should not.

Mr. Knudsen goes on to comment that we use the same approximation he conceived and which he proved valid mathematically and practically. His implication that he considers such an approximation as being somewhat profound is evident. Actually, such a step is rather straight-

forward, and the matter of principal interest is study of the trade-off between system complexity and dynamic response capability. Mr. Knudsen's statement that he has proved the approximation valid mathematically is hardly an accurate statement. Furthermore he does not consider at all the more general and actually more practical situation of quasi-stationary bang-bang control systems with complex roots, i.e., roots with a real and an imaginary part. Furthermore, from the presentation of his paper before the Institute of Radio Engineers it was clear at that time that Mr. Knudsen was not aware of the necessary techniques.

Finally, Mr. Knudsen states that he felt our work would have proceeded more

efficiently if we had referred to his paper. Mr. Knudsen has overlooked the fact that in our simulation studies we were going back and forth between the optimum system and the compromised optimum system and for our more general studies the manner in which we proceeded was preferable from our point of view. This comment of Mr. Knudsen's is beside the point, since we were primarily interested in obtaining valid experimental results, and this was certainly accomplished.

REFERENCE

1. SYNTHESIS OF OPTIMUM SYSTEMS WITH THE AID OF THE PHASE SPACE, A. A. Feldbaum. *Avtomatika Telemekhanika*, Moscow, USSR, vol. XVI, no. 2, 1955.

Wide-Range D-C Center-Wind Drive

BYRON JONES

ASSOCIATE MEMBER AIEE

THOMAS PARE

NONMEMBER AIEE

Synopsis: Continuous-process machines are employed in many different industries. Material processed on these machines must be handled, moved, and stored. One of the most commonly used packages is the reel, or roll, because material from this kind of package can be quickly unwrapped, processed, and then rewound. Several kinds of electric drives have been designed to perform the operation of rewinding material. This paper will deal with one particular class of constant-tension rewind drives. Direct-current motor drives are widely used for constant-tension rewind stands in which the roll being wound is driven by a motor attached to its shaft. When the d-c motor is controlled by varying its field, it exhibits an interesting property which allows for very economical drive design as well as economical machine design. One of the limitations of d-c motor rewind stands had been the limited speed range that is possible with field control of d-c motors. This paper will discuss a means for extending the range of a d-c winder drive.

IN MANY CASES a continuous-processing machine has positive control of the web being processed. When this is true, the speed of the web is determined by the driving means for the processing machine. The processed web must be rewound onto a package that is suitable for easy material handling.

The rewind stand, which picks up this material after it is processed by the machine, not only must maintain correct

position, so that the web is neither stretched nor broken, but also must be driven so that the tension in the web remains constant. Since the web is leaving the main machine at a constant velocity, and since the tension in the web must also be maintained constant, it is obvious that the power input to perform the winding operation is constant. This relationship is shown in equation 1.

$$P = FV \quad (1)$$

where

P = winding power

F = web tension

V = web velocity

Equation 1 is simply the time integral of the well-known force-distance equation. A satisfactory constant-tension drive could be obtained by maintaining constant power input to the web. This could be done by measuring web tension and web velocity, and regulating the drive to maintain their product constant. Some drives of this type have been used; how-

ever, many more d-c center-wind drives employ the principle of maintaining constant power input to the d-c motor. This is done because of the simplicity of the motor control system.

Basically, a d-c center-wind drive motor has constant armature voltage applied to it, maintains constant armature current, and has its speed variation accomplished by means of change in its field voltage. Fig. 1 shows such a drive system.

The windup drive motor as shown in Fig. 1 is powered from a direct-voltage source which is common to the main drive. As long as the voltage applied to the main drive is constant, the voltage applied to the windup drive will be constant also. The motor field is controlled by a regulator which maintains constant armature current. The armature current then is taken as a feedback signal.

The action of the system can be described as follows: Assume that the web tension, and hence the armature current, exceeds the value set by the tension reference voltage. Under this condition, the output of the motor field regulator will increase, thus causing the winder drive motor back-electromotive force to increase. This causes the armature current to decrease, which lowers the torque out-

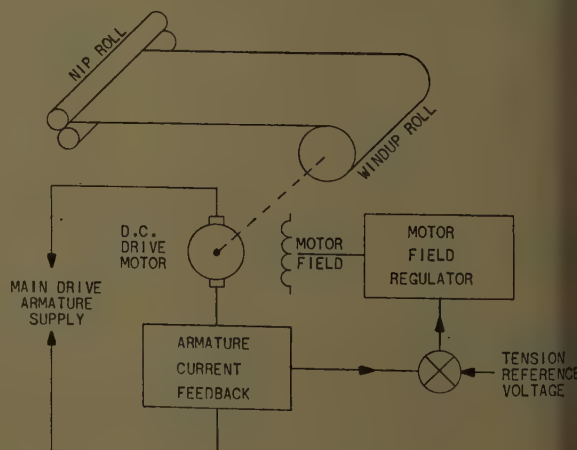


Fig. 1. Direct-current-motor armature current regulator

Paper 60-645, recommended by the AIEE Industrial Control Committee and approved by the AIEE Technical Operations Department for presentation at the AIEE Great Lakes District Meeting, Milwaukee, Wis., April 27-29, 1960, and represented for discussion only at the Winter General Meeting, New York, N. Y., January 29-February 3, 1961. Manuscript submitted February 23, 1960; made available for printing December 15, 1960.

BYRON JONES and THOMAS PARE are with The Louis Allis Company, Milwaukee, Wis.

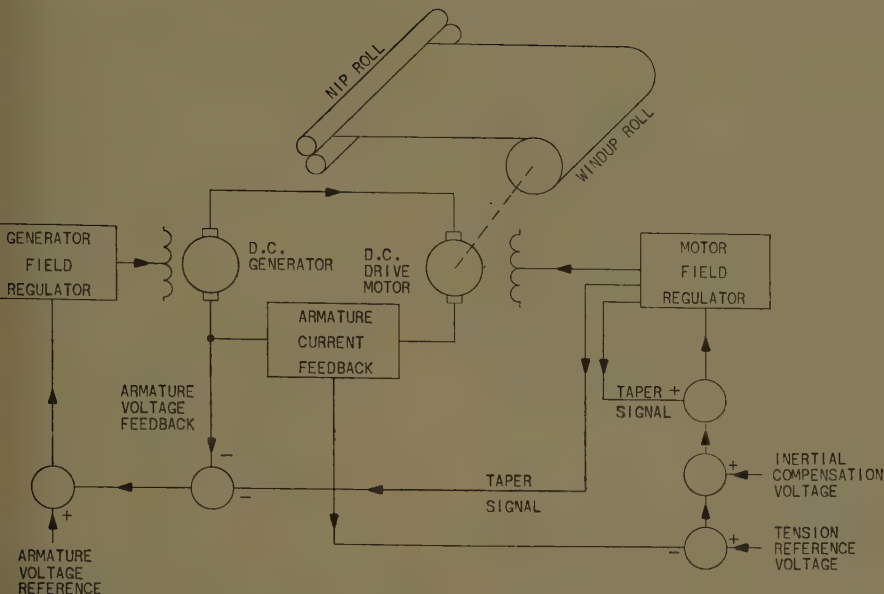


Fig. 2. Direct-current-motor dual-range tension regulator

out of the winder motor, and hence, the tension in the web decreases. For an increase in web tension, the reverse action takes place.

This drive system has two principal limitations. The first is that the regulator acts to maintain input power to the windup drive motor rather than to the web itself. The web tension will change because of drive motor and winder mechanical losses. This limitation can be overcome by care in the design of the drive motor and winder stand. The second limitation is that a field-controlled d-c motor has a limited speed range, partly because at extremely weak fields d-c motor commutation becomes difficult and motor stability is difficult to retain. Practical limitation of speed range for field-controlled d-c motors is 5 to 1 for small motors and 4 to 1 for larger motors. The dual-range winder described in this paper overcomes the second limitation.

Dual-Range D-C Winder Drive

Improvements in material-handling machinery have permitted the use of bigger packages. This could be accomplished by increasing the core diameter as well as the outside diameter, keeping the ratio of the two constant. Because the crushing forces on the core are very high, large-diameter cores are heavy and expensive and so a roll with small inside diameter and large outside diameter is desirable. To maintain constant web velocity and tension, the winder drive must operate over a wide speed range.

To provide a wide-range winder drive, the motor armature voltage is varied simultaneously with the motor field excitation during roll buildup. For instance,

if a 10-to-1 buildup is required and motor field is varied over a 5-to-1 range, the motor armature voltage will be varied over a 2-to-1 range. Since the winder-motor armature voltage must be varied, it must be derived from a generator other than the one supplying the processing-machine drive motor. Because the armature voltage is changing during roll buildup, it is necessary to change the winder-motor current in order to maintain constant input power. Fig. 2 is a block diagram of the system.

The dual-range tension regulator is composed of two closed-loop feedback systems. The winder-motor field is supplied from a regulator which receives armature current as a feedback signal. (This closed loop is the same as the one described previously for the common d-c motor tension regulator.) A second regulator supplies the generator field and, hence, the armature voltage to the winder drive motor. The feedback to this regulator is taken from armature voltage. At the beginning of the reeling operation the winder drive motor must be running at high speed, since the roll diameter is small. To attain this high speed, it is necessary to apply maximum armature voltage and minimum field current. At the end of the reeling operation the winder drive motor must be moving at low speed and so minimum armature voltage and maximum field voltage must be applied to the motor. A signal voltage from the motor field circuit is applied to the generator field regulator. This causes the generator armature voltage to reduce as the motor field voltage increases. In this manner, the armature voltage is reduced as the reel diameter increases. An additional signal voltage from the motor field

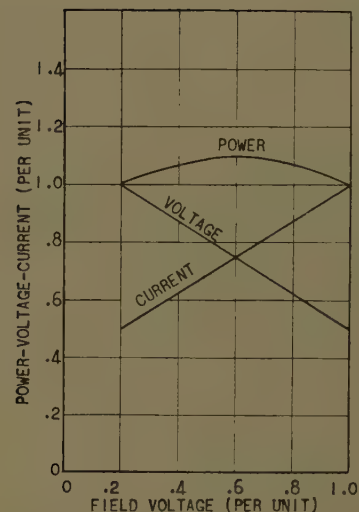


Fig. 3. Calculated power values

circuit is applied to the motor field regulator. This signal voltage causes the armature current to increase as the field voltage increases. In this manner, the conditions illustrated in Fig. 3 are obtained.

As might be expected, the cross-connection between the two regulators does give rise to some drive stability problems. It can be seen from the block diagram that the only cross-connection between the two closed-loop systems is the tie between motor field voltage and the input to the armature voltage regulator. If this signal is passed through a network with a fairly long time constant, the two regulator loops can be effectively separated and the result is a stable and well-behaved drive system.

THEORETICAL POWER DEVIATION

The power input to the d-c motor is the product of armature voltage and armature

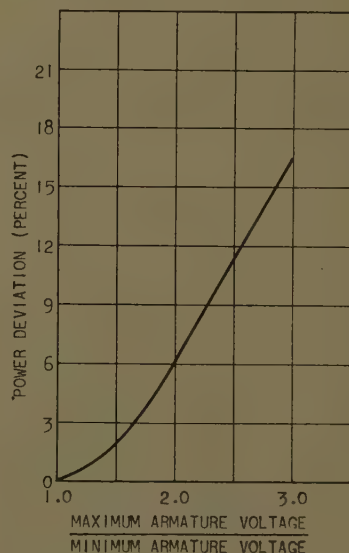


Fig. 4. Power deviation as a function of armature range

current. In the dual range, winder armature voltage and armature current are changed linearly, and are adjusted so that their product at both high and low speeds is the same. As might well be expected, the product of armature voltage and armature current is not constant over the entire speed range. This can be seen in Fig. 3. Equation 2 shows the per-cent deviation from constant power.

$$\% \text{ power deviation} = \frac{(1-K)^2}{8K} \times 100\% \quad (2)$$

where

$$K = \frac{\text{maximum armature voltage}}{\text{minimum armature voltage}}$$

As can be seen in equation 2, the per-cent deviation of power is determined solely by the amount of variation of armature voltage. The greater the armature voltage variation, the greater the deviation from theoretical constant power. Per-cent power deviation as a function of armature voltage range is shown in Fig. 4.

The derivation of equation 2 is given in the Appendix.

It is possible to eliminate the theoretical power deviation by using a multiplying device and controlling the output of this device to hold constant the product of armature voltage and current. This was not done on the dual-range winder drive because it was felt that the theoretical power deviation would not be objectionable. This feeling was based on the fact that the changes in motor losses cause greater power deviation than the error due to a straight-line relationship between current and voltage.

MEASURED POWER DEVIATION

Figs. 5-8 show the dynamometer performance of two different dual-range winder drives. Both of these drives have been installed in actual winding applications and are performing satisfactorily at this time. Fig. 5 shows the input and output power of a 10-hp (horsepower) winder. This winder has a buildup range

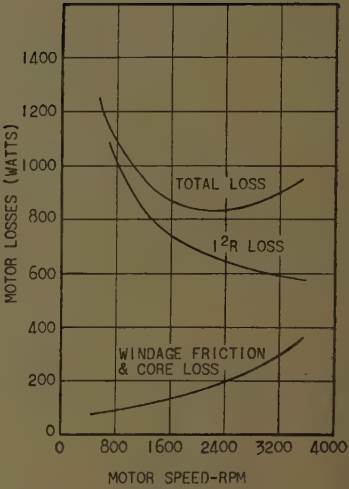


Fig. 6. Losses for 10-hp motor

of 8 to 1, which is accomplished by varying the motor field over a 4-to-1 range, and the armature voltage over a 2-to-1 range. Fig. 5 shows the performance of this drive at various values of tension and line speed (web velocity). Fig. 6 shows the separation of losses for this machine when it is operating at full line speed and full tension. It is obvious from Fig. 6 that the variation in I^2R loss is responsible for most of the deviation from constant horsepower.

Figs. 7 and 8 are performance characteristics for a 5-hp winder. The buildup range for this drive is 6.7 to 1, and this range is accomplished by varying the motor speed 4 to 1 by field control, and 1.7 to 1 by armature voltage control.

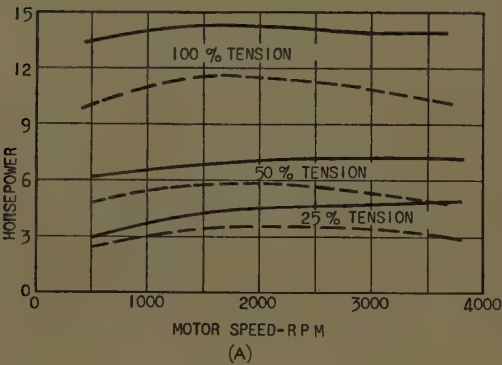


Fig. 5 (left). Tension characteristics for 10-hp winder

- A—At full line speed
- B—At one-half line speed
- C—At one-fourth line speed
- Power input
- - - Power output

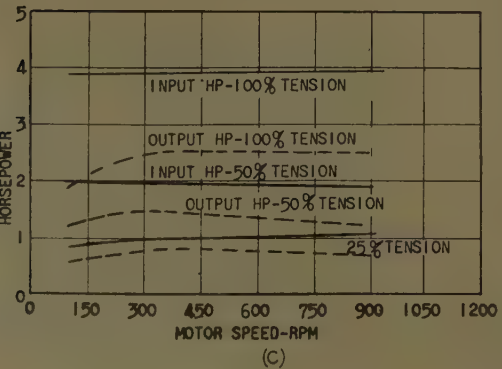
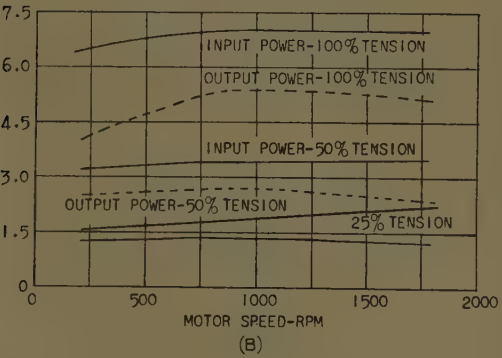
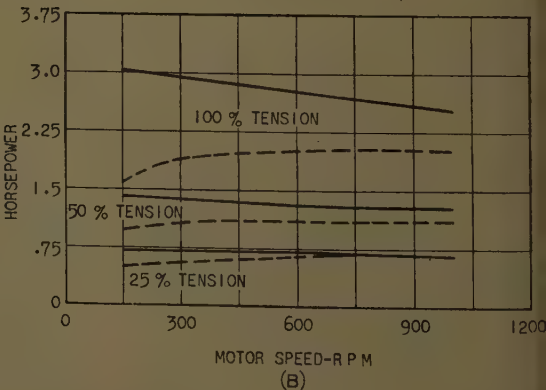
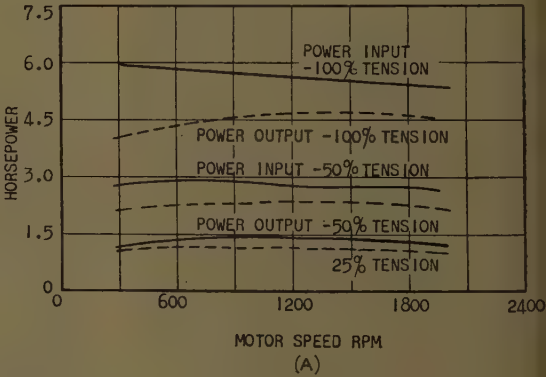
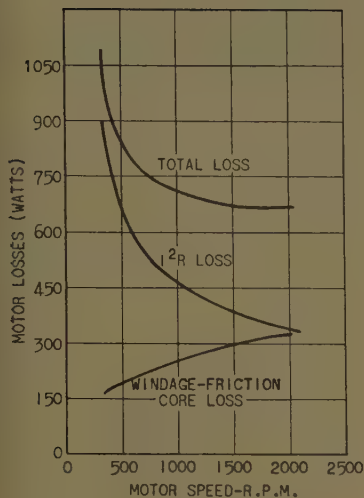


Fig. 7. (right). Tension characteristics for 5-hp winder

- A—At full line speed
- B—At one-half line speed
- Power input
- - - Power output





The effect of I^2R loss has been reduced in this drive, but this component of loss is still responsible for the major deviation of motor output power.

It is possible to correct the drive system and compensate for I^2R loss. This was not done because it was felt that correcting for I^2R loss would add further complexity to the drive regulator. Both of these drives are installed and are operating quite satisfactorily. The variation from constant tension shown in Figs. 8-9 apparently does not cause poor winder performance.

MODIFICATIONS

Any discussion of constant-tension winders would be incomplete unless mention were made of modifications such as tapered tension, stalled tension, and inertial compensation. When winding smooth-surfaced webs, the center of the roll sometimes slides out from under the upper layers of the roll along the axis of the core. This is known as "telescoping." Forces directed radially inward on the inner layers from the outside layers of the wound roll are responsible for this condition. For this reason it is sometimes desirable to reduce the tension as the roll builds up. This modification is called tapered tension and, on the dual-range winder drive, is obtained by simply decreasing the amount of motor field voltage signal which is fed back to the motor field regulator. For tapered tension the armature current is not required to build up as much as it does for constant tension.

It is usually necessary to provide tension between the processing machine and the roller when the web is not moving. Stalled tension prevents lurching of the roller at the instant of starting. On roller drives which take armature voltage from the main machine, a booster generator is necessary to provide stalled

tension. Since a separate generator is used on the dual-range winder, its voltage may be adjusted for stalled tension conditions.

Acceleration control in web-handling drives is important. Inertial compensation is employed to assist in maintaining constant tension during line speed changes. The inertial compensation signal is frequently derived from the armature voltage of the d-c motor driving the main processing machine. This voltage is taken through a derivative network, the output of which is proportional to the acceleration of the main machine. The importance of these control functions cannot be overemphasized. The system may function perfectly in the steady-state condition, but if the web cannot be handled during transient conditions, the entire drive system is useless.

Among other interesting modifications of this drive is one which allows for continuous reeling. This operation is obtained by using a tipover winding stand in which the drive motor powers two winding mandrels through a pair of mechanical clutches. During winding, one of the mandrels is stopped to permit changing of reels; the other mandrel is firmly engaged to the drive motor. Under this condition the drive functions as a constant-tension center winder. At the time of reel changeover the empty mandrel is moved up into position and by push-button signal the drive motor is switched to speed control. The empty mandrel is firmly clutched to the drive and accelerated to high speed. The mandrel containing the full reel is partially declutched and this reel continues to wind with tension being maintained by the slipping clutch. The web is then tagged onto the empty mandrel and the drive regulator is switched to tension control. The full reel is then stopped and while winding continues on the other reel, the full reel can be taken off the machine. In this way a continuous reeling operation is obtained.

Another modification came about because it is frequently desired to wind a wide range of web thicknesses and widths on a single machine. The winder drive is easy to control over a wide tension range; however, friction within the mechanical parts of the winder frequently leads to difficulties on light webs. Because of this problem, a windup drive was designed which uses normal tension control for heavy webs and a dancer-roll-operated induction regulator for light webs. In this drive the dancer roll was used simply as a vernier control of tension. The result was a drive system with excellent

transient response and stability. The performance was noted to be quite a bit superior to full dancer-roll-controlled drives.

Conclusions

A drive system has been described which will allow constant-tension center winding of material from continuous-process machines. This drive system has performance characteristics which are very similar to conventional d-c-motor center-wind systems. An extended winding range is achieved by varying the armature voltage applied to the d-c motor as well as its field voltage. This drive is capable of being modified to include all of the usual correcting signals. It has a functional error in that the product of armature voltage and current is not strictly controlled. However, it has been shown that this effect is not as responsible for deviation from constant tension as is the deviation of losses within the d-c motor. Field experience with the drive system described indicates that the performance obtained is adequate for most reeling applications.

Appendix

Nomenclature

e_a = armature voltage
 e_F = field voltage
 E_{F1} = minimum field voltage
 E_{F2} = maximum field voltage
 e' = field voltage displaced
 E_0 = armature voltage at $e' = 0$
 i_a = armature current
 I_0 = armature current at $e' = 0$
 $K = \frac{\text{maximum armature voltage}}{\text{minimum armature voltage}}$
 P = power
 ΔP = power deviation

Derivation

Refer to Fig. 3. If these curves were to be displaced to the left until the left end of the curves was coincident with the y -axis,

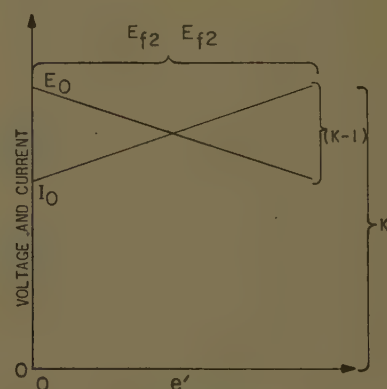


Fig. 9. Deviation construction

then the expression for y -intercept of current and voltage would be much simpler than at present. In equation form,

$$e' = e_F - E_{F1} \quad (3)$$

The plot of current and voltage versus e' is shown in Fig. 9. The y -intercept of e_a is equal to E_0 .

The slope of e_a is

$$\frac{E_0 \left(\frac{K-1}{K} \right)}{E_{F2} - E_{F1}}$$

Therefore the equation for e_a is

$$e_a = E_0 - \frac{e' E_0 \left(\frac{K-1}{K} \right)}{E_{F2} - E_{F1}} \quad (4)$$

The intercept of i_a is I_0 and the slope of i_a is

$$\frac{I_0 (K-1)}{E_{F2} - E_{F1}}$$

The equation for i_a is

$$i_a = I_0 + e' \frac{I_0 (K-1)}{E_{F2} - E_{F1}} \quad (5)$$

The power is given by multiplying equations 4 and 5.

$$P = E_0 I_0 \left(1 - \frac{e' K - 1}{E_{F2} - E_{F1}} \right) \left(1 + \frac{e' (K-1)}{E_{F2} - E_{F1}} \right) \quad (6)$$

Referring to Fig. 3 again, it can be seen that the maximum power point can be determined by differentiating the power equation and evaluating the equation when the slope is zero.

$$\frac{dP}{de'} = E_0 I_0 \left[\left(1 - \frac{e' K}{E_{F2} - E_{F1}} \right) \left(\frac{K-1}{E_{F2} - E_{F1}} \right) - \left(1 + \frac{e' (K-1)}{E_{F2} - E_{F1}} \right) \frac{K-1}{K(E_{F2} - E_{F1})} \right] \quad (7)$$

or when $dP/de' = 0$:

$$\left(1 - \frac{e' K}{E_{F2} - E_{F1}} \right) \left(\frac{K-1}{E_{F2} - E_{F1}} \right) = \left(1 + \frac{e' K - 1}{E_{F2} - E_{F1}} \right) \left(\frac{K-1}{K(E_{F2} - E_{F1})} \right) \quad (8)$$

Simplifying and solving for e' :

$$e' = \frac{E_{F2} - E_{F1}}{2} \quad (9)$$

At this point:

$$P = E_0 I_0 \left(1 - \frac{K-1}{2K} \right) \left(1 + \frac{K-1}{2} \right) \quad (10)$$

or

$$P = E_0 I_0 \left(1 + \frac{(1-K)^2}{2K} \right) \quad (11)$$

The change in power from $P = E_0 I_0$ is

$$\Delta P = E_0 I_0 \frac{(1-K)^2}{4K} \quad (12)$$

The per-cent deviation from mean power:

$$\% \text{ power deviation} = \frac{(1-K)^2}{8K} \times 100\% \quad (13)$$

References

1. CONTROLLING WEB TENSION, E. H. Dinger. *Machine Design*, Cleveland, Ohio, Oct. 1959, pp. 122-33.
2. WINDER DRIVES, L. W. Fisher. *Pulp and Paper Magazine of Canada*, Gardenvale, Que. Canada, vol. 53, 1952, pp. 206-14.
3. AUTOMATIC CONTROL OF PAPER TENSION, C. C. Ehemann, R. C. Berger, W. Mikelson. *The Paper Industry*, Chicago, Ill., vol. 33, Dec. 1951.
4. AN ELECTRONIC DRIVE FOR WINDUP REELS, K. P. Puchlowski. *AIEE Transactions*, vol. 65, Aug.-Sept. 1946, pp. 585-91.

Grounding of D-C Structures and Enclosures

D. C. HOFFMANN
MEMBER AIEE

THE GROUNDING of supporting structures and enclosures for d-c power circuits and apparatus has been a controversial subject ever since metal-enclosed power rectifiers and switchgear came into use in the electrochemical and other industries. Many users of d-c equipment naturally followed the well-established a-c practice of solidly grounding enclosures through a low-resistance conductor. Relatively few of these equipments included sensitive grounding protective relays. Many cases of serious injury and damage due to ground faults that might have been avoided by the use of grounding protective relays are recorded in an earlier paper.¹

As early as the 1920's, the transportation industry, recognizing the disadvantages and dangers of low-resistance grounding, insulated the metal supporting structures of d-c switchboards from ground. For many years it was the practice to ground the frames of 600-volt

rotary converters and generators through a low-resistance ground relay for flash-over protection. In 1957, an AIEE subcommittee recommended high-resistance grounding of enclosures for certain applications.¹ Several National Electrical Manufacturers Association (NEMA) standards touch lightly on the subject of low-resistance versus high-resistance grounding. In recent years, most users of d-c equipment for electrochemical service rated above 300 volts have grounded the enclosures through either low-resistance or high-resistance grounding protective devices.

The purpose of this paper is to present the advantages and disadvantages of high-

and low-resistance grounding of d-c structures and enclosures and to set forth guide rules for use in the design of new installations.

General Considerations

By d-c structures and enclosures is meant the metallic support, frame, or enclosure for power rectifier, rotary converters, generators, and d-c switchgear for power rectifiers, rotary converter, generator, and feeder circuits, including bus ducts and transition compartments close-connected thereto.

STANDARDS

NEMA standards²⁻⁴ and the AIEE¹ have made recommendations on the grounding of structures and enclosures but have left many questions unanswered. Some of the recommendations follow.

From NEMA SG5-5.02:²

Structures housing single-polarity direct-current circuits 275 volts and above shall be ungrounded.

It is recommended that they be connected to ground only by protective or indicating devices of relatively high resistance.

From NEMA 222-1952:³

Structures housing single-polarity direct-current circuits shall be designed for grounding through protective Device No. 64.

Paper 61-67, recommended by the AIEE Chemical Industry Committee and approved by the AIEE Technical Operations Department for presentation at the AIEE Winter General Meeting, New York, N. Y., January 29-February 3, 1961. Manuscript submitted October 31, 1960; made available for printing November 25, 1960.

D. C. HOFFMANN is with the General Electric Company, Philadelphia, Pa.

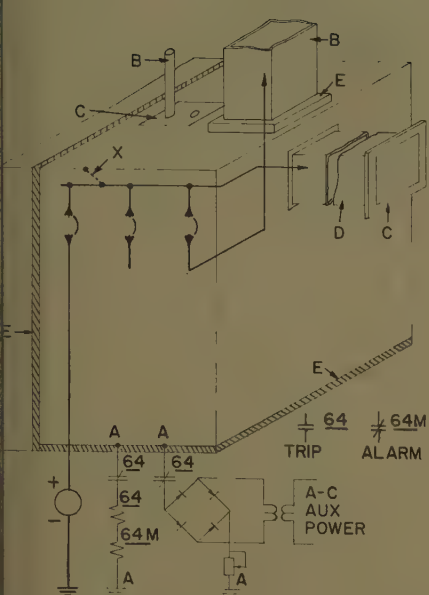


Fig. 1. Example of high-resistance grounding of indoor equipment

- Four physically separate electric connections
- Grounded conduit or bus duct not in protected zone
- Insulation oversize to insure ample creepage
- Bus duct in protected zone (connected to switchgear but insulated from ground)
- Insulation thick enough to insure ample creepage
- Fault between power circuit and enclosure
- 64—High-resistance instantaneous hand-reset ground relay
- 64M—Monitor relay

From NEMA 222-1952:⁴

When insulated structures are in a continuous line-up with grounded structures, they should be properly insulated from the grounded structures in the same line-up.

From AIEE Committee Report¹

It is strongly recommended that metallic structures of d-c power and control circuits be (a) insulated from ground and (b) grounded through a relatively high-resistance ground relay no. 64 when 1. the rated direct voltage is 275 and over (optional on lower direct voltages), and 2. when one polarity of the d-c circuit is grounded.

SINGLE-POLARITY AND DUAL-POLARITY EQUIPMENT

Large mercury-arc power rectifier equipments used for electrochemical processes usually employ the single-way circuit; hence the enclosures house only the positive polarity power circuit. The NEMA standards referred to in the preceding section refer to structures housing single-polarity d-c circuits. However, silicon power rectifiers now coming into general use for electrochemical processes usually employ the double-way circuit. Hence,

the enclosures house both positive and negative polarity power circuits. It will be understood that the discussions herein apply to d-c structures and enclosures for both single-polarity and dual-polarity equipment.

GROUND-FAULT PROTECTION OF ENCLOSURES

The grounding of d-c structures and enclosures through a protective device of some sort is no longer questioned by most users, as ground-fault protection is recognized as a necessary or desirable function. The question that has not been resolved is whether the enclosure should be grounded through a high-resistance or a low-resistance protective device. The two schemes should be reviewed and understood before the advantages and disadvantages of each are considered.

Fig. 1 shows a typical metal-enclosed d-c switchgear unit rated 600 volts insulated from ground and from close-connected grounded units. A sensitive high-resistance grounding protective relay device 64 is connected between enclosure and ground in series with the coil of a circuit monitor relay 64M. The monitor current is supplied from an auxiliary a-c source through a stepdown transformer, rectifier, and adjustable resistor. Devices 64 and 64M have a total resistance of 500 to 2,000 ohms, depending on the manufacturer. Such protective equipment is described in an earlier paper.¹

Normally the enclosure is substantially at ground potential, the actual voltage being that of the monitor circuit, about 25 volts d-c. If a fault develops between the d-c power circuit and the enclosure, such as at X, the potential difference between enclosure and ground will rise immediately to nearly 600 volts, the actual value depending on the resistance of the fault. This potential difference is applied to the ground protective relay 64 and if the potential difference is 30 volts or more, 64 operates instantly to clear the fault by tripping all of the circuit breakers and shutting down the source of d-c power. The fault current is limited to about 1 amp (ampere) or less; hence there is practically no damage, no burning, and no flashing.

While Fig. 1 illustrates the condition of a fault between a power bus and the enclosure, equally effective protection is provided against faults between the enclosure and control wiring or devices connected to the power circuit. This is especially true in the case of excitation devices and auxiliary circuits in power rectifier equipments.

Fig. 2 shows the same metal-enclosed

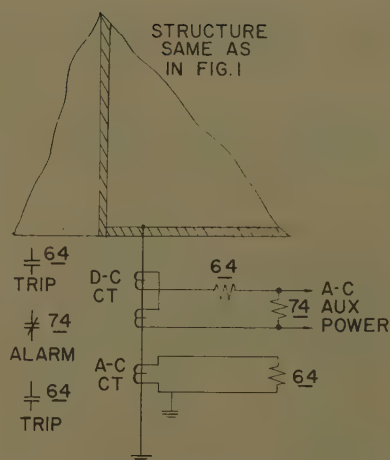


Fig. 2. Low-resistance grounding of indoor or outdoor equipment

- 64—Low-resistance instantaneous hand-reset ground relay
- 74—Auxiliary power failure alarm relay

switchgear unit connected to ground by means of a low-resistance conductor passing through window-type a-c and d-c current transformers. Sensitive instantaneous overcurrent relays 64 are connected to the secondary winding of each of the current transformers. The relays, set to pick up at as low as 20-amp a-c or 10-amp d-c primary ground-fault current, are connected to trip all circuit breakers supplying power to the equipment. The alarm relay 74, for indicating loss of a-c supply to the d-c current transformers, is optional.

Normally the enclosure is at ground potential. If a fault develops between the d-c power circuit and the enclosure, a heavy fault current will flow, the magnitude of the current depending on the total resistance in the path of the current. The current may approach short-circuit magnitude, resulting in considerable flashing, spreading, and burning during the operating time of 64 and interrupting time of the circuit breakers. A considerable potential difference may exist between the enclosure and surrounding grounded objects during the fault unless the grounding system has been carefully designed to prevent such potential differences under all conditions.

Comparison of High- and Low-Resistance Grounding

In the following discussion, it is assumed that the d-c system is grounded either intentionally for normal operation, or unintentionally owing to a ground fault external to the enclosure.

PERSONNEL SAFETY

If the enclosure is grounded through a low-resistance path and a short circuit

develops between the enclosure and the ungrounded polarity of the d-c power circuit, personnel may be endangered by:

1. A high-current power arc, which may cause severe burning of persons in the immediate vicinity.
2. A brilliant flash, which may cause fright and temporary blindness.
3. Flying objects, such as glass from an exploding instrument, splattering of hot metal, and the like.
4. High enough voltage between enclosure and ground to cramp muscles, making it impossible for the victim to free himself. Even though the resistance is low, the ground-fault current may be high enough to produce dangerous voltage differences between enclosure and ground in an improperly installed or maintained grounding system.
5. Consequential injury, such as broken bones and bruises due to fright, attempt to escape, or sudden release of cramped muscles, causing victim to fall or to strike other objects.

All five of the personnel hazards listed may exist during a ground fault in an enclosure grounded through a low resistance, whether or not a protective relay is used. However, if the enclosure is grounded through a high resistance, hazards 1, 2, and 3 cannot exist because there is no power arc. The only hazards are 4 and 5, and even in the case of 5, the danger is less because there is no flash, arc, or hot metal.

It should be noted further that in the case of the low-resistance grounded enclosure, personnel anywhere in the immediate vicinity of the unit is exposed to all of the hazards listed except 4, whereas in the case of the high-resistance grounded enclosure, a person must be in a definite position to be injured, i.e., bridging a gap with his body between the enclosure and a grounded object. The chances of this occurrence are small because in most installations the floor covering is insulating material such as rubber matting, and clearance to nearby grounded objects is ample, or the objects are covered with insulation.

DAMAGE TO EQUIPMENT

In high-resistance grounding, the fault current is limited to about 1 amp or less, which means that there is practically no damage to wiring, components, or equipment. Repairs may be made at very little cost and the unit can be restored to service quickly after the fault condition has been removed.

In low-resistance grounding, the fault current is high enough in most cases to do some damage in the 5 or 6 cycles required for the relays and circuit breakers to operate. Components and wiring may

require complete replacement. Steel panels, structural members, and copper bars may be deformed or burned, requiring extensive repairs or replacement. Such repairs may be costly and the unit may be out of service for a long time.

EASE OF INSTALLATION

For either low- or high-resistance grounding protection, the protected unit must be insulated from building steel, conduits, bus ducts, transformers, water pipes, air lines, ventilating ducts, and all other grounded metallic objects. Bus ducts may be included in the protected zone by insulating them from grounded metal and connecting them electrically to the protected enclosures, as shown in Fig. 1.

1. All of this is relatively easy to accomplish in the case of low-resistance grounding because the voltage across the insulation is low and because any accidental connection bridging the insulation would have to be extremely low in resistance to bypass effectively the low-resistance protective circuit.

In the case of high-resistance grounding, greater care must be taken in both the design and installation because the insulation may be subjected to rated voltage and because a relatively poor accidental connection bridging the insulation can bypass the protective circuit. Even though the ground relay itself may not be rendered inoperative, the monitor is adjusted to sound the alarm if the total resistance between enclosure and ground is reduced to a predetermined lower value. Four physically separate electric connections must be made at points *A*, *B*, *C*, and *D* of Fig. 1, to insure complete monitoring.

The installation should be designed so that a man cannot contact with his body the enclosure and a grounded metallic object at the same time. There should be ample clearance between the enclosure and building steel or other metallic objects, or such nearby grounded metal should be covered with insulation. In accordance with good station practice, the floor around the enclosure should be covered with rubber mats or the equivalent.

Special precautions must be observed in the case of water-cooled power rectifiers with water-to-water heat exchangers because the water columns can form conducting paths to raise the potential of the enclosure above ground or to bypass the grounding protective relay, depending on the arrangement. The circulating cooling water in the rectifier is at rectifier potential and the raw water supply and return pipes are at ground potential. The conductivity of the water, though

normally low, is variable, and could become high enough to cause operation of the ground relay or monitor relay, thus creating a maintenance problem. Depending on the location of the insulating hoses, the heat exchanger could be a rectifier potential, enclosure potential, ground potential, or floating.

Considering only the requirements of the high-resistance grounding protective scheme, any arrangement in which the heat exchanger is insulated from the enclosure is satisfactory. The water columns then can neither raise the enclosure potential nor bypass the insulation between enclosure and ground. If the heat exchanger is at rectifier potential, it is protected against ground faults the same as is the power circuit. If it is grounded, it need not be a hazard inside the insulated enclosure because it can be and usually is, in a separate compartment from the rectifier.

MAINTENANCE

High-resistance grounding requires more maintenance than low-resistance grounding. It is easier to bypass the high-resistance circuit.

The insulation between enclosure and ground may be bridged accidentally by an accumulation of conductive dirt or dust, iron filings, metallic sweepings, nails from building operations, spilled or leaking liquids, etc.

Gradual changes in the insulation between enclosure and ground may require occasional readjustment of the monitoring current to maintain the desired operating conditions. On the other hand, the monitor relay does act as a constant and reliable check on the continuity of the grounding relay circuit and the insulation between enclosure and ground. There is no easy way to check the low-resistance grounding protective relays either continuously or periodically. About all that can be done is to monitor the a-c supply to the d-c current transformer with an under-voltage alarm relay 74, as shown in Fig. 2.

Conclusions

Taking into account the advantages and disadvantages of high- and low-resistance grounding, the following rules are listed, which may be used as a guide in the design of new installations of d-c systems with different ratings, designated as cases 1, 2, and 3.

Case 1. D-C Systems Rated Above 300 Volts

Conditions:

One of the power conductors intentionally connected to ground through a resistance connection.

Structures and enclosures to be located outdoors in a dry place.

Access limited to authorized personnel.

All d-c structures and enclosures should be insulated from ground and from other electrically connected units. All such insulated structures and enclosures should be connected to ground through one or more high-resistance ground detector relays such as described above, and arranged to disconnect all sources of power upon occurrence of a fault between the power circuit and the structure or enclosure.

While case 1 applies especially to rapid transit and main-line haulage transportation systems, it also applies to those electrochemical systems in which the midpoint of the cell line is intentionally grounded through a current-limiting resistor that would permit relatively large ground-fault currents to flow.

Case 2. D-C Systems Rated Above 300 Volts

Conditions:

No power conductor intentionally grounded.

Characterized by unintentional grounds of varying magnitudes in varying locations.

Structures and enclosures to be located outdoors in a dry place.

Access limited to authorized personnel.

The method of grounding should be recommended with the purchaser or user. The recommendation would be the same as in case 1. The alternative is to ground the structures and enclosures through d-c and a-c current transformers with instantaneous overcurrent relays as shown in Fig. 2. Most electrochemical equipments are in this category.

Case 3. D-C Systems of Any Voltage Rating

Conditions:

No power conductor intentionally grounded.

Power conductor grounded through a high-resistance (such as a ground detector),

Structure or enclosure to be located outdoors or in a normally damp place, or

Unlimited access, such as in factory areas, public places, etc.

All structures and enclosures should be solidly grounded through d-c and a-c current transformers with instantaneous overcurrent relays as illustrated in Fig. 2.

Examples of case 3 are equipments for

steel mill main drive, general industrial power supplies, field excitation, and press drives, and all units located outdoors or in damp places.

GENERAL CONSIDERATIONS

The grounding protective relay 64 should trip all circuit breakers that can supply current to the protected unit, including outgoing feeder breakers and, in the case of rectifiers, the transformer primary breaker. Rotating machines should be shut down.

A circuit monitor is required in every case in which a high-resistance ground detector relay is used. The monitor relay 64M should sound a local and remote alarm and light a conspicuous local indicating lamp if the ground detector relay becomes inoperative because of the presence of an open circuit or a bypass circuit, or loss of a-c supply.

High-resistance grounding of d-c generators and motors is generally not feasible because it is difficult to insulate the frame of the machine from the prime mover or load. Motor-generator sets can be protected by high-resistance grounding protective relays as illustrated in Fig. 1, if driven by a low-voltage motor, and there is otherwise no objection to insulating the motor frame from ground. Motor-generator sets can also be protected by the low-resistance grounding protective relays shown in Fig. 2. High-resistance grounding provides excellent flashover and winding failure protection for rotary converters.

High-resistance grounding should not be used in a location to which access is unlimited or in which frequent changes are made in the surroundings. For example, an equipment in an open factory or other working area may become a maintenance problem because the floor cannot be kept insulated, clean, and dry, and because metallic objects may be placed against or close to the enclosure temporarily or permanently.

High-resistance grounding should not be used in outdoor, exposed, or normally damp locations because it is difficult to provide and maintain a dry insulated floor area around the unit for personnel. Even the low monitor circuit potential of 25 volts might be uncomfortable if hands and feet are damp.

Although a-c switchgear can be protected by the high-resistance grounding method described, it seldom meets the requirement of being in a location where access is limited to authorized personnel. High-resistance grounding of a-c switchgear therefore is not generally recommended.

Appendix. Case Histories

The following case histories of recent actual occurrences are presented in the words of the contributors, several large users of d-c equipment for aluminum reduction and other electrochemical processes.

Solidly Grounded Enclosures Without Grounding Protection

Conditions: Potline voltage of 750 volts with mid-point grounded through a 100-amp circuit breaker.

1. A flashover occurred as an electrician was replacing a fuse in a 2-pole fuse block mounted in a grounded metal box. The fuse block was connected to a 7,500-amp shunt in a 750-volt rectifier bus. Accidental contact of the fuse with the metal box caused grounding of rectifier bus. A d-c arc occurred that was cleared by burn-up of the wiring. The electrician received second-degree burns on one hand.

2. A cathode bus arced to 250 volts d-c control wiring of a cathode breaker. The battery circuit flashed to ground at the battery charger panel and also in an auxiliary relay on the rectifier switchboard. The glass cover was blown off the relay. The fault was cleared by burn-up of the wiring on the cathode breaker. The arcing on the various pieces of equipment and flying glass from the cover endangered operating personnel.

3. Flashover in a firing cubicle occurred during a lightning storm. The cubicle was solidly grounded and considerable damage occurred owing to the d-c feed from the rectifier. To minimize production loss, the entire firing cubicle was replaced with a spare and then was completely rewired at a later date.

4. Following an arc-back, a fire occurred in an excitation cubicle. Although all a-c power was disconnected, and d-c power was disconnected from all sources other than through the transformer from the negative bus, the fire persisted in burning. A number of CO₂ fire extinguishers were used in an attempt to extinguish the fire, but it was not extinguished until a ground fault had burned clear in the cubicle. The cubicle was damaged to such an extent as to merit replacement rather than an attempt to repair in place.

Low-Resistance Grounded Enclosures Protected as in Fig. 2

Conditions: Potline voltage of 750 volts with no intentional ground on the system.

5. Line relayed off on both a-c and d-c case ground. A burned spot was found on an anode bus support. It was surmised that some foreign object had grounded the bus, although none was found. No repairs were necessary. (This operation occurred in the first month of operation, during which time considerable difficulty was experienced with anode breakers.)

6. Line relayed off on a-c case ground. A control transformer supplying anode breaker holding cool rectifiers had failed. The transformer and some associated metallic

rectifiers and resistors were ruined and required replacement.

7. Potline relayed off on d-c case ground. A firing reactor had failed internally. The reactor and associated metallic rectifiers were ruined as a result and required replacement.

8. Potline relayed off on d-c case ground. The saturable reactor in the d-c case ground circuit had failed. The reactor was replaced. (This was an operation due to ground detector circuit failure, not one caused by the resulting fault.)

9. Potline relayed off on d-c case ground. A firing reactor had faulted to ground. Damage was confined to the reactor, which was replaced.

10 through 14. Same as or similar to case 9.

15. Potline relayed off on a-c and d-c case ground. The distilled-water connection at the top of an ignitron tank had come loose, spilling water on the frame and causing an anode bus to flash over to ground. The damage was minor, involving insulators, firing wiring, and capacitors mounted on the rectifier tanks, and required some cleanup work.

16. Potline relayed off on a-c and d-c case ground. An excitation transformer had failed. Damage was confined to the transformer.

17. Same as case 15.

Contributor's additional comment: "The case ground protection has operated a number of times to clear faults which were usually in auxiliary circuits. In no case has damage due to such faults been extensive, and it usually has been confined to the component whose failure created the fault in the first place."

High-Resistance Grounded Enclosures Protected as in Fig. 1

Conditions: Potline voltage of 750 volts with mid-point grounded through a 100-amp circuit breaker.

18. Man who was checking in a cubicle let one end of test lead drop to cubicle steel; the other end was connected to the cathode

bus. The rectifier tripped owing to resistance grounding relay action. Had cubicle been solidly grounded, man would probably have received a severe flash burn. No damage occurred to the equipment.

19. A metal retainer ring on the fingers of a drawout anode breaker broke and fell, establishing a path from anode bus to the cubicle enclosure. The rectifier tripped by ground relay action and negligible damage occurred. Damage would probably have been extensive with a solidly grounded cubicle. (Potline voltage assumed by author to be in 750-volt class. System assumed to be not intentionally grounded.)

20. Ionized gas path to ground created at anode breaker cubicle resulting from one pole and the cathode breaker interrupting approximately 100,000 amp, which occurred when all breakers cascaded out because of accidental loss of d-c control power.

Outage times: Potline no. 1, 14 minutes; one rectifier frame, 55 minutes.

Damage: None due to ground. Usual maintenance required on contacts and arc chute after severe interruption.

Comment: Solid cubicle grounding undoubtedly would have resulted in extensive damage and prolonged outages.

21. Short circuit from firing circuit phasing reactor to cubicle occurred when returning a rectifier transformer to service. Both a-c and d-c windings were short-circuited to the frame.

Outage time: Potline no. 2, 2 minutes.

Damage: None due to ground; faulty reactor was replaced.

Comment: Damage to other components and wiring nearby might have resulted with a low-resistance cubicle ground system.

22. Accidental short-circuiting of firing circuit leads to cubicle while two capacitors were being interchanged for test.

Outage times: Potline no. 1, 25 minutes
Potline no. 2, 26 minutes.

Note that the major portion of these outages was due to other causes, not the trouble mentioned above.

Damage: None.

Discussion

R. P. Stratford (General Electric Company, Schenectady, N. Y.): The author has presented the subject of d-c structure and enclosure grounding in a very clear and concise manner. However, we believe that a few points should be added or emphasized.

The first concerns insulation. How much is required on an enclosure? What materials should be used? What voltage does it have to withstand? What Megger value is acceptable?

Second, the paper states that motor-generator sets driven by low-voltage motors can be protected by high-resistance grounding protective relays. It would be helpful if an explanation of "low voltage" were given as well as why other "high-

voltage" motors would not receive better protection from a high-resistance grounding relay.

Third, in most electrochemical installations that use rectifiers, the high-resistance grounding relay is essential for protective relaying when d-c circuit breakers or main d-c fuses are not used. Without the relay, if a fault develops between one polarity and ground in the rectifier it is possible to remove the a-c source by the power circuit breaker, but there is no means of interrupting the cell line current which will continue to flow until the cells no longer act as a battery. With the high-resistance grounding relay, the fault current is limited to the order of 1 amp and the ground is removed when the relay operates so that the disconnecting switches can be operated without endangering the personnel.

Comment: Bodily injury to the man could have resulted from arc with a low-resistance grounding system.

23. Potline outage caused by accident making up a relay trip circuit when a relay was being removed for maintenance purposes.

Outage time: Potline no. 2, 2 minutes.

Damage: None.

Comment: The same thing could have happened with a low-resistance grounding system.

24. Accidental short-circuiting of a firing circuit capacitor to ground by maintenance man.

Outage time: Potline no. 2, 3 minutes.

Damage: None.

Comment: Possibility of damage to equipment and injury to man with a low-resistance grounding method.

25. Failure of phase shift reactor coil leads to control cubicle.

Outage time: Potline no. 2 off 1 minute; initial trouble and another minute in finding the cause. Rectifiers were off for 8 hours, 32 minutes.

Damage: None due to ground. Faulty phase shift reactor was replaced, and lat repaired.

Comment: Not likely that the reactor could have been repaired with a low-resistance grounding system; other components and wiring might have been damaged.

References

1. RECOMMENDED GROUNDING PRACTICES FOR SINGLE-POLARITY D-C STRUCTURES, AIEE Committee Report. *AIEE Transactions*, pt. III (*Power Apparatus and Systems*), vol. 76, Oct. 1957, p. 784-90.
2. POWER SWITCHGEAR ASSEMBLIES. *NEMA Standard SG5-1959*, National Electrical Manufacturers Association, New York, N. Y., Nov. 1959, pt. 5, p. 1.
3. STANDARDS FOR TRANSPORTATION RECTIFIER UNITS. *NEMA Publication no. 222-1952*, Sept. 1952, p. 9.
4. *Ibid.*, p. 18.

Last, it should be emphasized that the monitoring of ground circuits is a reliable and sensitive method of detecting faults, but care during installation is of the utmost importance. It is essential that, after insulating the structure or enclosure, either be grounded through the protective relay or grounded solidly with current transformers and relays to monitor the circuit. Under no condition should the structure or enclosure be left in an ungrounded condition.

Stuart N. Lovelace (Kaiser Aluminum and Chemical Corporation, Berkeley, Calif.) This paper provides well-organized general recommendations for the grounding of d-c structures and enclosures. The recommendations for ground-fault protection of d-c equipment supplying solidly ground-

case 1) and ungrounded systems (case 3) should receive general acceptance. The recommendations for unintentionally grounded systems (case 2), as characterized by electrochemical cell lines, may also be considered acceptable because they permit the user to choose either of the grounding methods described.

The paper indicates that high-resistance grounding is the preferred method because it is claimed to be safer for personnel and equipment. I would like to re-examine the comparisons which led to this preference, considering only enclosed d-c equipment applied to systems similar to electrochemical cell lines which are not intentionally grounded. Such systems are characterized by unintentional grounds of varying magnitude and location. Available ground-fault current at the d-c equipment is usually quite limited because of resistance in the unintentional grounds on the system. With the trend to enclosed semiconductor rectifiers on electrochemical cell lines, this combination of enclosed switchgear and unintentionally grounded system will probably become the most prevalent one. It is also likely to be the most controversial one in regard to equipment grounding.

PERSONNEL HAZARDS

Personnel hazards due to power arcs are attributed to low-resistance grounding. Actually, since all live parts are enclosed, power arcs can only originate inside the enclosure. With reasonable enclosure design and with fast clearing of the fault, it is very unlikely that personnel will be exposed to the arc at all. With high-resistance grounding, however, external shover of the enclosure ground insulation during a fault becomes a possibility. This could expose personnel to arc hazards.

EXPLOSION HAZARDS

Hazards due to flying objects such as glass from an exploding instrument, or splattering metal, were attributed to low-resistance grounding. Internal failure of an instrument solidly connected to the power circuit could, indeed, produce flying glass. However, the ground-fault current available within exposed instruments or trays can, and should, be held to safe values by isolating or current-limiting devices. Splattering metal and similar debris should be contained by the enclosure. Other explosion hazards should be slight because of limited fault current and fast fault clearing.

FATAL SHOCK HAZARDS

The paper states that enclosures with low-resistance grounding may reach dangerous potentials during faults. The main purpose of low-resistance grounding is, of course, to prevent this. It is difficult to imagine a realistic combination of unintentional system ground and equipment fault which could produce much potential across a properly installed low-resistance ground connection. This hazard for low-resistance grounding must be discounted as practically nonexistent.

With high-resistance grounding, however, the enclosure may be raised to potentials as high as the system voltage under some conditions. If we use Dalziel's proposed

criterion of $I^2t=0.054$ for a d-c impulse,¹ then with 6-cycle fault-clearing time we arrive at 735 milliamperes as a potentially fatal shock current. Assuming the conventional body resistance of 500 ohms, this current would be produced by 368 volts. For 60-cycle impulse shocks, which might occur on rectifying equipment, the established criterion is $I^2t=0.027$.¹ With 6-cycle fault duration and 500-ohm body resistance, a 260-volt a-c shock might be fatal. The hazards resulting from physical reaction to shock would, of course, occur at lower voltages than the potentially fatal ones.

It is evident that the enclosure potentials permitted by high-resistance grounding are dangerous. For safety it is necessary to treat the enclosure as though it were at high potential at all times. Even so, this is not as safe as an enclosure which can be considered grounded at all times.

EQUIPMENT DAMAGE

The amount of damage produced by a fault depends, to a great extent, on the energy released. With fast clearing and with moderate fault current, the damage is not likely to involve much more than the component whose failure causes the fault. This has been the experience in the case histories for sensitive low-resistance ground-fault protection which were cited in the paper. With high-resistance grounding the failed component must also be replaced or repaired.

It should be emphasized that low-resistance d-c and a-c case-ground protection must be sensitive. This permits detection and clearing of light or incipient faults before they spread and cause unnecessary damage. Sensitive d-c case-ground protection is of fairly recent origin. I believe it was first developed to meet specifications for enclosed rectifier equipment purchased by the General Electric Company in 1956.

INSTALLATION

The need to isolate or insulate-around high-resistance-grounded enclosures increases installation problems and costs. This need does not exist for low-resistance grounding. Where roll-out switchgear is involved, it is particularly advantageous to omit rubber matting from the floors, and low-resistance grounding makes this possible.

In order for low-resistance case-ground protection to be effective, the fault must be quickly cleared from all sources. This requires switchgear capable of interrupting the maximum foreseeable fault current. Fault-clearing requirements to make high-resistance case-ground protection effective are not so stringent, although delay in clearing does make enclosure potentials more dangerous. Under some conditions, however, the high-resistance method may permit a significant saving in switchgear requirements. For example, it may sometimes allow omission of circuit breakers which would otherwise be necessary to clear faults from the battery electromotive force of a cell line.

CONCLUSIONS

Sensitive low-resistance a-c and d-c case-ground protection provides excellent

safety to personnel. High-resistance case-ground protection permits enclosure potentials which can produce fatal shock, but the method can be made safe by suitable insulation, isolation, and operating practices. Ground-fault damage with low-resistance protection may be greater than with high-resistance protection, but the amount of repair work required is not likely to be much greater. Installation of low-resistance grounding is usually simpler and less costly than high-resistance grounding. For these reasons I believe that the tradition of effectively grounding metal enclosures should be maintained, and the low-resistance grounding method should be the preferred one. Under some circumstances high-resistance grounding may offer substantial cost savings due to reduced fault-clearing requirements. It might then be considered acceptable provided that enclosures are treated as though they were energized.

REFERENCE

1. A STUDY OF THE HAZARDS OF IMPULSE CURRENTS, Charles F. Dalziel. *AIEE Transactions*, pt. III (*Power Apparatus and Systems*), vol. 72, Oct. 1953, pp. 1032-43.

D. C. Hoffmann: Mr. Stratford has raised several interesting and important questions which I will attempt to answer. First, the amount of insulation is determined more by mechanical than by electrical considerations. Under normal conditions, only about 25 volts d-c is impressed across the insulation, hence there is no electrical deterioration of any kind. The leakage resistance can be relatively high without affecting the sensitivity of the ground detector. In one design, the monitor will sound the alarm if the leakage resistance is reduced to about 400 ohms. There are several installations of rotary converters in which dry concrete is the only insulation. The insulation, however, must be able to withstand full rated voltage, both alternating and direct, for at least as long as it takes to clear the fault, and preferably continuously.

Mechanically, the insulation is more of a problem because it must be designed so that dust, dirt, floor sweepings, moisture, etc., cannot bypass it readily. Stray flux from high-current units causes magnetic foreign particles to migrate toward the unit with the possibility of bypassing the insulation. Good housekeeping on the part of the user is a help in preventing such troubles.

In some early installations, a 1/8-inch-thick sheet of glass laminate was used as the insulation under the enclosure, but this proved unsatisfactory because it could be bypassed too easily by foreign matter on the floor. A thickness of 3/4 inch is much more satisfactory. In some installations, 3-inch standoff insulators have been used.

Second, the high-resistance grounding protective relay would provide very good protection for the motors of motor-generator sets of any voltage rating, but there are other considerations. During a ground fault in the motor winding, the frame of the machine is elevated to at least the line-to-neutral voltage of the a-c system. This same voltage is impressed upon the

commutator and windings of the d-c generator, which may not be able to take it. Therefore, one answer to this question is: Do not use the high-resistance grounding protective relay on any voltage higher than the voltage that the d-c generator windings and commutator can withstand. Another limitation is the availability of a relay of high-voltage design. In my opinion, the high-resistance grounding protective relay should not be used for motors rated higher than 600 volts alternating current.

I agree with Mr. Stratford's statements

regarding the operation of disconnecting switches and the importance of the monitoring relay and alarm. Under no conditions should the structure or enclosure be left ungrounded.

Mr. Lovelace's discussion presents some very valid additional reasons why low-resistance grounding protection should be used for d-c structures and enclosures in electrochemical service, and is therefore a valuable adjunct to the paper. He also mentioned a few additional points in favor of the use of high-resistance grounding protection.

Metal-enclosed equipment is, of course, much safer than the old open-type equipment, because it will protect personnel against faults in the equipment. However, this is true only if personnel are kept on the side of the equipment while it is energized either by interlocks or operating instructions.

Mr. Lovelace has helped considerably to accomplish the purpose of the paper which was, as stated, to present the advantages and disadvantages of high- and low-resistance grounding of d-c structures and enclosures.

Power Apparatus and Systems—April 1961

61-27	Improving Accuracy of Transformer Noise Tests.....Comm. Report . . .	1
60-1182	A-C System Voltage Nomenclature for Power Systems..Comm. Report . . .	3
61-3	Effect of Contact Synchronization on A-C Interruption.....Howatson . . .	10
61-240	Cable Jackets and Water Permeability.....Todd . . .	13
61-9	Amplidyne Exciter System...Harvey, Rubenstein, Temoshok, Morgan . . .	17
61-219	Weaknesses in Naval Insulation Systems.....Walker, Flaherty . . .	23
61-230	Bibliography on Power Capacitors 1956-1959.....Committee Report . . .	31
61-8	Synchronous Machine Simulator.....Adamson, El-Serafi . . .	36
60-1236	Line Entrance Gaps Protect Substation Insulation.....Watson, Hiatt . . .	43
60-1274	Protection of Multiterminal and Tapped Lines.....Comm. Report . . .	55
60-225	Thermal Relationships in Induction Motor..Martiny, McCoy, Margolis . . .	66
61-13	Tertiary Windings in Autotransformers.....Farry . . .	78
61-66	Long-Scale Ammeters and Voltmeters.....Van Bennekom, Rowell . . .	85
61-131	New Current-Limiting Motor-Starter Fuse.....Cameron . . .	89
61-58	Absolute Calibration of Current Transformers.....Kusters, Moore . . .	94
60-1247	Coaxial Cable for Protective Relaying Communications.....Linders . . .	104
61-46	Thermal Behavior of Silicon-Carbide Valve Blocks.....Bolen . . .	109
61-249	Study Discharges in Dielectric Voids by Photomultiplier.....Bashara . . .	115

Conference Papers Open for Discussion

Conference papers listed below have been accepted for AIEE Transactions and are now open for written discussion until June 27. Duplicate double-spaced typewritten copies for each discussion should be sent to Edward C. Day, Assistant Secretary for Technical Papers, American Institute of Electrical Engineers, 33 West 39th Street, New York 18, N.Y., on or before June 27.

Preprints may be purchased at 50¢ each to members; \$1.00 each to non-members if accompanied by remittance or coupons. Please order by number and send remittance to:

AIEE Order Department
33 West 39th Street
New York 18, N. Y.

60-599	Locomotive Repair Costs and Their Economic Meaning to the Railways of the United States.....Brown
61-190	Contact Wire Wear.....Gordon
61-208	The Economic Justification of Railway Electrification in the United States.....Cross

AIEE PUBLICATIONS

Electrical Engineering

Official monthly publication containing articles of broad interest, technical papers, digests, and news sections: Institute Activities, Current Interest, New Products, Industrial Notes, and Trade Literature. Automatically sent to all members and enrolled students in consideration of payment of dues. (Members may not reduce the amount of their dues payment by reason of nonsubscription.) Additional subscriptions are available at the nonmember rates.

Member Prices	Nonmember Prices	
	Basic Prices*†	Extra Postage for Foreign Subscriptions

annually
\$12* \$1.00

Single
copies
\$1.50*

Bimonthly Publications

Containing all officially approved technical papers collated with discussion (if any) in three broad fields of subject matter as follows:

Communication and Electronics
Applications and Industry
Power Apparatus and Systems

	annually	annually	
	\$5.00	\$8.00*	\$0.75
	\$5.00	\$8.00*	\$0.75
	\$5.00	\$8.00*	\$0.75

Each member may subscribe to any one, two, or all three bimonthly publications at the rate of \$5.00 each per year. A second subscription to any or all of the bimonthly publications may be obtained at the nonmember rate of \$8.00 each per year.

Single copies may be obtained when available. \$1.50 each \$1.50* each

AIEE Transactions

An annual volume in three parts containing all officially approved technical papers with discussions corresponding to six issues of the bimonthly publication of the same name bound in cloth with a stiff cover.

Part I Communication and Electronics
Part II Applications and Industry
Part III Power Apparatus and Systems

	annually	annually	
	\$4.00	\$8.00*	\$0.75
	\$4.00	\$8.00*	\$0.75
	\$4.00	\$8.00*	\$0.75

Annual subscription to all three parts (beginning with vol. 77 for 1958).

\$10.00	\$20.00*	\$2.25
	\$15.00*	\$1.50

Annual subscription to any two parts.

AIEE Standards

Listing of Standards, test codes, and reports with prices furnished on request.

Special Publications

Committee reports on special subjects, bibliographies, surveys, and papers and discussions of some specialized technical conferences, as announced in ELECTRICAL ENGINEERING.

*Discount 25% of basic nonmember prices to college and public libraries. Publishers and subscription agencies 15% of basic nonmember prices. For available discounts on Standards and special publications, obtain price lists from Order Department at Headquarters.

†Foreign prices payable in New York exchange

Send all orders to:

Order Department
American Institute of Electrical Engineers
33 West 39th Street, New York 18, N. Y.